AICL is a ligand for the human NK receptor NKp80/KLRF1 and mediates an activating crosstalk between NK cells and monocytes

AICL ist ein Ligand des humanen NK Rezeptors NKp80/KLRF1 und vermittelt eine aktivierende Interaktion zwischen NK-Zellen und Monozyten

DISSERTATION

der Fakultät für Chemie und Pharmazie
der Eberhard-Karls-Universität Tübingen

zur Erlangung des Grades eines Doktors
der Naturwissenschaften

2007

vorgelegt von

Stefan Welte

Tag der mündlichen Prüfung:	29. März 2007
Dekan:	Prof. Dr. L. Wesemann
1. Berichterstatter:	Prof. Dr. H.-G. Rammensee
2. Berichterstatter:	PD Dr. A. Steinle
3. Berichterstatter	Prof. Dr. H.-M. Jäck

Preface

All four chapters in the results and discussion section of this thesis have been published before. At the beginning of each chapter, it is indicated which experiments were done by the author of this thesis, which persons contributed to the publication, and in which journal the work has been published.

1 Introduction

1.1 Principles of the innate immune system

Pathogens infect the human body through a variety of routes. They can enter via the mucosal surfaces or the external epithelial surfaces during physical contact or in the case of wounds, punctures or bites. If a pathogen has successfully overcome these protective surfaces the human body launches a rapid innate response in order to prevent pathogen proliferation until the primary adaptive response consisting of T and B cells provides antigen-specific protection after 4 to 7 days. These innate mechanisms can act very fast within minutes or a few hours because there is no requirement for clonal expansion. In most cases pathogens are already eliminated at this stage and no clinical symptoms are evident. The innate arm of our immune system is the evolutionarily ancient and more universal among organisms. Invertebrates for example rely only on innate immunity.

Innate immunity was first described by the Russian pathologist Elie Metchnikoff by studying macrophages in sea stars [**1**], but soon immunological research focused mainly on the investigation of mechanisms underlying adaptive immune processes. The discoveries of the dendritic cells, of pathogen-specific receptors like Toll-like receptors and advances in NK cell biology triggered a broad interest in the field of innate immunity. It is now increasingly clear that the two arms of the immune system, the innate and the adaptive arm, are highly connected and it seems that nearly every aspect of the adaptive immune response is controlled by the innate immune system [**2-4**].

The two key features of the mammalian innate immune system are first the ability to recognize pathogen and/or tissue damage and second to signal the danger to the components of adaptive immune system both in a very rapid manner [**5**]. The innate immune system includes neutrophils, granulocytes, monocytes, macrophages, dendritic cells (DCs) and natural killer (NK) cells as the cellular components whereas the complement system and the interferons are the non-cellular components. The relative recent characterization of specialized lymphocyte subsets like the γδ T cells, NKT cells or $CD4^+CD25^+$ regulatory T cells to name a few underlines the close relationship of both arms of the immune system.

1.1.1 Immunobiology of NK cells

1.1.1.1 NK cell recognition and the “missing-self hypothesis”

Natural killer (NK) cells are large granular lymphocytes and account for 5-25% of the peripheral blood lymphocytes depending on the donor. They belong to the innate immunity because their receptors are encoded by germline genes that do not undergo somatic recombination. Functionally, however, NK cells are in many aspects more closely related to T cells than to any other leukocyte of the innate immune system, because they possess the same killing mechanism as cytotoxic T lymphocytes (CTL) and secrete IFNγ like CTL and T_H1 helper T cells [**6**]. NK cells express an impressing array of activating and inhibitory receptors. All signals received by this receptors are integrated and the final outcome decides whether the cell is activated or not by the respective target cell. Originally when the term “natural killer” was coined as early as 1975 when it was thought that NK cell recognition did not involve the MHC [**7-9**] and that NK cells are able to kill efficiently cells lacking MHC [**10**]. However Klas Kärre, in his doctoral thesis introduced the now classic "missing self-recognition" concept in 1984 [**11**], which means that NK cells are inhibited by self-MHC class I molecules and eliminate cells which fail to express self-MHC molecules. There were still many open questions, for example, why some MHC class I- positive tumor cells still can be lyzed by NK cells?
1989 Trinchieri postulated activating structures present on target cells [**12**], which could account for the conflicting results. In the late 1990s the new concept of “induced-self” was introduced by Diefenbach and Raulet, which was based on observations of Bauer, Spies and colleagues, which stated that NK cells eliminate cells expressing stimulatory ligands for activating receptors [**13-18**]. One of the key receptors mediating the recognition of induced-self is the NKC-encoded NKG2D molecule [**14**] which will be discussed in more detail in 1.1.1.3. An modified “missing-self hypothesis” would state, that NK cells kill targets that fail to express MHC class I molecules, but express ligands for activating receptors.

Importantly, without an activating signal the NK cell does not respond to a target cell even when the target fails to express inhibitory ligands. The inhibitory receptors weaken the signals from activating receptors rather terminating them totally, which implies that a strong activating signal overcomes the inhibitory signal and the target

will by lyzed [6]. Signal interpretation is more similar to an analog scale rather than a binary switch, an analogy which is symbolized by **Figure 1.1**.

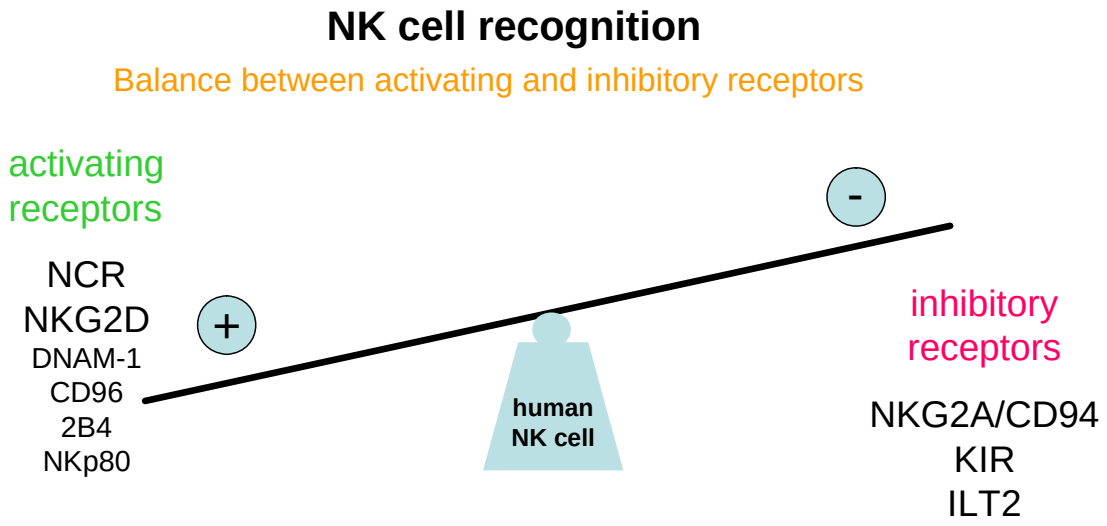

Figure 1.1 NK cell recognition as a balance between activating and inhibitory receptors. All signals received by activating and inhibitory receptors are integrated and the final outcome decides whether the NK cell is activated or not by the target cell, whereby the signal interpretation is more similar to an analog scale rather than a binary switch. Abbr.: NCR, natural cytotoxicity receptors; KIR, killer cell immunoglobulin-like receptors; DNAM-1, DNAX accessory molecule 1 (CD226); ILT2; inhibitory receptors Ig-like transcript 2.

1.1.1.2 Inhibitory receptors

NK cells express activating and inhibitory receptors, which can be subdivided into three classes. The first class is the killer cell immunoglobulin-like receptors (KIR), which belong to the immunoglobulin superfamily (IgSF), the second class is the C-type lectin-like receptors (CTLR) and finally the so called natural cytotoxicity receptors (NCR). Most CTLR are encoded within the natural killer gene complex (NKC), which is discussed in detail in **1.1.7**. However, all classes contain inhibitory and activating receptors.

Inhibitory receptors encompass members of the KIR family in humans, the Ly49 family in mice, and the CD94/NKG2A heterodimers in mouse and humans [**19-21**]. KIRs are expressed on NK cells and a subset of memory T cells [**22-25**], and are encoded in the leukocyte receptor complex (LRC) region on chromosome 19q [**26**]. KIRs are specific for allelic variants of HLA-A, -B and -C molecules, for example, KIR2DL1 binds HLA-C group 2 members (e.g. HLA-Cw2, -Cw4, -Cw6). The KIRs are thought to play an important role in a process called “NK licensing” which will be

described in **1.1.1.5**. In mice, monitoring of allelic loss of MHC class I expression is fulfilled by receptors of the Ly49 family, which are discussed in **1.1.7.3**.

All inhibitory NK receptors contain one (Ly49) or two (KIR2DL and KIR3DL) ITIMs (immunoreceptor tyrosin-based inhibitory motifs; I/VxxYxxL) in their cytoplasmic domains [**19**]. For details regarding signaling of inhibitory receptors see **Figure 1.2.**

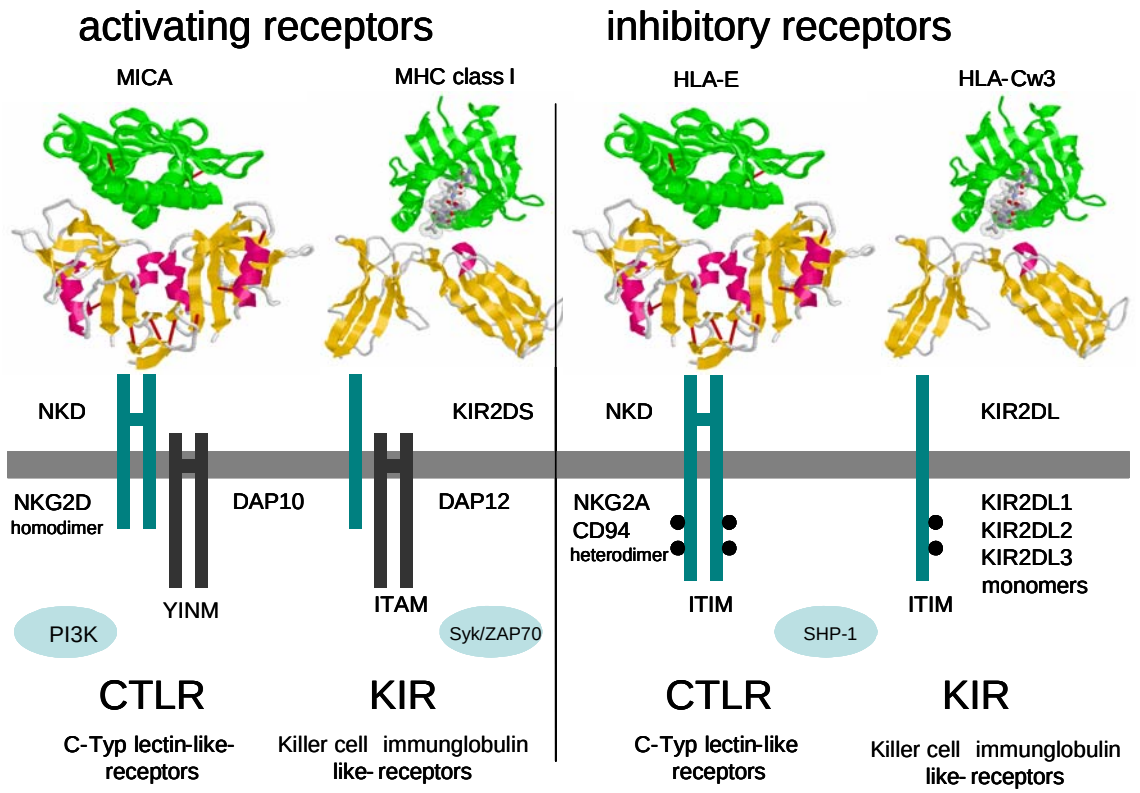

Figure 1.2 Activating and inhibitory receptors on NK cells. Both KIRs (killer cell immunoglobulin-like receptors) and CTLR (C-type lectin-like receptors) comprise activating and inhibitory receptors. The activating receptors do not contain ITAM themselves, but associate with adaptor molecules like DAP10 or DAP12 which contain an ITAM (DAP12) or YINM (DAP10) necessary for signal transduction. In humans, ligation of NKG2D leads to the phosphorylation of the YxxM-motif and activates the phosphatidylinositol-3-kinase (PI3K) pathway. In mouse there is a differential use of DAP10 and DAP12 [**15**]. DAP12 signals via the tyrosine kinases Syk and ZAP70, which are recruited via their SH2 domains. The ITIMs of the inhibitory receptors are tyrosine-phosphorylated upon receptor ligation by src-kinases and in turn recruit and activate SH2-domain-containing-protein tyrosine phosphatase 1 and 2 (SHP-1 and -2). Subsequently, SHP-1 and SHP-2 dephosphorylate and thus inactivate signal transducers of activating signaling pathways [**6**]. The cartoons of the crystal structures were created using ProteinExplorer [**27**] (www.proteinexplorer.org). The PDB code of the NKG2D-MICA-complex is 1HYR [**28**] and for KIR2DL-HLA-Cw3 1EFX [**29**]. For the KIR2DS/MHC class I and NKG2A/CD94/HLA-E complexes the crystal structures of KIR2DL/HLA-Cw3 and NKG2D/MICA were used respectively due to the lack of crystallographic data.

1.1.1.3 Activating NK receptors

In humans, a number of activating NK receptors including NKp30, NKp44, NKp46, NKp80 and NKG2D have been characterized, but, apart from NKG2D, the unidentified nature of the corresponding cellular ligands strongly curbs further advance in the understanding of their role in NK-mediated immunoregulation and immunosurveillance [**6,30**]. Since NKG2D-ligands are inducibly expressed on infected cells or upon genotoxic stress and are associated with malignant transformation, the hypothesis was put forward that NKG2D may serve as an immune detector of harmful cells promoting their elimination [**6,14,31,32**]. NKG2D is expressed by virtually all human NK cells, γδ T cells and $CD8^+$ T cells and, together with the adaptor protein DAP10, assembles into an activating immunoreceptor complex [**6,14**]. Upon ligation of its MHC class I-related, stress-inducible ligands encoded by the MIC and ULBP genes, NKG2D stimulates NK cytotoxicity and cytokine secretion [**14,18**].

The natural cytotoxicity receptors (NCR) NKp46, NKp44 and NKp30 were found by a screen for monoclonal antibodies (mAbs), which are capable of mediating redirected lysis of a Fc receptor expressing tumor cell line [**30**]. The NCRs were named after the molecular weight. NKp46 and NKp30 are present on all NK cells regardless of the activation status, therefore representing the only available truly NK-specific markers. NKp44 is only expressed by activated NK cells [**33**]. Cross-linking of NKp46 and NK30 induces Ca^{2+} influx, cytotoxicity and cytokine production [**34,35**]. NKp46 in encoded within the leukocyte receptor complex (LCR) on human chromosome 6. NKp46 has also been cloned in mice [**36**] and it was recently reported that mouse NKp46 is also the only marker which is truly NK specific. The cellular ligands of the NCRs are yet not known. NKp46-Fc fusion proteins bind to tumor cells as well as influenza virus–infected cells and it was also shown that NK cells are activated by recognition of haemagglutinins on virus-infected cells via NKp46 [**37**]. Using an NKp46 knock-out mouse Gazit *et al.* could show that NKp46 protects from lethal influenza virus infection, however the involvement of NKp46 in tumor immunity still remains unclear [**38,39**]. The role of NKp30 in the NK/DC crosstalk will be discussed in **1.1.6**. Regarding NKp44 it was published that NKp44-Fc fusion proteins bind to HIV-infected $CD4^+$ T cells [**40**] indicating also an involvement in the immunity against viruses.

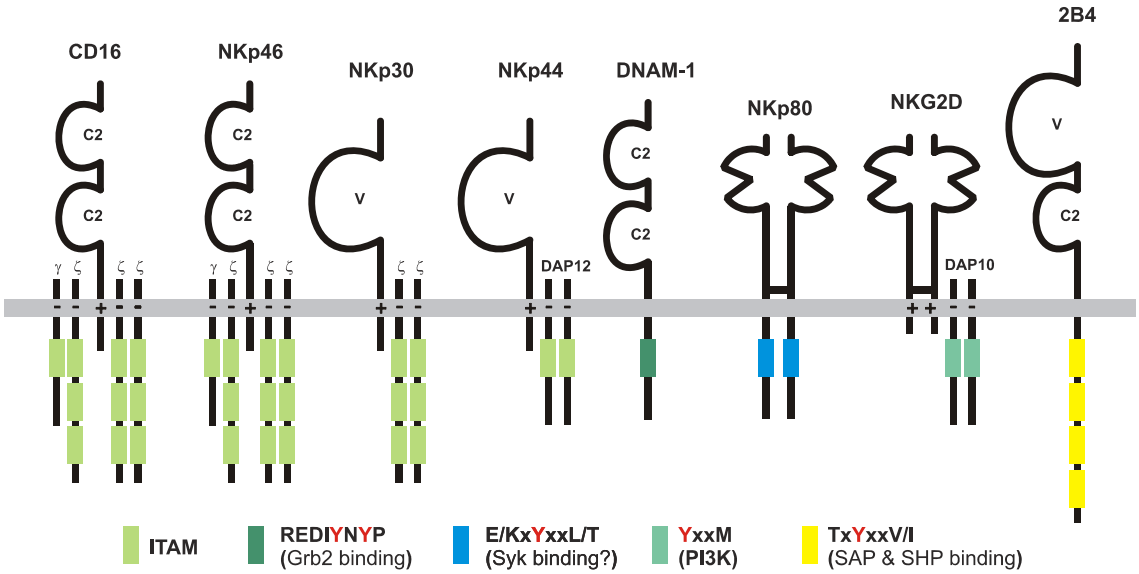

Figure 1.3 Activating receptors on human NK cells. CD16, NKp46, NKp30, NKp44, DNAM-1 and 2B4 are type I glycoproteins belonging to the Ig-SF containing either one or more Ig-like C2 type (C2) or a V-set domain (V). NKG2D and NKp80 are dimeric type II glycoproteins belonging to the C-type lectin-like receptor superfamily. Both the NCRs and NKG2D contain in their transmembrane region positively charged amino acids, which interact with signal-transducing adaptors, which contain negatively charged residues. The CD3ζ chain (ζ) and FcεRIγ chain (γ) are able to form disulfide-linked homodimers or heterodimers and contain ITAMs, which are phosphorylated by tyrosine kinases of the Src family followed by the recruitment of Syk and ZAP70 tyrosine kinases [**30**]. In contrast 2B4, DNAM-1 and NKp80 do not contain charged residues in the transmembrane region and are characterized by tyrosine-based motifs in their cytoplasmic tails [**30,41,42**]. 2B4 associates with SAP adaptor and SHP-1/SHP-2 tyrosin phosphatases, whereas NKp80 contains a tyrosin motif in its cytoplasmic domain, which could bind Syk analog to Dectin-1 [**43**]. The tyrosin motif of DNAM-1 is a possible binding site for Grb2, which activates the Ras pathway [**41**]. Data was compiled from [**30,41,44**].

1.1.1.4 Viral modulation of NK cell immunity

Viruses have coevolved together with their respective hosts and, hence, developed many mechanisms to avoid recognition by the hosts' immune system or to ensure detection of viral invaders, respectively. Together with cytotoxic T cells the major combatants against virus-infected cells are NK cells [**12**]. Amongst various viral pathogens, human and mouse cytomegalovirus (HCMV and MCMV) are the model pathogens regarding their overabundance of immunoevasive mechanisms that allow a life-long persistence in the host. Cytomegalovirus impairs T cell recognition by the down-modulation of MHC class I surface expression through various mechanisms. HCMV-encoded US6 blocks the transporter of antigenic peptides TAP, also HCMV-encoded US3 retains MHC class I heavy chains in the ER. In addition the two HCMV-encoded immunoevasins, US2 and US11, induce the dislocation of class I MHC

heavy chains in distinct pathways from the ER membrane and target them for proteasomal degradation in the cytosol [**45,46**]. Via the binding of US11 onto the channel-like protein Derlin-1 HCMV hijacks with Derlin-1 the cellular garbage-disposal machinery and disposes MHC class I molecules from the ER cytosol straight into the proteasome [**47**]. The strongly reduced MHC class I surface expression leads to a reduced engagement of inhibitory KIRs facilitating NK-mediated lysis. NK cells also indirectly monitor the expression of classical MHC class I molecules via HLA-E and Qa-1^b in human and mouse, respectively. Since cell surface expression of HLA-E and Qa-1^b is dependent on class I signal peptides, their surface expression indicates an intact MHC class I loading process in the ER. HLA-E and Qa-1^b is bound by the heterodimeric inhibitory CD94/NKG2A receptors expressed by a major subset of NK cells and a minor subset of memory T cells in humans and rodents [**48-50**]. Failure to express HLA-E and Qa-1^b on the cell surface leads to a reduced inhibitory signal to the NK cell.

However, HCMV evolved also several NK evasion mechanisms. On the one hand, HCMV exploits the NK recognition of MHC class I by expressing an MHC class I replica, the UL18 glycoprotein, which strongly binds the pan-HLA-class I-specific NK inhibitory receptor ILT2 (inhibitory receptors Ig-like transcript 2) [**51**]. Additionally a peptide derived from the HCMV UL40 glycoprotein mimics signal peptides from HLA-class I molecules, and ensures HLA-E surface expression and ligation of inhibitory CD94/NKG2A receptors [**52,53**].

1.1.1.5 NK licensing

Certain combinations of MHC class I alleles and KIR variants expressed by NK cells have been associated with the resistance to infections, the susceptibility to autoimmune diseases and even complications of pregnancy, as well as the outcome after a hematopoietic stem-cell transplantation [**54**]. The KIRs expressed by NK cells ensures that NK cells do not attack “self”. The genes for the MHC proteins and the KIR are inherited independently from one another and are highly polymorphic. One open question was how is it possible that receptors that are highly polymorphic recognize also highly polymorphic ligands? It was known already in the early 1990s, that in β_2-microglobulin knock-out mice ($\beta_2m^{-/-}$) (with an MHC class I-deficient phenotype) NK cells are not attacking “self” but rather NK cells from such $\beta_2m^{-/-}$ mice failed to kill $\beta_2m^{-/-}$ blasts, while they retained the ability to kill the prototype NK

cell target lymphoma YAC-1, however at reduced levels [**55**].

Recently, it was proposed that the acquisition of full NK functionality requires a process termed “licensing” during NK maturation on a clonal level [**56**]. Paradoxically, the ITIM-bearing inhibitory KIRs specific for self MHC class I molecules are crucially involved in this positive activation during NK development. The majority of individual NK cells express only one or rarely two such “self-restricted” KIRs [**57**]. Very recently it was reported, that in humans around 13% of the peripheral NK cells are even $KIR^{neg}NKG2A^{neg}$, which will be discussed later [**58**]. The “licensing model” states now that only such NK cells are licensed whose KIRs are engaged by the corresponding self-MHC molecules. NK cells, which are not licensed do not exhibit NK effector functions [**56**]. This model explains observations made in the past like the impaired NK killing capacity by NK cells from $\beta_2m^{-/-}$ mice as discussed above. Licensing could also be important in the problem why donor NK cells given to leukemia patients during bone marrow transplantation as treatment do not always have an anti-tumor effect. Leukemia patients can be treated by transplantation of bone marrow or hematopoietic stem cells. The patient's bone marrow and leukemia cells residing in the marrow are destroyed by irradiation and are replaced with marrow or stem cells from a donor (allogeneic transplantation). However, there is the risk of graft-versus-host (GvH) disease, which can be favorable for the patient by eradicating residual leukemia cells, called the graft-versus-leukemia or GvL effect. T cells are crucial mediators of these reactions. A different approach was used by the so called haploidentical (i.e. partly HLA-mismatched) hematopoietic cell transplantation pioneered by the Velardi group and others [**59-61**]. Haploidentical means that only one MHC-haplotype is matched with that of the recipient, which would be the case with either parent of the patient and with statistically 50% of the siblings of the patient. In certain donor-recipient combinations NK cells in the graft are not inhibited by HLA molecules of the host and are therefore alloreactive in the GvH direction. This leads especially in the case of acute myeloid leukemia (AML) to a greatly reduced probability of leukemia relapses and a reduced graft rejection (graft versus host, GvH), since the NK cells also eliminate host APCs, which are thought to be responsible for GvH effects [**61**]. Due to the absence of the appropriate recipient HLA ligands for the donor KIRs it is possible that the licensing is impaired, which influences the functional capacity of transplanted NK cells. It was shown that the licensing effect was less prominent in pre-activated NK cells [**56**], which means that licensing can be bypassed under

certain conditions. This could explain that certain transplantation protocols used in hematopoietic cell transplantation have more success than others [**54,58**].

As mentioned above recent studies in humans showed also that NK cells must encounter self MHC class I to become a fully functional NK effector [**58**]. Anfossi *et al.* described in humans a $KIR^{neg}NKG2A^{neg}$ subset accounting for ~13% of the peripheral NK cells. These cells are hyporesponsive to MHC class I-negative targets as well as to stimuli via NKp46-expressing targets or even CD16 cross-linking in cell-free stimulation assays. In contrast, bypassing surface receptors using PMA/ionomycin leads to a normal response by these cells. A very large fraction of $KIR^{+}NKG2A^{+}$ cells, however, did also not respond to classical NK stimuli indicating that there are other factors contributing to NK cell reactivity [**58**].

1.1.1.6 The $CD56^{dim}$ and $CD56^{bright}$ NK subsets in humans

It has been previously recognized that there are two functionally distinct NK cell subsets in humans: $CD56^{dim}$ and $CD56^{bright}$ NK cells. These NK cell populations differ in their localization properties: the $CD56^{bright}$ NK cells are more abundant in lymphoid organs than the $CD56^{dim}$ NK cells, and the latter being the most prominent subset in blood accounting for up to 90% [**62**]. The $CD56^{dim}$ NK cell population was also reported as being more prone to cytotoxicity, whereas the $CD56^{bright}$ NK cells tend to produce more cytokines such as IFNγ [**63**]. This distinction was recently modified stating that the $CD56^{dim}$ NK cells are more “target cell responsive”, which means they show higher CD107a and IFNγ expression upon stimulation with a MHC class I-deficient target. In contrast the $CD56^{bright}$ secrete more IFNγ in response to NK-stimulating cytokines like IL-12 and IL-15 being therefore more “cytokine responsive” [**58**].

1.1.1.7 Unconventional T cells subsets: T cells and NKT cells

Both subsets are T cells by definition as they express a TCR. However both T cell subsets are considered as components of the innate arm of the immune system, since both T cell subsets use a restricted TCR repertoire.

In contrast to "classical" αβ T cells, which account for the majority of T cells and

recognize short peptides bound to MHC molecules, the less frequent γδ T cells display a very restricted TCR repertoire. γδ T cells recognize a variety of possible antigens mostly self-molecules like CD1 or self-molecules associated with cellular stress like MICA, MICB or F1-ATP synthase in humans or T10/T22 in mice [**64,65**]. T22 recognition is dominated by a certain TCR-δ CDR3 motif, which is mainly germ-line encoded and could allow for a rapid and significant response without an initial need for clonal expansion [**66**]. γδ T cells express scavenger receptors like WC1, TLRs (Toll-like receptors) and NK receptors [**65,67**]. They exhibit functions similar to αβ T cells and NK cells such as cytokine production and cytolysis [**68**]. γδ T cells can kill *Listeria monocytogenes*-infected macrophages [**69**]. Triggering of NKG2D alone activates γδ T cells to secrete TNFα and to release cytotoxic granules [**70**]. Recently, it was demonstrated that γδ T cells like DCs can function as professional APCs [**71**]. In contrast to DCs γδ T cells need to be activated. After activation γδ T cells express the lymph node homing receptor CCR7 and express increased MHC class II as well as CD80/86 levels [**71**]. γδ T cells are mostly located within the intestinal epithelial layer [**64,72**]. γδ T cells have been found at relatively high proportion among tumor-infiltrating lymphocytes (TILs) of various origins [**73**] and several mouse models indicate that they likely play a role in tumor immunosurveillance [**74-76**]. The only well-characterized tumor ligands for human γδ T cells are the NKG2D ligands MICA and MICB. Since γδ T cells also express NKG2D, activation may occur via both, TCR and NKG2D binding. There are many reports that γδ T cells interact very closely with myeloid cells [**65**]. Half of the lung resident γδ T cells were shown to be in direct contact with DCs in the mouse [**77**] and in the skin a bi-directional activating crosstalk between DCs and γδ T cells was demonstrated in humans, which was cell-cell contact-dependent [**78**].

Classical or invariant NKT (iNKT) cells are defined as CD1d-dependent and express the invariant Vα14-Jα18 (mice), Vα24-Jα18 TCR (humans). Technically iNKT cells can be identified by staining with an α-galactosylceramide (α-GalCer) loaded CD1d tetramers [**79**]. iNKT cells include two subsets, either $CD4^{neg}$ or $CD4^{+}$. The $CD4^{neg}$ subset selectively produces the T_H1 cytokines IFNγ and TNFα, and expresses NKG2D. In contrast, $CD4^{+}$ CD1d-restricted iNKT cells potently produce both T_H1 and T_H2 cytokines [**79**]. All invariant NKT cells recognize α-GalCer, a marine-

sponge-derived glycosphingolipid [**80**]. Yet α-GalCer is not a likely physiological antigen of iNKT cells, since it is very rare in microorganisms and absent in mammalian cells [**81**]. Additionally, bacterially derived glycosylceramides can activate all iNKTs [**82**]. Recently, iGb3 (a glycosphingolipid) was identified as an important endogenous, lysosomal ligand for iNKT cells, which is required for iNKT development in the thymus and is also able to activate iNKT cells albeit weaker than α-GalCer [**83**]. iGb3 plays critical role in the activation of NKT cells during infections with Gram-negative bacteria that contain LPS in their cell wall. CD1d-mediated iGb3 presentation by DCs and TLR-mediated IL12 secretion also by DCs leads to iNKT activation, which in turn secrete IFNγ. In the case of LPS-negative bacteria, it was shown that iNKT are solely activated via CD1d-expessing DCs via above mentioned glycosylceramides [**81,82**].

1.1.2 Monocytes and macrophages

Cells of the monocyte lineage have important functions in the innate arm of the immunity since they phagocytose foreign material or cell debris, present antigen to T cells and produce important cytokines initiating the immune response like TNF, IL-6, IL1β or IL-8. In addition there are also inflammatory mediators like prostaglandins or leukotrienes, which are secreted by macrophages in response to pathogens. In order to detect pathogens the monocytic cells possess a wide variety of cell surface receptors like the Toll-like receptor (TLR) family or pattern recognition receptors, which will be discussed in detail in **1.1.4**.

1.1.2.1 Hematopoietic differentiation of myeloid cells

Circulating monocytes in the blood differentiate from a common myeloid progenitor, which they share with granulocytes (see **Figure 1.4** for details). They circulate for up to 3 days [**84**] before they are recruited into tissues upon different stimuli and differentiate into tissue macrophages, a process, which was shown already as early as 1939 by Ebert and Florey [**85**].

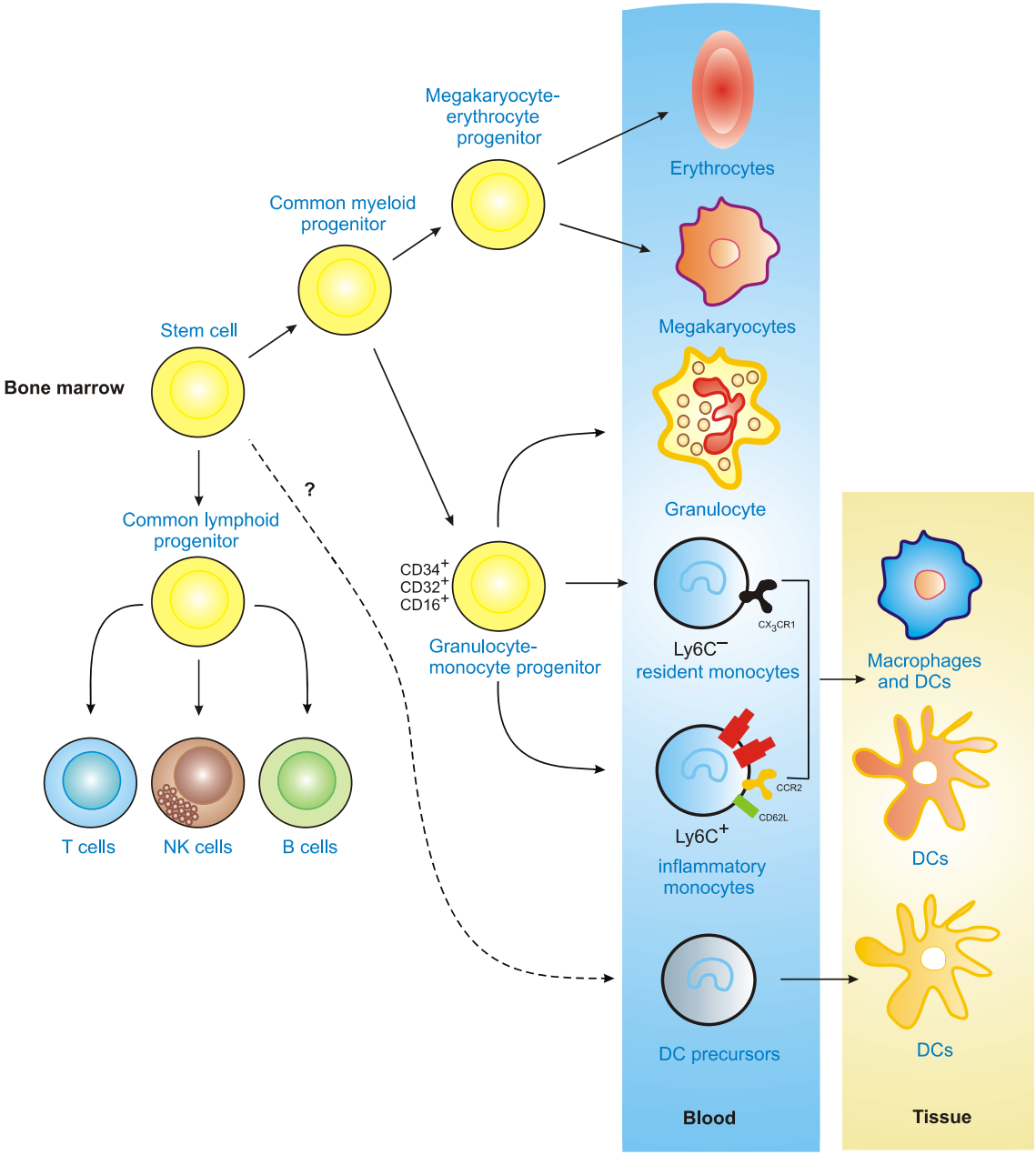

Figure 1.4 Hematopoietic differentiation of mouse myeloid cells. In the bone marrow stem cells differentiate into myeloid and lymphoid progenitor cells. The myeloid progenitors subsequentially give rise to granulocyte-monocyte progenitors, which differentiate into granulocytes and monocytes. For more details see main text. Del Hoyo *et al.* [**86**] decribe a common precursor population, which can give rise to all DCs including plasmacytoid DCs. This pathway is indicated with an "?". This illustration was drawn after [**87**].

Blood monocytes can also differentiate into myeloid dendritic cells in the tissue, but it seems that at least mouse monocytes are not the only source for DCs since a common precursor population for DCs was also described [**86**]. In the human system DCs can be generated *in vitro* by cultivating monocytes in the presence of IL-4 and GM-CSF for 7 days [**88**]. In humans, however, the *in vivo* development and differentiation pathway from monocytes to DCs is only poorly understood.

1.1.2.2 Monocyte heterogeneity

The main surface marker for monocytes is CD14, which is part of the lipopolysaccharide (LPS) receptor. Although there is quite some morphologically heterogeneity among monocytes regarding size or granularity, only with the discovery of differential expressed surface markers one could define different monocytes subsets.

Table 1.1 Markers of circulating monocytes subsets in human and mice. The minor $CD14^+CD16^+CD64^+$ population was omitted since it is not well-characterized yet. Adapted from [**89**]. ND, not determined. NC, antigen is not conserved.

Markers	human $CD14^{hi}CD16^{neg}$	human $CD14^+CD16^+$	mouse $Ly6C^+CD62L^+$ "inflammatory"	mouse $Ly6C^{neg}CD62L^{neg}$ "resident"
Chemokine receptors				
CCR2	+		+	
CCR5		+	ND	ND
CCR7	+		ND	ND
CX_3CR1	+	++	+	++
other markers				
CD11c	++	+++		+
CD14	+++	+	ND	ND
CD32	+++	+	++	+
CD62L	++		+	
Ly6C	NC	NC	+	
MHC class II	+	++		
7/4	ND	ND	+	

In humans, there are altogether three different subsets known so far: the $CD14^{hi}CD16^{neg}$ cells, which are regarded the classical monocytes, the $CD14^+CD16^+CD64^{neg}$ subset [**90**] and finally the minor $CD14^+CD16^+CD64^+$ population [**91**]. Compared to the classical subset the $CD14^+CD16^+$ cells express more MHC class II, more CX_3CR1 (CX_3C-chemokine receptor) and they are CC-chemokine receptor 5 (CCR5) positive in contrast to the classical, which are $CCR2^+CCR5^{neg}$ [**89**]. Another important difference among the surface receptor expression is CD62L (or L-selectin), which is expressed only on the classical monocytes. A summary of important markers in human and mouse monocytes is shown in **Table 1.1.**

With the observation that there are mouse counterparts to the human monocyte

subsets it seems appropriate to draw conclusions from *in vivo* studies in mice regarding the relevance in humans. With the help of adoptively transferred GFP-expressing monocytes it could be shown that the $CCR2^{+}$ subset is short-lived and is quickly recruited to the site of experimentally induced inflammation and upregulates CD11c and MHC class II.

In contrast the $CCR2^{neg}$ monocytes persist longer in the blood and it could be shown that some cells could be detected in the spleen expressing a DC-like phenotype [**92**]. There is evidence, however, that also $CCR2^{+}$ monocytes can differentiate into DCs [**92**]. Using an *in vitro* transendothelial-migration model Randolph *et al.* [**93**] could show that the human $CD14^{+}CD16^{+}$ subset preferentially differentiates into DCs. *In vitro* both monocyte subsets in human and in mice differentiate into DCs upon cultivation in IL-4 and GM-CSF [**88,92,94**]. It is not clear yet, at what point in the development the two subsets separate. There is evidence in mice that after the complete depletion of monocytes the $CCR2^{+}$ monocytes are the first to recover in the circulation [**95**]. Together with the description of a population with an intermediate Ly6C expression one could discuss following development model as depicted in **Figure 1.5**.

In healthy donors ~ 10% of the monocytes belong to the $CD14^{+}CD16^{+}$ subset. Regarding functionality of the $CD14^{+}CD16^{+}$ monocytes it was shown that this subset is a major source for TNFα producing threefold more of TNFα upon LPS stimulation and up to tenfold more TNFα after Pam_3Cys-stimulation compared to $CD14^{hi}CD16^{neg}$ cells [**96**]. The expression level of TLR2 (the receptor for Pam_3Cys) was twofold higher in the $CD14^{+}CD16^{+}$ subset again compared to $CD16^{neg}$ cells [**96**]. Details regarding TLR ligands will be discussed in detail in **1.1.4**. In patients with severe infections this subset is strongly expanded [**97,98**].

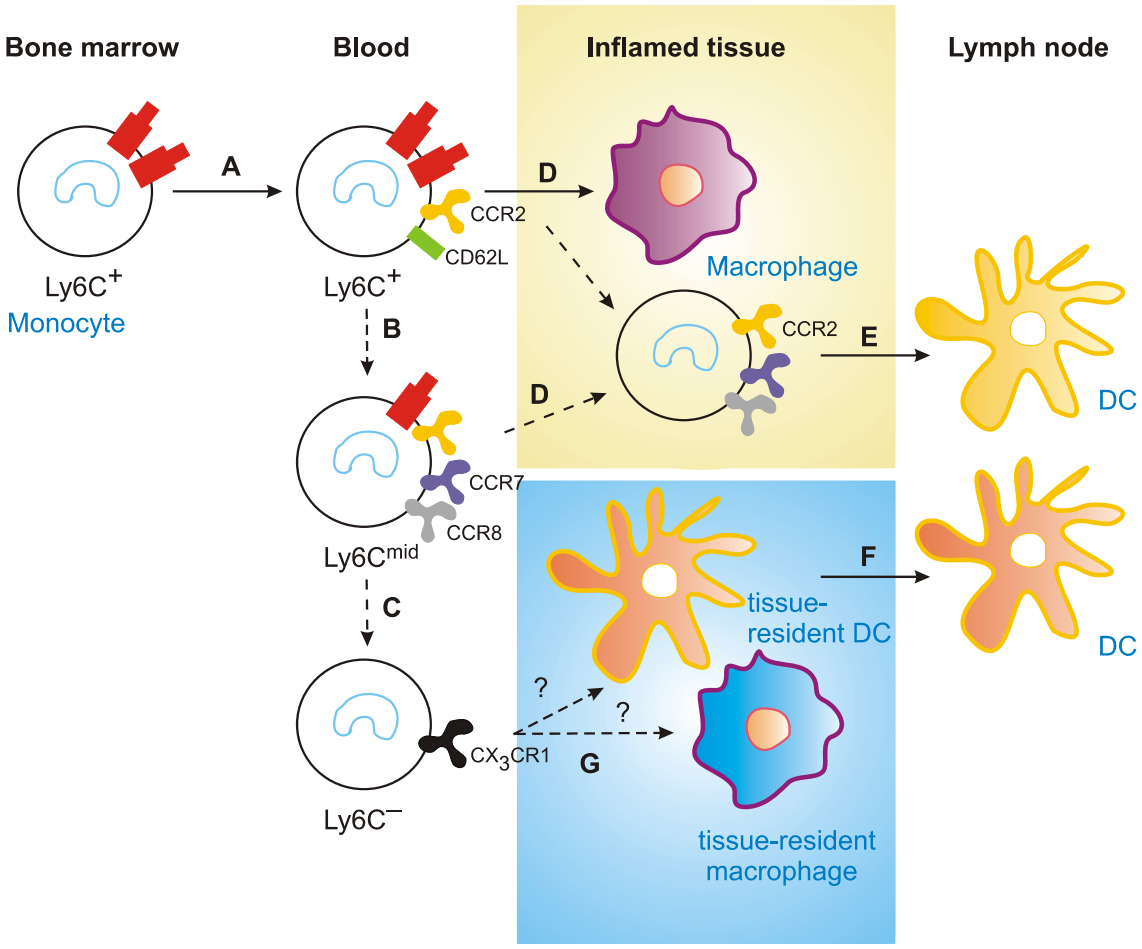

Figure 1.5 Developmental model of mouse and human monocytes subsets. Ly6C^{+} monocytes are released into the blood (**A**) and without an inflammatory stimuli they develop into Ly6C^{neg} CX$_3$CR1^{+} resident monocytes (**B**, **C**). Upon inflammatory stimuli like CCL2 binding to its receptor CCR2 most of the Ly6C^{+} and the Ly6C^{mid} monocytes are recruited into the tissue and develop into macrophages (**D**). Some monocytes are migrating to the draining lymph node and differentiate to DC. A process, which was shown to be dependent on CCR7/CCR8 expression (**E**). The Ly6C^{neg}CX$_3$CR1^{+} resident monocytes finally replenish the tissue-resident macrophages like the aleveolar macrophages, osteoclasts or tissue-resident DC (**G, F**). The solid arrows indicate that the pathways are supported by *in vivo* mouse data, whereas the dashed arrows indicate a more hypothetical status. This model was drawn after [**89**].

1.1.2.3 Specialized tissue macrophages

The very heterogeneous nature of tissue macrophages is a consequence of their specialization of function in very different parts of the body. The professional antigen-presenting Langerhans cells, for example, are found in the epidermis of the skin. The osteoclasts are responsible for remodeling bone, whereas the alveolar macrophages are responsible for the clearance of environmental particles, viruses and other microorganisms in the lung. The Kupffer cells in the hepatic sinusoids of the liver remove debris and dying cells of the blood similar to splenic macrophages in the white

pulp, which are by themselves again very heterogeneous. Finally there are many subsets of macrophages in the central nervous system (CNS) like the microglia or the perivascular macrophages in the small blood vessel near the brain [**89**].
Under steady-state conditions this tissue macrophages undergo local proliferation to replenish their resident populations whereas under stress conditions circulating monocytes are recruited into the tissue. This could be shown for the Langerhans cells [**99**] in the epidermis or for the alveolar macrophages in the lung [**100,101**] and for most of the other tissue macrophages like the Kupffer cells [**102**]. Generally there are three modes of macrophage activation: the classical via an IFNγ priming signal and a subsequent LPS exposure as a second signal, which leads to a strong TNFα production, higher antimicrobial activity and to an activation of cellular immunity by upregulating MHC class II and CD86 expression. The innate activation is the second mode of activation only via TLR ligands like LPS or peptidoglycans, which again leads to secretion of pro-inflammatory cytokines and increased production of reactive oxygen species (ROS). The third kind of activation is the so called alternative activation via IL-4 and IL-13, which results in higher activity in tissue repair, increased cell growth and reduced inflammatory function. IL-10 and TGFβ are strongly deactivating for macrophages, which results in MHC class II downregulation and anti-inflammatory cytokine production [**89,103**].

1.1.3 Dendritic cells

The first description of dendritic cells (DCs) stems from Paul Langerhans [**104**] in the human skin, but he erroneously thought that this cells are nerve cells. Nearly a century later Steinman and Cohn discovered DCs in the mouse spleen and termed them “dendritic cells” [**105**]. Dendritic cells are professional antigen-presenting cells and have the exceptional ability to induce primary immune responses. DCs sample the environment and transfer this information to the cells of the adaptive immune system and are therefore crucial linkers of the innate and the adaptive arm of the immune system. Mature DCs are the most effective APCs for T cell priming [**106**] whereby without costimulatory signals an interaction between an immature DC and a T cell can induce tolerance [**107**]. So DCs determine not only whether an adaptive immune response is mounted, but also what type of immune response is induced.

1.1.3.1 Mouse and human dendritic cell subsets

Mouse DC subsets are much better defined than the human one. In mice there are three different subsets [**108,109**]; two are considered conventional DCs, which express high levels of CD11c and differentially express CD8α. The $CD8\alpha^{neg}$ are found in the marginal zones of the spleen, whereas the $CD8\alpha^{+}$ express also high levels of CD205 and are found in the T cell zones of the spleen. The $CD8\alpha^{+}$ are able to cross-present exogenous antigen to $CD8^{+}$ T cells [**110**]. The third category are the plasmacytoid DCs (pDCs), which are also called natural interferon-producing cells since they produce large amounts of type I interferons in response to viral infections [**111**]. It took nearly fifty years from the first description to clearly define that the cell subset described already 1958 by Lennert *et al.* [**112**] are the interferon-producing cells described by Trinchieri 1978 [**113**]. Lennert *et al.* reported cells in the T cell zone of lymphoid tissue displaying a plasma cell like morphology, but lacking B cell and plasma cell markers yet expressing some monocyte markers and therefore termed them plasmacytoid monocytes. The question whether the pDCs are of lymphoid or myeloid origin is still an ongoing matter of debate [**111**]. As discussed in **1.1.2.1** a common precursor population for DCs was described [**86**], which could give rise to all DC subsets. There are also several hints that pDCs are of lymphoid origin, but it seems that there is a certain plasticity in the development of pDCs [**114**] and DCs in general.

Human DCs are all bone marrow-derived leukocytes and are distinct from follicular DCs, which are no leukocytes [**115**]. It is possible to generate, under cytokine-driven conditions, *ex vivo*, four different type of human DCs: the Langerhans cells (LC), the dermal DCs (interstitial DCs, IDC), the plasmacytoid DCs (pDCs) and the monocyte-derived DCs (moDCs), which are the best-characterized type of human DCs [**116**]. Human DCs don't express CD8α but there are several markers, which differentiate human DCs: CD11c, CD123 and the four monoclonal antibodies BDCA-1 through BDCA-4 (blood dendritic cell antigen 1-4) generated by Dzionek *et al.*, which define clearly three distinct populations of DCs present in the blood, which account together of ~ 1% of the PBMC [**117**]. The so called myeloid DC subset 1 (MDC-1) cells are efficient APCs and secrete large amounts of IL-12 in response to bacteria and represents 0.6% of all PBMCs. In contrast the pDCs account for 0.37% of the PBMCs and secrete large amounts of type I IFN in response to viruses, which strongly activates NK cells, but only little IL-12 and they are only poor APCs. The smallest

population of blood DCs are the myeloid DC subset 2 (MDC-2) and constitute only 0.03% of the PBMC of a healthy donor. The role of this subset remains to be established. It is important to note that after maturation in culture the expression profile of BDCA-2, BDCA-3 and BDCA-4 on the three blood DC subsets is indistinguishable [**117**]. The differentiation markers expressed by the different human DCs subsets is displayed in detail in Table **1.2**.

Table 1.2 Markers of DC subsets in humans. The nomenclature MDC-1 and MDC-2 stands for myeloid DC subset 1 or 2 respectively. The expression levels of the different markers of the pDCs, and the MDC-1/2 subset was determined *ex vivo*. The expression levels of the *in vitro* IL-4/GM-CSF monocyte-derived DCs are shown of immature DCs only. Due to the lack of TLR-specific antibodies most data regarding TLR expression in literature was acquired using RT-PCR, which resulted in conflicting results (indicated in the table by +/-). Data complied from [**108,116-118**]. ND, not determined/found in the literature.

DC subset	human pDC	human MDC-1	human MDC-2	*in vitro* monocyte-derived DCs
CD1a				+
CD1c/BDCA-1		+		+
CD4	++	+	+	ND
CD11b		+/		+
CD11c		++	+	+
CD14		+/		
CD16				
CD56		**subset +/**	**subset +/**	ND
CD80				+
CD83				+
CD86	+	+++	++	++
CD123	++	+	+	++
CD208 (DC-LAMP)		ND	ND	
BDCA-2	+			
BDCA-3			+	
BDCA-4	+			+
TLR1	+	++	ND	+
TLR2	+/	++	ND	++
TLR3		++	ND	+
TLR4			ND	+/
TLR5	+/	+	ND	+
TLR6	+	++	ND	+
TLR7	+	+	ND	+/
TLR8		++	ND	+
TLR9	++		ND	
TLR10	+/	+	ND	+

Only after developing of these cytokine-driven methods for the generation of larger

quantities of human DCs large scale studies were made possible during the 1990s. Still, the question of the *in vivo* relevance of all this data generated with these *in vitro* generated DCs is not answered completely. With the availability of appropriate reagents, however, it is now it is possible to directly purify human blood DCs and evaluate the cells *ex vivo*.

1.1.3.2 Antigen capture and maturation of DCs

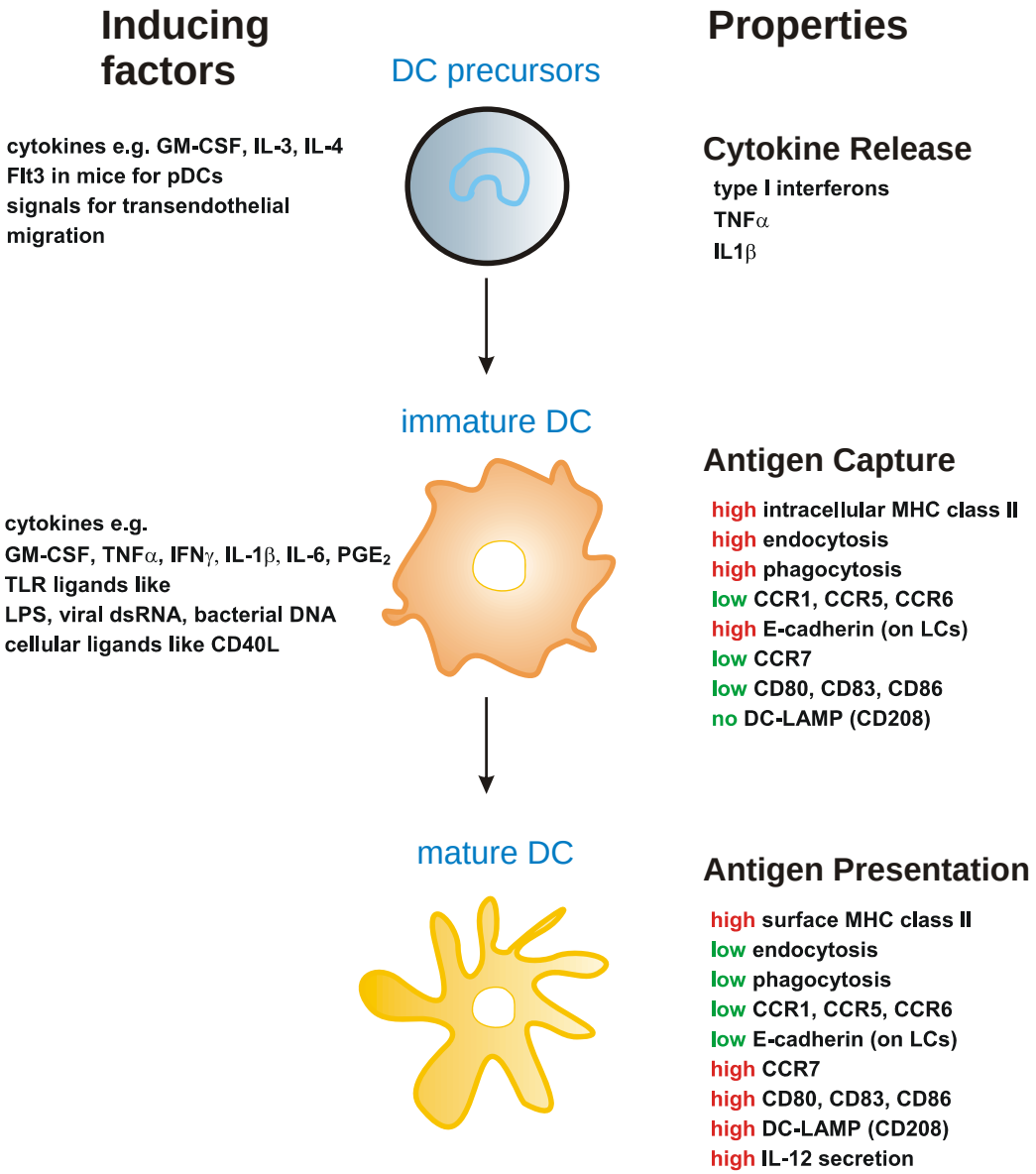

Figure 1.6 Maturation of dendritic cells. The environmental stimuli necessary for each maturation step is outlined in the left panel, while the characteristic properties of the DCs at each level is shown on the right side. Important appr: TLR, Toll-like receptor; ds, double stranded RNA; LC, Langerhans cell; PGE_2, Prostaglandin E_2; Flt3-L, fms-like tyrosine kinase 3 ligand. This scheme was drawn after [109].

DCs use phagocytosis, endocytosis, pinocytosis and specific receptors to sample their environment and to capture cell debris, immunocomplexes, pathogens or other antigens to process and present it to T cells as other professional antigen presenting cells (APC) also do. Ag can be presented classically via MHC class II or class I, additionally DCs are also able to cross-present exogenous Ag via MHC class I.

In order to be fully immunogenic all DCs have to undergo a process called maturation, which is a crucial step in the activation of the adaptive immune system. Maturation can be induced by a whole variety of stimuli provided by (a) components of pathogens like LPS or bacterial DNA (b) the local cytokine environment where inflammatory cytokines like TNFα or IFNγ drive maturation or finally (c) stimuli provided by membrane-bound ligands e.g. CD40L on T cells. The most potent inducers for maturation are the ligands for the TLRs expressed by the DCs [**109,116**]. The maturation process is outlined in **Figure 1.6.**

1.1.3.3 The final outcome of antigen-presentation by DCs: induction of immunity or tolerance

Dendritic cells constitutively phagocytose both microbial and host apoptotic cells [**119**]. This results in the induction of immunity against invading pathogens or tolerance to peripheral self antigens, respectively [**107**]. Toll-like receptor (TLR)-induced dendritic cell activation makes DCs immunogenic, whereas the steady-state presentation of self antigens induces tolerance [**107**]. One mechanisms of self/non-self discrimination is the TLR-inducible expression of co-stimulatory signals [**118**]. The question remains, if DCs are capable of distinguishing between the two sources of antigens for their selective presentation by MHC class II when both are encountered by dendritic cells during an infection. How is the immunogenic presentation of self antigens avoided by DCs? Very recently Blander *et al.* could describe a new mechanism of antigen selection on a subcellular level in DCs for presentation on MHC class II, which is based on the origin of the antigen [**120**]. They show that antigens are only presented when there are TLR ligands present within the cargo of the same phagosome. The degradation of the MHC class II-associated invariant chain (Ii) to CLIP seems to be TLR-dependent. Using this mechanism, DCs can distinguish between different sources of antigens if it is of self or non-self origin

at a subcellular level. The generation of peptide–MHC II complexes from pathogens takes only place in context of TLR-mediated co-stimulation, whereas presentation self-antigen is avoided in such a costimulatory context [**120**].

1.1.3.4 C-type lectin receptors on dendritic cells

Many lectins on DCs are considered non-TLR pattern recognition receptors since they have been associated with antigen uptake, but there is more and more evidence that lectins are important for DC migration and interaction with other leukocytes. The structural aspects of lectins are discussed in detail in **1.1.7.1**. C-type lectins bind sugar in a Ca^{2+}-dependent manner using their so-called carbohydrate recognition domain (CRD), whereas the C-type lectin-like receptors lack the Ca^{2+} ligating elements and are not able to bind sugar residues in a manner analogous to the C-type lectins. C-type lectins are type I or type II transmembrane proteins depending on the orientation of the N termini. Type I transmembrane proteins have their N termini pointing outwards of the cell or into the cytoplasm for the type II proteins respectively [**121**]. Unfortunately, the same nomenclature is used for another distinction regarding lectins. Type I means also that the C-type lectins have more than one carbohydrate recognition domain (CRD) in contrast to type II, which have only one CRD. There are also soluble C-type lectins like the mannose binding protein known (MBP), which is present in the plasma [**122**].

The **macrophage mannose receptor (MMR)** is the prototype of lectins on DCs involved in antigen uptake. Using its CRD 4 and 5 MMR binds to mannosylated proteins on pathogens. MMR is constitutively internalized into early endosomes where under the acidic conditions MMR is unloaded and recycles back to the cell surface [**123**]. **CD205** and **DC-SIGN** (dendritic cell-specific ICAM-3 grabbing non-integrin) are just internalized after ligand binding. It was shown that up to 20% of the membrane-bound MMR is shed by the DCs and serves as agglutinins and opsonins by binding to the surface of pathogens [**124**]. The role of C-type lectins in cell migration and trafficking is demonstrated by the reported binding of the intercellular adhesion molecule 2 (ICAM-2) to DC-SIGN. ICAM-2 is expressed by endothelial cells and promotes the adhesion of DCs during migration [**125**]. Finally are C-type lectins involved in DC-T-cell interaction. DC-SIGN mediates transient adhesion with T cells by high-affinity binding to ICAM-3 expressed by T cells. Blocking of this interaction

inhibited DC-induced T cell proliferation [**126**].

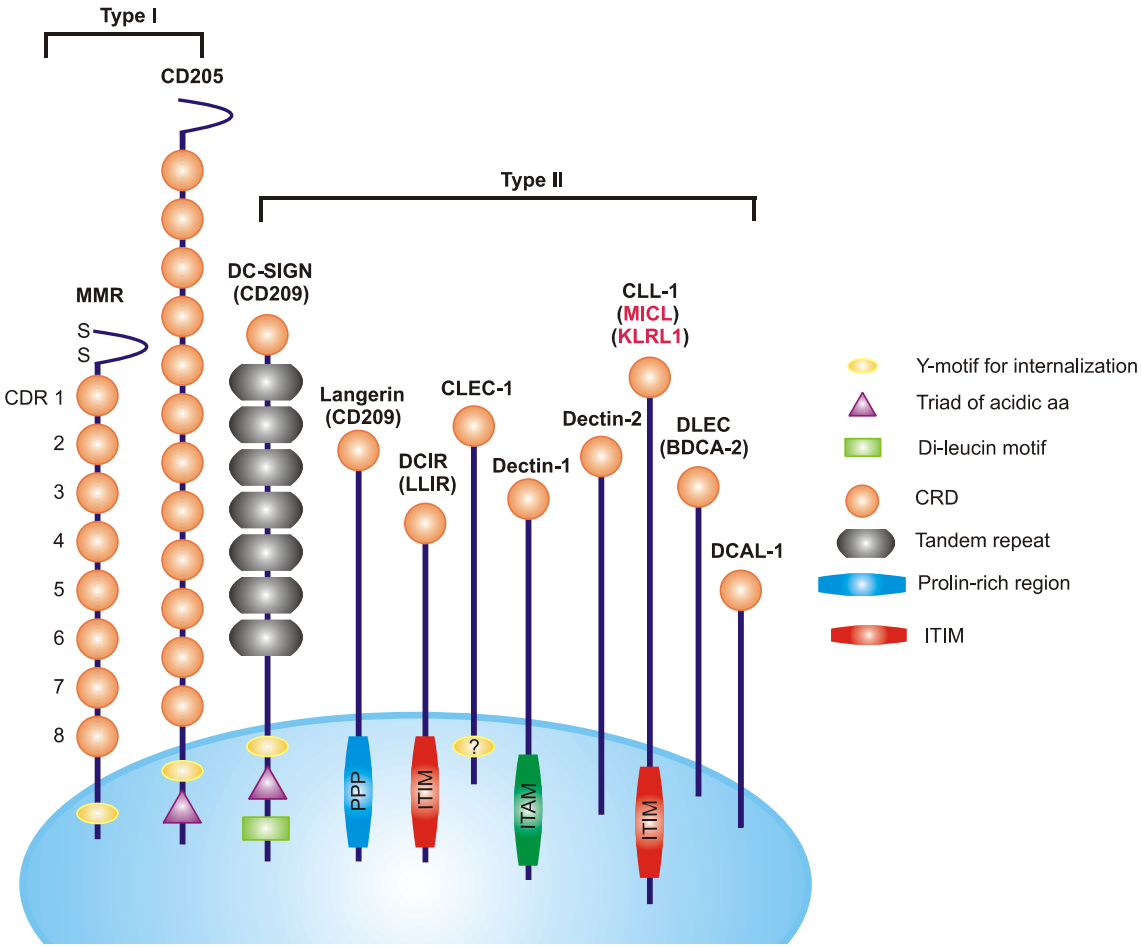

Figure 1.7 C-type lectins on human dendritic cells. Type I means in this figure that the C-type lectins have more than one carbohydrate recognition domain (CRD) in contrast to type II, which have only one CRD. The cytoplasmic tails are very diverse and contain several motifs all related with antigen uptake: a tyrosin-containing motif, which targets into coated pits or a di-leucin motif. CLEC-1, C-type lectin receptor; DCIR, dendritic cell immunoreceptor; LLIR, lectin-like immunoreceptor; DC-SIGN, dendritic cell-specific ICAM-3 grabbing non-integrin; DCLEC, dendritic cell lectin; MMR, macrophage mannose receptor; dectin-1 und -2, DC-associated C-type lectins 1 and 2; CLL-1, C-type lectin-like molecule 1; MICL, myeloid inhibitory C-type lectin -like receptor. MICL is a truncated form of CLL-1. This illustration was drawn after [126]. Additional data was compiled from: [127-130].

Dectin-1 (DC-associated C-type lectin 1) is a quite unusual C-type lectin like molecule. First its main ligand is a polysaccharide though its CRD lacks the known residues important for sugar binding. Dectin-1 binds β-glucans found in the cells walls of fungi, some bacteria and plants. It also binds to zymosan, which is a cell-wall extract of *S. cerevisiae* [**131**]. There is also evidence for proteinaceous ligand of Dectin on T cells. Blocking of this interaction inhibited Dectin-1-induced T cell proliferation [**132**]. Hence Dectin-1 could serve as a co-stimulatory molecule. This leads to the

second unusual property of Dectin-1. It contains in its cytoplasmic tail a single ITAM (YXXL) and is therefore the only known non-TLR pattern recognition receptor capable of mediating signals on its own. It is also the first description of signaling of C-type lectins occurs via the spleen tyrosin kinase (Syk) [**43**]. There is a second unusual ITAM repeat (YXXXL) present but it seems dispensable for signaling [**43**]. Dectin-1 was originally thought to be DC specific (hence its name) [**132**], but is now clear that it is also expressed by many cell types including macrophages, monocytes, a subset of T cells, eosinophils and B cells [**133**]. In mice, Dectin-1 expression can be increased by IL-4 and IL-13, cytokines associated with the alternative activation of macrophages (see **1.1.2.3** for details) and the expression is reduced by LPS [**133**]. After ligand binding Dectin-1 induces multiple responses ranging from cytokine and chemokine secretion (TNFα, CXCL2, IL-2, IL-10, IL-12), respiratory burst and ligand uptake through phagocytosis. However for some responses co-signaling via TLR is necessary e.g. TNFα secretion needs TLR2 triggering [**134**]. Such responses are also independent of Syk, however how such dectin-1 signaling integrates the TLR pathway is unknown [**43**]. Dectin-1 and TLR2 colocalize after zymosan-binding. So a signaling complex analog to the TLR2, MD2 and CD14 complex of the LPS signaling pathway seems possible [**133**].

C-type lectin-like molecule 1 (CLL-1) was described by three groups independently [**127,128,135**] (official gene symbol **C-type lectin domain family 12, member A**, CLEC12A). Consequently the C-type lectin-like molecule 1 (CLL-1), the myeloid inhibitory C-type lectin-like receptor (MICL) and the killer cell C-type lectin-like receptor L 1 are the same molecules (KLRL1). There have been three alternative splice forms described and the published MICL sequence is a truncated form of CLL-1. CLEC12A is exclusively expressed on cells of the myeloid lineage. It contains an ITIM motif in its cytoplasmic tail and is rapidly internalized upon ligation with specific monoclonal antibodies [**127,128,135**].

As reflected by **Table 1.3** lectins expressed on DCs are very diverse and different subsets of DCs or even different activations states of DCs show wide differences in surface expression. Beyond the role of C-type lectins on DCs in antigen capture C-type lectins are important in DC migration and even more dominant in the emerging DC cross-talk with other players of the immune system.

Table 1.3 Functions of C-type lectins on dendritic cells in humans. Some receptors are discussed in more detail in the main text. Abbr.: actDCs, activated DCs; LCs, Langerhans cells; mono, monocytes, MΦ, macrophage; PBMC, polymorphic mononuclear cells; EC, endothelial cells; neutro, neutrophils, eosino, eosinophils; for more see **Figure 1.7**. Birbeck granules are cytoplasmic organelles in LC associated mature DCs only. Type I means that the C-type lectins have more than one carbohydrate recognition domain (CRD) in contrast to type II, which have only one CRD. Data compiled from [**126**] and the references cited within the table. ?, not known yet. $, expressed on RNA level.

C-type lectin	Type	Location chrom.	Expression	Ligand	Function	Ref.
MMR (CD206)	I	10p13	DCs, LCs, mono, MΦ	Mannose, fucose, sialyl lewis X	antigen uptake	[**136**]
DEC-205 (CD205)	I	2q24	DCs, LCs, actDCs, thymic EC	?	antigen uptake	[**137**]
Dectin-1	II	12p13	DCs, LCs, mono, MΦ, B cells, T cell subset, neutro, eosino,	β-glucan zymosan	T cell proliferation, cytokine release, antigen uptake, respiratory burst	[**132,133**]
Dectin-2	II	12p13	DCs, LCs	mouse Dectin-2 binds mannose	antigen uptake, ligand(s) on regulatory T cells?	[**132**]
Langerin (CD207)	II	2p13	LCs	?	formation of Birbeck granules	[**138**]
DC-SIGN (CD209)	II	19p13	DCs	gp120 (HIV-1), mannan, ICAM-2, ICAM-3	antigen uptake	[**139**]
BDCA-2 (CD303) HECL DLEC	II	12p13	pDCs	?	antigen uptake? induces Ca^{2+} influx, putative activating adapter molecule? induces IL-12 & type I interferons	[**140,141**]
DCIR (LLIR)	II	12p13	DCs, mono, MΦ, PMN, B cells	?	?	[**142**]
CLEC-1	II	12p13	DCs$	?	?	[**143**]
CLEC-2	II	12p13	liver$	?	?	[**143**]
L-SIGN	II	??	??	?	?	[**144**]
CLEC12A (CLL-1)	II	12p13	mono, gran, HL-60, U937, THP-1, blood DCs,	?	? ITIM	[**127**]
MICL						[**128**]
KLRL1						[**135**]
DCAL-1	II	12p13	DC, B cells	?	truncated CRD, no sugar binding possible	[**130**]

1.1.4 Pattern recognition in the innate immune system

1.1.4.1 Pathogen-associated molecular patterns (PAMPs) and pattern-recognition receptors (PRRs)

The innate immune system employs a whole range of so called pattern- recognition-receptors (PRRs), which recognize highly conserved molecular patterns found only in pathogens but not in mammalian cells and thereby activate the innate immune system. Important examples are the Toll-like receptor family (TLRs) or as already discussed in **1.1.3.4** the non-TLR dectin-1. The molecular structures recognizes by PRR are commonly called pathogen-associated molecular patterns (PAMPs). PAMPs are essential for the pathogens and are therefore in general immutable. The induction of an inflammatory immune response after a pathogen encounter is mainly mediated by the TLR family, but the non-TLRs can contribute to a TLR-mediated activation. Dectin-1 is so far the only example of a non-TLR PRR capable of inducing an inflammatory response [**133**].

Table 1.4 Non-TLR pattern-recognition-receptors (PRR). Abbr.: LBP, lipid binding protein; CR, complement receptor; LOX-1, lectin-like oxidized LDL receptor; MARCO, macrophage receptor with collagenous structure; LPS, lipopolysaccharide; MMR, macrophage mannose receptor; SP-A and SP-D, surfactant protein A and D; NOD1 and NOD2, nucleotide-binding oligomerization domain; NLR, NACHT-leucin-rich repeat. Data compiled from [**133**].

Class	Member	Recognized microorganism or PAMP.
soluble in serum or tissue fluid		
Complement	C3, C1q	microbial surfaces, *L. monocytogenes*, *E.coli*
Lipid transferases	LBP	LPS
Collectins	SP-A, SP-D	influenza virus, *A. fumigatus*, *C. albicans*
membrane-bound PRR		
Leucin-rich repeats proteins	CD14	LPS, LTA, *E.coli*, peptidoglycan
Scavenger proteins	LOX-1, MARCO	*E.coli, L. monocytogenes*, *S. aureus, Heliobacter pylori,* LPS, LTA, bacterial DNA
classical C-type lectins	MMR, DC-SIGN	*C. albicans, E. coli, M. tuberculosis,* zymosan, HIV, Ebola virus
non-classical C-type lectins	Dectin-1	*C. albicans, S. cerevisiae, A. fumigatus* zymosan
Integrins	CR3, CR4	complement-coated microorganisms, LPS
cytoplasmic		
NLR	NOD1, NOD2	muramyl dipeptide, *shigella flexneri*

PRRs can be soluble in the serum or tissue fluid, membrane bound or cytoplasmic. Leukocytes can detect pathogens directly using PRRs or via so-called opsonic recognition, whereby opsonic receptors like the complement receptor 3 (CR3) bind to PRR-coated pathogens. Some PRR are acting intracellularly like the NACHT-leucin-rich repeat (NLR) family [**145**]. In **Table 1.4** some typical non-TLR PRR for each class of PRR are listed.

1.1.4.2 Toll-like receptors

Toll genes were described originally in *Drosophila melanogaster* by Nüsslein-Volhard and colleagues [**146**] where these proteins are involved in the establishment of dorso-ventral polarity of the developing embryo [**147**] and anti-fungal immune response of the adult fly [**148**]. “Toll” is a German word and means "amazing" or "crazy". The similarities of the signaling pathways of *Drosophila* Toll and the mammalian IL-1 receptor and the highly conserved cytoplasmic domains of both receptors led to the identification of a family of mammalian homologues of the Toll protein, the so called Toll-like receptors (TLRs) by Ruslan Medzhitov and Charles Janeway in 1997 [**149**]. This discovery turned out to be a fundamental breakthrough in the way we think about the innate immune system, since the TLRs are the key mediators of an inflammatory immune response after a pathogen encounter. So far the TLR family consists of 11 members in mammals [**150-155**] and specificity for different ligands either resides within one receptor itself or is mediated through heterodimerization. Nine out of eleven TLRs are conserved between human and mouse. The orphan TLR10 is non-functional in the mouse while TLR11 is not expressed in humans [**155,156**].

Only the biology of TLR4 will be discussed here in more detail. TLR4 is the receptor for lipopolysaccharide (LPS), which is the main component of the outer cell membrane of gram-negative bacteria. There are in addition to TLR4 several other molecules involved in the LPS-mediated cellular activation. In serum LPS forms micelles, which form a complex with the LPS-binding protein (LBP). This LPS-LBP complex binds to the GPI-anchored CD14 on the cell surface of cells of the myeloid lineage i.e. monocytes, macrophages and granulocytes. [**157,158**]. In contrast to *in vitro*-generated DCs freshly isolated DCs do not express TLR4 [**118**]. The CD14/LPS/LBP complex associates then with TLR4 [**159,160**] leading to the downstream activation of the receptor pathway. With MD-2 there is yet another

molecule involved in LPS-recognition. MD-2 is associated with the extracellular domain of TLR4 and binds directly to LPS and amplifies LPS responsiveness of cells [**161,162**].

Several other PAMPs from viruses like the F protein of RSV [**163**] or endogenous ligands like heat shock proteins [**164**] activate TLR4 in addition to LPS. It is thought that receptor agonists from endogenous origin, which are released from dead or injured cells, indicate an inflammatory process and therefore function as danger signals [**165**]. However, under certain conditions the TLR-mediated recognition of endogenous components may break tolerance and lead to autoimmunity [**118**].

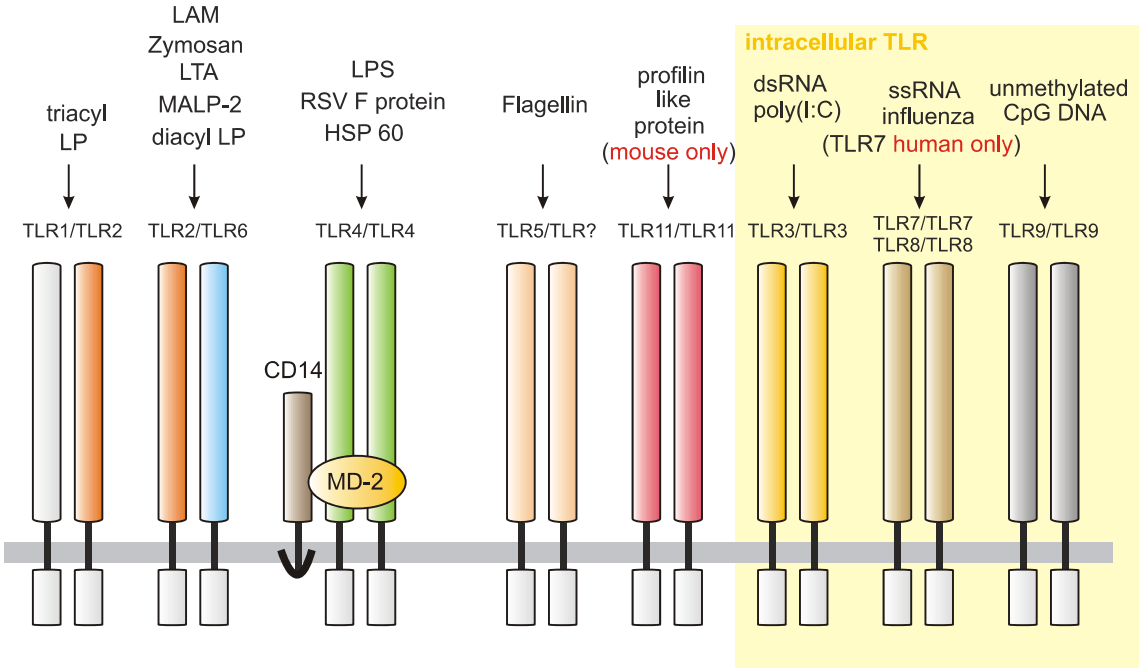

Figure 1.8 Ligand specificities of Toll-like receptors (TLR). TLRs recognize a wide range of pathogen-derived products, which are indicated by the black arrows for each individual TLR. The TLR4 homodimer associates with the GPI-anchored CD14/LPS complex together with MD-2. TLR2 associated either with TLR1 or TLR6 to form a functional heterodimer. Abbr.: LP, lipoprotein; LPS, lipopolysaccharide; MALP-2, macrophage-activating lipopeptide; LAM, lipoarabinomannan; RSV, respiratory syncytial virus; HSP, heat shock protein; dsRNA, double stranded RNS; poly(I:C), polyinosinic: polycytidylic acid; CpG, cytosin-phosphatidyl-guanosin. The orphan TLR10 in humans is not shown. TLR10 is able to homodimerize, but also to heterodimerize with TLRs 1 and 2 [**166**]. Data was compiled from [**118,167,168**].

Upon binding of the respective specific ligand, TLR signaling is initiated by homodimerization (e.g. TLR4) or heterodimerization (e.g. TLR2 and TLR1). All TLRs except TLR3 signal via the adaptor protein MyD88 initiating several signaling pathways [**118,169**]. This triggers the expression of various genes that are involved in immune responses, such as inflammatory cytokines and costimulatory molecules on cells of the innate immune system. This activation is essential for the generation of

adaptive immune responses. DCs are central in priming of antigen-specific naïve T lymphocytes. For example TLR4-mediated LPS-recognition initiates DC maturation and migration to the draining lymph node [**167**]. Inside the draining lymph node the DCs provide naïve T cells with two signals necessary for T cell priming: the first via the T cell receptor and the second one via CD80/CD86 binding to CD28. The TLR mediated activation translates the signal received by the pathogen recognition into the clonal expansion of antigen specific T cells yielding to a T_H1 response. There are some reports, however, that TLR2 ligands like Pam_3Cys are able to induce a T_H2 response, which may play a role in the initiation of T_H2-mediated immune disorders, such as asthma [**170**]. The different subsets of DCs show differential TLR expression (see **Table 1.2** for details). Freshly isolated human pDCs express TLR7 and TLR9, whereas mDCs express TLR1, TLR2, TLR3, TLR5, TLR6, TLR7 and TLR8. Importantly both subsets do not express TLR4 [**118**]. It is also possible that the very same TLR ligands induce different answers in different DC subsets e.g. stimulation of human pDC with TLR7 induces Type I IFN but IL-12 secretion by mDCs [**171**].

1.1.5 Cytokines as regulators of innate and adaptive immunity

An important component of innate immune reactions is the production of various cytokines by various cells in the body upon an activating stimulus. Type I interferons play a central role in innate immunity not only because of their antiviral activity, but also due to their role in the regulation of cells of the innate and adaptive immunity.

Type I interferon secretion (IFNα by leukocytes and pDCs and IFNβ by fibroblasts), is induced by viral infection and is one of the first events in the innate immune response after antigen recognition [**172**]. Type I interferons induce resistance to viral replication in all cells, increase of MHC class I and II expression and the necessary antigen processing and presentation pathways, thus enabling effective T cell responses. Importantly IFNγ is not induced directly by viral infection however IFNα and IFNβ are strong activators of NK cells and NK-mediated IFNγ-release [**173**]. NK cells and certain T cell subsets like the $CD8^+$ T cells, NKT or γδ T cells are the major source for IFNγ [**174**]. IFNγ in synergy with TNFα provide a differentiation and maturation signal for DCs [**175**]. In addition, IFNγ is crucial for the induction of Interleukin-12 (IL-12) secretion by phagocytic cells and DCs.

IL-12 is a heterodimeric pro-inflammatory cytokine and plays a central role at the interface of innate and adaptive immunity. It has important effects on T cells and NK

cells and is produced mainly by activated inflammatory cells like monocytes, macrophages, neutrophils, DCs and to a minor extent by B cells. IL-12 was originally named natural killer cell stimulatory factor (NKSF) based on its NK-activating capacity and is also secreted by the EBV-transformed human B lymphoblastoid cell line RPMI 8866, which is frequently used for the *in vitro* proliferation of NK cells [**176**]. It is the major cytokine for T_H1-cell differentiation allowing potent IFNγ production especially by NK cells [**177**]. Dependent on the presence of NK, NKT, and T cells, which IL-12 can drive towards their most active effector functions against tumors, this cytokine has a potent anti-tumor activity [**178**].

Activated monocytes/macrophages secrete in a TLR-mediated manner various cytokines and chemokines in response to pathogens such as IL-1β, TNFα, IL-6, IL-12 and IL-8 (CXCL8). A central role plays here TNFα, which leads to local inflammation and the activation of the endothelial cell wall, which includes increased permeability for cells, immunoglobulins and complement. TNFα is also released by activated NK cells. The chemokine IL-8 attracts neutrophils, basophils and T cells to the site of infection.

IL-18 is produced by the same cell populations as IL-12 and induces synergistically with IL-12 IFNγ secretion by NK and T cells leading to a T_H1 polarization. Interestingly IL-18 alone in the absence of IL-12 can also stimulate T_H2 responses [**179**].

Granulocyte-macrophage colony stimulating factor (GM-CSF) is mainly produced by T cells and NK cells and has essential effects on DC maturation necessary for the induction of potent adaptive immune responses [**180**].

The last cytokines to be discussed are IL-2 and IL-15 the latter originally called T-cell growth factor. The properties of IL-2 and IL-15 are detailed in **Table 1.5**. The receptors for IL-2 and IL-15 are members of the common cytokine-receptor γ-chain (γ_c) (also known as CD132) family of cytokine receptors which includes the receptors for IL-4, IL-7, IL-9, and IL-21 since all contain γ_c. Additionally the IL-2 receptor (IL-2R) and the IL-15R have a second shared subunit, the β-chain IL-2/15Rβ, and the high affinity forms of both also contain a unique subunit, IL-2Rα (also known as CD25) or IL-15Rα, respectively [**181**]. Due to the shared receptor subunits many functions of IL-2 and IL-15 are overlapping like the proliferation and differentiation of NK cells, T and B cells. In adaptive immunity, however, there are significant differences (see **Table 1.5** for details). IL-15 is secreted only in small quantities and is

mainly membrane-bound. IL-15 is especially important in NK biology since in the absence of IL-15Rα-mediated trans-presentation NK cells are not generated from bone marrow precursor cells and NK cells are also depend on IL-15 for their survival *in vivo*. Trans-presentation means that IL-15 is membrane-bound by IL-15Rα, which is mainly expressed on the surface of APCs like monocytes or dendritic cells. Such membrane-bound IL-15 binds in the immunological synapse to IL-2/15Rβ γ_c on NK cells or $CD8^+$ T cells.

Table 1.5 Key features of IL-2 and IL-15. Abbr.: AICD, activation-induced cell death; γ_c, common cytokine-receptor-chain; IL, interleukin; IL-2R, IL-2 receptor-chain; IL-2/15R, the γ_c -chain of the IL-2 receptor and IL-15 receptor; IL-15R, IL-15 receptor-chain; T_{Reg} cell, $CD4^+CD25^+$ regulatory T cell. Table adapted from [**181**].

Properties	IL-2	IL-15
Producer cells	activated T cells	dendritic cells and monocytes
Receptor	IL-2R, IL-2/15R and γ_c are co-expressed by activated T and B cells	IL-15R on the surface of monocytes and dendritic cells presents in trans IL-15 to NK cells and $CD8^+$ memory T cells expressing IL-2/15R and γ_c
Function	proliferation and differentiation of NK cells, and T and B cells; elimination of self-reactive T cells, mediated by AICD, maintenance of T_{Reg} cells	Proliferation and differentiation of NK cells, and T and B cells; maintenance of $CD8^+CD44^{hi}$ memory T cells
Effect of cytokine or cytokine-receptor knockout	enlargement of peripheral lymphoid organs and polyclonal expansion of T- and B-cell populations; associated with autoimmune diseases	strongly reduced number of NK and NKT cells and $CD8^+CD44^{hi}$ memory T cells

1.1.6 NK cell/DC crosstalk

Having introduced most of the key components of the innate immune system, the original statement at the beginning of this introduction that the two arms of the immune system are closely connected and that many aspects of the adaptive immune response are in fact controlled by the innate immune system can be revisited again [**2-4,108**]. Two key players of the immune system, the DCs and the NK cells took center stage in recent years in a process commonly called NK/DC crosstalk. In the past five years there have been many reports supporting the notion that NK cells and DCs not only influence innate and adaptive immunity but are also able to regulate both of them. However, NK cells are not the only innate lymphocytes committed in the cross-

talk with DCs. The unconventional T cells subsets, γδ T cells and iNKT cells, are also crucially involved in the initiation of adaptive immunity. The next paragraph **1.1.6.1** will summarize how innate lymphocytes mature DCs before the further sections discuss the NK/DC crosstalk in greater detail (**1.1.6.2 -1.1.6.4**).

1.1.6.1 DC interaction with innate lymphocytes

The induction of DC maturation is a critical step in the activation of adaptive immunity. Maturation can be initiated either by TLR ligands [**118**] or by interaction with innate lymphocytes like γδ T cells, NKT cells or most importantly with NK cells [**182**].
DC maturation has been shown after NK cell recognition of MHC class I low tumor cells [**183**], iNKT cell activation by α-GalCer presented by CD1d on DCs [**184**], and activation of phosphoantigen-specific and also CD1c-restricted γδ T cell subsets [**78,185**]. All above named innate lymphocyte subsets induced DC maturation, which is indicated by increased CD86 expression, IL-12 production, and T cell priming [**183-186**]. TNFα is hereby an important mediator of DC maturation [**182**]. Additionally, CD40 on iNKT cells plays a crucial role in DC maturation, since in $CD40^{-/-}$ mice DCs failed to initiate adaptive immunity after stimulation with α-GalCer activated iNKT cells [**187**]. Thus, NK, iNKT, and γδ T cells are able to induce DC maturation by a cytokine- and cell contact–dependent signals [**182**].

In the innate lymphocyte-mediated DC maturation the nature of the ligands involved is quite different to the TLR ligands. γδ T cells and NK cells can be activated by stress-induced self-antigens like the MHC class I related molecules (e.g. MICA/MICB in humans or T10/T22 in the mouse). In addition, γδ T cells recognize CD1c on the surface of immature DCs in the absence of a specific foreign antigen (which implies reactivity against yet to be identified self-lipids). iNKT are activated via CD1d-presented glycopeptides expressed also on DCs (details of this NKT/DC cross-talk are already discussed in section **1.1.1.7**).

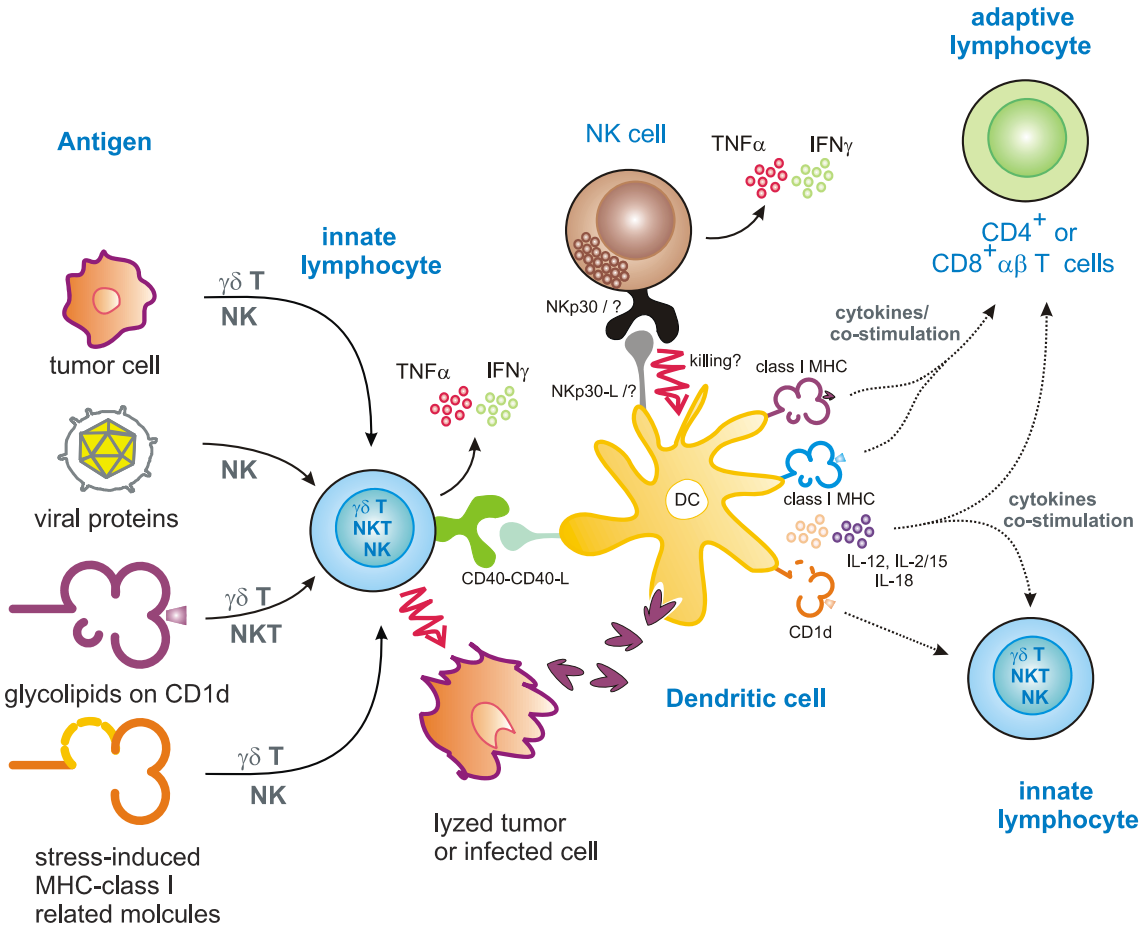

Figure 1.9 Innate lymphocytes mature DCs. Innate lymphocytes like γδ T, iNKT, and NK cells recognize pathogen-derived and self-antigens on infected cells, tumors, and stressed self-tissues. Their activation leads to DC maturation, most likely under conditions where the DCs are also presenting ligands recognized by innate lymphocytes. The DCs further stimulate the innate response and also trigger adaptive immunity including antigen presentation of antigens derived from cells lyzed by innate lymphocytes. Cytokines and cell contact–dependent molecules mediate DC activation by different types of innate lymphocytes, whereas DCs produce cytokines that expand and differentiate additional innate and adaptive lymphocytes. Additionally, there are more yet unknown ligands systems involved in the cell-cell contact-dependent NK/DC cross-talk. This illustration was drawn after [**182**].

In detail, CD1c-restricted γδ T cells can mediate the maturation of DCs. The maturation is cell-cell contact-dependent as well as TNFα-mediated (which is secreted by the γδ T cells in response to CD1c recognition [**185**]). For the secretion of IL-12 by maturing DCs, both CD1-restricted γδ T cells and LPS are required. Importantly, DCs matured by CD1c-restricted γδ T cells were able to efficiently present peptide antigens to naïve $CD4^+$ T cells [**185**].

Additionally, the lysis of infected or tumor cells by innate lymphocytes provides DC with antigenic material, which is presented either via MHC class I or class II. **Figure 1.9** outlines how innate lymphocytes mature DCs in response to different antigenic

stimuli and how matured DCs mediate via cytokines and co-stimulation the expansion and differentiation of innate and adaptive lymphocytes.

1.1.6.2 DC/NK interactions in peripheral and in secondary lymphoid tissues

Generally, triggering of an immune response takes place in peripheral tissues. DCs detect via their PRRs PAMPs on the surface of microorganisms (see **1.1.4**) and attract other cells of the immune system via chemokines like RANTES/CCL5, fractalkine/CX_3CL1 or IL-8/CXCL8. $CD56^{dim}$ NK cells express the receptors for IL-8 and fractalkine, whereas the $CD56^{bright}$ subset migrates in response to RANTES and others. It was shown *in vivo*, that DCs and NK cells encounter each other in Gleevec-induced lichenoid dermatitis, were NK cells and DCs are recruited into inflamed tissues [**188**]. Gleevec (imatinib mesylate; an inhibitor for the kinase activity of the three related kinases: BCR/ABL, PDGFR, and KIT) was shown to be effective against gastrointestinal stromal tumors. Gleevec can act on host DCs to promote NK cell activation and IFNγ secretion resulting in an increased anti-tumor activity [**188,189**]. During maturation mDCs and pDCs undergo a complex remodelling. They also acquire CCR7, which allows them to enter the lymph node, where they encounter T cells as well as NK cells (e.g $CD205^+$ mDCs and NK cells have been shown to co-localize in the T cell zone of human lymph nodes [**190**]). The main NK subsets present in the lymph nodes resemble the subsets in the blood, however in an inverse composition. 90% of the lymph nodes NK cells belong to the $CD56^{bright}CD16^{neg}KIR^{neg}$ subset [**190,191**]. Martin-Fontecha *et al.* could show when mature DCs are injected in the mouse, they migrate CCR7-dependently to the draining lymph node [**192**] and that NK cells are actively recruited to the lymph nodes in a CXCR3-dependent manner. NK cells then secrete IFNγ, which provides an early source of IFNγ in polarization towards T_H1 responses [**193**].

1.1.6.3 Reciprocal activating cross-talk between NK cells and DCs

Besides chemokines the most important DC-derived cytokines involved in NK activation are IL-12, IL-15, and IL-18 as well as type I interferons [**108,194**]. IL-12 is the key player in the induction of the secretion of IFNγ by NK cells, which was shown in several systems: LPS-activated human monocyte-derived DCs, human splenic DCs [**190**], or poly(I:C)-stimulated human blood myeloid DCs [**195**]. IL-18 acts in synergy

with IL-12 to induce the secretion of IFNγ but also to enhance cytotoxicity (shown with human cord-blood $CD34^+$-derived DCs [**196**]). Type I IFN – mainly derived from pDCs, particularly when activated through TLR7 and TLR9 [**111**] – together with IL-15 have been shown to induce cytotoxicity of NK cells (demonstrated with human monocyte-derived DCs [**186**]). In response to bacteria, DC-derived IL-2 can induce IFNγ-secretion by NK cells in mice [**197**]. The role of DC-derived IL-15 is manifold; IL-2 secretion by DCs in humans and mice is IL-15 dependent [**190,198**]. IL-15 bound on human splenic DCs stimulates NK cell proliferation and is essential for their survival [**190**]. IL-15 leads (like IFNα) to the expression of the NKG2D ligands MICA/B by human monocyte-derived DCs as well as to an upregulation of NKG2D on NK cells itself [**199,200**].

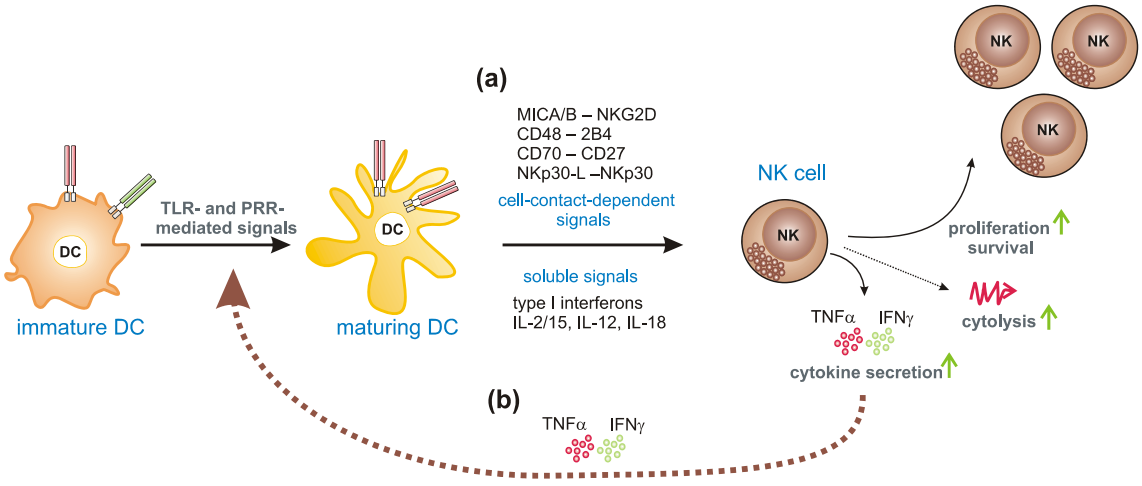

Figure 1.10 TLR-induced reciprocal interplay between NK cells and DCs. **(a)** The DC-mediated NK cell activation and proliferation is dependent on cell-cell contacts as well as soluble signals. NK activation by DCs leads to increased NK cytotoxicity, NK proliferation and survival. **(b)** NK-derived TNFα and IFNγ induces DC maturation in a reciprocal fashion. All data depicted have been derived from human *in vitro* monocytes-derived DCs (moDCs) [**186,194,199,201,202**]. This illustration was drawn after [**108**].

Soluble factors are not the only mediators of the NK/DC cross-talk. There have been many reports on the role of cell-cell contacts; however, the relevant molecules involved are poorly defined. The NKG2D and the CD48-2B4 ligand systems [**203**], the orphan activating NK receptor NKp30 as well as TRAIL and CD94/NKG2A-meditated signals have been implicated in NK/DC cross-talk. Jinushi *et al.* showed, using trans-well experiments and MICA/B blocking antibodies, that IFNα-mediated MICA/B induction on DCs may be a mechanism by which IFNα indirectly activates

NK cells via DC-expressed NKG2D ligands [**199**].

The peculiar finding that immature human monocyte-derived DCs are killed by NK cells in an NKp30-dependent manner was published 2002 by different groups [**186,201,202**] and is depicted in **Figure 1.11.** It was proposed that this killing occurs after a rapid influx of both DCs and NK cells and NK cells abolish DC-mediated immune responses by killing immature DCs [**189,204**]. Piccioli *et al.* showed that the outcome between DC activation or killing depends on the DC/NK cell ratio [**201**]. At high NK:DC ratios (5 to 1) NK cell killing of immature DC was observed, whereas at low activated NK/immature DC ratios (1/5 and up to 1/40) both DC maturation by NK-derived IFNγ and DC cytokine production (TNFα, IL-12) was observed, which could be blocked selectively by an α-NKp30 mAb (and not by α-NKp44, NKp46, NKG2D, 2B4, NKp80 mAbs) [**202**]. In contrast, mature DCs are resistant to NK cell lysis, presumably due to the expression of inhibitory CD94/NKG2A ligands [**201,202**].

On the contrary, Gerosa *et al.* recently published similar experiments with freshly isolated myeloid and plasmacytoid blood DCs instead of monocyte-derived DCs and no killing of immature blood mDCs or pDCs could be observed [**195**]. The reason for this different susceptibility to NK cell-mediated lysis is not clear, but it emphasizes the problem regarding the physiological relevance of *in vitro* monocyte-derived DCs. Until the identification of reliable markers and isolation procedures for blood DCs (see **1.1.3.1** for details, [**117**]) the only feasible source for DCs have been the *in vitro*-generated DCs, so most of above discussed findings result from *in vitro* monocyte-derived DCs.

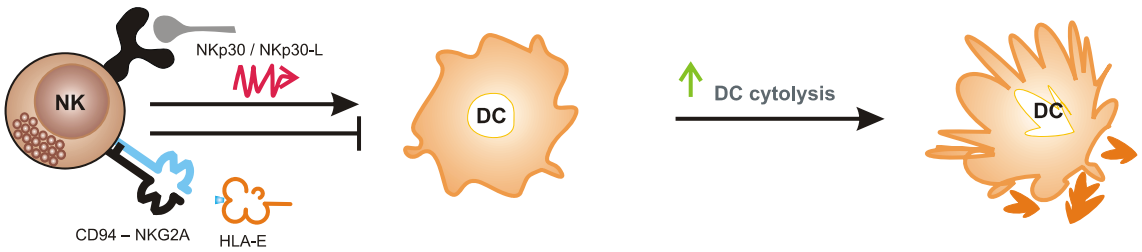

Figure 1.11 NKp30-mediated lysis of immature moDCs by DCs. NKp30-mediated killing of immature *in vitro* generated monocyte-derived DCs (moDCs) was shown; however, immature blood mDCs as well as pDC are not lyzed by activated NK cells [**195**]. This illustration was drawn and modified after [**108**].

Vitale *et al.* reported that upon NK/DC interaction NK cells produced TNFα and IFNγ and, in turn, promoted DC maturation Both effects were like the DC-killing NKp30-mediated [**205**]. Again these results were obtained by using monocyte-derived DCs, however, this was corroborated by experiments using poly(I:C) stimulated blood myeloid DC, which induce NK cells also to produce IFNγ. This effect was dependent on both, IL-12 secretion and cell contact between NK cells and myeloid DC, but independent of type I IFN [**195**]. Reciprocally, NK cells also induce the maturation of myeloid and plasmacytoid dendritic cells, as well as their production of type I interferons and TNFα [**195**].

1.1.6.4 Cross-talk during viral infection

In the very early phase of a viral infection, one of the most important cells are the pDCs, since in humans they express TLR7 and TLR9 (which recognize ssRNA and CpG DNA respectively; mouse pDCs express TLR8, which also recognizes ssRNA [**206,207**]. Both TLRs induce MyD88-dependent inflammation and type I IFN production. As discussed already in **1.1.5** type I IFN are potent activators of NK cell cytotoxicity [**195,208**].
After recognition of an activating ligand, NK cells kill the infected cells either via ADCC, granule exocytosis or death-receptor engagement, which all induces apoptosis. These infected apoptotic cells can be phagocytosed by mDCs and the viral components interact with TLR3 leading to mDC maturation. It was shown recently that this activation path way is particularly important for viral antigen cross-presentation to $CD8^+$ T cells [**209**]. This is an essential mechanism against viruses, which do not directly infect professional antigen-presenting cells [**209**].

1.1.7 Genes encoded in the natural killer gene complex (NKC)

1.1.7.1 Structural aspects of C-type lectin-like molecules

The term ‘C-type lectin’ was brought in to distinguish a group of Ca^{2+}-dependent (C-type) carbohydrate-binding lectins from the Ca^{2+}-independent lectins [**210**]. The carbohydrate-binding activity is mediated by the carbohydrate recognition domain (CRD), which is present in all Ca^{2+}-dependent lectins but not in other types of lectins. This domain has been called ‘C-type CRD’ or ‘C-type lectin domain’. Since not all

proteins containing C-type CRDs can actually bind carbohydrates or even Ca^{2+}, a more general term “C-type lectin-like domains” (CTLD) is used to refer to such domains [**210**]. All proteins containing one or more such CTLD belong to the C-type lectin superfamily (CLSF), which can be subdivided into 14 groups designated I-XIV [**211**] and up to now there are more than a thousand known members most of them lacking the lectin capacity to bind to sugar.

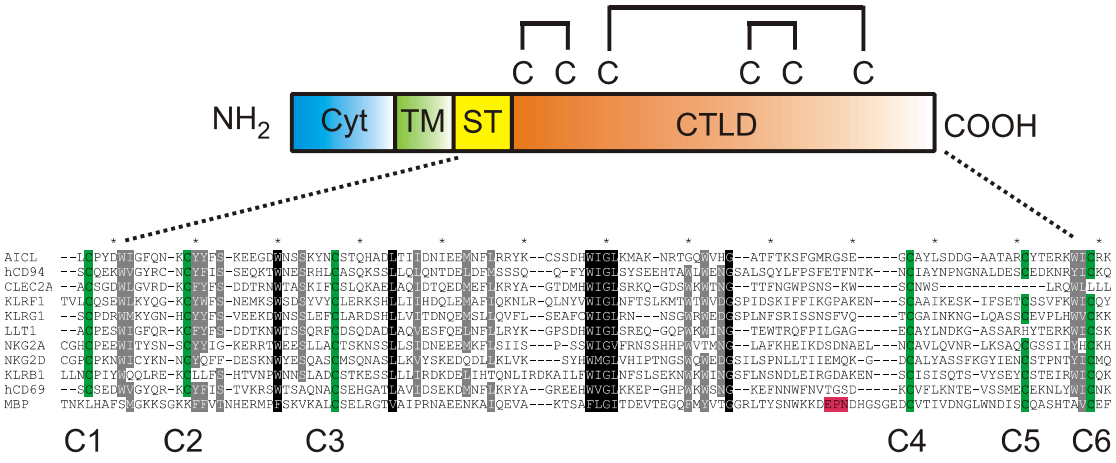

Figure 1.12 Structure of C-type lectin-like molecules encoded by the NKC. There are six conserved cysteines colored in green in the C-type lectin-like domain (CTLD), which form intra-chain disulfide bonds. The highly conserved “WIGL” motif in black is a landmark of CTLD containing proteins. In the last line the sequence of rat mannose-binding protein (MBP) is aligned to the NKC-encoded proteins for comparison. The mannose binding residues represented by the “EPN” motif drawn in red is only present in the MBP indicating that none of the above aligned proteins are able to bind oligosaccharides. Between the CTLD domain and the transmembrane (TM) domain there is usually a stalk region (ST) of varying length. All NKC encoded proteins are type II transmembrane proteins with an amino-terminal end representing the cytoplasmic tail (Cyt).

Each group can be distinguished by additional domains present. All group II and V members contain only one CTLD and originally it was thought that all group V members are NK receptors and were therefore assigned to the group V separately from group II, however, with the discovery of more gene products, which are not NK-specific, the distinction of group II and V is not clear anymore. Within the NKC all proteins are either group II or V proteins [**212**] with only one CTLD and do not bind to carbohydrates, but are engaged in protein-protein interactions.

A remarkable exception known so far is Dectin-1 as discussed in **1.1.3.4**, which binds β-glucan in a Ca^{2+}-independent manner. The lectin-like molecules can be classified into families. All C-type lectin-like molecules have related general structural features (**Figure 1.12**) but are only distantly related in sequence (25% amino-acid identity).

Figure 1.12 shows an alignment of 10 members of the human NKC together with the sugar-binding C-type lectin mannose-binding protein (MBP). Not all members of the NKC are dimers or heterodimers as some function as monomers like LOX-1 or Dectin-1.

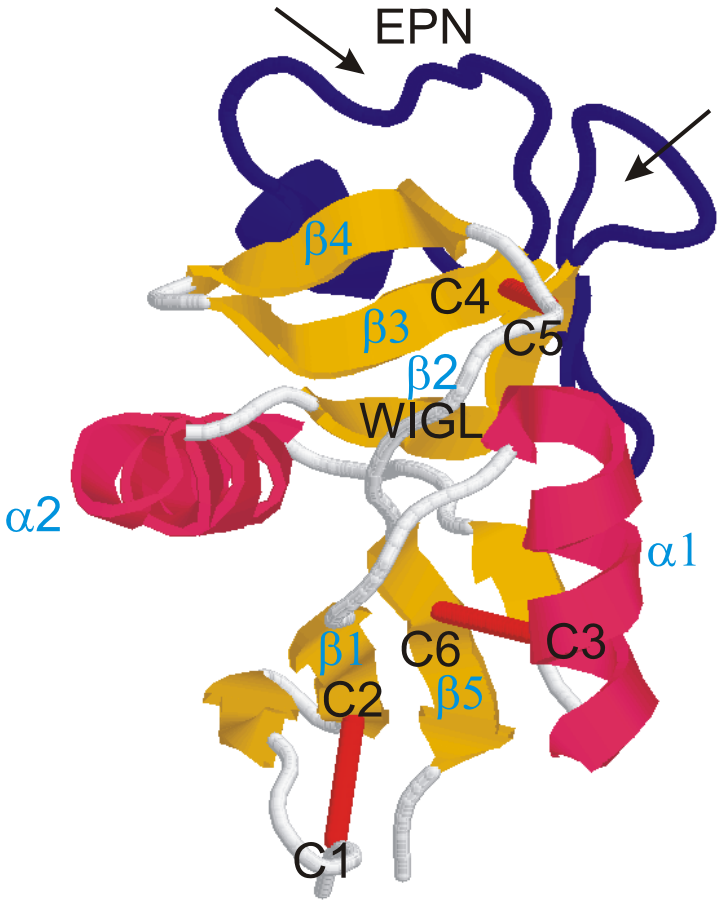

Figure 1.13 CTLD structure. A cartoon of the C-type lectin-like domain of DC-SIGN (pdb code 1k9i [**213**]) was created using ProteinExplorer [**27**] (www.proteinexplorer.org). Only the amino acids ranging from Pro 244 to Ala 382 are shown. The three disulfide bonds created by the highly conserved cysteines (C1-C6) are depicted in red. The characteristic "WIGL" motif is located within the β2 strand, whereas the "EPN" motif is located in the long loop region, which is drawn in blue. DC-SIGN is able to bind to high-mannose oligosaccharides. Ca^{2+} binding sites are indicated by black arrows.

Figure 1.13 provides a cartoon from the crystal structure of the C-type lectin-like domain (CTLD) of DC-SIGN, which binds Ca^{2+}-dependent to high-mannose oligosaccharides [**213**]. Mannose-dependent interactions are also responsible for the ability of DC-SIGN to bind HIV [**214**]. The highly conserved cysteines are labeled C1-C6 comparable to **Figure 1.12**.

1.1.7.2 Overall organization and evolution of the NKC

The NKC is located in a single chromosomal region in man (12p13) and in the mouse (6), whereas in cattle it is spread onto two chromosomes. The human NKC encompasses ~25 genes (without pseudogenes) and 2.8 Megabases (Mb) in length, the mouse NKC ~57 genes (depending on the strain) and 8.7 Mb [**212**]. In the two-page **Figure 1.14** all known lectin-like molecules encoding the NKC of mouse and man are depicted. The killer cell lectin-like receptors (KLR) and the C-type lectins (CLEC) are clustered together except KLRF1 in humans and KLRB1 and KLRG1 in mouse and human, which are intermingled among the CLEC2 genes.

Hao *et al.* [**212**] identified 28 lineages of orthologous genes (11 KLRs, 15 CLECs, 1 OLR1 and 1 CD69) in human, mouse, rat, dog and cattle. In the mouse and rat NKC four gene lineages (CLEC4, CLEC2D, KLRA1 and KLRB1) have expanded e.g. the KLRA1 or Ly49 into 15 members compared to just one pseudogene in humans. These expansions have occurred mainly by tandem duplications. Since some of the KLRB1 proteins bind to CLEC2D proteins and supported by the fact that the genes of these two lineages are intermingled, it could be that the observed expansion is related to the co-evolution of the receptor with its ligand [**212**].

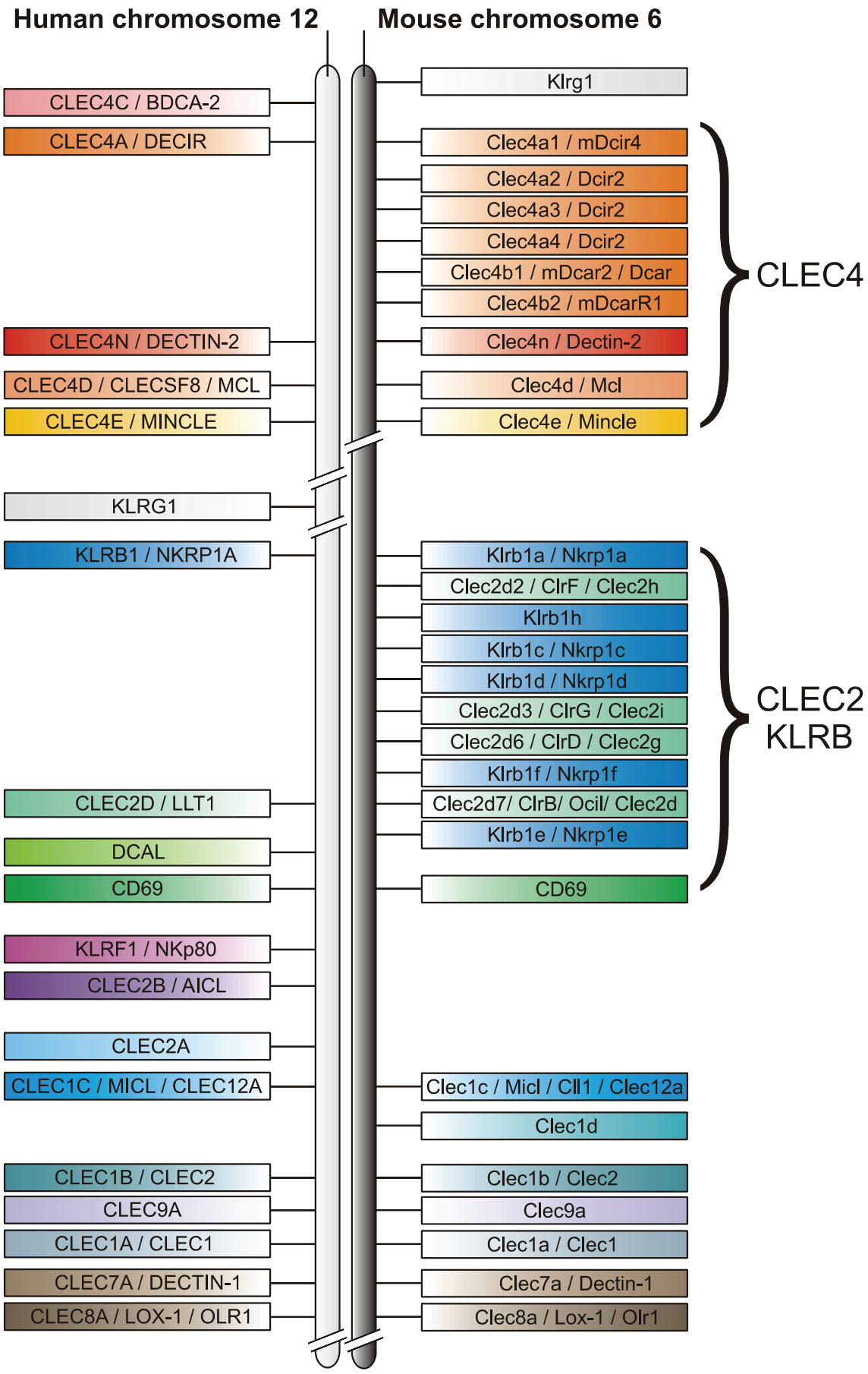
Human chromosome 12
Mouse chromosome 6
CLEC4C / BDCA-2
CLEC4A / DECIR
CLEC4N / DECTIN-2
CLEC4D / CLECSF8 / MCL
CLEC4E / MINCLE
KLRG1
KLRB1 / NKRP1A
CLEC2D / LLT1
DCAL
CD69
KLRF1 / NKp80
CLEC2B / AICL
CLEC2A
CLEC1C / MICL / CLEC12A
CLEC1B / CLEC2
CLEC9A
CLEC1A / CLEC1
CLEC7A / DECTIN-1
CLEC8A / LOX-1 / OLR1
Klrg1
Clec4a1 / mDcir4
Clec4a2 / Dcir2
Clec4a3 / Dcir2
Clec4a4 / Dcir2
Clec4b1 / mDcar2 / Dcar
Clec4b2 / mDcarR1
Clec4n / Dectin-2
Clec4d / Mcl
Clec4e / Mincle
CLEC4
Klrb1a / Nkrp1a
Clec2d2 / ClrF / Clec2h
Klrb1h
Klrb1c / Nkrp1c
Klrb1d / Nkrp1d
Clec2d3 / ClrG / Clec2i
Clec2d6 / ClrD / Clec2g
Klrb1f / Nkrp1f
Clec2d7/ ClrB/ Ocil/ Clec2d
Klrb1e / Nkrp1e
CD69
CLEC2
KLRB
Clec1c / Micl / Cll1 / Clec12a
Clec1d
Clec1b / Clec2
Clec9a
Clec1a / Clec1
Clec7a / Dectin-1
Clec8a / Lox-1 / Olr1

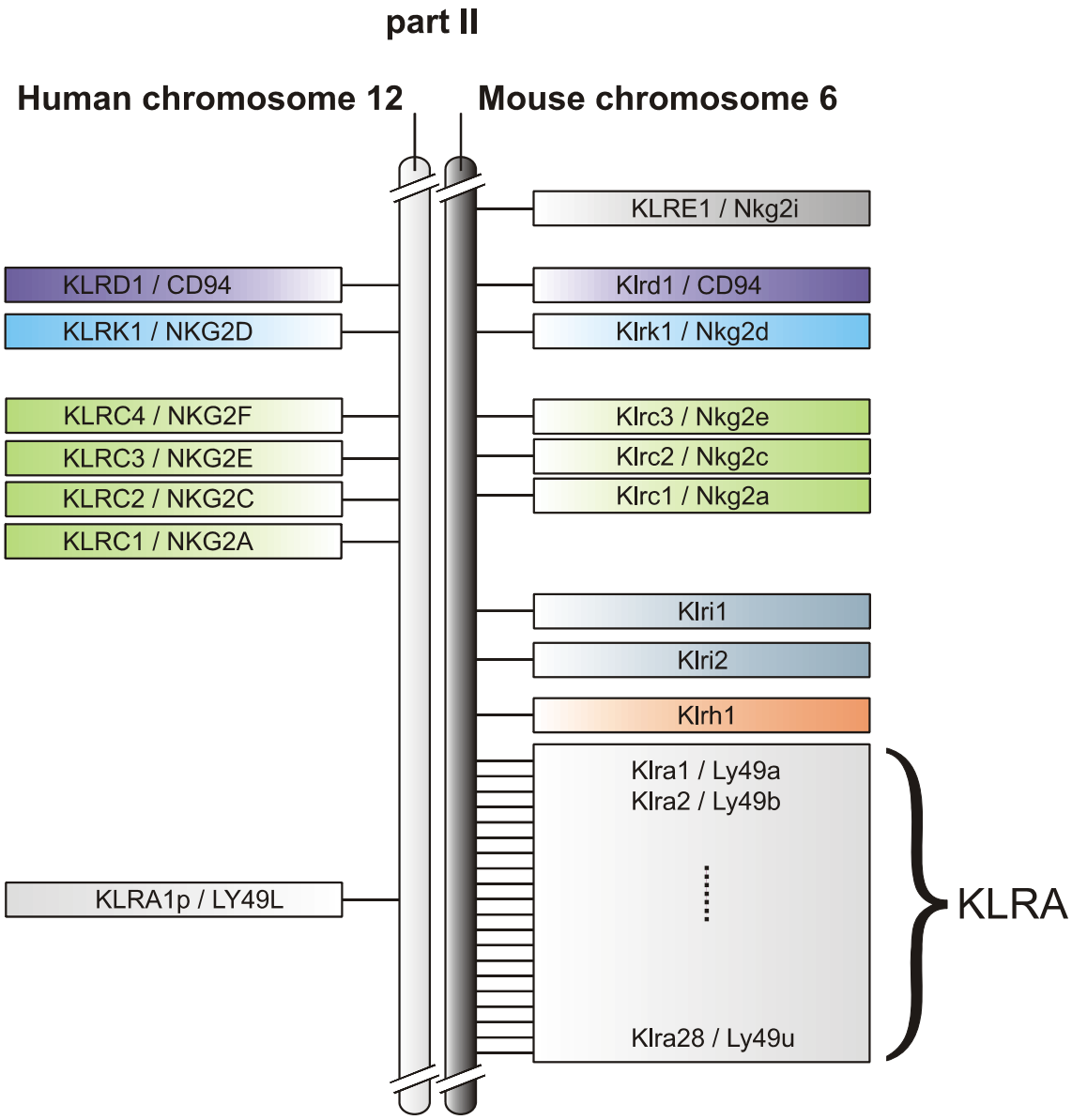

Figure 1.14 C-type lectins encoded in the natural killer gene complex (NKC). In humans the NKC is located on chromosome 12p13, in mouse on chromosome 6. Boxes colored in the same color indicate that the gene(s) have corresponding homologues in mouse and human. The distance between the genes is not drawn to scale. The four gene lineages KLRA, KLRB, CLEC2D and CLEC4 have expanded in mice compared to human, which is indicated by the curly braces. Some of the Klra1 genes are allelic variants only. NKC-encoded pseudogenes are not included except the human LY49L. // - segments indicate non-C-type lectins encoded by the NKC, which are also not depicted. This scheme was modified and updated from [**212,215**]. In mouse the official gene symbol assigned by Mouse Genome Informatics **(MGI)** (**http://www.informatics.jax.org/**) and in humans the official names provided by the HUGO Gene Nomenclature Committee (HUGO) (**http://www.gene.ucl.ac.uk/nomen clature/**) were used along with other commonly used names in literature.

1.1.7.3 Important NKC-encoded receptors and their ligands

The best-studied NKC family is the **Ly49 family** in the mouse, which is mainly responsible for the monitoring of allelic loss of MHC class I expression. Ly49A was

the first identified inhibitory receptor with specificity for MHC class I molecules [**216**]. Ly49A binds to allelic variants of H-2D^d molecules and is expressed on NK cells and T cells with a memory phenotype [**25,216,217**]. As Ly49A, many other members of the Ly49 family like Ly49C and Ly49G are MHC class I-specific inhibitory receptors and contain an ITIM (immunoreceptor-tyrosine-based inhibition motif) in their cytoplasmatic domains, whereas Ly49D and Ly49H contain charged amino acid residues in their transmembrane region and associate with the DAP12 signaling adapter molecule [**215**]. They are predominantly monoallelically expressed [**218,219**] and bind to classical MHC class I molecules except for Ly49H, which binds a viral protein encoded by MCMV [**6**]. There is only one Ly49 gene in humans, Ly49L, which apparently gives rise to a non-functional molecule [**220**].

The members of the Nkrp1 family are listed in **Table 1.6.** and the genes are clustered near the CD69 locus. The best-known representative is the NK1.1 or Nkrp1c receptor, which is a well-established serological marker for C57BL/6J NK cells. Nkrp1c is an activating NK receptor due to the lack of an ITIM and its association with the ITAM-containing FcεRIγ chain [**221**]. Nkrp1d like Nkrp1b has an ITIM in their cytoplasmic tail in contrast to Nkrp1a and Nkrp1f, which are thought to associate also with the FcεRIγ chain [**215**]. In humans there is only one member of the NKRP1A family, the CD161 or KLRB1 molecule.

Table 1.6 Members of the Nkrp1 family. Abbr.: Clr, C-type lectin-related molecules; MGI, Mouse Genome Informatics; HUGO, Human Genome Organisation. Data compiled from [**222**].

Species	Genes	Other names (MGI, HUGO)	function, expression
Mouse			
C57BL/6J	Nkrp1a	Klrb1a	ligands?
C57BL/6J	Nkrp1c	Klrb1c, NK1.1	ligands?, serological NK marker in C57BL/6J mice, activating receptor, FcεRIγ associated
C57BL/6J	Nkrp1d	Klrb1d	binds to Clrb, ITIM
C57BL/6J	Nkrp1e	Klrb1e	pseudogene
C57BL/6J	Nkrp1f	Klrb1f	binds to Clrg
SJL/j	Nkrp1b	Klrb1b	ligands?, ITIM
Human			
	CD161	KLRB1	binds to LLT1

In 2003, it was shown that the Nkrp1d inhibitory receptor binds to the genetically-linked Clrb molecule and the activating Nkrp1f receptor binds to Clrg molecules [**223,224**]. This was the first demonstration that the ligand of a C-type lectin-like

molecule is another C-type lectin-like molecule. The members of the C-type lectin-related molecules (Clr) are listed in **Table 1.7**.

Table 1.7 Members of the Clr family. The Clr family displays homology with CD69. Abbr.: Clr, C-type lectin-related molecules; MGI, Mouse Genome Informatics; HUGO, Human Genome Organisation. Data compiled from [**222**].

Species	Genes	Other names (MGI, HUGO)	function, expression
Mouse			
	Clra	Clec2e	no transcripts identified yet
	Clrb	Clec2d	binds to Nkrp1d, transcripts found in NK
	Clrc	Clec2f	no transcripts identified yet
	Clrd	Clec2g	?
	Clre	-	pseudogene
	Clrf	Clec2h	transcripts found in NK
	Clrg	Clec2i	binds to Nkrp1f, transcripts found in NK
Human			
	LLT1	CLEC2D	binds to CD161, KLRB1
	AICL	CLEC2B	?
	CD69	CLEC2C	?
	DCAL	-	?

In 2005 two groups reported that with the binding of human KLRB1/CD161 to LLT1 another genetically-linked receptor-ligand pair encoded by the NKC was discovered [**225,226**]. The functional consequences of these ligand-receptor interactions are only poorly understood. Expression of Ocil/Clrb on mouse tumor cell lines inhibits NK cell-mediated killing. The same inhibiting effect for NK-mediated cytotoxicity and IFNγ secretion was shown for binding of human LLT1 (the human homologue to Clrb) to is receptor CD161 [**225,226**]. Ocil/Clrb is expressed at high levels on nearly all hematopoietic cells, with the exception of erythrocytes, in a pattern that is similar to that of class I MHC molecules [**224**]. In contrast LLT1 is expressed only on some cell lines (the NK cell lines YT and NKL, the B cell lines 721.221 and RPMI 8866) and activated B and T cells (J. Pfeiffer, unpublished observations). Clrg specific reagents are not available yet. The proposed hypothesis that the Clr molecules constitute a MHC class I-independent back-up mechanism for tissues with low MHC class I expression like the liver or the brain in order to be protected against NK-mediated lysis [**223**] has to be re-evaluated in the light of the new data.

1.1.7.4 The activating NK receptor NKp80/KLRF1

Killer cell lectin-like receptor subfamily F1 (KLRF1), also known as NKp80, is encoded by the NKC. There are only a few reports regarding NKp80 in the literature. NKp80 has been reported to be expressed by NK cells as well as by a $CD56^{+}CD3^{+}$ subset [**42**]. None of the NK cell lines analyzed, including NKL, NK3.3 and YT expressed NKp80. Similar to NKG2D, NKp80 stimulates NK cytotoxicity and induces Ca^{2+}-influx in human NK cells upon triggering by appropriate antibodies [**42**]. At difference to NKG2D, NKp80 contains neither charged amino acids in the transmembrane domain disfavouring association with activating adaptor proteins like CD3ζ, DAP12, DAP10 or FcεRIγ nor any known activation motifs in the cytoplasmic sequence. There is, also at difference to NKG2D, no known NKp80 homologue in rodents impeding elucidation of its function *in vivo* [**215**]. Recently, two reports on NKp80 in non-human primates corroborated that NKp80 is a NK-specific stimulatory receptor [**227,228**]. Using NKp80-specific monoclonal antibodies it was shown by immunoprecipitation that under non-reducing conditions a band of approximately 80 kDa could be detected (hence the name NKp80). Under reducing conditions the band displayed a molecular mass of 40 kDa, which indicates that the surface molecule is expressed at the NK cell surface as a dimer [**42**]. Adding mAb to Nkp80 reduces the lysis of T cell PHA blasts by polyclonal activated NK cells, which indicates that such PHA blasts express a putative NKp80 ligand. Analysis of NK clones in redirected killing experiments showed that only NKp46 expressing clones show NKp80-mediated killing, whereas $NKp80^{+}NKp46^{dull}$ clones and $NKp80^{dull}NKp46^{dull}$ clones do not kill via NKp80. Vitale *et al.* suggested therefore that NKp80 plays a rather costimulatory role in NK-mediated killing [**42**].

1.2 Aims of the thesis

NK cells are activated by several immunoglobulin-like and C-type lectin-like receptors. In humans, the cellular ligands of the major activating NK receptors, apart from NKG2D, remained unknown. The characterization of NKG2D ligands has profoundly improved our understanding of NK cell activation; this provided the rationale to identify ligand(s) of the orphan NK receptor NKp80, which like NKG2D, is encoded in the natural killer gene complex (NKC).

Similar to NKG2D, the activating NK receptor NKp80, which was first described 5 years ago [**16**], has been reported to stimulate NK cell cytotoxicity. However, in contrast to NKG2D, NKp80 is expressed almost exclusively on human NK cells [**16**]. Since the unknown nature of the NKp80-ligand(s) represents a major obstacle in elucidating the role of NKp80 for NK cell biology, it was the aim of this thesis to identify and characterize the ligand(s) of NKp80.

Two approaches were chosen to identify NKp80-ligand (NKp80-L)-expressing cells: first, the generation of a reporter cell line expressing NKp80-CD3ζ reporter constructs, and second, the production of NKp80 ectodomains to generate NKp80 tetramers using the BirA technology [**229**]. Both detecting systems should be used to screen for NKp80-L-expressing cDNA clones by expression cloning using cDNA from NKp80-L-expressing cells. Additionally, the soluble ectodomain should aid in the generation of NKp80-specific monoclonal antibodies. After identification of NKp80-ligand(s), the expression of NKp80-L and the biological relevance of the NKp80-NKp80-L interaction should be established and characterized.

1.3 References

1. Metschnikoff, Elias. Immunität bei Infektionskrankheiten, L' Immunité dans les maladies infectieuses. Fischer, Jena (XI, 456 S. : Mit 45 Fig. im Text ; 4). 1902.

2. Janeway, C. A., Jr. 1989. Approaching the asymptote? Evolution and revolution in immunology. *Cold Spring Harb.Symp.Quant.Biol.* 54 Pt 1:1-13.

3. Fearon, D. T. and R. M. Locksley. 1996. The instructive role of innate immunity in the acquired immune response. *Science* 272:50-53.

4. Janeway, C. A., Jr. and R. Medzhitov. 2002. Innate immune recognition. *Annu.Rev.Immunol.* 20:197-216.

5. Matzinger, P. 1994. Tolerance, danger, and the extended family. *Annu.Rev.Immunol.* 12:991-1045.

6. Lanier, L. L. 2005. NK cell recognition. *Annu.Rev.Immunol.* 23:225-274.

7. Becker, S., E. M. Fenyö, ., and E. Klein. 1976. The natural killer cell in the mouse does not require H-2 homology and is not directed against type or group-specific antigens of murine c viral proteins. *SO: European Journal of Immunology* 6:882-885.

8. Kiessling, R., E. Klein, and H. Wigzell. 1975. "Natural" killer cells in the mouse. I. Cytotoxic cells with specificity for mouse Moloney leukemia cells. Specificity and distribution according to genotype. *Eur.J.Immunol.* 5:112-117.

9. Kiessling, R., E. Klein, H. Pross, and H. Wigzell. 1975. "Natural" killer cells in the mouse. II. Cytotoxic cells with specificity for mouse Moloney leukemia cells. Characteristics of the killer cell. *Eur.J Immunol* 5:117-121.

10. Stern, P., M. Gidlund, A. Orn, and H. Wigzell. 1980. Natural killer cells mediate lysis of embryonal carcinoma cells lacking MHC. *Nature* 285:341-342.

11. Karre, K., H. G. Ljunggren, G. Piontek, and R. Kiessling. 1986. Selective rejection of H-2-deficient lymphoma variants suggests alternative immune defence strategy. *Nature* 319:675-678.

12. Trinchieri, G. 1989. Biology of natural killer cells. *Adv.Immunol.* 47:187-376.

13. Diefenbach, A. and D. H. Raulet. 2001. Strategies for target cell recognition by natural killer cells. *Immunol Rev.* 181:170-184.

14. Bauer, S., V. Groh, J. Wu, A. Steinle, J. H. Phillips, L. L. Lanier, and T. Spies. 1999. Activation of NK cells and T cells by NKG2D, a receptor for stress-inducible MICA. *Science* 285:727-729.

15. Wu, J., Y. Song, A. B. Bakker, S. Bauer, T. Spies, L. L. Lanier, and J. H. Phillips. 1999. An activating immunoreceptor complex formed by NKG2D and DAP10. *Science* 285:730-732.

16. Cerwenka, A., A. B. Bakker, T. McClanahan, J. Wagner, J. Wu, J. H. Phillips, and L. L. Lanier. 2000. Retinoic acid early inducible genes define a ligand family for

the activating NKG2D receptor in mice. *Immunity.* 12:721-727.

17. Steinle, A., P. Li, D. L. Morris, V. Groh, L. L. Lanier, R. K. Strong, and T. Spies. 2001. Interactions of human NKG2D with its ligands MICA, MICB, and homologs of the mouse RAE-1 protein family. *Immunogenetics* 53:279-287.

18. Cosman, D., J. Mullberg, C. L. Sutherland, W. Chin, R. Armitage, W. Fanslow, M. Kubin, and N. J. Chalupny. 2001. ULBPs, novel MHC class I-related molecules, bind to CMV glycoprotein UL16 and stimulate NK cytotoxicity through the NKG2D receptor. *Immunity.* 14:123-133.

19. Lanier, L. L. 1998. NK cell receptors. *Annu.Rev.Immunol.* 16:359-393.

20. Long, E. O., D. N. Burshtyn, W. P. Clark, M. Peruzzi, S. Rajagopalan, S. Rojo, N. Wagtmann, and C. C. Winter. 1997. Killer cell inhibitory receptors: diversity, specificity, and function. *Immunol.Rev.* 155:135-144.

21. Yokoyama, W. M. 1993. Recognition structures on natural killer cells. *Curr.Opin.Immunol.* 5:67-73.

22. Moretta, A., C. Bottino, M. Vitale, D. Pende, R. Biassoni, M. C. Mingari, and L. Moretta. 1996. Receptors for HLA class-I molecules in human natural killer cells. *Annu.Rev.Immunol.* 14:619-648.

23. Mingari, M. C., F. Schiavetti, M. Ponte, C. Vitale, E. Maggi, S. Romagnani, J. Demarest, G. Pantaleo, A. S. Fauci, and L. Moretta. 1996. Human CD8+ T lymphocyte subsets that express HLA class I-specific inhibitory receptors represent oligoclonally or monoclonally expanded cell populations. *Proc.Natl.Acad.Sci.U.S.A* 93:12433-12438.

24. McMahon, C. W. and D. H. Raulet. 2001. Expression and function of NK cell receptors in CD8+ T cells. *Curr.Opin.Immunol.* 13:465-470.

25. Vivier, E. and N. Anfossi. 2004. Inhibitory NK-cell receptors on T cells: witness of the past, actors of the future. *Nat.Rev.Immunol.* 4:190-198.

26. Trowsdale, J., R. Barten, A. Haude, C. A. Stewart, S. Beck, and M. J. Wilson. 2001. The genomic context of natural killer receptor extended gene families. *Immunol.Rev.* 181:20-38.

27. Martz, E. 2002. Protein Explorer: easy yet powerful macromolecular visualization. *Trends Biochem.Sci.* 27:107-109.

28. Li, P., D. L. Morris, B. E. Willcox, A. Steinle, T. Spies, and R. K. Strong. 2001. Complex structure of the activating immunoreceptor NKG2D and its MHC class I-like ligand MICA. *Nat.Immunol.* 2:443-451.

29. Boyington, J. C., S. A. Motyka, P. Schuck, A. G. Brooks, and P. D. Sun. 2000. Crystal structure of an NK cell immunoglobulin-like receptor in complex with its class I MHC ligand. *Nature* 405:537-543.

30. Moretta, A., C. Bottino, M. Vitale, D. Pende, C. Cantoni, M. C. Mingari, R. Biassoni, and L. Moretta. 2001. Activating receptors and coreceptors involved in human natural killer cell-mediated cytolysis. *Annu.Rev.Immunol.* 19:197-223.

31. Raulet, D. H. 2003. Roles of the NKG2D immunoreceptor and its ligands. *Nat.Rev.Immunol.* 3:781-790.

32. Vivier, E., E. Tomasello, and P. Paul. 2002. Lymphocyte activation via NKG2D: towards a new paradigm in immune recognition? *Curr.Opin.Immunol.* 14:306-311.

33. Vitale, M., C. Bottino, S. Sivori, L. Sanseverino, R. Castriconi, E. Marcenaro, R. Augugliaro, L. Moretta, and A. Moretta. 1998. NKp44, a novel triggering surface molecule specifically expressed by activated natural killer cells, is involved in non-major histocompatibility complex-restricted tumor cell lysis. *J.Exp.Med.* 187:2065-2072.

34. Sivori, S., M. Vitale, L. Morelli, L. Sanseverino, R. Augugliaro, C. Bottino, L. Moretta, and A. Moretta. 1997. p46, a novel natural killer cell-specific surface molecule that mediates cell activation. *J.Exp.Med.* 186:1129-1136.

35. Pende, D., S. Parolini, A. Pessino, S. Sivori, R. Augugliaro, L. Morelli, E. Marcenaro, L. Accame, A. Malaspina, R. Biassoni, C. Bottino, L. Moretta, and A. Moretta. 1999. Identification and molecular characterization of NKp30, a novel triggering receptor involved in natural cytotoxicity mediated by human natural killer cells. *J.Exp.Med.* 190:1505-1516.

36. Biassoni, R., A. Pessino, C. Bottino, D. Pende, L. Moretta, and A. Moretta. 1999. The murine homologue of the human NKp46, a triggering receptor involved in the induction of natural cytotoxicity. *Eur.J.Immunol.* 29:1014-1020.

37. Mandelboim, O., N. Lieberman, M. Lev, L. Paul, T. I. Arnon, Y. Bushkin, D. M. Davis, J. L. Strominger, J. W. Yewdell, and A. Porgador. 2001. Recognition of haemagglutinins on virus-infected cells by NKp46 activates lysis by human NK cells. *Nature* 409:1055-1060.

38. Gazit, R., R. Gruda, M. Elboim, T. I. Arnon, G. Katz, H. Achdout, J. Hanna, U. Qimron, G. Landau, E. Greenbaum, Z. Zakay-Rones, A. Porgador, and O. Mandelboim. 2006. Lethal influenza infection in the absence of the natural killer cell receptor gene Ncr1. *Nat.Immunol.* 7:517-523.

39. Spies, T. and V. Groh. 2006. Natural cytotoxicity receptors: influenza virus in the spotlight. *Nat.Immunol.* 7:443-444.

40. Vieillard, V., J. L. Strominger, and P. Debre. 2005. NK cytotoxicity against CD4+ T cells during HIV-1 infection: a gp41 peptide induces the expression of an NKp44 ligand. *Proc.Natl.Acad.Sci.U.S.A* 102:10981-10986.

41. Shibuya, A., D. Campbell, C. Hannum, H. Yssel, K. Franz-Bacon, T. McClanahan, T. Kitamura, J. Nicholl, G. R. Sutherland, L. L. Lanier, and J. H. Phillips. 1996. DNAM-1, a novel adhesion molecule involved in the cytolytic function of T lymphocytes. *Immunity* 4:573-581.

42. Vitale, M., M. Falco, R. Castriconi, S. Parolini, R. Zambello, G. Semenzato, R. Biassoni, C. Bottino, L. Moretta, and A. Moretta. 2001. Identification of NKp80, a novel triggering molecule expressed by human NK cells. *Eur.J.Immunol.* 31:233-242.

43. Rogers, N. C., E. C. Slack, A. D. Edwards, M. A. Nolte, O. Schulz, E. Schweighoffer, D. L. Williams, S. Gordon, V. L. Tybulewicz, G. D. Brown, and Reis e Sousa. 2005. Syk-dependent cytokine induction by Dectin-1 reveals a novel pattern recognition pathway for C type lectins. *Immunity* 22:507-517.

44. Ravetch, J. V. and B. Perussia. 1989. Alternative membrane forms of Fc gamma RIII(CD16) on human natural killer cells and neutrophils. Cell type-specific expression of two genes that differ in single nucleotide substitutions. *J.Exp.Med.* 170:481-497.

45. Tortorella, D., B. E. Gewurz, M. H. Furman, D. J. Schust, and H. L. Ploegh. 2000. Viral subversion of the immune system. *Annu.Rev.Immunol.* 18:861-926.

46. Alcami, A. and U. H. Koszinowski. 2000. Viral mechanisms of immune evasion. *Immunol.Today* 21:447-455.

47. Lilley, B. N. and H. L. Ploegh. 2004. A membrane protein required for dislocation of misfolded proteins from the ER. *Nature* 429:834-840.

48. Braud, V. M., D. S. Allan, C. A. O'Callaghan, K. Soderstrom, A. D'Andrea, G. S. Ogg, S. Lazetic, N. T. Young, J. I. Bell, J. H. Phillips, L. L. Lanier, and A. J. McMichael. 1998. HLA-E binds to natural killer cell receptors CD94/NKG2A, B and C. *Nature* 391:795-799.

49. Vance, R. E., J. R. Kraft, J. D. Altman, P. E. Jensen, and D. H. Raulet. 1998. Mouse CD94/NKG2A is a natural killer cell receptor for the nonclassical major histocompatibility complex (MHC) class I molecule Qa-1(b). *J.Exp.Med.* 188:1841-1848.

50. Lee, N., M. Llano, M. Carretero, A. Ishitani, F. Navarro, M. Lopez-Botet, and D. E. Geraghty. 1998. HLA-E is a major ligand for the natural killer inhibitory receptor CD94/NKG2A. *Proc.Natl.Acad.Sci.U.S.A* 95:5199-5204.

51. Chapman, T. L., A. P. Heikeman, and P. J. Bjorkman. 1999. The inhibitory receptor LIR-1 uses a common binding interaction to recognize class I MHC molecules and the viral homolog UL18. *Immunity.* 11:603-613.

52. Tomasec, P., V. M. Braud, C. Rickards, M. B. Powell, B. P. McSharry, S. Gadola, V. Cerundolo, L. K. Borysiewicz, A. J. McMichael, and G. W. Wilkinson. 2000. Surface expression of HLA-E, an inhibitor of natural killer cells, enhanced by human cytomegalovirus gpUL40. *Science* 287:1031.

53. Vales-Gomez, M., H. T. Reyburn, R. A. Erskine, M. Lopez-Botet, and J. L. Strominger. 1999. Kinetics and peptide dependency of the binding of the inhibitory NK receptor CD94/NKG2-A and the activating receptor CD94/NKG2-C to HLA-E. *EMBO J.* 18:4250-4260.

54. Parham, P. 2005. MHC class I molecules and KIRs in human history, health and survival. *Nat.Rev.Immunol.* 5:201-214.

55. Hoglund, P., C. Ohlen, E. Carbone, L. Franksson, H. G. Ljunggren, A. Latour, B. Koller, and K. Karre. 1991. Recognition of beta 2-microglobulin-negative (beta 2m-) T-cell blasts by natural killer cells from normal but not from beta 2m- mice: nonresponsiveness controlled by beta 2m- bone marrow in chimeric mice. *Proc.Natl.Acad.Sci.U.S.A* 88:10332-10336.

56. Kim, S., J. Poursine-Laurent, S. M. Truscott, L. Lybarger, Y. J. Song, L. Yang, A. R. French, J. B. Sunwoo, S. Lemieux, T. H. Hansen, and W. M. Yokoyama. 2005. Licensing of natural killer cells by host major histocompatibility complex class I molecules. *Nature* 436:709-713.

57. Moretta, L. and A. Moretta. 2004. Unravelling natural killer cell function: triggering and inhibitory human NK receptors. *EMBO J.* 23:255-259.

58. Anfossi, N., P. Andre, S. Guia, C. S. Falk, S. Roetynck, C. A. Stewart, V. Breso, C. Frassati, D. Reviron, D. Middleton, F. Romagne, S. Ugolini, and E. Vivier. 2006. Human NK cell education by inhibitory receptors for MHC class I. *Immunity* 25:331-342.

59. Handgretinger, R., T. Klingebiel, P. Lang, M. Schumm, S. Neu, A. Geiselhart, P. Bader, P. G. Schlegel, J. Greil, D. Stachel, R. J. Herzog, and D. Niethammer. 2001. Megadose transplantation of purified peripheral blood CD34(+) progenitor cells from HLA-mismatched parental donors in children. *Bone Marrow Transplant.* 27:777-783.

60. Karre, K. 2002. Immunology. A perfect mismatch. *Science* 295:2029-2031.

61. Ruggeri, L., M. Capanni, E. Urbani, K. Perruccio, W. D. Shlomchik, A. Tosti, S. Posati, D. Rogaia, F. Frassoni, F. Aversa, M. F. Martelli, and A. Velardi. 2002. Effectiveness of donor natural killer cell alloreactivity in mismatched hematopoietic transplants. *Science* 295:2097-2100.

62. Ferlazzo, G. and C. Munz. 2004. NK cell compartments and their activation by dendritic cells. *J Immunol* 172:1333-1339.

63. Cooper, M. A., T. A. Fehniger, S. C. Turner, K. S. Chen, B. A. Ghaheri, T. Ghayur, W. E. Carson, and M. A. Caligiuri. 2001. Human natural killer cells: a unique innate immunoregulatory role for the CD56(bright) subset. *Blood* 97:3146-3151.

64. Groh, V., A. Steinle, S. Bauer, and T. Spies. 1998. Recognition of stress-induced MHC molecules by intestinal epithelial gammadelta T cells. *Science* 279:1737-1740.

65. Born, W. K., C. L. Reardon, and R. L. O'Brien. 2006. The function of gammadelta T cells in innate immunity. *Curr.Opin.Immunol.* 18:31-38.

66. Shin, S., R. El Diwany, S. Schaffert, E. J. Adams, K. C. Garcia, P. Pereira, and Y. H. Chien. 2005. Antigen recognition determinants of gammadelta T cell receptors. *Science* 308:252-255.

67. Rogers, A. N., D. G. Vanburen, E. E. Hedblom, M. E. Tilahun, J. C. Telfer, and C. L. Baldwin. 2005. Gammadelta T cell function varies with the expressed WC1 coreceptor. *J.Immunol.* 174:3386-3393.

68. Carding, S. R. and P. J. Egan. 2002. Gammadelta T cells: functional plasticity and heterogeneity. *Nat Rev.Immunol.* 2:336-345.

69. Dalton, J. E., G. Howell, J. Pearson, P. Scott, and S. R. Carding. 2004. Fas-Fas ligand interactions are essential for the binding to and killing of activated macrophages by gamma delta T cells. *J.Immunol.* 173:3660-3667.

70. Rincon-Orozco, B., V. Kunzmann, P. Wrobel, D. Kabelitz, A. Steinle, and T. Herrmann. 2005. Activation of V gamma 9V delta 2 T cells by NKG2D. *J.Immunol.* 175:2144-2151.

71. Brandes, M., K. Willimann, and B. Moser. 2005. Professional antigen-presentation function by human gammadelta T Cells. *Science* 309:264-268.

72. Steinle, A., V. Groh, and T. Spies. 1998. Diversification, expression, and gamma delta T cell recognition of evolutionarily distant members of the MIC family of major histocompatibility complex class I-related molecules. *Proc.Natl.Acad.Sci.U.S.A* 95:12510-12515.

73. Kabelitz, D., D. Wesch, E. Pitters, and M. Zoller. 2004. Potential of human gammadelta T lymphocytes for immunotherapy of cancer. *Int.J Cancer* 112:727-732.

74. Girardi, M., D. E. Oppenheim, C. R. Steele, J. M. Lewis, E. Glusac, R. Filler, P. Hobby, B. Sutton, R. E. Tigelaar, and A. C. Hayday. 2001. Regulation of cutaneous malignancy by gammadelta T cells. *Science* 294:605-609.

75. Gao, Y., W. Yang, M. Pan, E. Scully, M. Girardi, L. H. Augenlicht, J. Craft, and Z. Yin. 2003. Gamma delta T cells provide an early source of interferon gamma in tumor immunity. *J Exp.Med* 198:433-442.

76. Street, S. E., Y. Hayakawa, Y. Zhan, A. M. Lew, D. MacGregor, A. M. Jamieson, A. Diefenbach, H. Yagita, D. I. Godfrey, and M. J. Smyth. 2004. Innate immune surveillance of spontaneous B cell lymphomas by natural killer cells and gammadelta T cells. *J Exp.Med* 199:879-884.

77. Wands, J. M., C. L. Roark, M. K. Aydintug, N. Jin, Y. S. Hahn, L. Cook, X. Yin, J. Dal Porto, M. Lahn, D. M. Hyde, E. W. Gelfand, R. J. Mason, R. L. O'Brien, and W. K. Born. 2005. Distribution and leukocyte contacts of gammadelta T cells in the lung. *J Leukoc.Biol.* 78:1086-1096.

78. Conti, L., R. Casetti, M. Cardone, B. Varano, A. Martino, F. Belardelli, F. Poccia, and S. Gessani. 2005. Reciprocal Activating Interaction Between Dendritic Cells and Pamidronate-Stimulated {gamma}{delta} T Cells: Role of CD86 and Inflammatory Cytokines. *J Immunol* 174:252-260.

79. Gumperz, J. E., L. D. Barber, N. M. Valiante, L. Percival, J. H. Phillips, L. L. Lanier, and P. Parham. 1997. Conserved and variable residues within the Bw4 motif of HLA-B make separable contributions to recognition by the NKB1 killer cell-inhibitory receptor. *J.Immunol.* 158:5237-5241.

80. Kawano, T., J. Cui, Y. Koezuka, I. Toura, Y. Kaneko, K. Motoki, H. Ueno, R. Nakagawa, H. Sato, E. Kondo, H. Koseki, and M. Taniguchi. 1997. CD1d-restricted and TCR-mediated activation of valpha14 NKT cells by glycosylceramides. *Science* 278:1626-1629.

81. Van Kaer, L. and S. Joyce. 2005. Innate immunity: NKT cells in the spotlight. *Curr.Biol.* 15:R429-R431.

82. Mattner, J., K. L. Debord, N. Ismail, R. D. Goff, C. Cantu, III, D. Zhou, P. Saint-Mezard, V. Wang, Y. Gao, N. Yin, K. Hoebe, O. Schneewind, D. Walker, B. Beutler, L. Teyton, P. B. Savage, and A. Bendelac. 2005. Exogenous and endogenous glycolipid antigens activate NKT cells during microbial infections. *Nature* 434:525-529.

83. Zhou, D., J. Mattner, C. Cantu, III, N. Schrantz, N. Yin, Y. Gao, Y. Sagiv, K. Hudspeth, Y. P. Wu, T. Yamashita, S. Teneberg, D. Wang, R. L. Proia, S. B. Levery, P. B. Savage, L. Teyton, and A. Bendelac. 2004. Lysosomal glycosphingolipid recognition by NKT cells. *Science* 306:1786-1789.

84. van Furth, R. and Z. A. Cohn. 1968. The origin and kinetics of mononuclear phagocytes. *J.Exp.Med.* 128:415-435.

85. Ebert, R. H. and H. W. Florey. 1939. The extravascular development of the mononuclear phagocytosis observed in vivo. *Brit.J.Exp.Pathol.* 20:415-435.

86. del Hoyo, G. M., P. Martin, H. H. Vargas, S. Ruiz, C. F. Arias, and C. Ardavin. 2002. Characterization of a common precursor population for dendritic cells. *Nature* 415:1043-1047.

87. Imhof, B. A. and M. Aurrand-Lions. 2004. Adhesion mechanisms regulating the migration of monocytes. *Nat.Rev.Immunol.* 4:432-444.

88. Sallusto, F. and A. Lanzavecchia. 1994. Efficient presentation of soluble antigen by cultured human dendritic cells is maintained by granulocyte/macrophage colony-stimulating factor plus interleukin 4 and downregulated by tumor necrosis factor alpha. *J.Exp.Med.* 179:1109-1118.

89. Gordon, S. and P. R. Taylor. 2005. Monocyte and macrophage heterogeneity. *Nat.Rev.Immunol.* 5:953-964.

90. Passlick, B., D. Flieger, and H. W. Ziegler-Heitbrock. 1989. Identification and characterization of a novel monocyte subpopulation in human peripheral blood. *Blood* 74:2527-2534.

91. Grage-Griebenow, E., R. Zawatzky, H. Kahlert, L. Brade, H. Flad, and M. Ernst. 2001. Identification of a novel dendritic cell-like subset of CD64(+) / CD16(+) blood monocytes. *Eur.J.Immunol.* 31:48-56.

92. Geissmann, F., S. Jung, and D. R. Littman. 2003. Blood monocytes consist of two principal subsets with distinct migratory properties. *Immunity.* 19:71-82.

93. Randolph, G. J., G. Sanchez-Schmitz, R. M. Liebman, and K. Schakel. 2002. The CD16(+) (FcgammaRIII(+)) subset of human monocytes preferentially becomes migratory dendritic cells in a model tissue setting. *J.Exp.Med.* 196:517-527.

94. Sanchez-Torres, C., G. S. Garcia-Romo, M. A. Cornejo-Cortes, A. Rivas-Carvalho, and G. Sanchez-Schmitz. 2001. CD16+ and. *Int.Immunol.* 13:1571-1581.

95. Sunderkotter, C., T. Nikolic, M. J. Dillon, N. Van Rooijen, M. Stehling, D. A. Drevets, and P. J. Leenen. 2004. Subpopulations of mouse blood monocytes differ in maturation stage and inflammatory response. *J.Immunol.* 172:4410-4417.

96. Belge, K. U., F. Dayyani, A. Horelt, M. Siedlar, M. Frankenberger, B. Frankenberger, T. Espevik, and L. Ziegler-Heitbrock. 2002. The proinflammatory CD14+CD16+DR++ monocytes are a major source of TNF. *J.Immunol.* 168:3536-3542.

97. Fingerle, G., A. Pforte, B. Passlick, M. Blumenstein, M. Strobel, and H. W. Ziegler-Heitbrock. 1993. The novel subset of CD14+/CD16+ blood monocytes is expanded in sepsis patients. *Blood* 82:3170-3176.

98. Nockher, W. A. and J. E. Scherberich. 1998. Expanded CD14+ CD16+ monocyte subpopulation in patients with acute and chronic infections undergoing

hemodialysis. *Infect.Immun.* 66:2782-2790.

99. Merad, M., M. G. Manz, H. Karsunky, A. Wagers, W. Peters, I. Charo, I. L. Weissman, J. G. Cyster, and E. G. Engleman. 2002. Langerhans cells renew in the skin throughout life under steady-state conditions. *Nat.Immunol.* 3:1135-1141.

100. Tarling, J. D., H. S. Lin, and S. Hsu. 1987. Self-renewal of pulmonary alveolar macrophages: evidence from radiation chimera studies. *J.Leukoc.Biol.* 42:443-446.

101. Thomas, E. D., R. E. Ramberg, G. E. Sale, R. S. Sparkes, and D. W. Golde. 1976. Direct evidence for a bone marrow origin of the alveolar macrophage in man. *Science* 192:1016-1018.

102. Crofton, R. W., M. M. Diesselhoff-den Dulk, and R. van Furth. 1978. The origin, kinetics, and characteristics of the Kupffer cells in the normal steady state. *J.Exp.Med.* 148:1-17.

103. Gordon, S. 2003. Alternative activation of macrophages. *Nat.Rev.Immunol.* 3:23-35.

104. Langerhans, P. 1868. Über die Nerven der menschlichen Haut. *Archiv für pathologische Anatomie und Physiologie, und für Klinische Medicin.Berlin.* 44:325-337.

105. Steinman, R. M. and Z. A. Cohn. 1973. Identification of a novel cell type in peripheral lymphoid organs of mice. I. Morphology, quantitation, tissue distribution. *J.Exp.Med.* 137:1142-1162.

106. Banchereau, J. and R. M. Steinman. 1998. Dendritic cells and the control of immunity. *Nature* 392:245-252.

107. Steinman, R. M., D. Hawiger, and M. C. Nussenzweig. 2003. Tolerogenic dendritic cells. *Annu.Rev.Immunol.* 21:685-711.

108. Degli-Esposti, M. A. and M. J. Smyth. 2005. Close encounters of different kinds: dendritic cells and NK cells take centre stage. *Nat.Rev.Immunol.* 5:112-124.

109. Banchereau, J., F. Briere, C. Caux, J. Davoust, S. Lebecque, Y. J. Liu, B. Pulendran, and K. Palucka. 2000. Immunobiology of dendritic cells. *Annu.Rev.Immunol.* 18:767-811.

110. den Haan, J. M., S. M. Lehar, and M. J. Bevan. 2000. CD8(+) but not CD8(-) dendritic cells cross-prime cytotoxic T cells in vivo. *J.Exp.Med.* 192:1685-1696.

111. Colonna, M., G. Trinchieri, and Y. J. Liu. 2004. Plasmacytoid dendritic cells in immunity. *Nat.Immunol.* 5:1219-1226.

112. Lennert, K., W. Remmele, and . 1958. [Karyometric research on lymph node cells in man. I. Germinoblasts, lymphoblasts & lymphocytes.]. *Acta Haematol.* 19:99-113.

113. Trinchieri, G., D. Santoli, R. R. Dee, and B. B. Knowles. 1978. Anti-viral activity induced by culturing lymphocytes with tumor-derived or virus-transformed cells. Identification of the anti-viral activity as interferon and characterization of the human effector lymphocyte subpopulation. *J.Exp.Med.* 147:1299-1313.

114. Corcoran, L., I. Ferrero, D. Vremec, K. Lucas, J. Waithman, M. O'Keeffe, L. Wu, A. Wilson, and K. Shortman. 2003. The lymphoid past of mouse plasmacytoid cells and thymic dendritic cells. *J.Immunol.* 170:4926-4932.

115. Tew, J. G., J. Wu, M. Fakher, A. K. Szakal, and D. Qin. 2001. Follicular dendritic cells: beyond the necessity of T-cell help. *Trends Immunol.* 22:361-367.

116. Rossi, M. and J. W. Young. 2005. Human dendritic cells: potent antigen-presenting cells at the crossroads of innate and adaptive immunity. *J.Immunol.* 175:1373-1381.

117. Dzionek, A., A. Fuchs, P. Schmidt, S. Cremer, M. Zysk, S. Miltenyi, D. W. Buck, and J. Schmitz. 2000. BDCA-2, BDCA-3, and BDCA-4: three markers for distinct subsets of dendritic cells in human peripheral blood. *J.Immunol.* 165:6037-6046.

118. Iwasaki, A. and R. Medzhitov. 2004. Toll-like receptor control of the adaptive immune responses. *Nat.Immunol.* 5:987-995.

119. Ravichandran, K. S. 2003. "Recruitment signals" from apoptotic cells: invitation to a quiet meal. *Cell* 113:817-820.

120. Blander, J. M. and R. Medzhitov. 2006. Toll-dependent selection of microbial antigens for presentation by dendritic cells. *Nature* 440:808-812.

121. Kogelberg, H. and T. Feizi. 2001. New structural insights into lectin-type proteins of the immune system. *Curr.Opin.Struct.Biol.* 11:635-643.

122. Kawasaki, N., T. Kawasaki, and I. Yamashina. 1983. Isolation and characterization of a mannan-binding protein from human serum. *J.Biochem.(Tokyo)* 94:937-947.

123. Stahl, P., P. H. Schlesinger, E. Sigardson, J. S. Rodman, and Y. C. Lee. 1980. Receptor-mediated pinocytosis of mannose glycoconjugates by macrophages: characterization and evidence for receptor recycling. *Cell* 19:207-215.

124. Jordens, R., A. Thompson, R. Amons, and F. Koning. 1999. Human dendritic cells shed a functional, soluble form of the mannose receptor. *Int.Immunol.* 11:1775-1780.

125. Geijtenbeek, T. B., D. J. Krooshoop, D. A. Bleijs, S. J. van Vliet, G. C. van Duijnhoven, V. Grabovsky, R. Alon, C. G. Figdor, and Y. van Kooyk. 2000. DC-SIGN-ICAM-2 interaction mediates dendritic cell trafficking. *Nat.Immunol.* 1:353-357.

126. Figdor, C. G., Y. van Kooyk, and G. J. Adema. 2002. C-type lectin receptors on dendritic cells and Langerhans cells. *Nat.Rev.Immunol.* 2:77-84.

127. Bakker, A. B., O. S. van den, A. Q. Bakker, N. Feller, M. van Meijer, J. A. Bia, M. A. Jongeneelen, T. J. Visser, N. Bijl, C. A. Geuijen, W. E. Marissen, K. Radosevic, M. Throsby, G. J. Schuurhuis, G. J. Ossenkoppele, J. de Kruif, J. Goudsmit, and A. M. Kruisbeek. 2004. C-type lectin-like molecule-1: a novel myeloid cell surface marker associated with acute myeloid leukemia. *Cancer Res.* 64:8443-8450.

128. Marshall, A. S., J. A. Willment, H. H. Lin, D. L. Williams, S. Gordon, and G. D. Brown. 2004. Identification and characterization of a novel human myeloid inhibitory C-type lectin-like receptor (MICL) that is predominantly expressed on

granulocytes and monocytes. *J.Biol.Chem.* 279:14792-14802.

129. Kanazawa, N., K. Tashiro, and Y. Miyachi. 2004. Signaling and immune regulatory role of the dendritic cell immunoreceptor (DCIR) family lectins: DCIR, DCAR, dectin-2 and BDCA-2. *Immunobiology* 209:179-190.

130. Ryan, E. J., A. J. Marshall, D. Magaletti, H. Floyd, K. E. Draves, N. E. Olson, and E. A. Clark. 2002. Dendritic cell-associated lectin-1: a novel dendritic cell-associated, C-type lectin-like molecule enhances T cell secretion of IL-4. *J.Immunol.* 169:5638-5648.

131. Brown, G. D. and S. Gordon. 2001. Immune recognition. A new receptor for beta-glucans. *Nature* 413:36-37.

132. Ariizumi, K., G. L. Shen, S. Shikano, S. Xu, R. Ritter, III, T. Kumamoto, D. Edelbaum, A. Morita, P. R. Bergstresser, and A. Takashima. 2000. Identification of a novel, dendritic cell-associated molecule, dectin-1, by subtractive cDNA cloning. *J.Biol.Chem.* 275:20157-20167.

133. Brown, G. D. 2006. Dectin-1: a signalling non-TLR pattern-recognition receptor. *Nat.Rev.Immunol.* 6:33-43.

134. Underhill, D. M., A. Ozinsky, A. M. Hajjar, A. Stevens, C. B. Wilson, M. Bassetti, and A. Aderem. 1999. The Toll-like receptor 2 is recruited to macrophage phagosomes and discriminates between pathogens. *Nature* 401:811-815.

135. Han, Y., M. Zhang, N. Li, T. Chen, Y. Zhang, T. Wan, and X. Cao. 2004. KLRL1, a novel killer cell lectinlike receptor, inhibits natural killer cell cytotoxicity. *Blood* 104:2858-2866.

136. Sallusto, F., M. Cella, C. Danieli, and A. Lanzavecchia. 1995. Dendritic cells use macropinocytosis and the mannose receptor to concentrate macromolecules in the major histocompatibility complex class II compartment: downregulation by cytokines and bacterial products. *J.Exp.Med.* 182:389-400.

137. Kato, M., T. K. Neil, G. J. Clark, C. M. Morris, R. V. Sorg, and D. N. Hart. 1998. cDNA cloning of human DEC-205, a putative antigen-uptake receptor on dendritic cells. *Immunogenetics* 47:442-450.

138. Valladeau, J., O. Ravel, C. Dezutter-Dambuyant, K. Moore, M. Kleijmeer, Y. Liu, V. Duvert-Frances, C. Vincent, D. Schmitt, J. Davoust, C. Caux, S. Lebecque, and S. Saeland. 2000. Langerin, a novel C-type lectin specific to Langerhans cells, is an endocytic receptor that induces the formation of Birbeck granules. *Immunity.* 12:71-81.

139. Geijtenbeek, T. B., R. Torensma, S. J. van Vliet, G. C. van Duijnhoven, G. J. Adema, Y. van Kooyk, and C. G. Figdor. 2000. Identification of DC-SIGN, a novel dendritic cell-specific ICAM-3 receptor that supports primary immune responses. *Cell* 100:575-585.

140. Eichler, W., P. Ruschpler, M. Wobus, and K. Drossler. 2001. Differentially induced expression of C-type lectins in activated lymphocytes. *J.Cell Biochem.* 81:201-208.

141. Dzionek, A., Y. Sohma, J. Nagafune, M. Cella, M. Colonna, F. Facchetti, G. Gunther, I. Johnston, A. Lanzavecchia, T. Nagasaka, T. Okada, W. Vermi, G.

Winkels, T. Yamamoto, M. Zysk, Y. Yamaguchi, and J. Schmitz. 2001. BDCA-2, a novel plasmacytoid dendritic cell-specific type II C-type lectin, mediates antigen capture and is a potent inhibitor of interferon alpha/beta induction. *J.Exp.Med.* 194:1823-1834.

142. Bates, E. E., N. Fournier, E. Garcia, J. Valladeau, I. Durand, J. J. Pin, S. M. Zurawski, S. Patel, J. S. Abrams, S. Lebecque, P. Garrone, and S. Saeland. 1999. APCs express DCIR, a novel C-type lectin surface receptor containing an immunoreceptor tyrosine-based inhibitory motif. *J.Immunol.* 163:1973-1983.

143. Colonna, M., J. Samaridis, and L. Angman. 2000. Molecular characterization of two novel C-type lectin-like receptors, one of which is selectively expressed in human dendritic cells. *Eur.J.Immunol.* 30:697-704.

144. Bashirova, A. A., T. B. Geijtenbeek, G. C. van Duijnhoven, S. J. van Vliet, J. B. Eilering, M. P. Martin, L. Wu, T. D. Martin, N. Viebig, P. A. Knolle, V. N. KewalRamani, Y. van Kooyk, and M. Carrington. 2001. A dendritic cell-specific intercellular adhesion molecule 3-grabbing nonintegrin (DC-SIGN)-related protein is highly expressed on human liver sinusoidal endothelial cells and promotes HIV-1 infection. *J.Exp.Med.* 193:671-678.

145. Martinon, F. and J. Tschopp. 2005. NLRs join TLRs as innate sensors of pathogens. *Trends Immunol.* 26:447-454.

146. Nusslein-Volhard, C., M. Lohs-Schardin, K. Sander, and C. Cremer. 1980. A dorso-ventral shift of embryonic primordia in a new maternal-effect mutant of Drosophila. *Nature* 283:474-476.

147. Hashimoto, C., K. L. Hudson, and K. V. Anderson. 1988. The Toll gene of Drosophila, required for dorsal-ventral embryonic polarity, appears to encode a transmembrane protein. *Cell* 52:269-279.

148. Lemaitre, B., E. Nicolas, L. Michaut, J. M. Reichhart, and J. A. Hoffmann. 1996. The dorsoventral regulatory gene cassette spatzle/Toll/cactus controls the potent antifungal response in Drosophila adults. *Cell* 86:973-983.

149. Medzhitov, R., P. Preston-Hurlburt, and C. A. Janeway. 1997. A human homologue of the *Drosophila* Toll protein signals activation of adaptive immunity. *Nature* 388:394-397.

150. Rock, F. L., G. Hardiman, J. C. Timans, R. A. Kastelein, and J. F. Bazan. 1998. A family of human receptors structurally related to Drosophila Toll. *Proc.Natl.Acad.Sci.U.S.A.* 95:588-593.

151. Takeuchi, O., T. Kawai, H. Sanjo, N. G. Copeland, D. J. Gilbert, N. A. Jenkins, K. Takeda, and S. Akira. 1999. TLR6: A novel member of an expanding toll-like receptor family. *Gene* 231:59-65.

152. Chuang, T. and R. J. Ulevitch. 2001. Identification of hTLR10: a novel human Toll-like receptor preferentially expressed in immune cells. *Biochim.Biophys.Acta* 1518:157-161.

153. Du, X., A. Poltorak, Y. Wei, and B. Beutler. 2000. Three novel mammalian toll-like receptors: gene structure, expression, and evolution. *Eur Cytokine Netw.* 11:362-371.

154. Chuang, T.-H. and R. J. Ulevitch. 2000. Cloning and characterization of a sub-family of human toll-like receptors: hTLR7, hTLR8 and hTLR9. *Eur.Cytokine Netw.* 11:372-378.

155. Zhang, D., G. Zhang, M. S. Hayden, M. B. Greenblatt, C. Bussey, R. A. Flavell, and S. Ghosh. 2004. A toll-like receptor that prevents infection by uropathogenic bacteria. *Science* 303:1522-1526.

156. Yarovinsky, F., D. Zhang, J. F. Andersen, G. L. Bannenberg, C. N. Serhan, M. S. Hayden, S. Hieny, F. S. Sutterwala, R. A. Flavell, S. Ghosh, and A. Sher. 2005. TLR11 Activation of Dendritic Cells by a Protozoan Profilin-Like Protein. *Science* 308:1626-1629.

157. Ulevitch, R. J. and P. S. Tobias. 1995. Receptor-dependent mechanisms of cell stimulation by bacterial endotoxin. *Annu.Rev.Immunol.* 13:437-457.

158. Wright, S. D., R. A. Ramos, P. S. Tobias, R. J. Ulevitch, and J. C. Mathison. 1991. CD14, a receptor for complexes of lipopolysaccharide (LPS) and LPS binding protein. *science* 252:1321-1322.

159. Jiang, Q., S. Akashi, K. Miyake, and H. R. Petty. 2000. Lipopolysaccharide induces physical proximity between CD14 and toll-like receptor 4 (TLR4) prior to nuclear translocation of NF-kappa B. *J.Immunol.* 165:3541-3544.

160. da Silva Correia, J., K. Soldau, U. Christen, P. S. Tobias, and R. J. Ulevitch. 2001. Lipopolysaccharide is in close proximity to each of the proteins in its membrane receptor complex. transfer from CD14 to TLR4 and MD-2. *J.Biol.Chem.* 276:21129-21135.

161. Shimazu, R., S. Akashi, H. Ogata, Y. Nagai, K. Fukudome, M. Kensuke, and M. Kimoto. 1999. MD-2, a molecule that confers lipopolysaccharide responsiveness on Toll-like receptor 4. *J.Exp.Med.* 189:1777-1782.

162. Akashi, S., R. Shimazu, H. Ogata, N. Yoshinori, K. Takeda, M. Kimoto, and K. Miyake. 2000. Cutting edge: cell surface expression and lipopolysaccharide signaling via the toll-like receptor 4-MD-2 complex on mouse peritoneal macrophages. *J.Immunol.* 164:3471-3475.

163. Kurt-Jones, E. A., L. Popova, L. Kwinn, L. M. Haynes, L. P. Jones, R. A. Tripp, E. E. Walsh, M. W. Freeman, D. T. Golenbock, L. J. Anderson, and R. W. Finberg. 2000. Pattern recognition receptors TLR4 and CD14 mediate response to respiratory syncytial virus. *Nat.Immunol.* 1:398-401.

164. Ohashi, K., V. Burkart, S. Flohe, and H. Kolb. 2000. Cutting edge: heat shock protein 60 is a putative endogenous ligand of the toll-like receptor-4 complex. *J.Immunol.* 164:558-561.

165. Gallucci, S. and P. Matzinger. 2001. Danger signals: SOS to the immune system. *Curr.Opin.Immunol.* 13:114-119.

166. Hasan, U., C. Chaffois, C. Gaillard, V. Saulnier, E. Merck, S. Tancredi, C. Guiet, F. Briere, J. Vlach, S. Lebecque, G. Trinchieri, and E. E. Bates. 2005. Human TLR10 is a functional receptor, expressed by B cells and plasmacytoid dendritic cells, which activates gene transcription through MyD88. *J.Immunol.* 174:2942-2950.

167. Goldstein, D. R. 2004. Toll-like receptors and other links between innate and acquired alloimmunity. *Curr.Opin.Immunol.* 16:538-544.

168. Liew, F. Y., D. Xu, E. K. Brint, and L. A. O'Neill. 2005. Negative regulation of toll-like receptor-mediated immune responses. *Nat.Rev.Immunol.* 5:446-458.

169. Akira, S. and K. Takeda. 2004. Toll-like receptor signalling. *Nat Rev.Immunol.* 4:499-511.

170. Redecke, V., H. Hacker, S. K. Datta, A. Fermin, P. M. Pitha, D. H. Broide, and E. Raz. 2004. Cutting edge: activation of Toll-like receptor 2 induces a Th2 immune response and promotes experimental asthma. *J.Immunol.* 172:2739-2743.

171. Ito, T., R. Amakawa, T. Kaisho, H. Hemmi, K. Tajima, K. Uehira, Y. Ozaki, H. Tomizawa, S. Akira, and S. Fukuhara. 2002. Interferon-alpha and interleukin-12 are induced differentially by Toll-like receptor 7 ligands in human blood dendritic cell subsets. *J.Exp.Med.* 195:1507-1512.

172. Siegal, F. P., N. Kadowaki, M. Shodell, P. A. Fitzgerald-Bocarsly, K. Shah, S. Ho, S. Antonenko, and Y. J. Liu. 1999. The nature of the principal type 1 interferon-producing cells in human blood. *Science* 284:1835-1837.

173. Biron, C. A., G. Sonnenfeld, and R. M. Welsh. 1984. Interferon induces natural killer cell blastogenesis in vivo. *J Leukoc.Biol.* 35:31-37.

174. Trinchieri, G. 2003. Interleukin-12 and the regulation of innate resistance and adaptive immunity. *Nat.Rev.Immunol.* 3:133-146.

175. Santini, S. M., C. Lapenta, M. Logozzi, S. Parlato, M. Spada, T. Di Pucchio, and F. Belardelli. 2000. Type I interferon as a powerful adjuvant for monocyte-derived dendritic cell development and activity in vitro and in Hu-PBL-SCID mice. *J Exp.Med* 191:1777-1788.

176. Kobayashi, M., L. Fitz, M. Ryan, R. M. Hewick, S. C. Clark, S. Chan, R. Loudon, F. Sherman, B. Perussia, and G. Trinchieri. 1989. Identification and purification of natural killer cell stimulatory factor (NKSF), a cytokine with multiple biologic effects on human lymphocytes. *J.Exp.Med.* 170:827-845.

177. Trinchieri, G. 1995. Interleukin-12: a proinflammatory cytokine with immunoregulatory functions that bridge innate resistance and antigen-specific adaptive immunity. *Annu.Rev.Immunol.* 13:251-276.

178. Smyth, M. J., M. Taniguchi, and S. E. Street. 2000. The anti-tumor activity of IL-12: mechanisms of innate immunity that are model and dose dependent. *J Immunol.* 165:2665-2670.

179. Reddy, P. 2004. Interleukin-18: recent advances. *Curr.Opin.Hematol.* 11:405-410.

180. Dranoff, G. 2002. GM-CSF-based cancer vaccines. *Immunol.Rev.* 188:147-154.

181. Waldmann, T. A. 2006. The biology of interleukin-2 and interleukin-15: implications for cancer therapy and vaccine design. *Nat.Rev.Immunol.* 6:595-601.

182. Munz, C., R. M. Steinman, and S. Fujii. 2005. Dendritic cell maturation by innate lymphocytes: coordinated stimulation of innate and adaptive immunity. *J.Exp.Med.* 202:203-207.

183. Mocikat, R., H. Braumuller, A. Gumy, O. Egeter, H. Ziegler, U. Reusch, A. Bubeck, J. Louis, R. Mailhammer, G. Riethmuller, U. Koszinowski, and M. Rocken. 2003. Natural killer cells activated by MHC class I(low) targets prime dendritic cells to induce protective CD8 T cell responses. *Immunity.* 19:561-569.

184. Fujii, S., K. Shimizu, M. Kronenberg, and R. M. Steinman. 2002. Prolonged IFN-gamma-producing NKT response induced with alpha-galactosylceramide-loaded DCs. *Nat.Immunol.* 3:867-874.

185. Leslie, D. S., M. S. Vincent, F. M. Spada, H. Das, M. Sugita, C. T. Morita, and M. B. Brenner. 2002. CD1-mediated gamma/delta T cell maturation of dendritic cells. *J.Exp.Med.* 196:1575-1584.

186. Gerosa, F., B. Baldani-Guerra, C. Nisii, V. Marchesini, G. Carra, and G. Trinchieri. 2002. Reciprocal activating interaction between natural killer cells and dendritic cells. *J.Exp.Med.* 195:327-333.

187. Fujii, S. i., K. Liu, C. Smith, A. J. Bonito, and R. M. Steinman. 2004. The Linkage of Innate to Adaptive Immunity via Maturing Dendritic Cells In Vivo Requires CD40 Ligation in Addition to Antigen Presentation and CD80/86 Costimulation. *J.Exp.Med.* 199:1607-1618.

188. Borg, C., M. Terme, J. Taieb, C. Menard, C. Flament, C. Robert, K. Maruyama, H. Wakasugi, E. Angevin, K. Thielemans, A. Le Cesne, V. Chung-Scott, V. Lazar, I. Tchou, F. Crepineau, F. Lemoine, J. Bernard, J. A. Fletcher, A. Turhan, J. Y. Blay, A. Spatz, J. F. Emile, M. C. Heinrich, S. Mecheri, T. Tursz, and L. Zitvogel. 2004. Novel mode of action of c-kit tyrosine kinase inhibitors leading to NK cell-dependent antitumor effects. *J Clin.Invest* 114:379-388.

189. Moretta, A. 2002. Natural killer cells and dendritic cells: rendezvous in abused tissues. *Nat.Rev.Immunol* 2:957-964.

190. Ferlazzo, G., M. Pack, D. Thomas, C. Paludan, D. Schmid, T. Strowig, G. Bougras, W. A. Muller, L. Moretta, and C. Munz. 2004. Distinct roles of IL-12 and IL-15 in human natural killer cell activation by dendritic cells from secondary lymphoid organs. *Proc.Natl.Acad.Sci.U.S.A* 101:16606-16611.

191. Ferlazzo, G., D. Thomas, S. L. Lin, K. Goodman, B. Morandi, W. A. Muller, A. Moretta, and C. Munz. 2004. The abundant NK cells in human secondary lymphoid tissues require activation to express killer cell Ig-like receptors and become cytolytic. *J Immunol* 172:1455-1462.

192. Martin-Fontecha, A., S. Sebastiani, U. E. Hopken, M. Uguccioni, M. Lipp, A. Lanzavecchia, and F. Sallusto. 2003. Regulation of dendritic cell migration to the draining lymph node: impact on T lymphocyte traffic and priming. *J Exp.Med* 198:615-621.

193. Martin-Fontecha, A., L. L. Thomsen, S. Brett, C. Gerard, M. Lipp, A. Lanzavecchia, and F. Sallusto. 2004. Induced recruitment of NK cells to lymph nodes provides IFN-gamma for T(H)1 priming. *Nat.Immunol* 5:1260-1265.

194. Lui, G., P. Carrega, and G. Ferlazzo. 2006. Principles of NK Cell/DC Crosstalk: The Importance of Cell Dialogue for a Protective Immune Response. *Transfus Med Hemother* 33:50-57.

195. Gerosa, F., A. Gobbi, P. Zorzi, S. Burg, F. Briere, G. Carra, and G. Trinchieri.

2005. The reciprocal interaction of NK cells with plasmacytoid or myeloid dendritic cells profoundly affects innate resistance functions. *J Immunol* 174:727-734.

196. Yu, Y., M. Hagihara, K. Ando, B. Gansuvd, H. Matsuzawa, T. Tsuchiya, Y. Ueda, H. Inoue, T. Hotta, and S. Kato. 2001. Enhancement of human cord blood CD34+ cell-derived NK cell cytotoxicity by dendritic cells. *J Immunol* 166:1590-1600.

197. Granucci, F., I. Zanoni, N. Pavelka, S. L. Van Dommelen, C. E. Andoniou, F. Belardelli, M. A. Degli Esposti, and P. Ricciardi-Castagnoli. 2004. A contribution of mouse dendritic cell-derived IL-2 for NK cell activation. *J Exp.Med* 200:287-295.

198. Feau, S., V. Facchinetti, F. Granucci, S. Citterio, D. Jarrossay, S. Seresini, M. P. Protti, A. Lanzavecchia, and P. Ricciardi-Castagnoli. 2005. Dendritic cell-derived IL-2 production is regulated by IL-15 in humans and in mice. *Blood* 105:697-702.

199. Jinushi, M., T. Takehara, T. Kanto, T. Tatsumi, V. Groh, T. Spies, T. Miyagi, T. Suzuki, Y. Sasaki, and N. Hayashi. 2003. Critical role of MHC class I-related chain A and B expression on IFN-alpha-stimulated dendritic cells in NK cell activation: impairment in chronic hepatitis C virus infection. *J.Immunol.* 170:1249-1256.

200. Roberts, A. I., L. Lee, E. Schwarz, V. Groh, T. Spies, E. C. Ebert, and B. Jabri. 2001. NKG2D receptors induced by IL-15 costimulate CD28-negative effector CTL in the tissue microenvironment. *J.Immunol.* 167:5527-5530.

201. Piccioli, D., S. Sbrana, E. Melandri, and N. M. Valiante. 2002. Contact-dependent stimulation and inhibition of dendritic cells by natural killer cells. *J.Exp.Med.* 195:335-341.

202. Ferlazzo, G., M. L. Tsang, L. Moretta, G. Melioli, R. M. Steinman, and C. Munz. 2002. Human dendritic cells activate resting natural killer (NK) cells and are recognized via the NKp30 receptor by activated NK cells. *J.Exp.Med.* 195:343-351.

203. Morandi, B., R. Costa, M. Falco, S. Parolini, A. De Maria, G. Ratto, M. C. Mingari, G. Melioli, A. Moretta, and G. Ferlazzo. 2005. Distinctive lack of CD48 expression in subsets of human dendritic cells tunes NK cell activation. *J Immunol* 175:3690-3697.

204. Zitvogel, L. 2002. Dendritic and natural killer cells cooperate in the control/switch of innate immunity. *J Exp.Med* 195:F9-14.

205. Vitale, M., C. M. Della, S. Carlomagno, D. Pende, M. Arico, L. Moretta, and A. Moretta. 2005. NK-dependent DC maturation is mediated by TNFalpha and IFNgamma released upon engagement of the NKp30 triggering receptor. *Blood* 106:566-571.

206. Heil, F., H. Hemmi, H. Hochrein, F. Ampenberger, C. Kirschning, S. Akira, G. Lipford, H. Wagner, and S. Bauer. 2004. Species-specific recognition of single-stranded RNA via toll-like receptor 7 and 8. *Science* 303:1526-1529.

207. Scheel, B., S. Braedel, J. Probst, J. P. Carralot, H. Wagner, H. Schild, G. Jung, H. G. Rammensee, and S. Pascolo. 2004. Immunostimulating capacities of stabilized RNA molecules. *Eur.J Immunol* 34:537-547.

208. Biron, C. A., K. B. Nguyen, G. C. Pien, L. P. Cousens, and T. P. Salazar-Mather. 1999. Natural killer cells in antiviral defense: function and regulation by innate cytokines. *Annu.Rev.Immunol.* 17:189-220.

209. Schulz, O., S. S. Diebold, M. Chen, T. I. Naslund, M. A. Nolte, L. Alexopoulou, Y. T. Azuma, R. A. Flavell, P. Liljestrom, and Reis e Sousa. 2005. Toll-like receptor 3 promotes cross-priming to virus-infected cells. *Nature* 433:887-892.

210. Zelensky, A. N. and J. E. Gready. 2005. The C-type lectin-like domain superfamily. *FEBS J.* 272:6179-6217.

211. Drickamer, K. and A. J. Fadden. 2002. Genomic analysis of C-type lectins. *Biochem.Soc.Symp.*59-72.

212. Hao, L., J. Klein, and M. Nei. 2006. Heterogeneous but conserved natural killer receptor gene complexes in four major orders of mammals. *Proc.Natl.Acad.Sci.U.S.A* 103:3192-3197.

213. Feinberg, H., D. A. Mitchell, K. Drickamer, and W. I. Weis. 2001. Structural basis for selective recognition of oligosaccharides by DC-SIGN and DC-SIGNR. *Science* 294:2163-2166.

214. Curtis, B. M., S. Scharnowske, and A. J. Watson. 1992. Sequence and expression of a membrane-associated C-type lectin that exhibits CD4-independent binding of human immunodeficiency virus envelope glycoprotein gp120. *Proc.Natl.Acad.Sci.U.S.A* 89:8356-8360.

215. Yokoyama, W. M. and B. F. Plougastel. 2003. Immune functions encoded by the natural killer gene complex. *Nat.Rev.Immunol.* 3:304-316.

216. Karlhofer, F. M., R. K. Ribaudo, and W. M. Yokoyama. 1992. MHC class I alloantigen specificity of Ly-49+ IL-2-activated natural killer cells. *Nature* 358:66-70.

217. Yokoyama, W. M. and W. E. Seaman. 1993. The Ly-49 and NKR-P1 gene families encoding lectin-like receptors on natural killer cells: the NK gene complex. *Annu.Rev.Immunol.* 11:613-635.

218. Held, W., J. Roland, and D. H. Raulet. 1995. Allelic exclusion of Ly49-family genes encoding class I MHC-specific receptors on NK cells. *Nature* 376:355-358.

219. Held, W. and D. H. Raulet. 1997. Expression of the Ly49A gene in murine natural killer cell clones is predominantly but not exclusively mono-allelic. *Eur.J.Immunol.* 27:2876-2884.

220. Westgaard, I. H., S. F. Berg, S. Orstavik, S. Fossum, and E. Dissen. 1998. Identification of a human member of the Ly-49 multigene family. *Eur.J.Immunol.* 28:1839-1846.

221. Arase, N., H. Arase, S. Y. Park, H. Ohno, C. Ra, and T. Saito. 1997. Association with FcRgamma is essential for activation signal through NKR-P1 (CD161) in natural killer (NK) cells and NK1.1+ T cells. *J.Exp.Med.* 186:1957-1963.

222. Plougastel, B. F. and W. M. Yokoyama. 2006. Extending missing-self? Functional interactions between lectin-like NKrp1 receptors on NK cells with lectin-like ligands. *Curr.Top.Microbiol.Immunol.* 298:77-89.

223. Iizuka, K., O. V. Naidenko, B. F. Plougastel, D. H. Fremont, and W. M. Yokoyama. 2003. Genetically linked C-type lectin-related ligands for the NKRP1 family of natural killer cell receptors. *Nat.Immunol.* 4:801-807.

224. Carlyle, J. R., A. M. Jamieson, S. Gasser, C. S. Clingan, H. Arase, and D. H. Raulet. 2004. Missing self-recognition of Ocil/Clr-b by inhibitory NKR-P1 natural killer cell receptors. *Proc.Natl.Acad.Sci.U.S.A* 101:3527-3532.

225. Aldemir, H., V. Prod'homme, M. J. Dumaurier, C. Retiere, G. Poupon, J. Cazareth, F. Bihl, and V. M. Braud. 2005. Cutting edge: lectin-like transcript 1 is a ligand for the CD161 receptor. *J.Immunol.* 175:7791-7795.

226. Rosen, D. B., J. Bettadapura, M. Alsharifi, P. A. Mathew, H. S. Warren, and L. L. Lanier. 2005. Cutting edge: lectin-like transcript-1 is a ligand for the inhibitory human NKR-P1A receptor. *J.Immunol.* 175:7796-7799.

227. Biassoni, R., M. Fogli, C. Cantoni, P. Costa, R. Conte, G. Koopman, A. Cafaro, B. Ensoli, A. Moretta, L. Moretta, and A. De Maria. 2005. Molecular and functional characterization of NKG2D, NKp80, and NKG2C triggering NK cell receptors in rhesus and cynomolgus macaques: monitoring of NK cell function during simian HIV infection. *J.Immunol.* 174:5695-5705.

228. Mavilio, D., J. Benjamin, D. Kim, G. Lombardo, M. Daucher, A. Kinter, E. Nies-Kraske, E. Marcenaro, A. Moretta, and A. S. Fauci. 2005. Identification of NKG2A and NKp80 as specific natural killer cell markers in rhesus and pigtailed monkeys. *Blood* 106:1718-1725.

229. Altman, J. D., P. A. Moss, P. J. Goulder, D. H. Barouch, M. G. McHeyzer-Williams, J. I. Bell, A. J. McMichael, and M. M. Davis. 1996. Phenotypic analysis of antigen-specific T lymphocytes. *Science* 274:94-96.

2 Results and Discussion

2.1 The biology of NKG2D and its ligands

2.1.1 Selective intracellular retention of virally induced NKG2D ligands by the human cytomegalovirus UL16 glycoprotein

This chapter has been published in *European Journal of Immunology* **33**(1): 194-203 (2003) by the following authors:

Stefan Welte, Christian Sinzger, Stefan Lutz, Harpreet Singh-Jasuja, Kerstin Laib Sampaio, Ute Eknigk, Hans-Georg Rammensee and Alexander Steinle.

The author of this thesis performed all experiments except following parts: HCMV infections, cloning UL16-EGFP expression construct, production of soluble recombinant proteins, generation of monoclonal antibodies and ELISA, (for details see the material section in 2.1.1.3). Harpreet Singh-Jasuja provided essential support with confocal microscopy. Parts of the work discussed in 2.1.1 have been performed during the diploma thesis of the author of this thesis. Further contributions are mentioned in the acknowledgements section.

2.1.1.1 Abstract

Human cytomegalovirus (HCMV) has evolved a multitude of molecular mechanisms to evade the antiviral immune defense of the host. Recently, using soluble recombinant molecules, the HCMV UL16 glycoprotein was shown to interact with some ligands of the activating immunoreceptor NKG2D and therefore may also function as a viral immunomodulator. However, the role of UL16 during the course of HCMV infection remained unclear. Here we demonstrate that HCMV infection of fibroblasts induces expression of all known NKG2D ligands (NKG2DL). However, solely MICA and ULBP3 reach the cellular surface to engage NKG2D, whereas MICB, ULBP1 and ULBP2 are selectively retained in the endoplasmic reticulum by UL16. UL16-mediated reduction of NKG2DL cell surface density diminished NK

cytotoxicity. Thus, UL16 functions by capturing activating ligands for cytotoxic lymphocytes that are synthesized in response to HCMV infection.

2.1.1.2 Introduction

Human cytomegalovirus (HCMV) is a β herpesvirus that establishes lifelong infections. The infection is critically controlled by the cellular immune system and associated with severe morbidity in immunocompromised individuals [**1**]. HCMV encodes a battery of immunomodulatory molecules that interfere with recognition of infected cells by NK and $CD8^+$ T cells. In a concerted action, the HCMV glycoproteins US2, US3, US6 and US11 down-regulate MHC class I surface expression to prevent recognition of HCMV derived peptides by $CD8^+$ αβ T cells (reviewed in [**2,3**]). As reduction of MHC class I molecules on the cell surface would render HCMV-infected cells susceptible to NK cell lysis, HCMV also expresses the MHC class I-like UL18 and an UL40 encoded peptide ligand for HLA-E. Both UL18 and HLA-E/UL40 suppress NK cell activity by engaging the inhibitory receptors LIR-1 and CD94/NKG2A, respectively [**4-6**].

Recently, evidence for an immunomodulatory function of the orphan HCMV UL16 glycoprotein was provided [**7**]. UL16, a 50-kDa type I transmembrane glycoprotein, is dispensable for growth of HCMV in fibroblasts and lacks homology to other known proteins [**8**]. In a search for cellular targets of UL16, Cosman and co-workers identified the MHC class I-like molecules MICB, UL16 binding protein (ULBP)1 and ULBP2 which function as ligands of the activating immunoreceptor NKG2D [**7**].

NKG2D is a member of the C-type lectin-like receptor family expressed by most human $CD8^+$ αβ T cells, γδ T cells and NK cells [9]. NKG2D homodimers form an activating immunoreceptor complex with DAP10 adaptor molecules that transmit signals through recruitment of the p85 subunit of the phosphatidylinositol-3-kinase (PI-3K) [**10,11**]. Engagement of NKG2D leads to costimulation of $CD8^+$ αβ T cells and triggers effector functions of NK cells [**7,9**,**12,13**]. NKG2D interacts with several MHC class I-like cell surface glycoproteins, hereafter collectively designated as NKG2D ligands (NKG2DL). In humans, there are two families of NKG2DL, the MIC and ULBP molecules. MICA and MICB are highly polymorphic, MHC-encoded glycoproteins and their expression can be induced by cell stress [**14,15**]. In contrast to MHC class I molecules, MIC molecules do not associate with β_2-microglobulin and antigenic peptides and their *in vivo* expression on healthy cells is highly restricted

[**14**]. However, MIC molecules were detected on many epithelial tumors and infected cells [**12,16,17**] which led to the hypothesis that they may act as danger signals [**18,19**].

ULBPs are atypical MHC class I-like molecules, since they lack a α3 domain and are attached to the cell surface via a glycosylphosphatidylinositol anchor. They are encoded by a multigene family which apparently contains at least six functional proteins [**20**]. However, NKG2D interaction has only been demonstrated for ULBP1, ULBP2 und ULBP3 [**21, 22**]. Like MIC molecules they trigger effector functions of NK cells [**7**]. Crystal structures of human NKG2D in complex with either MICA*01 or ULBP3 show that NKG2DL interact in a similar fashion with NKG2D that is reminiscent of the T cell receptor binding to MHC molecules [**23,24**]. Thus far, ULBP protein expression has only been shown for cell lines and its regulation is largely unknown [**7**].

Soluble, recombinant UL16 binds ULBP1 and ULBP2, and also MICB, but not ULBP3 and MICA *in vitro* [**7**]. This was surprising since MICA and MICB are closely related by sequence, but only distantly related to ULBPs. Binding of soluble UL16 to soluble ULBP1 impaired the ULBP1/NKG2D interaction and thus, UL16 may block the NKG2D-mediated triggering of NK cell effector functions by MICB, ULBP1 and ULBP2 [**7**].

Since these findings suggested a suppression of NKG2D mediated immunosurveillance of HCMV-infected cells by UL16, it was unexpected when another group reported that HCMV infection caused induction of MIC expression on fibroblasts allowing recognition by HCMV-specific $CD8^+$ T cells in spite of reduced MHC class I levels [**12**]. Accordingly, MIC molecules appear to function as potent enhancers of TCR mediated recognition of HCMV infected cells, thereby compensating for HCMV-mediated down-regulation of MHC class I. At this state, it was of interest to reconcile these contrasting findings on the role of NKG2DL for immunosurveillance of HCMV. Therefore, we scrutinized the induction of individual NKG2DL upon HCMV infection, the interference of UL16 with virally induced NKG2DL and its consequences for NKG2D-mediated recognition.

2.1.1.3 Materials and Methods

Cell lines, transfectants. The human embryonic kidney-derived cell line 293T and the mouse mastocytoma cell lines P815 were cultured in IMDM supplemented with

10% FCS, transfected 293T cells in 10% FCS-IMDM with 2.0 mg G418/ml. HFF and MRC-5 fibroblasts were cultured in alpha-MEM supplemented with 10% FCS. The NK cell line NKL, kindly provided by M. J. Robertson (Indiana University School of Medicine, Indianapolis, IN), was grown in RMPI 1640 with 15% FCS and 200 U/ml IL-2 (Proleukin, Chiron, Ratingen, Germany). 8 days prior to cellular cytotoxicity assays, NKL cells were cultured without IL-2. All media were supplemented with penicillin (100 IU/ml)/streptomycin (100 µg/ml) (Life Technologies, Karlsruhe, Germany), 2 mM L-glutamine and 1 mM sodium pyruvate. Transfections were performed with the FuGENE 6 reagent according to manufacturer's intructions (Roche, Mannheim, Germany).

HCMV infections. HFF, MRC-5, or 293T were grown to confluence and infected with HCMV AD169 at a multiplicity of infection (m.o.i.) of 5 to achieve an infection efficiency of ~100 %. Infections were performed with cell free supernatant from productively infected HFF cultures with 100 % late stage cytopathic effects; mock infections were done by using the same supernatants after removal of infectious virus by ultracentrifugation at 80.000xg for 70 min. Briefly, media were replaced by infectious or non-infectious supernatant, incubated for 2 h at 37ºC, and finally replaced with fresh media. Cells were then incubated at 37ºC in 5 % CO_2 for time intervals (p.i.) as indicated. The exact efficiency of infection in the respective experiment was determined at 24 h p.i. by immunodetection of viral immediate early antigen using monoclonal antibody E13 (Biosoft, Paris, France) or at 72 h p.i. by the appearance of characteristic nuclear inclusions.

UL16-EGFP expression construct. Viral DNA was prepared from HCMV AD169-infected HFF monolayers 4 p.i. by phenol/chloroform extraction. The complete HCMV-UL16 ORF excluding the stop codon was amplified using the oligonucleotides 5'ATG GAG CGT CGC CGA GGT ACG GTA C 3' (sense) and 5' GTC CTC GGT GCG TAA CCG CTG GTA T 3' (antisense) by PCR. PCR products were cloned into the EcoRI site of the EGFP-N3 vector (Clontech, Palo Alto, CA) in front of the EGFP ORF and verified by sequencing. The resulting UL16-EGFP ORF contains seventeen additional codons between the last UL16 codon (GAC) and the first EGFP codon (ATG).

Production of soluble MICA*04, MICB*02 and NKG2D tetramers. Soluble MICA was produced and purified as previously described [**21**]. In brief, the cDNA encoding

the MICA*04 ectodomain (Glu1 through Lys276) in pET20b (Novagen, Madison, WI) was introduced in *E. coli* and MICA*04 production induced by addition of isopropyl thiogalactose (IPTG). Inclusion bodies were solubilized and successively dialyzed against decreasing concentrations of urea. Refolded MICA*04 was purified by gel filtration, dialyzed against PNEA (50 mM PIPES pH 7.0, 0.15 M NaCl, 1 mM EDTA, 0.02% NaN_3) and eventually examined by SDS-PAGE and immunoblotting. Accordingly, the MICB*02 ectodomain was amplified with oligonucleotides 5' ACA TGC ATA TGG AGC CCC ACA GTC TTC G-3' (sense) and 5'-CTG ACT CGA GCT TCC CAG AGG GCA CAG GGT G-3' (anti-sense), cloned in pET21a (Novagen) via NdeI and XhoI, and soluble MICB*02 produced as described above. The cDNA fragment encoding the extracellular portion of human NKG2D (Asn80 through Thr147) was amplified with oligonucleotides 5´-ATC ATA TGG AAA GTT ACT GTG GCC CAT GTC-3`(sense) and 5`- ATA AGC TTA CTC GTG CCA CTC GAT CTT TTG AGC CTC GAA GAT GTC GTT CAG AGT CCT TTG CAT GCA GAT GTA TG-3` (anti-sense) adding a BirA recognition sequence at the carboxyterminus and ligated into pET20b. Soluble NKG2D was produced in *E. coli* as described above. Biotinylation of NKG2D was done overnight at 27ºC with the BirA enzyme (Avidity, Denver, CO) according to manufacturer's instruction. Excess biotin was removed by FPLC with a Superdex S75 HL 26/60 column and biotinylated NKG2D tetramerized by gradual addition of phycoerythrin-conjugated streptavidin (Molecular Probes, Leiden, Netherlands) over 4 h.

Generation of monoclonal antibodies. The murine P815 mastocytoma cell line was transfected using FuGENE 6 with full length cDNA of MICA*01, MICA*04, MICB*02, ULBP1, ULBP2 and ULBP3 in RSV.5 neo, respectively [**21**]. Transfectants were selected with 1 mg/ml G418 and expression of the respective NKG2DL mRNA was verified by RT-PCR. BALB/c mice were immunized either with a mixture of MICA*01-, MICA*04-, and MICB*02- or ULBP1-, ULBP2-, and ULBP3- expressing P815 cells. Splenocytes of immunized mice were fused with P3X63Ag8.653 myeloma cells. Hybridoma supernatants were tested by indirect immunofluorescence using a FACSCalibur (Becton Dickinson, Heidelberg, Germany) for selective binding to P815-NKG2DL transfectants and to COS cells transiently transfected with the various NKG2DL cDNA. Hybridoma producing NKG2DL-specific mAbs were subcloned twice and immunoglobulins isotyped using an isotyping kit (Roche). BAMO-1 (IgG_1) and BAMO-3 (IgG_{2a}) recognize MICA and MICB, AMO-1 (IgG_1) is MICA specific, BMO-1 (IgG_1) and BMO-2 (IgG_{2a}) MICB

specific, AUMO-1 (IgG_1) ULBP1-specific, BUMO-1 (IgG_1) ULBP2-specific and CUMO-1 and CUMO-2 (IgM) ULBP3-specific.

Real-time RT-PCR. Total fibroblast RNA was prepared using TRIZOL (Life Technologies) followed by DNase I treatment and reverse transcription using SuperScript RTII (Invitrogen, Karlsruhe, Germany) according to the manufacturer's protocol. The resulting cDNA was amplified with NKG2DL, UL16 and 18S rRNA specific primer pairs in duplicates (40 cycles, 95ºC x 15 s, 60ºC x 1 min) using SYBRGreen chemistry on the ABI PRISM 7000 Sequence Detection System (Applied Biosystems, Weiterstadt, Germany). Samples were independently analyzed 2 to 3 times. Primers were selected to flank an intron, where possible, and specificity was validated using cloned NKG2DL. Data analysis was done by using the ΔC_T method for relative quantification. Similar amplification efficiencies for NKG2DL and 18S were demonstrated by analyzing serial cDNA dilutions with values of the slope of log cDNA amount vs. ΔC_T of < 0.1. Oligonucleotide sequences (forward; reverse) were for 18S rRNA: 5´-CGGCTACCACATCCAAGGAA-3´; 5´-GCTGGAATTACCGCGGCT-3´; MICA: 5´-CCTTGGCCATGAACGTCAGG-3´; 5´-CCTCTGAGGCCTCRCTGCG-3´; MICB: 5´-ACCTTGGCTATGAACGTCACA-3´; 5´-CCCTCTGAGACCTCGCTGC A-3´; ULBP1: 5´-GTACTGGGAACAAATGCTGGAT-3´; 5´-AACTCTCCTCATC TGCCAGCT-3´; ULBP2: 5´-TTACTTCTCAATGGGAGACTGT-3´; 5´-TGTGCCT GAGGACATGGCGA-3´; ULBP3: 5´-CCTGATGCACAGGAAGAAGAG-3´; 5´-TATGGCTTTGGGTTGAGCTAAG-3´; UL16: 5´-TAATCGAGCGCCTCTACGTC C-3´; 5´-AAGGTCGCGGACAGTTCCTCG-3´. PCR products were analyzed on 3% agarose gels for purity.

Flow cytometry. Cells were incubated with NKG2DL-specific mAb or appropriate mouse immunoglobulin isotypes and then, after washing, with goat anti-mouse-PE conjugate (1:100) (Jackson ImmunoResearch Laboratories, West Grove, PA, USA) as secondary reagent. PE-labeled NKG2D tetramers were used at 5 µg/ml. Intracellular staining was done using Cytofix/Cytoperm following the manufacturer's protocol (BD PharMingen, Heidelberg, Germany). Samples were analyzed on a FACSCalibur.

Confocal microscopy. 293T-UL16-EGFP cells were seeded on round cover slips in

12-well culture plates and grown to ~50% confluency. Coverslips were washed in PBS and cells fixed with methanol/aceton (1:1, -20°C) for 20 min. After a washing step, cells were incubated for 20 min with the respective primary mAb. In case of Figs. 4C, E and F, cells were first stained with W6/32 (anti-MHC class I), then washed and fixed. As organelle-specific markers for ER and lysosomes, an anti-PDI mAb (Stressgen Biotechnologies, Victoria BC, Canada) and anti-lamp-1 (kindly provided by M. Fukuda, La Jolla Research Center, La Jolla, CA), respectively, were used. For detection, fixed cells were incubated with Alexa 546-conjugated anti-mouse IgG (Molecular Probes). Microscopy was done with a ZEISS LSM 510 laser scanning microscope (Carl Zeiss, Göttingen, Germany). "bleeding" of emission into other detection channels was excluded using the multitracking modus of the LSM 510. Thickness of the optical plane was adjusted by the pinhole to be <0.7 µm.

Cellular cytotoxicity assays. Cytotoxicity was analyzed in a 24 h ^{51}Cr assay. Target cells were labeled with 50 µCi of ^{51}Cr (Amersham, Freiburg, Germany) for 2 h at 37°C and washed three times. In blocking experiments mAb were added at 10 µg/ml during labelling procedure. Effector cells were titrated on target cells and incubated for 24h at 37°C. Spontaneous release of target cells alone was less than 15% of the maximum release taken from target cells lyzed in 1% Triton X-100. Percentage of lysis was calculated as follows: 100 x (experimental release – spontaneous release): (maximum release – spontaneous release). Experiments were performed in duplicates.

ELISA. For the detection of sMICA plates were coated with the capture anti-MICA mAb AMO-1 at 2 µg/ml in PBS, then blocked by addition of 15% BSA-PBS for 2 h at 37°C and washed. Next, the standard (recombinant MICA*04 in 7.5% BSA-PBS) and samples were incubated for 2h at 37° C, plates were washed and the detection mAb BAMO-3 added at 5 µg/ml in 7.5% BSA-PBS and incubated for 2h at 37° C. Plates were then washed and incubated with anti-mouse IgG_{2a}-HRP (1:8000 in 7.5% BSA-PBS) for 1 h at 37° C. Finally, plates were washed, developed using the TMB Peroxidase Substrate System (KPL, Gaithersburg, MD), and the absorbance measured at 450 nm. Results are shown as means of duplicates using recombinant sMICA*04 as a standard. A similar ELISA was established to detect sMICB by using the anti-MICA/B mAb BAMO-1 as capture antibody and the MICB specific mAb BMO-2 as detection antibody. For standardization, recombinant sMICB*02 was used.

For analysis of release of sMICA and MICB, confluent 293T , 293T-UL16 and 293T-

EGFP cells were cultured for 5 days, supernatants removed, tenfold concentrated using Centriprep (Amicon, Bedford, MA) and subjected to ELISA.

2.1.1.4 Results

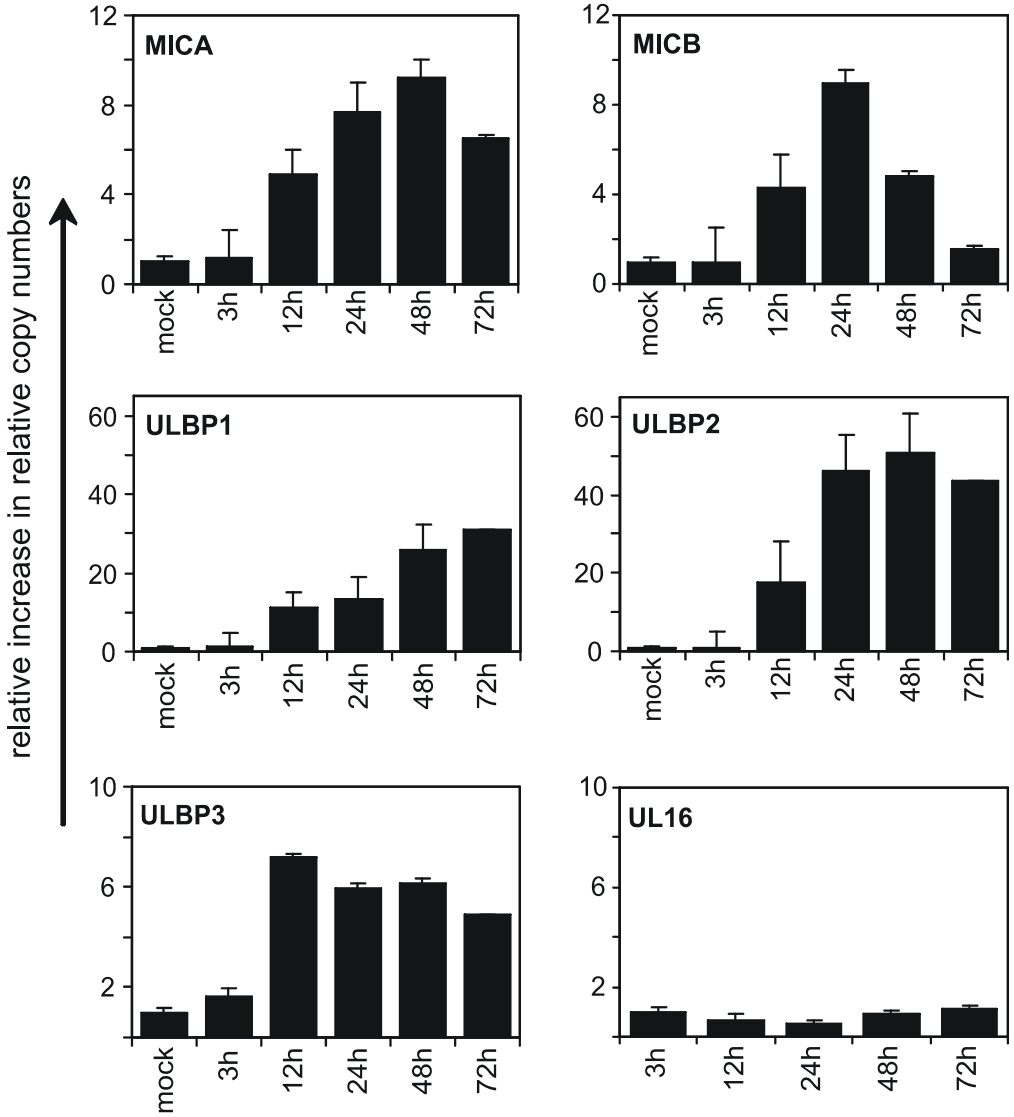

Figure 2.1. Induction of NKG2DL mRNA expression upon HCMV infection. MRC-5 monolayers were infected with HCMV AD169 3, 12, 24, 48 and 72 h, respectively, before RNA extraction. Relative copy numbers were determined by real-time PCR. Increase in relative copy numbers was calculated by defining relative copy numbers of mock-infected cells as 1, except for UL16 where relative copy numbers at 3 h p.i. were defined as 1.

Induction of NKG2DL expression upon HCMV infection

HCMV infection has been reported to induce MIC cell surface expression on fibroblasts [**12**]. However, it remained unclear whether HCMV infection induces surface expression of both human MIC species, MICA and MICB, and how it affects

ULBP expression. To investigate HCMV-induced expression of all known NKG2DL, we established NKG2DL specific real-time PCR using sets of oligonucleotides specific for MICA, MICB, ULBP1, ULBP2, and ULBP3, respectively.

Human MRC-5 fibroblasts were infected with HCMV strain AD169 and harvested at 3, 12, 24, 48 and 72 h p.i. Relative NKG2DL mRNA levels of infected fibroblasts were quantified by real-time PCR. Expression of all NKG2DL was strongly induced after HCMV infection and increased mRNA levels were detected already 12 h p.i. (**Figure 2.1**) However, kinetics and induction rates substantially varied between the individual ligands. Both, MICA and MICB were induced about tenfold, but whereas MICA levels gradually reached a maximum at 48 h and slightly dropped at 72 h, kinetics of MICB were faster with a maximum at 24 h followed by a sharp decline. ULBP3 levels rose to about sixfold at 12 h p.i. and remained stable thereafter. In contrast, ULBP1 mRNAs gradually accumulated over 72 h to about 30 fold above background. ULBP2 mRNA levels were most dramatically induced to about 50 fold at 24 h p.i. and remained high until 72 h p.i. Altogether, all NKG2DL were clearly induced already 12 h p.i., but their maxima varied between 12 and 72 h p.i. To corroborate these results, we also analyzed mRNA levels of HCMV-infected primary human foreskin fibroblasts (HFF). Similarly to MRC-5, expression of all NKG2DL was strongly induced by HCMV infection and kinetics characteristically varied between the individual NKG2DL as described above (data not shown).
Thus, HCMV infection concomitantly induces mRNA expression of all NKG2DL resulting in drastically increased NKG2DL mRNA levels throughout early and late stages of HCMV infection.

Restricted NKG2DL surface expression on HCMV-infected fibroblasts

Having shown that HCMV infection is paralleled by a pronounced increase in NKG2DL mRNA levels, we next investigated NKG2DL cell surface expression by HCMV infected fibroblasts. In order to survey expression of NKG2DL, we generated a panel of mAb specific for MICA, MICB, ULBP1, ULBP2, and ULBP3, respectively, by immunizing BALB/c mice with P815 cells transfected with the respective NKG2DL cDNAs. Specificity of the antibodies was demonstrated on P815, COS, and C1R cells transfected with the respective antigens. For MICA and MICB specific mAb, direct and mutually exclusive binding to recombinant MICA and MICB, respectively, was demonstrated by ELISA (data not shown). HFF and MRC-5 cells were infected with HCMV strain AD169 and surface NKG2DL expression analyzed at

24 h, 48 h, and 72 h p.i. by flow cytometry. For both, HFF and MRC-5, low constitutive expression of MICA and ULBP2 was detected, but not for MICB, ULBP1 and ULBP3 (**Figure 2.2a** and data not shown). No significant changes were observed 24h and 48h p.i., respectively (data not shown), but 72 h p.i. MICA surface expression was clearly increased, whereas ULBP2 was no more detectable. No MICB and ULBP1 molecules were detected at any time post-infection on the cell surface, whereas a pronounced expression of ULBP3 was detected 72 h p.i.

Since NKG2DL mRNA induction was observed for all NKG2DL, we wondered whether MICB, ULBP1 and ULBP2 molecules were selectively retained in HCMV-infected cells. To test interference of HCMV with NKG2DL expression, 293T cells which constitutively express all five NKG2DL on the cell surface were infected with HCMV strain AD169. In contrast to HFF and MRC-5 fibroblasts, infection of 293T cells was only partial as judged by detection of viral antigens and cytopathic effects.

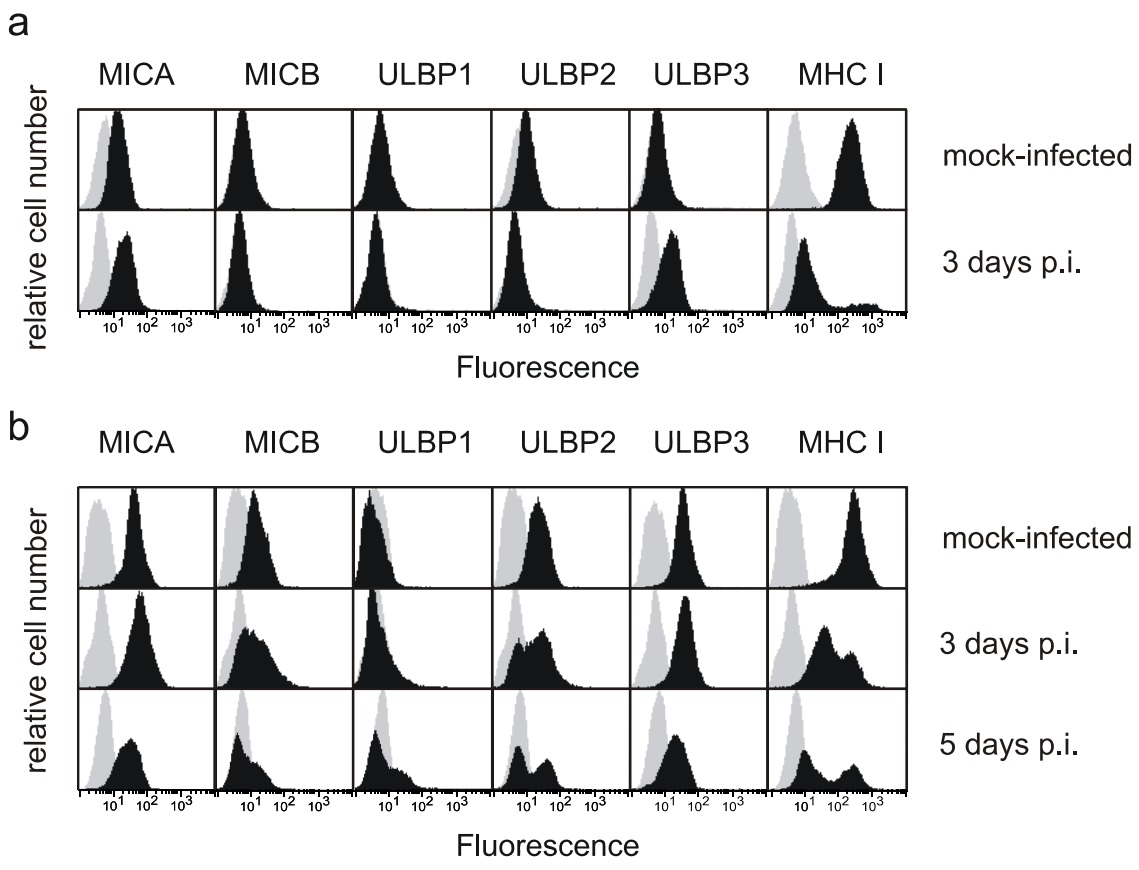

Figure 2.2. Selective NKG2DL surface expression upon HCMV infection. The human primary MRC-5 fibroblasts (**a**) and the 293T kidney fibroblast cell line (**b**) were infected with HCMV AD169 or mock-infected and NKG2DL surface expression monitored with NKG2DL mAbs in flow cytometry. The following mAbs were used: AMO-1 (MICA), BMO-1 (MICB), AUMO-1 (ULBP1), BUMO-1 (ULBP2), CUMO-1 (ULBP3) and W6/32 (MHC class I).

This is also reflected by partial down-regulation of MHC class I molecules (**Figure 2.2 b**). Analysis of NKG2DL cell surface expression three and five days p.i. revealed that

MICA and ULBP3 expression remained unaffected by the HCMV infection. However, in parallel to MHC class I down-regulation, MICB and ULBP2 vanished on a subpopulation of 293T cells. HCMV-associated down-regulation was most impressive for ULBP2 where two distinct populations became apparent five days p.i. These results demonstrate that HCMV infection is associated with increased cell surface expression of MICA and ULBP3 and a loss of cell surface MICB and ULBP2.

UL16 inhibits cell surface expression of MICB, ULBP1 and ULBP2

Selective down-regulation of MICB and ULBP2, but not MICA and ULBP3 perfectly matches the binding preferences described for a recombinant soluble variant of the HCMV glycoprotein UL16 [**7**]. The UL16 ORF encodes a heavily glycosylated 230 amino acid (aa) protein of 50 kDa [**8**]. It is predicted as a type I transmembrane protein with an N-terminal ER signal sequence, a large luminal domain (163 aa) containing eight potential N-linked glycosylation sites followed by a short transmembrane domain (17 aa) and positively charged cytoplasmic domain (25 aa).

In order to investigate whether down-regulation of MICB and ULBP2 surface expression can be attributed to UL16, we generated an UL16 expression construct where the putative full length UL16 open reading frame was fused at the carboxyterminus to enhanced green fluorescent protein (EGFP). 293T cells were stably transfected with plasmids encoding UL16-EGFP or EGFP, respectively.

For controlled assessment of changes in NKG2DL expression, we used transfectants representing mixtures of neomycin resistant UL16-EGFP positive and UL16-EGFP negative 293T cells. Cell surface expression of MICB, ULBP1 and ULBP2 was strongly reduced on UL16-EGFP expressing transfectants versus UL16-EGFP negative transfectants (**Figure 2.3a**). In contrast, expression of MICA, ULBP3 and MHC class I molecules did not differ between UL16-EGFP expressing and non-expressing cells. Surface expression of NKG2DL was not altered on 293T-EGFP transfectants and comparable to untransfected 293T cells (data not shown). Failure to detect MICB, ULBP1 and ULBP2 on the cell surface of 293T-UL16-EGFP transfectants may be either due to their intracellular retention and/or degradation or to masking of the respective mAb epitopes by UL16. To address this issue we analyzed intracellular NKG2DL expression of permeabilized 293T-UL16-EGFP cells. Staining intensities for MICA and MHC class I did not significantly differ between intact and permeabilized UL16-EGFP positive and negative cells (**Figure 2.3b** and data not shown). In contrast, intracellular stainings of UL16-EGFP positive cells detected significantly higher MICB and ULBP2 levels as compared to cell surface

analysis and were almost (MICB) or fully equivalent (ULBP2) to levels of UL16-EGFP negative cells. These results strongly suggested that MICB and ULBP2 are intracellularly retained by UL16 and do not reach the cell surface (**Figure 2.3b**.

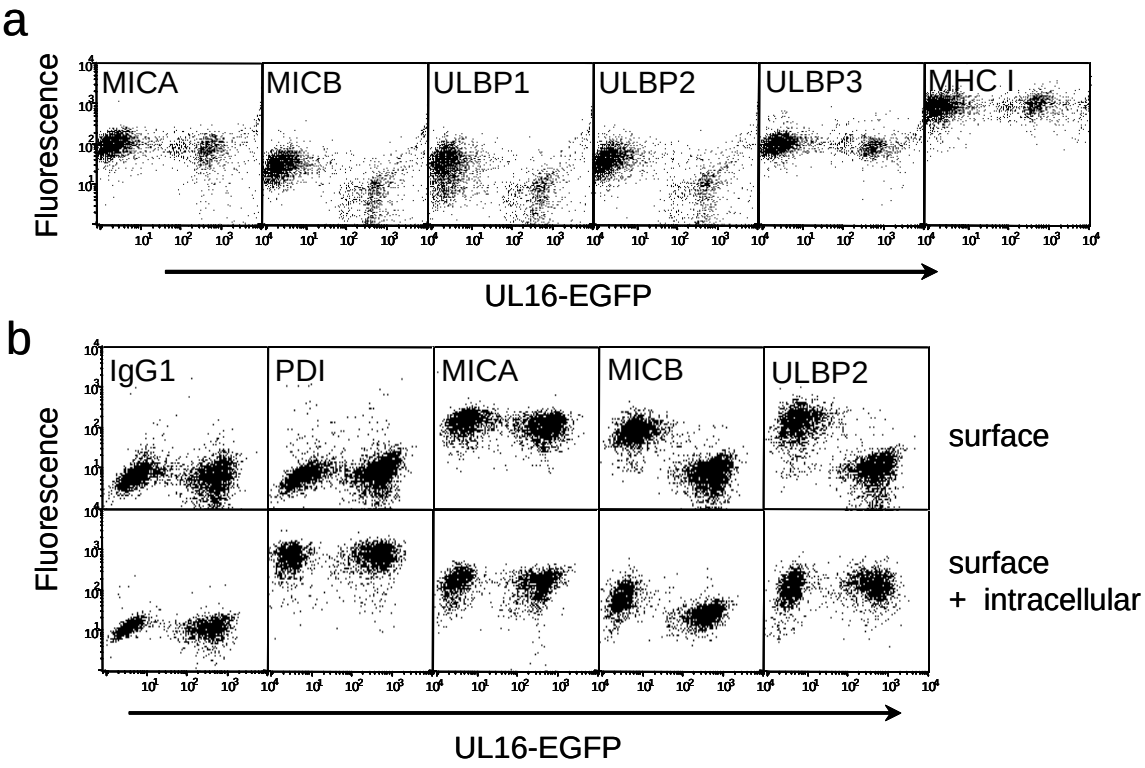

Figure 2.3. UL16 impairs surface expression of MICB, ULBP1 and ULBP2. Cell surface (**a**) and total NKG2DL expression (**b**) of intact and permeabilized UL16-EGFP transfected 293T cells, respectively, were detected with NKG2DL specific mAbs. Following mAbs were used: AMO-1 (MICA), BMO-1 (MICB), AUMO-1 (ULBP1), BUMO-1 (ULBP2), CUMO-2 (ULBP3) and W6/32 (MHC class I). Cell permeability and integrity, respectively, was monitored by PDI-staining.

To corroborate these results we analyzed soluble MICA (sMICA) and MICB (sMICB) in the supernatants of 293T cells. We observed recently, using a highly sensitive ELISA for sMICA, that MICA molecules are shed from the surface of tumor cells by metalloproteinases [**25**]. To extend these studies, we also established a Sandwich-ELISA for MICB with a comparable range of sensitivity. Here, we employed these ELISAs to analyze interference of UL16 with the release of MIC molecules. In full agreement with our other observations, we found no differences for release of sMICA between 293T, 293T-EGFP and 293T-UL16-EGFP cells (**Figure 2.4**). However, supernatants of 293T-UL16-EGFP cells contained 10-20 fold less MICB in comparison to 293T and 293T-EGFP cells, again suggesting that cell surface transport of MICB molecules is selectively inhibited by UL16.

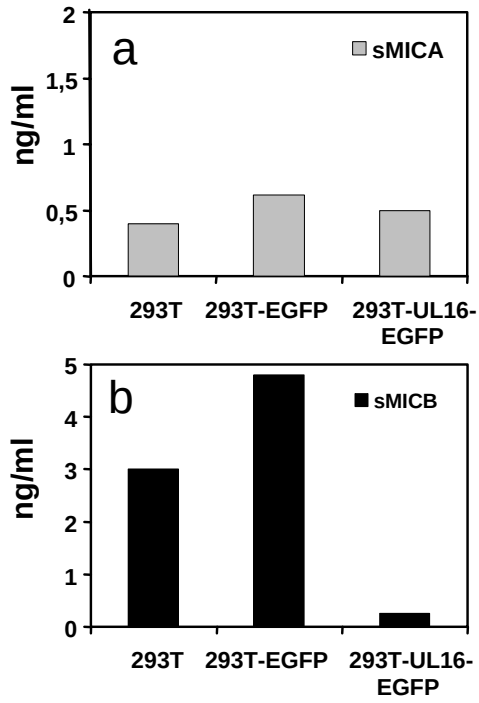

Figure 2.4. UL16 selectively blocks release of sMICB. Release of sMICA and sMICB in culture supernatants by 293T, 293T-EGFP and 293T-UL16-EGFP was determined by a sMICA and a sMICB specific Sandwich-ELISA, respectively.

Subcellular localization of UL16

We used confocal microscopy to visualize the different fate of MICA and MICB in UL16 expressing cells and to localize UL16 intracellularly. Confirming flow cytometric results, MICA surface and intracellular staining was observed for both UL16-EGFP positive and negative 293T cells (**Figure 2.5a**). In contrast, surface and bright intracellular MICB staining was detected only for UL16-EGFP negative 293T cells, whereas only residual intracellular MICB was detected in UL16-EGFP positive cells (**Figure 2.5b**).

These data further substantiated selective intracellular retention of MICB, but not MICA by UL16. To address cellular localization of UL16 we analyzed colocalization of UL16-EGFP with the ER-resident Protein-Disulfide-Isomerase (PDI), the lysosomal lamp-1 protein and surface MHC class I, respectively, in confocal microscopy. There was a prominent colocalization of UL16-EGFP with PDI expression (**Figure 2.5c**), a partial colocalization with lamp-1 (data not shown), but none with cell surface MHC class I molecules (**Figure 2.5d-f**).

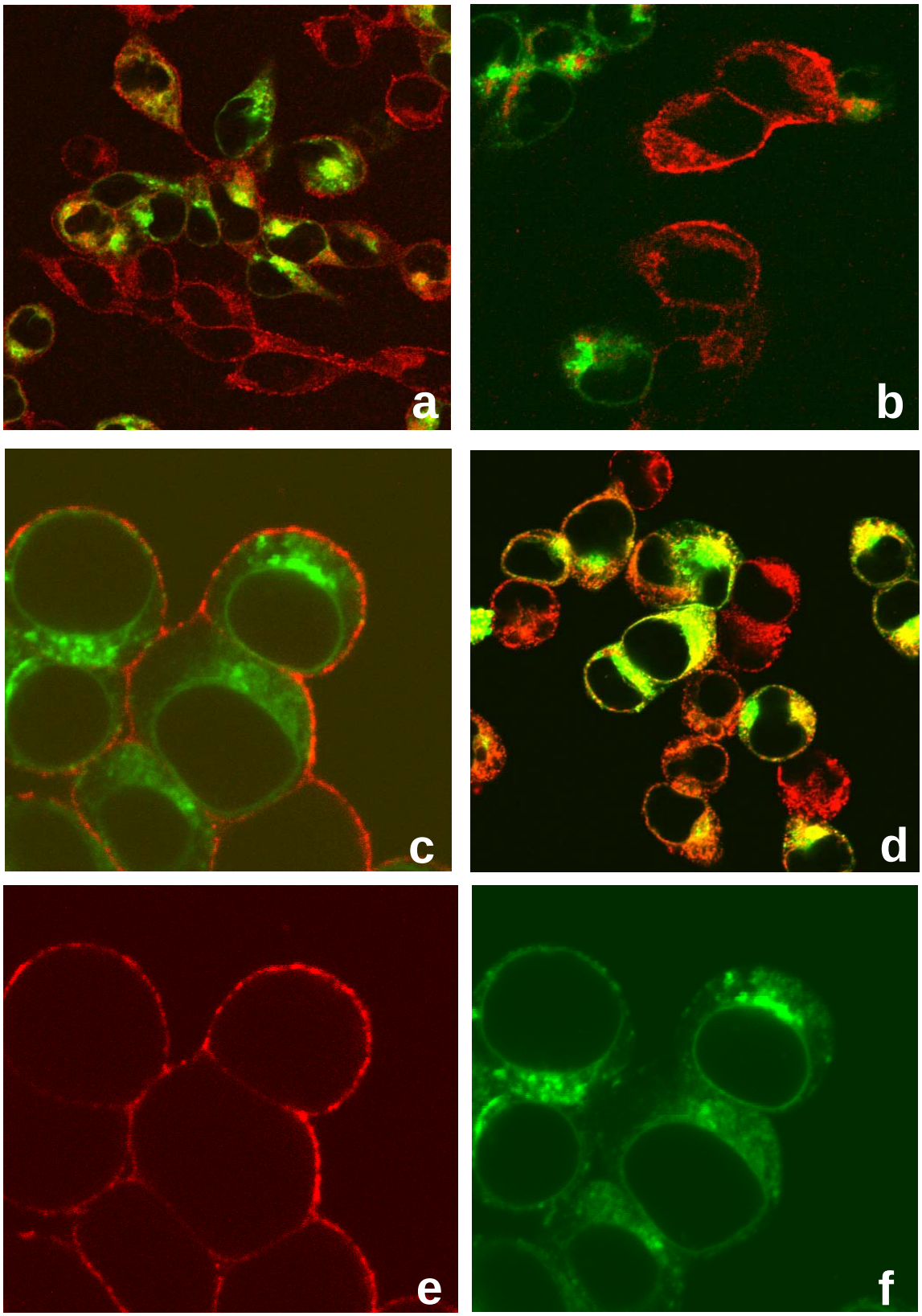

Figure 2.5. Subcellular localization of UL16, MICA and MICB in 293T-UL16-EGFP cells. Confocal microscopy was implemented for colocalization studies of MICA (**a**), MICB (**b**), surface MHC class I (**c**), PDI (**d**) (all in red) with UL16-EGFP (green). Colocalization appears in yellow. For demonstration of mutually exclusive surface MHC class I and UL16-EGFP localization, single color photographs showing only surface MHC I (**e**) or UL16-EGFP stainings (**f**) were added. In **a**, **b** and **d** approximately 50% of the cells were UL16-EGFP negative 293T transfectants.

These results suggest that UL16 is mainly resident in the ER which is in concordance with predictions based on the UL16 primary sequence and the intracellular retention of MICB and ULBP2. They also indicate that UL16 does not reach the cell surface to block NKG2DL interaction with NKG2D in a direct fashion as proposed elsewhere [**25**]. At present, we do not know whether lysosomal localization is a feature of UL16 or simply an experimental artifact due to overexpression of the UL16-EGFP fusion protein. Unambiguous organelle-assignment of UL16 has to be addressed in future studies when UL16 specific reagents become available.

UL16 mediated NKG2DL down-regulation reduces NK cell reactivity

The sole function known for MICB, ULBP1 and ULBP2 consists in their capacity to ligate NKG2D and thereby to trigger NK cells and costimulate $CD8^+$ T cells [**7,9,12,13**]. To address the impact of UL16 on NKG2D-mediated immune responses, we analyzed binding of soluble human NKG2D tetramers to 293T-UL16-EGFP transfectants. As expected, binding levels of sNKG2D were significantly reduced on UL16-EGFP expressing as compared to UL16-EGFP negative transfectants (**Figure 2.6a**).

Next, we investigated whether UL16-mediated reduction of surface NKG2DL levels modulates NKG2D mediated recognition by NK cells. In first experiments, we analyzed recognition of 293T-EGFP and 293T-UL16-EGFP by polyclonal NK cells from healthy donors. However, both 293T transfectants were highly susceptible to lysis and addition of anti-NKG2D mAb did not greatly reduce lysis suggesting that 293T cells express several other activating ligands besides NKG2DL recognized by the various activating receptors on polyclonal NK cells (data not shown). Therefore, we used the NK cell line NKL which has been well characterized for its NKG2D expression and NKG2D-mediated effector functions [**9**]. In cytotoxicity assays, both 293T and 293T-EGFP cells were lyzed by NKL whereas lysis of 293T-UL16 cells was strongly reduced (**Figure 2.6b**). As MICA and ULBP3 remain the only known NKG2DL surface-expressed on 293T-UL16-EGFP cells, we addressed NK cytotoxicity in the presence of anti-MICA and anti-ULBP3 antibodies. Blocking interaction of NKG2D with MICA and ULBP3 completely abrogated lysis of 293T-UL16 cells, and reduced lysis of 293T and 293T-EGFP cells by NKL (**Figure 2.6c**).

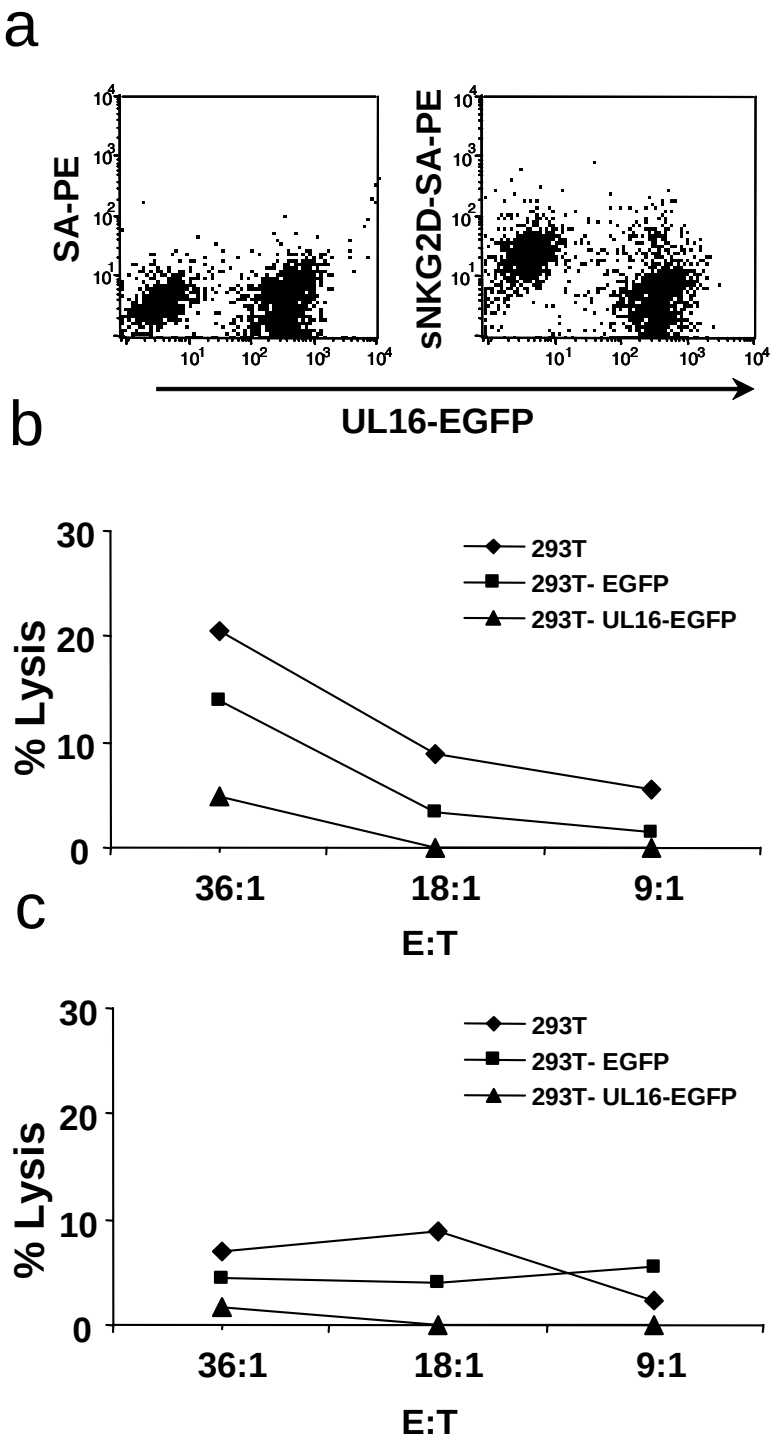

Figure 2.6. Reduced NKG2DL expression impairs NK cytotoxicity. (**a**) Binding of soluble NKG2D tetramers is reduced on UL16-EGFP expressing as compared to UL16-EGFP non-expressing 293T cells (right panel). No staining was observed with streptavidin-PE (SA-PE) only (left panel). Lysis of 293T, 293T-EGFP and 293T-UL16-EGFP pretreated with AMO-1 and CUMO-1 (**c**) or irrelevant isotype-matched Ab (**b**) by NKL cells.

2.1.1.5 Discussion

HCMV implements diverse molecular strategies to escape anti-viral NK and T cell responses. The concerted action of US2, US3/US11 and US6 proteins, for example, results in down-regulation of MHC class I molecules on HCMV infected cells minimizing $CD8^+$ T cell reactivity [**2,3**]. In addition, products of the UL18 and UL40 ORF are thought to provide protection against NK cell killing by constituting ligands engaged by inhibitory receptors on NK cells [**4-6**]. The HCMV UL16 glycoprotein now emerges as antagonist of another immune surveillance principle: the surface expression of cell-stress induced ligands of activating NK cell receptors. Our data demonstrate that UL16 intracellularly retains ligands of the activating receptor NKG2D which are induced in the course of HCMV infection. Cosman and colleagues proposed two models of action for UL16: intracellular retention of NKG2DL or masking NKG2D binding sites of NKG2DL on the cell surface [**25**]. Although our data clearly support the first model, we cannot rule out that some UL16 molecules reach the cell surface.

We also demonstrate that expression of all five known NKG2DL is strongly induced upon HCMV infection. Only three of them (MICB, ULBP1, ULBP2) are retained by UL16, whereas MICA and ULBP3 reach the cell surface (**Figure 2.7**). These data reconcile the description of UL16 as an HCMV encoded NKG2D antagonist with findings that $CD8^+$ T cell recognition of HCMV infected fibroblasts is augmented by virally induced MIC expression compensating for MHC class I down-regulation [**7,12**]. The selective binding of UL16 to NKG2DL is intriguing from a structural point of view, since MICA and MICB are closely related by sequence (~85% amino acid identity), but quite dissimilar from ULBPs (~25% identity) which are also more divergent amongst each other (~55% identity). One might speculate that UL16, as does NKG2D, rather recognizes a common structural element of NKG2DL, which is altered in MICA and ULBP3, than an array of particular amino acid side chains. MICA and MICB appear to be products of a recent gene duplication [**26**] and may have consequently evolved differently under selective pressure, one of which may be UL16 binding. Interestingly, MICA and ULBP3, but not MICB, ULBP1 and ULBP2, contain an N-linked glycosylation site at position 8 that is located in the center of the β-pleated sheet platform [**27**] and may be involved in precluding UL16 binding.

Selective binding of UL16 to NKG2DL may also have been evolved as a consequence of different functions of the respective NKG2DL. For example, MIC and ULBP

molecules may also serve as ligands for receptors other than NKG2D. In fact, a recent report provides direct evidence for binding of MICA tetramers to γδ T cell receptors of some Vδ1 γδ T cells [**28**]. Of note, some allelic MICA variants and ULBP3 apparently have a lower affinity for NKG2D as compared to MICB, ULBP1 and ULBP2 [**21,22**]. Thus, UL16 is selective for higher affinity NKG2DL which may be sufficient to dampen a NKG2D-mediated anti-viral response. In this context, it will be of interest to compare anti-HCMV immune responses in individuals homozygous for low versus high affinity MICA allelic variants.

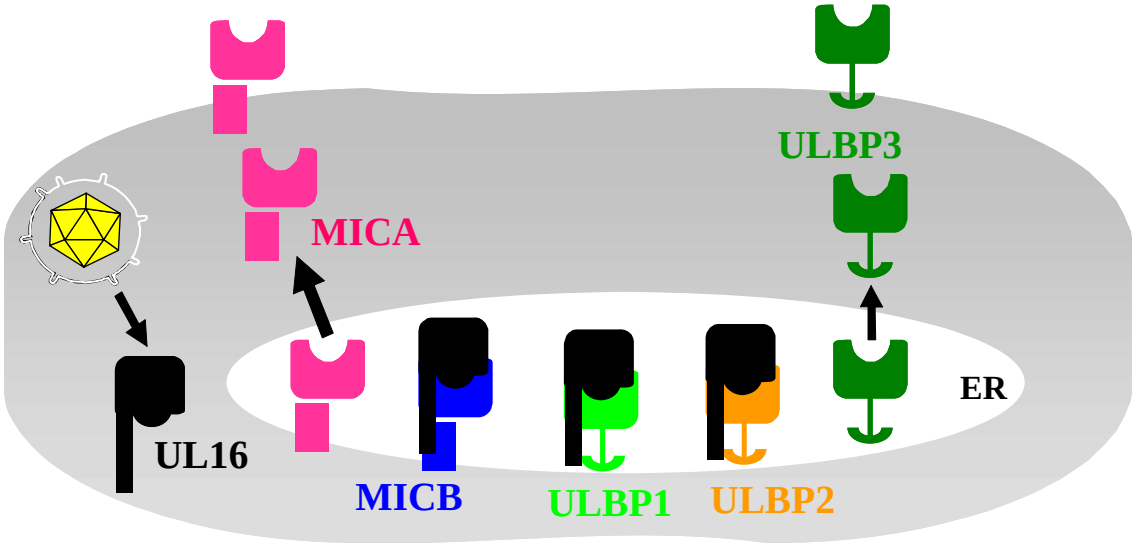

Figure 2.7. Model of UL16 function. Upon HCMV infection, expression of all five NKG2DL is induced, but only MICA and ULBP3 reach the cell surface. HCMV-encoded UL16 selectively binds to MICB, ULBP1, and ULBP2, retaining them in the ER.

An urging question concerns the redundancy of NKG2DL. Besides differences in affinity for NKG2D and the interaction of MIC molecules with some γδ T cell receptors, there are no features known distinguishing NKG2DL with respect to their function. In particular, little is known about differences in regulation of gene expression. We show that expression of all NKG2DL is induced upon HCMV infection, but kinetics and induction rates varied considerably between the individual ligands. For example, induction of MICB was faster and shorter-lived as compared to MICA. This is in parallel with previous findings on induction of MICA and MICB by heat-shock [**14**]. Future studies have to establish whether NKG2DL are distinct in their expression kinetics. It also remains to be clarified what molecular events drive induction of NKG2DL expression in response to HCMV infection. It is known that

infection of adenoviruses and herpes viruses is accompanied by a cell-stress response and since promoters of MIC genes contain a heat-shock response element, expression of MIC genes during HCMV infection has been suggested to be regulated via heat-shock factors [**12,29**].

Taken together, our data provide another example for the delicate balance between host immune defense mechanisms and viral evasion strategies. They also strengthen the notion of the NKG2D/NKG2DL system as a surveillance system for dysfunctional cells.

2.1.1.6 Acknowledgements

We would like to thank Oliver Schoor and Toni Weinschenk for eminent support with the real-time PCR. We also thank Iris Kehrer (now Seyboldt) for excellent technical assistance. This work was supported in part by the fortüne programme of the Faculty of Medicine of the Eberhard-Karls-Universität Tübingen to A.S. (1010-0-0).

2.1.1.7 References

1. Walter, E. A., P. D. Greenberg, M. J. Gilbert, R. J. Finch, K. S. Watanabe, E. D. Thomas, and S. R. Riddell. 1995. Reconstitution of cellular immunity against cytomegalovirus in recipients of allogeneic bone marrow by transfer of T-cell clones from the donor. *N.Engl.J.Med.* 333:1038-1044.

2. Alcami, A. and U. H. Koszinowski. 2000. Viral mechanisms of immune evasion. *Immunol.Today* 21:447-455.

3. Tortorella, D., B. E. Gewurz, M. H. Furman, D. J. Schust, and H. L. Ploegh. 2000. Viral subversion of the immune system. *Annu.Rev.Immunol.* 18:861-926.

4. Wang, E. C., B. McSharry, C. Retiere, P. Tomasec, S. Williams, L. K. Borysiewicz, V. M. Braud, and G. W. Wilkinson. 2002. UL40-mediated NK evasion during productive infection with human cytomegalovirus. *Proc.Natl.Acad.Sci.U.S.A* 99:7570-7575.

5. Tomasec, P., V. M. Braud, C. Rickards, M. B. Powell, B. P. McSharry, S.

Gadola, V. Cerundolo, L. K. Borysiewicz, A. J. McMichael, and G. W. Wilkinson. 2000. Surface expression of HLA-E, an inhibitor of natural killer cells, enhanced by human cytomegalovirus gpUL40. *Science* 287:1031.

6. Cosman, D., N. Fanger, L. Borges, M. Kubin, W. Chin, L. Peterson, and M. L. Hsu. 1997. A novel immunoglobulin superfamily receptor for cellular and viral MHC class I molecules. *Immunity* 7:273-282.

7. Cosman, D., J. Mullberg, C. L. Sutherland, W. Chin, R. Armitage, W. Fanslow, M. Kubin, and N. J. Chalupny. 2001. ULBPs, novel MHC class I-related molecules, bind to CMV glycoprotein UL16 and stimulate NK cytotoxicity through the NKG2D receptor. *Immunity.* 14:123-133.

8. Kaye, J., H. Browne, M. Stoffel, and T. Minson. 1992. The UL16 gene of human cytomegalovirus encodes a glycoprotein that is dispensable for growth *in vitro*. *J.Virol.* 66:6609-6615.

9. Bauer, S., V. Groh, J. Wu, A. Steinle, J. H. Phillips, L. L. Lanier, and T. Spies. 1999. Activation of NK cells and T cells by NKG2D, a receptor for stress-inducible MICA. *Science* 285:727-729.

10. Wu, J., Y. Song, A. B. Bakker, S. Bauer, T. Spies, L. L. Lanier, and J. H. Phillips. 1999. An activating immunoreceptor complex formed by NKG2D and DAP10. *Science* 285:730-732.

11. Wu, J., H. Cherwinski, T. Spies, J. H. Phillips, and L. L. Lanier. 2000. DAP10 and DAP12 form distinct, but functionally cooperative, receptor complexes in natural killer cells. *J.Exp.Med.* 192:1059-1068.

12. Groh, V., R. Rhinehart, J. Randolph-Habecker, M. S. Topp, S. R. Riddell, and T. Spies. 2001. Costimulation of CD8alphabeta T cells by NKG2D via engagement by MIC induced on virus-infected cells. *Nat.Immunol.* 2:255-260.

13. Roberts, A. I., L. Lee, E. Schwarz, V. Groh, T. Spies, E. C. Ebert, and B. Jabri. 2001. NKG2D receptors induced by IL-15 costimulate CD28-negative effector CTL in the tissue microenvironment. *J.Immunol.* 167:5527-5530.

14. Groh, V., S. Bahram, S. Bauer, A. Herman, M. Beauchamp, and T. Spies. 1996. Cell stress-regulated human major histocompatibility complex class I gene

expressed in gastrointestinal epithelium. *Proc.Natl.Acad.Sci.U.S.A* 93:12445-12450.

15. Groh, V., A. Steinle, S. Bauer, and T. Spies. 1998. Recognition of stress-induced MHC molecules by intestinal epithelial gammadelta T cells. *Science* 279:1737-1740.

16. Groh, V., R. Rhinehart, H. Secrist, S. Bauer, K. H. Grabstein, and T. Spies. 1999. Broad tumor-associated expression and recognition by tumor-derived gamma delta T cells of MICA and MICB. *Proc.Natl.Acad.Sci.U.S.A* 96:6879-6884.

17. Tieng, V., C. Le Bouguenec, M. L. du, P. Bertheau, P. Desreumaux, A. Janin, D. Charron, and A. Toubert. 2002. Binding of Escherichia coli adhesin AfaE to CD55 triggers cell-surface expression of the MHC class I-related molecule MICA. *Proc.Natl.Acad.Sci.U.S.A* 99:2977-2982.

18. Vance, R. E. 2000. Cutting edge: cutting edge commentary: a Copernican revolution? Doubts about the danger theory. *J.Immunol.* 165:1725-1728.

19. Vivier, E., E. Tomasello, and P. Paul. 2002. Lymphocyte activation via NKG2D: towards a new paradigm in immune recognition?. *Curr.Opin.Immunol.* 14:306-311.

20. Radosavljevic, M., B. Cuillerier, M. J. Wilson, O. Clement, S. Wicker, S. Gilfillan, S. Beck, J. Trowsdale, and S. Bahram. 2002. A cluster of ten novel MHC class I related genes on human chromosome 6q24.2-q25.3. *Genomics* 79:114-123.

21. Steinle, A., P. Li, D. L. Morris, V. Groh, L. L. Lanier, R. K. Strong, and T. Spies. 2001. Interactions of human NKG2D with its ligands MICA, MICB, and homologs of the mouse RAE-1 protein family. *Immunogenetics* 53:279-287.

22. Sutherland, C. L., N. J. Chalupny, K. Schooley, T. VandenBos, M. Kubin, and D. Cosman. 2002. UL16-binding proteins, novel MHC class I-related proteins, bind to NKG2D and activate multiple signaling pathways in primary NK cells. *J.Immunol.* 168:671-679.

23. Radaev, S., B. Rostro, A. G. Brooks, M. Colonna, and P. D. Sun. 2001.

Conformational plasticity revealed by the cocrystal structure of NKG2D and its class I MHC-like ligand ULBP3. *Immunity.* 15:1039-1049.

24. Li, P., D. L. Morris, B. E. Willcox, A. Steinle, T. Spies, and R. K. Strong. 2001. Complex structure of the activating immunoreceptor NKG2D and its MHC class I-like ligand MICA. *Nat.Immunol.* 2:443-451.

25. Salih, H. R., H. G. Rammensee, and A. Steinle. 2002. Cutting edge: down-regulation of MICA on human tumors by proteolytic shedding. *J.Immunol.* 169:4098-4102.

26. Sutherland, C. L., N. J. Chalupny, and D. Cosman. 2001. The UL16-binding proteins, a novel family of MHC class I-related ligands for NKG2D, activate natural killer cell functions. *Immunol.Rev.* 181:185-192.

27. Steinle, A., V. Groh, and T. Spies. 1998. Diversification, expression, and gamma delta T cell recognition of evolutionarily distant members of the MIC family of major histocompatibility complex class I-related molecules. *Proc.Natl.Acad.Sci.U.S.A* 95:12510-12515.

28. Li, P., S. T. Willie, S. Bauer, D. L. Morris, T. Spies, and R. K. Strong. 1999. Crystal structure of the MHC class I homolog MIC-A, a gammadelta T cell ligand . *Immunity.* 10:577-584.

29. Wu, J., V. Groh, and T. Spies. 2002. T cell antigen receptor engagement and specificity in the recognition of stress-inducible MHC class I-related chains by human epithelial gamma delta T cells. *J.Immunol.* 169:1236-1240.

30. Glotzer, J. B., M. Saltik, S. Chiocca, A. I. Michou, P. Moseley, and M. Cotten. 2000. Activation of heat-shock response by an adenovirus is essential for virus replication. *Nature* 407:207-211.

.

2.1.2 NKG2D dysfunction impairs NK and CD8$^+$ T cell responses *in vivo*

This chapter has been published in *Journal of Immunology* **175**(2): 720-729 (2005) by the following authors:

Katrin Wiemann, Hans-Willi Mittrücker, Ute Feger, Stefan Welte, Wayne M. Yokoyama, Thomas Spies, Hans-Georg Rammensee, and Alexander Steinle

The author of this thesis performed the Real-Time PCR analyses.

2.1.2.1 Abstract

The immunoreceptor NKG2D stimulates activation of cytotoxic lymphocytes upon engagement with MHC class I-related NKG2D-ligands (NKG2DL) of which at least some are inducibly expressed upon exposure to carcinogens, cell stress, or viruses. Here, we investigated consequences of a persistent NKG2DL expression *in vivo* by employing transgenic mice expressing MICA under control of the H2-K^b promoter. Although MICA functions as a potent activating ligand of mouse NKG2D, H2-K^b-MICA mice appear healthy without aberrations in lymphocyte subsets. However, NKG2D-mediated cytotoxicity of H2-K^b-MICA NK cells is severely impaired *in vitro* and *in vivo*. This deficiency concurs with a pronounced down-regulation of surface NKG2D that is also seen on activated CD8$^+$ T cells. As a consequence, H2-K^b-MICA mice fail to reject MICA-expressing tumors and to mount normal CD8$^+$ T cell responses upon Listeria infection emphasizing the importance of NKG2D in immunity against tumors and intracellular infectious agents.

2.1.2.2 Introduction

NKG2D is a C-type lectin-like activating receptor broadly expressed on cytotoxic lymphocytes. In humans, NKG2D is present on most NK cells, CD8$^+$ T cells, and γδ T cells in association with the adaptor protein DAP10 [**1,2**]. In mice, CD8$^+$ T cells express NKG2D only upon activation, whereas NK cells, NKT cells and some γδ T cells constitutively express NKG2D [**3,4**]. At difference to humans, activated mouse NK cells generate a second NKG2D isoform with a shortened cytoplasmic domain (NKG2D-S) which is capable of pairing with both DAP10 and DAP12, whereas the

constitutively expressed NKG2D-L isoform exclusively associates with DAP10 [**5,6**]. DAP10 mediates costimulation of $CD8^+$ T cells and
triggers cytotoxicity by NK cells, whereas signal transduction via DAP12 augments cytotoxicity and is strictly required for activation of cytokine release [**7-9**].

A peculiarity of NKG2D resides in its interaction with a multitude of MHC class I-related ligands of which at least the MIC molecules are inducibly expressed in association with cell stress, infection or malignant transformation [**10-12**]. Whereas the ectodomain of NKG2D is fairly conserved in mouse and man, the various MHC class I-related binding partners of NKG2D are highly diverged. In humans, the MHC-encoded MIC molecules (MICA and MICB) and five members of the ULBP family (ULBP1-4; RAET1G) ligate NKG2D and consequently trigger NK cells [**13-15**]. *In vitro*, cell stress-inducible MIC molecules are expressed by many tumor cell lines and up-regulated upon infection with Human Cytomegalovirus, M. tuberculosis, and *E. coli* [**12,16**]. *In vivo*, MIC molecules are not detectable on most healthy tissues, but are expressed on gastrointestinal epithelium, on tumors and on Human Cytomegalovirus-infected cells [**8,16**]. Recently, MICA expression was reported for tissues affected by autoimmune reactions in patients with rheumatoid arthritis and celiac disease together with evidence for an involvement of NKG2D in the autoimmune pathogenesis of these diseases [**17-19**].

In mice, members of the RAE-1 protein family, the minor histocompatibility antigen H60, and MULT1 act as ligands of NKG2D [**20-22**]. Similarly to ULBP molecules they all lack an α3 domain. Recently, upregulation of RAE-1 molecules on macrophages by various ligands of Toll-like receptors has been demonstrated [**23**]. RAE-1 expression is also induced by carcinogens and stimulates anti-tumor activity of γδ T cells [**24**]. RAE-1-transduced tumor cell lines were rejected *in vivo* due to NK and $CD8^+$ T cell responses and induced tumor immunity against the parental cell line supporting a role for NKG2D in tumor immunity [**25,26**], though no direct evidence for an involvement of NKG2D was provided.

Recent findings that tumor cells release soluble MIC molecules may account for the failure of tumor surveillance by the NKG2D system in human cancer patients. MICA molecules are shed from tumor cells by metalloproteases resulting in a reduced NKG2DL surface density [**27**]. Further, sMICA was shown to down-regulate NKG2D surface expression and thereby to impair the anti-tumor reactivity of cytotoxic lymphocytes *in vitro* [**28**]. Substantial levels of sMICA were detected in sera of patients with various malignancies and correlated with a systemic NKG2D

downregulation on peripheral NK and $CD8^+$ T cells [**27,29,30**]. However, direct evidence for an *in vivo* impairment of NKG2D-mediated tumor immunosurveillance by persistent MICA expression was lacking. Another study reported NKG2D down-regulation upon co-culture with NKG2DL expressing cells that was at least in part due to signaling of the DAP10 adaptor. In addition, down-regulation of NKG2D was observed for NK cells from NOD mice and attributed to co-expression of RAE-1 [**31**], but consequences for NK cell activation *in vivo* were not investigated.

Here we explored implications of persistent NKG2DL expression *in vivo*. We investigated consequences of persistent MICA expression for NKG2D-mediated immunosurveillance as it may occur in cancer patients. In addition, we took advantage of the strongly impaired NKG2D function in H2-K^b-MICA mice to address the role of NKG2D for NK and $CD8^+$ T cell responses *in vivo*.

2.1.2.3 Materials and Methods

Mice. C57BL/6 mice were obtained from Charles River Wiga. For the generation of mice constitutively expressing MICA, one-cell embryos of (C57BL/6 x SJL)F1/J hybrid mice were microinjected with a 4.75-kb XhoI/KpnI DNA fragment excised from the pHSE plasmid [**32**] containing the H2-K^b promoter followed by the 1.15-kb MICA*07 open reading frame (accession number AY750850) and the 3' untranslated region of the β-globin gene. Eggs were transferred into the oviducts of B6 CBA mice (transgenic mouse facility, Fred Hutchinson Cancer Research Center). Offspring were tested for the presence of the MICA transgene by PCR from genomic tail DNA using the oligonucleotides MICAEX2F (5'-GAC TTG ACA GGG AAC GGA AAG G-3') and MICAEX4R (5'-CCC CCC ACT GCT GGG TGT TG-3'). Several H2-K^b-MICA transgenic lines were obtained, and one of them (tg24) exhibiting high surface MICA expression was backcrossed with C57BL/6 mice at least 12 times for further studies. Litters were tested for MICA transgenes by PCR and/or for MICA surface expression on PBL by flow cytometry using biotinylated anti-MICA/B mAb BAMO1. RAG2-deficient and β_2-microglobulin-deficient C57BL/6 mice were kindly provided by H. Schild (University of Mainz, Mainz, Germany). Animals were maintained under specific pathogen-free conditions in the animal facilities of the Department of Immunology at the University of Tübingen. All animal experiments were conducted according to the German animal protection law.

Cell lines and transfectants. All cell culture media were supplemented with 10% FCS (PAA Laboratories), 2 mM glutamine, 100 U/ml penicillin, 100 µg/ml streptomycin (Cambrex), 1 mM sodium pyruvate (c.c. pro), and 50 µM 2-ME. The cell lines RMA (T cell lymphoma), RMA-S (TAP2-deficient RMA variant), and CHO (Chinese hamster ovary carcinoma) were cultured in RPMI 1640 (Cambrex). The RMA cell line was transfected by electroporation (250 V, 950 µF) using 15 µg of the vector RSV.5neo or RSV.5neo containing the MICA*07 open reading frame [**15**]. Stable transfectants (RMA-neo and RMA-MICA*07) were selected in RPMI 1640 supplemented with 1 mg/ml G418 (PAA Laboratories).

Cells. Thymocytes and splenocytes were prepared by passing the respective organs through a 40 µm cell strainer (BD Biosciences Europe). For analysis of PBL, blood was collected from the orbital sinus. RBC in PBL and splenocyte suspensions were lyzed by ammonium chloride treatment. For isolation of NK cells, nylon wool nonadherent cells were positively selected from splenocytes by magnetic cell sorting using DX5 MicroBeads (Miltenyi Biotec) according to the manufacturer's instructions. Resulting cells were 65–85% $NK1.1^+$. For *in vitro* analyses DX5-sorted cells were cultured in RPMI 1640 (Cambrex) supplemented with 1500 U/ml human IL-2 (R&D Systems). For analysis of *in vivo*-activated NK cells, mice were injected i.p. with 300 µg of polyinosinic-polycytidylic acid potassium salt (poly(I:C), Sigma-Aldrich). Twelve to 18 h later, DX5-positive cells were isolated from splenocytes as described above. Con A blasts were generated by culturing splenocytes for 48 h in Alpha-MEM (Cambrex) containing 2.5 µg/ml Con A. Hepatocytes were isolated by a two-step perfusion protocol [**33**]. In brief, 60 ml of PBS containing 0.5 mM EGTA and 0.05 M HEPES was used as a first perfusate. Liver was perfused with 60 ml of collagenase (40 U/ml in RPMI 1640; Sigma-Aldrich) and subsequently excised from the body cavity, the gall bladder was removed, and the liver was pushed through a tea strainer and incubated for 10 min at 37°C in collagenase. To get a single-cell suspension, the digested liver was additionally rinsed through a 70-µm cell strainer (BD Biosciences Europe).

For isolation of $CD8^+$ T cells, nylon wool nonadherent splenocytes were first depleted for NK cells using DX5 MicroBeads (Miltenyi Biotec). DX5-depleted cells were then positively selected with anti-CD8 (clone Ly-2) MicroBeads (Miltenyi Biotec) according to the manufacturer's instructions. Purified $CD8^+$ T cells were either directly analyzed for NKG2D expression or after 3 days culture in anti-CD3 (clone 17A2) coated microwells.

mAbs and recombinant proteins. Anti-CD3ε FITC (145-2C11), anti-H2-K^b FITC (AF6-88.5), anti-NK1.1 PE (PK136), anti-CD8 PE (Ly-2), anti-CD19 PE (1D3), anti-γδ TCR PE (GL3), anti-TNP-KLH PE (A110-1; rat Ig control), anti-TNP hamster IgG PE (A19-3; hamster Ig control), and anti-CD4 PerCP (GK1.5) were purchased from BD Pharmingen. Anti-NKG2D PE (CX5), anti-NKG2D allophycocyanin (CX5), and anti-NK1.1 FITC (PK136) were obtained from eBioscience. Anti-NKG2D mAb C7 was described elsewhere [**3**]. Rat IgG Abs, anti-CD16/CD32 mAb (clone 2.4G2), anti-IFNγ mAb (XMG1.2), anti-CD8α mAb (YTS169), and anti-CD62L mAb (Mel-14) were purified from rat serum or hybridoma supernatants with protein G-Sepharose. mAbs were Cy5- or FITC-conjugated according to standard protocols. The mAbs AMO1 and BAMO1 recognizing MICA and MICA/B, respectively, were generated and purified as described [**27**]. BAMO1 was biotinylated using EZ-Link Sulfo-NHS-Biotin (Pierce) according to the manufacturer's protocol. Streptavidin-PE (Molecular Probes) was used as a secondary reagent. Soluble mouse NKG2D was produced in insect cells using the baculovirus system as described elsewhere [**15**]. Binding of FLAG-tagged mouse NKG2D was detected with the biotinylated anti-FLAG mAb M2 (Sigma-Aldrich) in combination with streptavidin-PE. Stained cells were analyzed on a FACSCalibur (BD Biosciences) using CellQuest software for evaluation.

ELISA. Concentrations of sMICA in sera of H2-K^b-MICA and nontransgenic littermates (nontgLM) were determined by sandwich-ELISA using a modified protocol of the previously published MICA-ELISA [**27**]. In brief, plates were coated with 2 µg/ml of the MICA-specific capture mAb AMO1 overnight at 4°C. After blocking with 7.5% BSA-PBS, plates were washed with 0.05% Tween 20. Samples or recombinant sMICA*04 serving as a standard were added in 2% BSA-PBS. After incubation and washing, biotinylated BAMO1 was added at a concentration of 1 µg/ml. After incubation and washing, HRP-conjugated streptavidin (BD Pharmingen) was applied as a 1/1000 dilution. Plates were washed extensively before adding the peroxidase substrate TMB (Kirkegaard & Perry Laboratories) according to the manufacturer's instructions. HRP activity was stopped by addition of 1 M phosphoric acid, and absorbance was measured at 450 nm.

Chromium release assay. Cytotoxicity of NK cells *in vitro* was assessed in a ^{51}Cr

release assay. NK effector cells were isolated from splenocytes with DX5-coated beads and either used immediately or after 5 days of cultivation with human IL-2 at 1500 U/ml (R&D Systems). Target cells were labeled with 50 µCi of ^{51}Cr (Amersham) for 1 h at 37°C and washed three times. Effector cells were titrated on target cells and incubated for 4 h at 37°C unless noted otherwise. Spontaneous release of target cells alone was <15% of the maximum release taken from target cells lyzed in 1% Triton X-100. Percentage of lysis was calculated as follows: 100 x (experimental release – spontaneous release)/(maximum release – spontaneous release). Data are means of duplicates. For NKG2D blocking studies, NK cells were preincubated for 20 min with the mAb C7 (30 µg/ml) before addition to the target cells. Hamster Ig (ICN Pharmaceuticals) served as a control.

Intracellular IFNγ analysis of NK cells. Purified NK cells were cocultured for 17 h with RMA transfectants at a ratio of 2:1 in medium containing 1000 U IL-2/ml. During the final 11 h of culture, GolgiStop (BD Biosciences) was added according to manufacturer's instructions. Subsequently, cells were stained with FITC-conjugated anti-NK1.1, permeabilized with Cytofix/Cytoperm (BD Biosciences), and stained with PE-conjugated anti-IFNγ-mAb (BD Biosciences). After a further 20-min incubation, cells were washed and analyzed by flow cytometry.

Real-time PCR. RNA was isolated from purified NK cells using TRIZOL (Invitrogen Life Technologies) followed by reverse transcription using SuperScript II (Invitrogen Life Technologies) according to the manufacturer's protocol. The resulting cDNA was amplified with primer pairs specific for NKG2D, DAP10, DAP12, and 18S rRNA, respectively, in duplicates (40 cycles: 95°C x 15 s, 60°C x 1 min) using SYBRGreen chemistry on the ABI PRISM 7000 Sequence Detection System (Applied Biosystems). PCR products were analyzed on 3% agarose gels for purity und validated by direct sequencing. Data were analyzed by the ΔC_T method for relative quantification and calculated as the relative increase in relative copy numbers. Oligonucleotide sequences (forward, reverse) are: 18S rRNA: 5'-CGGCTACCACATCCAAGGAA-3', 5'-GCTGGAATTACCGCGGCT3'; NKG2D: 5'-ACG TTT CAG CCA GTA TTG TGC-3', 5'-GGA AGC TTG GCT CTG GTT C-3'; DAP10: 5'-CCC AGG CTA CCT CCT GTT C-3', 5'-CTA CAA TTA GGA GTG ACA TGA CCG-3'; DAP12: 5'-CTG GGA TTG TTC TGG GTG AC-3', 5'-CTG AAG CTC CTG ATA AGG CG-3'. The NKG2D primer pair amplifies both the NKG2D-S and

NKG2D-L variants.

***In vivo* cytotoxicity assay.** Freshly isolated splenocytes were washed in PBS and resuspended at a final concentration of 2 x 10^7 cells/ml in PBS. Cells were labeled either with 8 µM CFSE (Molecular Probes) or with 5–7 µM PKH26 (Sigma-Aldrich) for 4 min at room temperature. The reaction was stopped by adding FCS, and cells were washed once in RPMI 1640 and twice in PBS. Labeled cells were mixed at defined ratios, and a total of 1.5 x 10^7 cells was adoptively transferred into H2-K^b-MICA mice or nontgLM, respectively. Immediately after adoptive transfer, labeled cells were analyzed in the peripheral blood. Six or 14 h after transfer, mice were sacrificed and PBL, splenocytes, and lymph node cells were analyzed for labeled cells by flow cytometry.

Tumor inoculation. Growth of RMA-neo and RMA-MICA*07 cells was analyzed in H2-K^b-MICA mice, nontgLM, and RAG2-deficient mice. Mice were injected s.c. with 10^5 RMA-neo in the right flank and 10^5 RMA-MICA*07 cells in the left flank, respectively. Tumor growth was monitored by measuring tumor surface with a metric caliper at the indicated time points. Animals were sacrificed at day 17 when some tumors reached a size of 200 mm^2. Data are representative of two independent experiments.

Infection with *Listeria monocytogenes*. Mice were infected with *L. monocytogenes* strain EGD or with a *L. monocytogenes* strain recombinant for a secreted form of OVA [**34**]. For i.v. infection, listeriae were injected into a lateral tail vein. Inocula were controlled by plating serial dilutions on tryptic soy broth agar.

Quantitation of T cell responses by analysis of cellular cytokine expression. For determination of cytokine expression, at day 9 postinfection, 4 x 10^6 splenocytes were stimulated for 5 h with 10–6 M of peptides derived from listeriolysin O (LLO190–201, NEKYAQAYPNVS) or OVA (OVA257–264, SIINFEKL). During the final 4 h of culture, 5 µg/ml brefeldin A (Sigma-Aldrich) was added. Cultured cells were incubated for 10 min with rat IgG and anti-CD16/CD32 mAb. Subsequently, cells were stained with PE-conjugated anti-CD4 mAb or anti-CD8 mAb, and after 30 min on ice, fixed for 20 min at room temperature with PBS 4% paraformaldehyde. Cells were washed with PBS 0.1% BSA, permeabilized with PBS 0.1% BSA/0.5% saponin (Sigma-Aldrich), and incubated with rat IgG and anti-CD16/CD32 mAb. After 5 min,

FITC-conjugated anti-IFNγ-mAb was added. After a further 20 min incubation, cells were washed with PBS, fixed with PBS 1% paraformaldehyde, and analyzed by flow cytometry.

Quantitation of $CD8^+$ T cell responses by MHC class I tetramer staining. Modified full-length cDNA of H2-K^b and human β_2-microglobulin were kindly provided by D. Busch (Technical University of Munich, Munich, Germany). H2-K^b/OVA257–264-tetramers were generated as described [**35**]. For flow cytometric analysis, at day 9 postinfection, 2 x 10^6 splenocytes were incubated for 15 min at 4°C with rat IgG, anti-CD16/CD32 mAb, and streptavidin (Molecular Probes) in PBS with 0.5% BSA and 0.01% sodium azide. After incubation, cells were stained for 60 min at 4°C either with Cy5-conjugated anti-CD8α mAb, FITC-conjugated anti-CD62L mAb, and PE-conjugated MHC class I-OVA257–264-tetramers, or with allophycocyanin-conjugated anti-NKG2D mAb, FITC-conjugated anti-CD8α mAb, and PE-conjugated MHC class I-OVA257–264-tetramers. Subsequently, cells were washed with PBS 0.5% BSA/0.01% sodium azide and diluted in PBS. Propidium iodide was added before four-color flow cytometric analysis.

2.1.2.4 Results

MICA expression by H2-K^b-MICA mice.

In order to gain insight into consequences of a persistent NKG2DL expression *in vivo*, we established transgenic mice constitutively and ubiquitously expressing the human NKG2DL MICA. We corroborated previous data of MIC-molecules acting as a ligands of mouse NKG2D by demonstrating that MICA*07-expressing cells bind soluble mouse NKG2D (**Figure 2.8**) [**22,36**]. To achieve constitutive and ubiquitous MICA expression, a transgene containing the coding sequence of MICA*07 under control of the MHC class I H2-K^b promoter was introduced into the germline of (C57BL/6 x SJL)F1/J mice (**Figure 2.9a**). Offspring expressing MICA on PBL was selected and a transgenic line (H2-K^b-MICA) established that was repeatedly backcrossed with C57BL/6 mice (B6 mice).

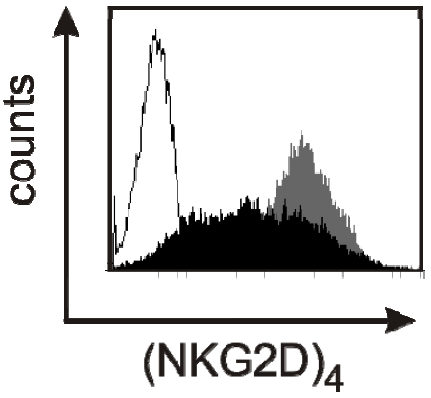

Figure 2.8. MICA*07 ligates NKG2D. Flow cytometric analysis of RMA cells ectopically expressing MICA*07 (RMA-MICA*07) with soluble mouse NKG2D (black histogram) and anti-MICA/B mAb BAMO1 (gray histogram). Mock-transfected RMA cells (RMA-neo) did not bind mouse NKG2D (open histogram).

H2-K^b-MICA mice presented phenotypically normal and healthy, and did not display any overt signs of autoimmunity. No significant alterations in frequencies of lymphocyte subsets were observed when splenocytes of H2-K^b-MICA mice and non-transgenic littermates (nontgLM) were compared (data not shown). Most splenocytes from H2-K^b-MICA mice strongly expressed MICA (**Figure 2.9b**). In particular, B and NK cells expressed high levels of MICA, whereas MICA expression of $CD4^+$ and $CD8^+$ T cells reached intermediate levels (**Figure 2.9c**). Accordingly, MICA expression by PBL varied over a broad range (**Figure 2.9b**).

In contrast, most thymocytes representing the $CD4^+/CD8^+$ subpopulation had only low amounts of MICA, while other thymocyte subsets displayed a more pronounced MICA expression (**Figure 2.9b,c**). As for thymocytes, MICA expression of hepatocytes paralleled H2-K^b expression levels (**Figure 2.9b**). No expansions of intraepithelial $CD4^+/CD8\alpha\alpha^+$ T cells were observed as previously described for transgenic mice with a gut-specific MICA expression [**37**] (data not shown). Sera from H2-K^b-MICA mice, but not from nontgLM, contained high levels of soluble MICA (~ 50 ng/ml) exceeding sMICA levels previously detected in tumor patients [**27-29**], suggesting substantial MICA shedding by non-malignant cells (**Figure 2.9d**).

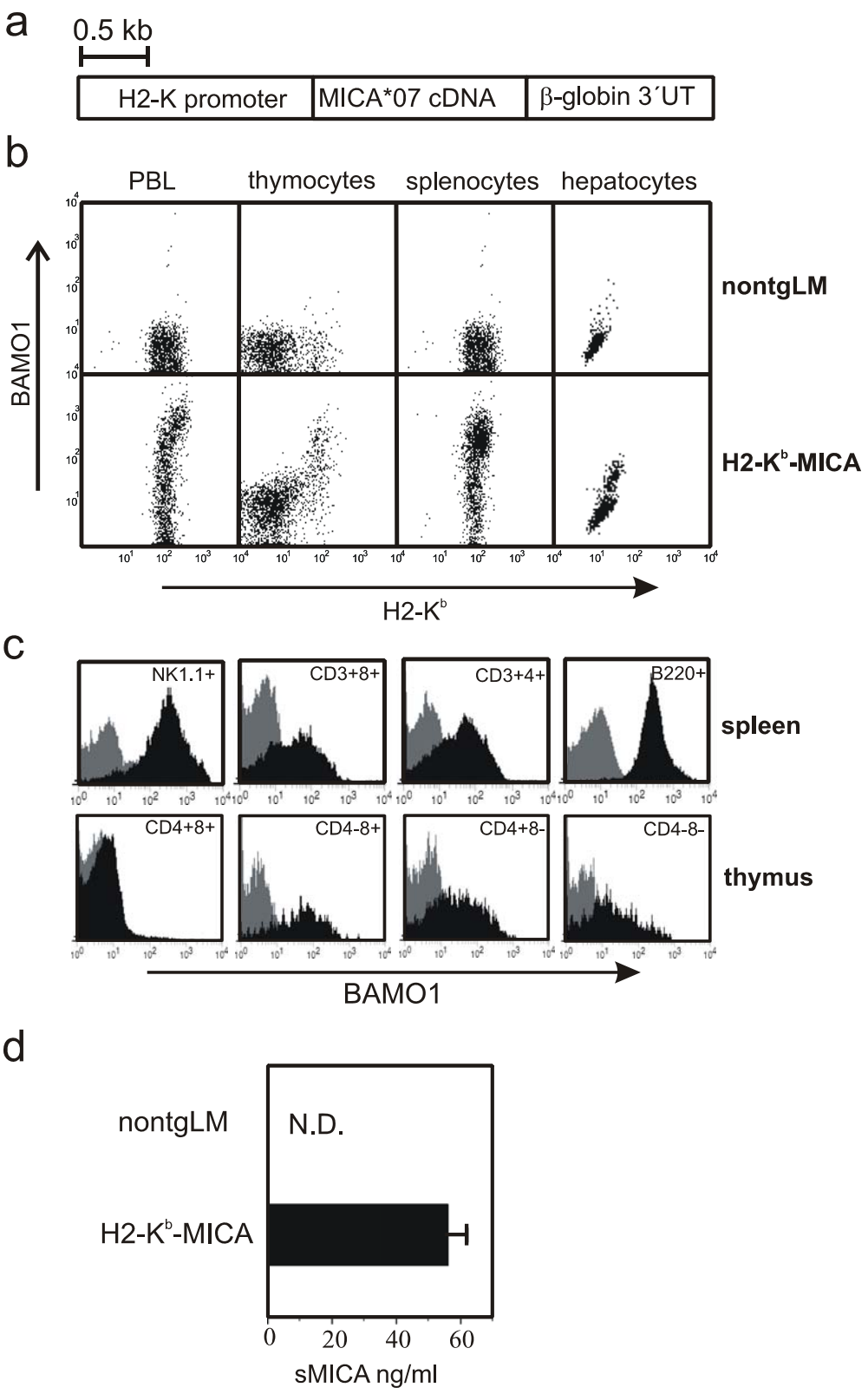

Figure 2.9. Constitutive MICA expression by H2-K^b-MICA mice. (**a**), H2-K^b-MICA transgene encompassing the H2-K^b promoter, the 1.15 kb MICA*07 coding sequence, and the 3' untranslated region (UT) of the β-globin gene. (**b**) MICA cell surface expression by PBL, thymocytes, splenocytes, and hepatocytes of H2-K^b-MICA mice as detected by BAMO1. Cells were co-stained with anti-H2-K^b. (**c**) MICA expression by gated subpopulations of splenocytes and thymocytes from nontgLM (gray histograms) and H2-K^b-MICA mice (black histograms) as analyzed with BAMO1. (**d**) sMICA levels in sera of H2-K^b-MICA mice detected with a MICA-Sandwich-ELISA. The mean of sMICA levels from four representative mice is shown. NontgLM tested negative (N. D. = not detectable).

Constitutive MICA expression induces NKG2D down-regulation and dysfunction. To address functional consequences of constitutive MICA expression, we analyzed expression and functionality of NKG2D on NK cells. NKG2D surface levels of NK cells from H2-K^b-MICA were reduced when compared to NK cells of nontgLM (**Figure 2.10a**). Differences in surface expression were even more pronounced when poly (I:C) activated NK cells of H2-K^b-MICA mice and nontgLM were analyzed *ex vivo*. NKG2D down-regulation coincided with a strong impairment of NKG2D function.

In contrast to NK cells from nontgLM, poly (I:C) activated NK cells from H2-K^b-MICA mice failed to lyze RMA-MICA*07 cells *ex vivo* (**Figure 2.8**, **Figure 2.10b**). When poly (I:C) activated NK cells from nontgLM were stimulated *ex vivo* with RMA-MICA*07 cells, we observed a markedly higher frequency of $NK1.1^+$ IFNγ producing cells (~16%) as opposed to simulation with RMA-neo cells (~ 8%). In contrast, frequencies of $NK1.1^+$ cells from H2-K^b-MICA mice producing IFNγ were only slightly increased when stimulated with RMA-MICA*07 cells as compared to RMA-neo stimulation (**Figure 2.10c**).

To assess a general defect in cytotoxicity, we tested the lytic capacity of NK cells from H2-K^b-MICA mice towards CHO and RMA-S cells. CHO cells are recognized by mouse NK cells via the activating receptor Ly49D in complex with DAP12 [**38**]. Activated NK cells from H2-K^b-MICA mice and nontgLM displayed similar lytic potential for CHO cells arguing against a general impairment of cytotoxicity (**Figure 2.10d**).

Similarly, RMA-S cells that are also recognized NKG2D-independently were lyzed by NK cells from H2-K^b-MICA mice and nontgLM at comparable rates (**Figure 2.10e**). When NK cells from H2-K^b-MICA mice were cultivated *in vitro* with high dose of IL-2 (1500 U/ml), NKG2D surface levels increased, but did not reach wildtype levels presumably due to MICA expression by NK cells (**Figure 2.10f**).

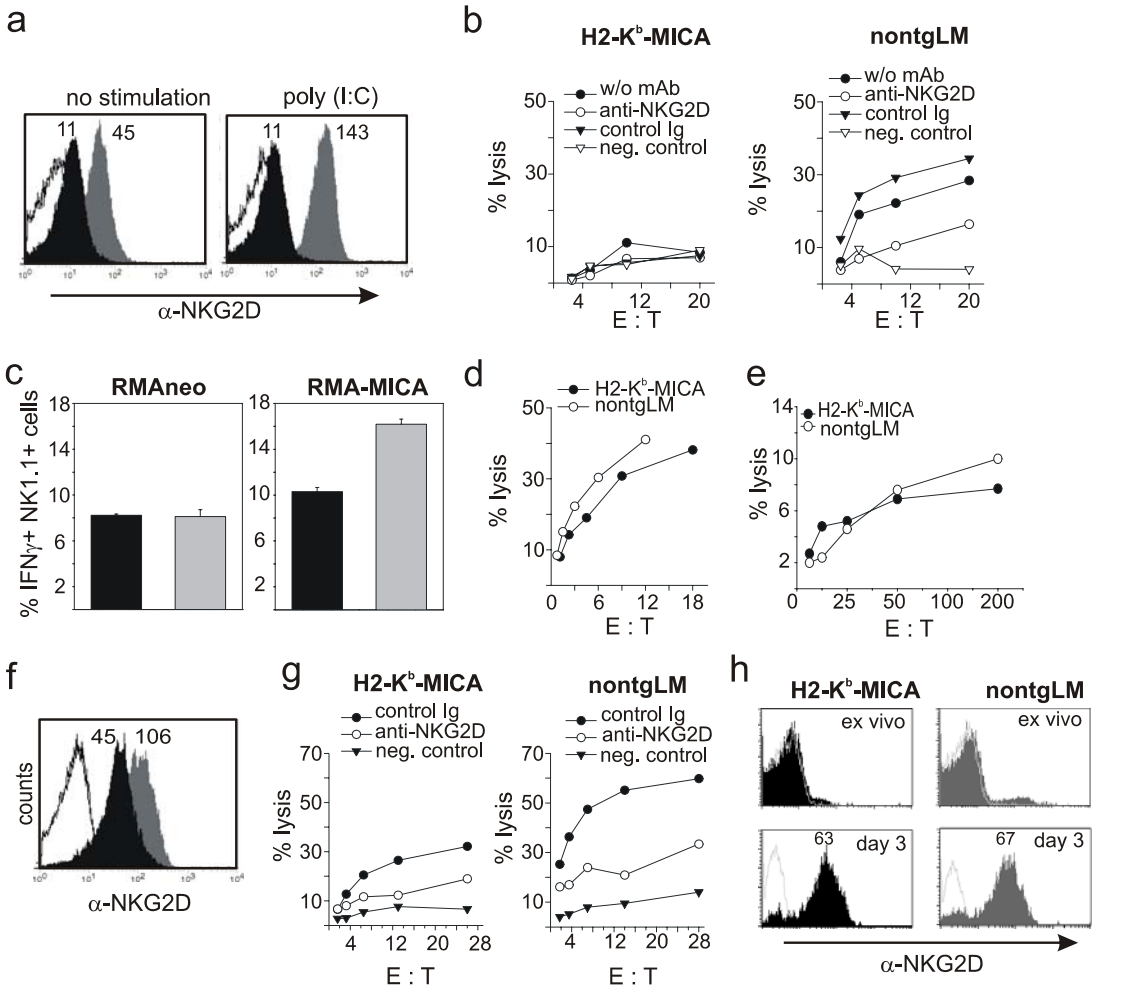

Figure 2.10. NKG2D on H2-K^b-MICA NK cells is dysfunctional. (**a**) NKG2D cell surface expression by resting and poly (I:C) activated NK cells from H2-K^b-MICA mice is strongly reduced. Purified NK cells from H2-K^b-MICA mice (black histograms) and nontgLM (gray histograms) were stained *ex vivo* with the anti-NKG2D mAb CX5 or with an isotype control (open histograms). Mean fluorescence intensities of gated NK1.1 cells are shown. (**b**) In contrast to poly (I:C) activated non-transgenic NK cells, poly (I:C) activated H2-K^b-MICA NK cells fail to lyze RMA-MICA*07 cells *ex vivo* in the presence (anti-NKG2D; control Ig) or absence (w/o mAb) of antibodies. Both types of NK cells fail to lyze RMA-neo cells (neg. control). Cytotoxicity was measured by a 12 h chromium-release assay. (**c**), IFNγ production by H2-K^b-MICA NK cells. Freshly isolated, poly (I:C) activated NK cells from H2-K^b-MICA mice and ntgLM were co-cultured with RMA-neo or RMA-MICA cells. After 17h frequencies of IFNγ producing NK1.1+ cells were evaluated by intracellular staining. Data represent means of triplicates. (**d**,**e**) Lysis of CHO cells (**d**) and RMA-S cells (**e**) by poly (I:C) activated NK cells *ex vivo* isolated from H2-K^b-MICA mice and nontgLM. (**f**) NKG2D expression of purified H2-K^b-MICA NK cells increases upon *in vitro* culture. NKG2D surface expression of NK1.1$^+$ cells from H2-K^b-MICA mice (black histogram) and nontgLM (gray histogram) cultured for 5 days with IL-2 was analyzed with CX5. Isotype controls are shown as open histograms. (**g**) *In vitro* cultivated H2-K^b-MICA NK cells lyze RMA-MICA*07 cells. Purified NK cells from H2-K^b-MICA mice and nontgLM were cultivated 5 days with IL-2 and subsequently assayed for lysis of RMA-MICA*07 cells. Lysis was blocked by mAb C7 (anti-NKG2D), but not by control immunoglobulin (control Ig). RMA-neo cells were not lyzed (neg. control). (**h**) NKG2D up-regulation on purified CD8$^+$ T cells from H2-K^b-MICA mice and nontgLM upon *in vitro* stimulation with anti-CD3 mAb is comparable. NKG2D expression by freshly isolated CD8$^+$ T cells or by purified CD8$^+$ T cells after 3 days culture in the presence of anti-CD3 mAb was analyzed with PE-conjugated CX5. NKG2D surface expression of CD8$^+$ gated cells from H2-K^b-MICA mice (black histogram) and nontgLM (gray histogram) are shown. Isotype controls are open histograms.

Accordingly, RMAMICA*07 cells were lyzed by IL-2 cultivated H2-K^b-MICA NK cells, but less efficiently when compared to lysis by non-transgenic NK cells (**Figure 2.10g**). $CD8^+$ T cells freshly isolated from H2-K^b-MICA mice and nontgLM contained a small fraction of NKG2D-positive cells which presumably are activated $CD8^+$ T cells. Again, NKG2D expression was greatly reduced on cells from H2-K^b-MICA mice as compared to cells from nontgLM (**Figure 2.10h**). However, after three days of stimulation with anti-CD3, NKG2D expression of $CD8^+$ T cells from both mice was almost indistinguishable.

Reduced NKG2D staining was not due to epitope-masking by soluble MICA, since complexes formed between recombinant MICA and NKG2D bound anti-NKG2D and NKG2D staining of H2-K^b-MICA NK cells was not increased following mild acid treatment (data not shown). An impact of different transcriptional regulation on NKG2D expression was excluded by real-time PCR that did not reveal differences in NKG2D, DAP10, or DAP12 transcripts between NK cells from H2-K^b-MICA mice and nontgLM (**Figure 2.11a**). Previous reports described NKG2D down-regulation by NK cells upon exposure to NKG2DL-expressing cells *in vitro* and *in vivo* [**23,28,31**]. We observed that down-regulation of surface NKG2D on non-transgenic splenocytes was most pronounced after co-cultivation with splenocytes from mice *in vitro*, and only marginally following treatment with sera from H2-K^b-MICA mice, whereas incubation with control cells and sera from nontgLM, respectively, had no effect (**Figure 2.11b,c**). *In vivo*, NKG2D surface expression on splenocytes from B6 mice was down-regulated after adoptive transfer into H2-K^b-MICA mice, but not after transfer into nontgLM (**Figure 2.11d**). Altogether, these data suggest that reduced surface NKG2D on H2-K^b-MICA NK cells results in NKG2D dysfunction and that NKG2D downregulation is primarily caused by a persistent exposure to cell-bound MICA *in vivo*.

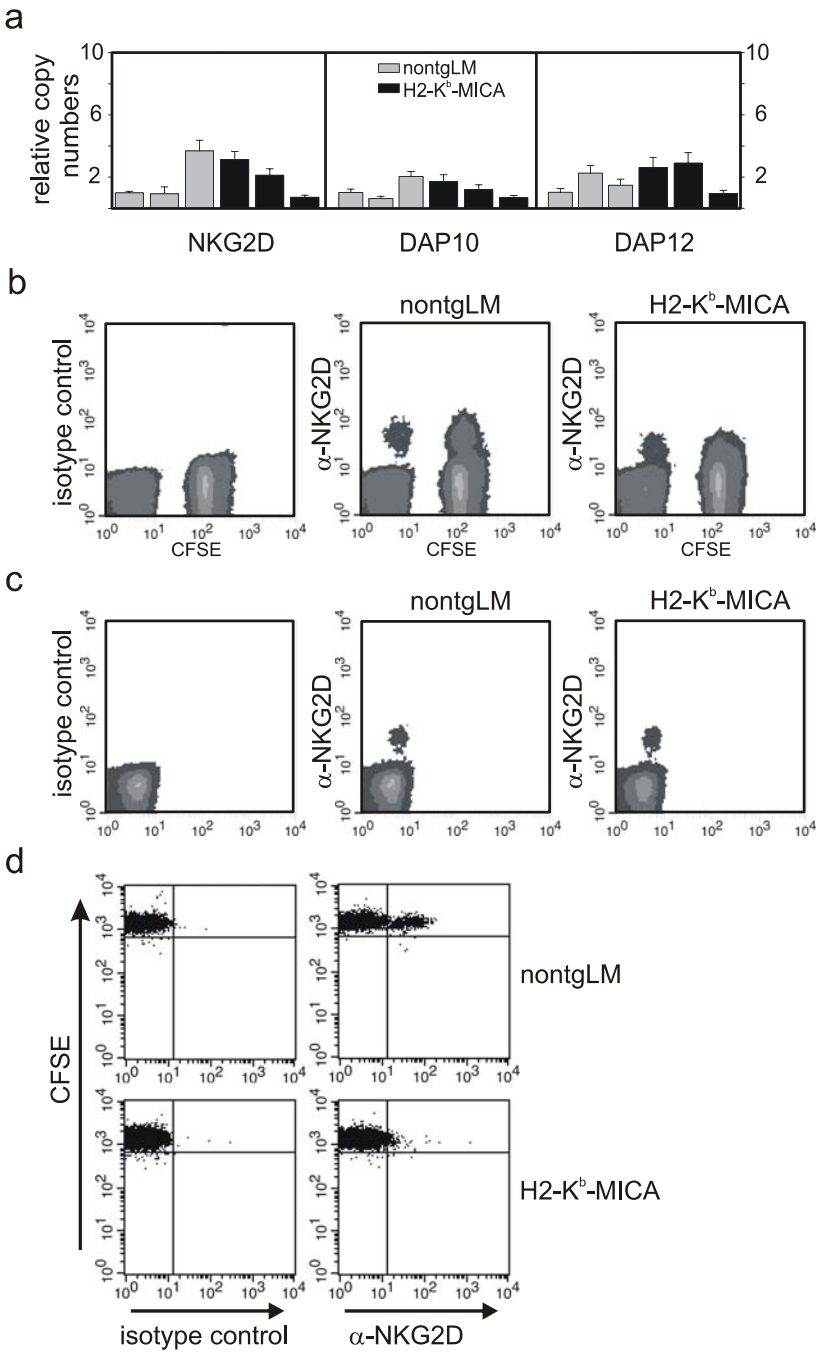

Figure 2.11. NKG2D-downregulation by MICA. (**a**) Transcript levels of DAP10, DAP12, and NKG2D are unaltered in NK cells from H2-K^b-MICA mice as compared to nontgLM. Bars show the relative copy numbers in purified unstimulated NK cells from three individual H2-K^b-MICA mice (black bars) and three nontgLM (gray bars). (**b**,**c**) NKG2D downregulation by cell-bound and soluble MICA. (**b**) Splenocytes from nontgLM (5 x 10^5) were co-incubated with CFSE-*labeled* splenocytes (1 x 10^6) either from H2-K^b-MICA mice or from nontgLM for 12 h *in vitro* and, subsequently, NKG2D surface expression of CFSE-negative cells analyzed by flow cytometry. (**c**) Splenocytes from nontgLM were incubated for 12 h in sera (1:2 dilution with medium) from H2-K^b-MICA mice and nontgLM, respectively, and, subsequently, analyzed for NKG2D surface expression. The fluorescence intensities of unlabeled NKG2D expressing cells after incubation were 55.0 ± 0.5 (nontg splenocytes co-culture), 37.9 ± 1.2 (H2-K^b-MICA splenocytes co-culture), 49.3 ± 0.4 (nontg serum), and 46.6 ± 1.3 (H2-K^b-MICA serum) representing means of triplicates of y mean fluorescence intensities. (**d**) NKG2D down-regulation *in vivo*. 8 x 10^6 CFSE-labeled nylon wool nonadherent splenocytes from B6 mice were injected intravenously into H2-K^b-MICA mice or nontgLM. After 10 hours splenocytes were isolated and analyzed for NKG2D surface expression on CFSE-labeled cells with APC-conjugated CX5.

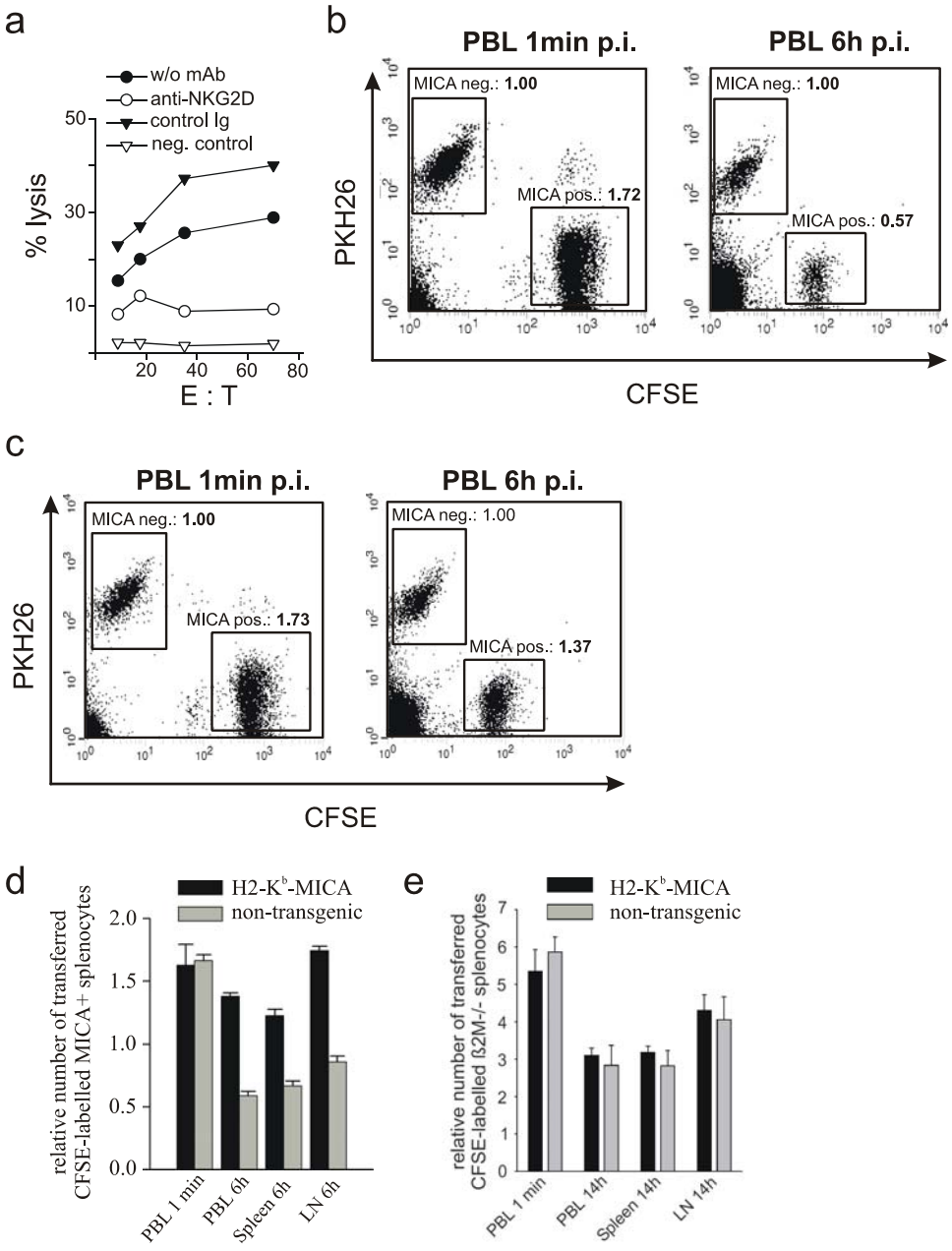

Figure 2.12. Deficient NKG2D-mediated natural cytotoxicity in H2-K^b-MICA mice. (**a**) poly (I:C) activated B6 NK cells *ex vivo* lyze Con A blasts from H2-K^b-MICA mice (w/o mAb). Lysis was inhibited by addition of the mAb C7 (anti-NKG2D), but not by control immunoglobulin (control Ig). Con A blasts from B6 mice were not lyzed (neg. control). (**b**-**d**) H2-K^b-MICA splenocytes are readily eliminated in non-transgenic mice, but not in H2-K^b-MICA mice. Splenocytes of H2-K^b-MICA mice (CFSE-labeled) and nontgLM (PKH26-labeled) were adoptively co-transferred into nontgLM (**b**) or in H2-K^b-MICA mice (**c**) and their presence among PBL was analyzed by flow cytometry 1 min and 6 h post-injection (p.i.). In addition to PBL, spleen and lymph nodes were analyzed 6h p.i. and all results are summarized in (**d**). The number of MICA-negative splenocytes was set as 1 and the relative number of MICA-positive splenocytes recovered from nontgLM (black bars) or H2-K^b-MICA (gray bars) calculated accordingly. Data represent the means of the relative number of transferred MICA-positive splenocytes from three mice per indicated organ. Results are representative of two independent experiments. (**e**) Splenocytes of CFSE-labeled β_2-microglobulin-deficient ($\beta_2M^{-/-}$) and PKH26-labeled wildtype controls were adoptively cotransferred and analyzed by flow cytometry 1 min and 14 h p.i. in PBL, spleens and lymph nodes of nontgLM (black bars) or H2-K^b-MICA mice (gray bars).

NKG2D-mediated natural cytotoxicity is deficient in H2-K^b-MICA mice.

To address functional consequences of NKG2D down-regulation for NK cell activation *in vivo*, we took advantage of H2-K^b-MICA splenocytes. In contrast to Concanavalin A-activated splenocytes (Con A blasts) from B6 mice, H2-K^b-MICA Con A blasts were subject of substantial lysis by freshly isolated poly (I:C) activated B6 NK cells, and lysis was blocked by addition of anti-NKG2D antibody (**Figure 2.12a**). To test the efficacy of NKG2D-mediated NK cytotoxicity *in vivo*, we adoptively co-transferred CFSE-labeled MICA-transgenic and PKH26-labeled non-transgenic splenocytes into nontgLM. Within six hours, the relative number of MICA-expressing splenocytes in the peripheral blood was reduced to one third (**Figure 2.12b**) indicating an efficient and preferential elimination of MICA-expressing cells *in vivo*. A similar preferential elimination of H2-K^b-MICA splenocytes was observed when lymph nodes and spleens were analyzed (**Figure 2.12d**). However, when CFSE-labeled MICA-transgenic splenocytes were adoptively co-transferred together with PKH26-labeled non-transgenic splenocytes into H2-K^b-MICA mice, relative numbers of MICA-transgenic splenocytes were only slightly decreased indicating that NKG2D-mediated activation of NK cytotoxicity is deficient in H2-K^b-MICA mice (**Figure 2.12c,d**). To address functionality of NKG2D-independent NK cytotoxicity, we adoptively transferred CFSE-labeled splenocytes from β_2-microglobulin-deficient mice. Both H2-K^b-MICA mice and nontgLM exhibited similar clearance rates of β2-microglobulin-deficient cells excluding a general impairment of NK cytotoxicity in H2-K^b-MICA mice (**Figure 2.12e**).

Impaired tumor rejection by H2-K^b-MICA mice.

Tumor cells ectopically expressing NKG2DL stimulate tumor immunity. For example, RAE-1-expressing RMA cells have been shown to be rejected by NK cells and/or CD8$^+$ T cells [**25,26**]. We adopted this experimental setting to evaluate functional consequences of NKG2D impairment *in vivo* and injected 10^5 RMA-neo and 10^5 RMA-MICA*07 cells into the right and left flank, respectively, of nontgLM. As expected RMA-neo cells gave rise to tumors in all mice, but RMA-MICA*07 cells were rejected analogous to previous findings with RAE-1-expressing RMA cells [**25,26**] (**Figure 2.13**). To assess a potential contribution of T cells recognizing putative MICA peptides presented by MHC class I in the rejection of RMA-MICA cells, we tested RAG2-deficient mice: RMA-MICA*07 cells were rejected by RAG2-deficient mice whereas RMA-neo cells expanded to tumors demonstrating that

rejection of RMA-MICA*07 cells occurred independently of T cell recognition, but rather is due to the NKG2D-mediated activation of NK cells reaffirming the functionality of MICA as surrogate ligand of mouse NKG2D. However, when we challenged H2-K^b-MICA mice with injections of RMA cells, both RMA-neo and RMA-MICA*07 gave rise to tumors demonstrating that the NKG2D-mediated tumor rejection is strongly impaired in these mice (**Figure 2.13**).

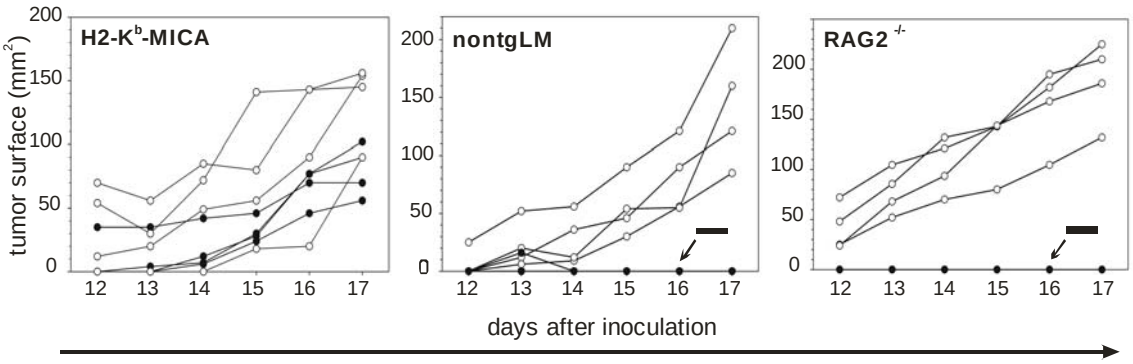

Figure 2.13. NKG2D-mediated tumor rejection is impaired in H2-K^b-MICA mice. H2-K^b-MICA mice, nontgLM, and B6 RAG2-deficient mice, respectively, were inoculated subcutaneously with 1x10^5 RMA-neo (into the right flank) and 1x10^5 RMA-MICA*07 cells (left flank). Each panel displays the tumor growth of RMA-neo (open circles) and RMAMICA (closed circles) in four mice monitored for 17 days post-inoculation.

NKG2D dysfunction compromises CD8$^+$ T cell responses to *Listeria monocytogenes*.

To address the role of NKG2D in the immune defence against infectious pathogens and for the generation of T cell responses, we scrutinized the immune response of H2-K^b-MICA mice upon infection with *L. monocytogenes*. The control of the intracellular pathogen *L. monocytogenes* involves both cells of the innate and of the acquired immune system [**39**]. To evaluate consequences of NKG2D impairment for the early control of *L. monocytogenes* by innate mechanisms, H2-K^b-MICA mice and nontgLM were infected with 5 x 10^4 listeriae, and the bacteria titers in spleen and liver were determined at day 2 and 3 post-infection. Both groups of mice did not differ significantly in their bacterial load, indicating that NKG2D-mediated effector functions of NK cells are not relevant for the early control of *L. monocytogenes* (data not shown).

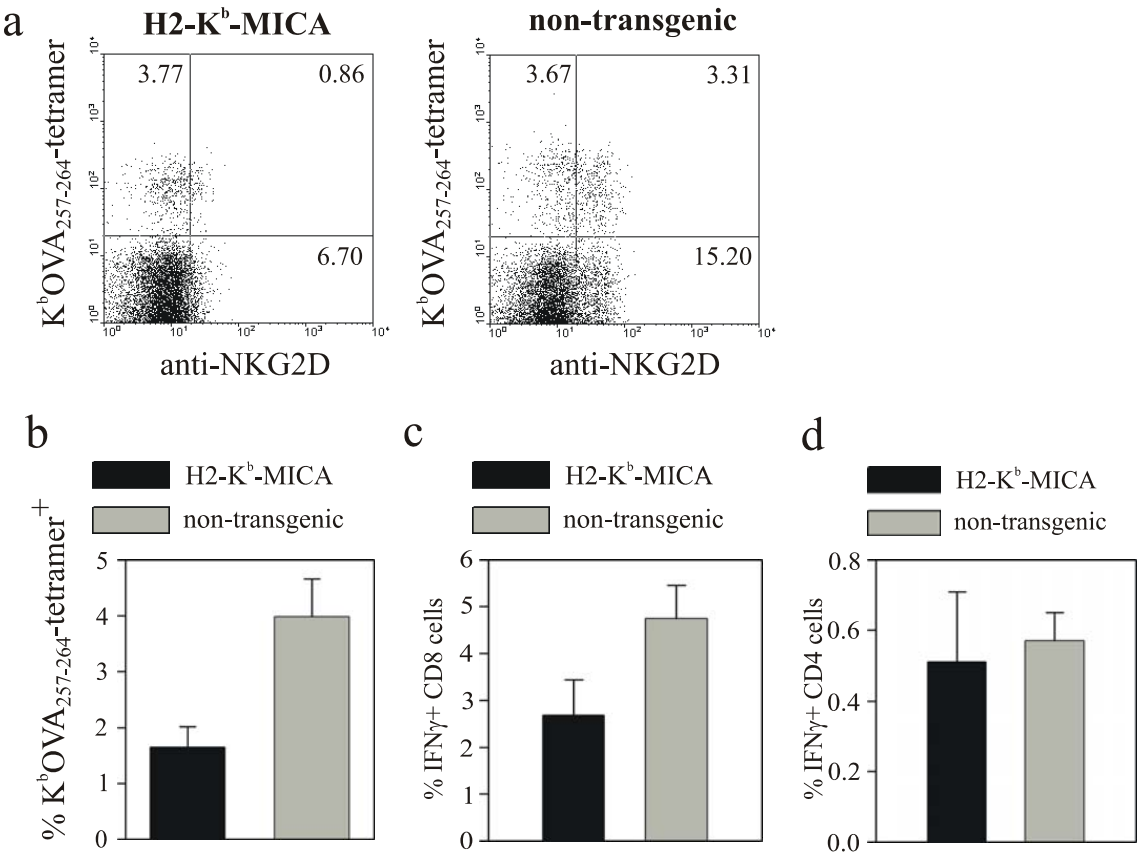

Figure 2.14. Impaired anti-Listeria CD8$^+$ T cell response in H2-K^b-MICA mice. H2-K^b-MICA mice and nontgLM were i. v. infected with 5 x 10^3 listeriae encoding a secreted form of ovalbumin. On day 9 post-infection, spleen cells of infected mice were analyzed. (**a**) NKG2D surface expression by H2-K^b/OVA257-264-tetramer-positive cells. Only viable CD8$^+$-gated splenocytes stained with anti-NKG2D mAb CX5 are shown. (**b**) Frequencies of H2-K^b/OVA257-264-tetramer-positive CD62LlowCD8$^+$ T cells in H2-K^b-MICA mice (black bars) versus nontgLM (gray bars) as assessed by flow cytometry. (**c**) Frequencies of IFN**γ**-producing CD8$^+$ T cells after *in vitro* stimulation with peptide OVA257-264 analyzed by intracellular cytokine staining. (**d**) Frequencies of IFN**γ**-producing CD4$^+$ T cells after *in vitro* stimulation with peptide LLO190-201 analyzed by intracellular cytokine staining. (**b-d**) Values represent means of three infected mice per group.

For the analysis of listeria-specific T cell responses, we applied a *L. monocytogenes* strain recombinant for a secreted form of ovalbumin [**34**]. This strain induces a strong ovalbumin-specific CD8$^+$ T cell response, which can be detected with H2-K^b/OVA257-264-tetramers. At the peak of the primary T cell response against *L. monocytogenes* (day 9 post-infection), we analyzed tetramer-positive T cells in both H2-K^b-MICA mice and nontgLM. Co-staining with anti-NKG2D mAb revealed a significant NKG2D expression on the majority of tetramer-positive cells from non-transgenic mice. This in accord with earlier studies reporting that CD8$^+$ T cells, but not CD4$^+$ T cells, show induced NKG2D expression several days after antigenic activation [**4**]. In contrast to non-transgenic mice, NKG2D surface expression of tetramer-positive cells from H2-K^b-MICA mice was strongly reduced (**Figure 2.14a**).

Interestingly, spleens of H2-K^b-MICA mice contained significant lower frequencies and total numbers of tetramer-positive $CD8^+$ T cells (**Figure 2.14b** and data not shown). These results were confirmed by the analysis of frequencies and numbers of $CD8^+$ T cells responding to *in vitro* peptide stimulation with IFNγ production (**Figure 2.14c** and data not shown). When we compared the frequencies of $CD62L^{low}$ cells among $CD8^+$ T cells of infected mice, H2-K^b-MICA mice had a significantly reduced percentage of $CD62L^{low}$ cells (20,0 ± 3,7 % and 32,8 ± 3,8 % in H2-K^b-MICA mice and littermate controls, respectively), revealing a general impairment of the anti-Listeria $CD8^+$ T cell response in H2-K^b-MICA mice. In contrast, listeria-specific $CD4^+$ T cell responses were only marginally affected in H2-K^b-MICA mice. Compared to littermate controls, H2-K^b-MICA mice showed similar frequencies and only slightly reduced total numbers of $CD4^+$ T cells responding to the immunodominant listeria epitope LLO190-201 (**Figure 2.14d** and data not shown).

2.1.2.5 Discussion

A hallmark of the NKG2D/NKG2DL-system is the inducible surface expression of at least some of the MHC class I-related NKG2DL in response to cell stress, microbial infection or malignant transformation, thereby marking dysfunctional cells for elimination by cytotoxic lymphocytes via NKG2D-mediated mechanisms ("induced-self" hypothesis) [**10,11,40**]. Conversely, a sustained NKG2DL expression as described in patients with malignant or autoimmune diseases may desensitize NKG2D-mediated immune responses. Here, we analyzed transgenic mice constitutively expressing MICA to address functional consequences of persistent NKG2DL expression *in vivo*. MICA was chosen, because it is the bestcharacterized NKG2DL with regard to expression in normal and diseased tissues, regulation of expression and soluble release, and availability of biochemical and structural data [**10,12**]. Although the amino acid sequence of the MICA ectodomain is fairly divergent from any mouse NKG2DL, crystal structures of MICA and RAE1 α1/α2 platform domains interacting with NKG2D are highly related as are crystal structures of human and mouse NKG2D ectodomains [**41-43**]. Structural homology is reflected in functional equivalence of MICA/B and RAE1 with regard to mouse NKG2D ligation and NKG2D-mediated activation of mouse NK cells qualifying MICA as a bona fide surrogate ligand of mouse NKG2D (**Figure 2.8**) [**22,36**]. MICA expression in H2-K^b-MICA mice generally parallels H2-K^b expression with a strong expression

by B and NK cells and an intermediate to low expression by thymocytes and hepatocytes. A disparate expression of K^b and MICA molecules was only observed for peripheral $CD4^+$ and $CD8^+$ T cells that remains to be addressed. MICA-expressing splenocytes were utilized to evaluate the efficiency of NKG2D-mediated activation of natural cytotoxicity *in vivo*. Hitherto, NKG2D-mediated cytotoxicity has been extensively demonstrated *in vitro* using tumor cell lines expressing NKG2DL. Previous studies also demonstrated that ectopic expression of NKG2DL by tumors induces strong NK and CTL responses *in vivo*, however, no direct evidence for an involvement of NKG2D-mediated cytotoxicity in the rejection of NKG2DL-expressing tumor cells was provided [**25, 26**].
By adoptive transfer of MICA-expressing splenocytes, we here demonstrate that ectopic expression of NKG2DL renders “normal” syngeneic cells highly susceptible to cytotoxicity *in vivo*, vividly underscoring that NKG2DL-expression potently overrides inhibitory signals by MHC class I molecules for NK cell activation.

To our surprise, H2-K^b-MICA mice were vital, fertile and did not exhibit any overt signs of autoimmunity in spite of a strong MICA surface expression. A previous study reported hyperkeratosis and leukocytosis in transgenic mice with a MICB cDNA under control of a chicken beta-actin promoter, but neither the underlying molecular cause nor functionality of NKG2D was analyzed [**44**]. The difference in phenotype of these mice as compared to the H2-K^b-MICA mice may be due to a different tissue expression of the MIC molecules though no evidence for MICB protein expression was provided by the authors. It turned out that in H2-K^b-MICA mice “tolerance” towards MICA expressing cells is established by downmodulation of NKG2D which is due to permanent exposure to MICA. In fact, downmodulation of surface NKG2D by NK cells after exposure to NKG2DL-expressing cells *in vitro* and *in vivo* has been previously reported [**23,31**]. It remains to be investigated whether a high local NKG2D ligand expression also leads to a systemic NKG2D down-regulation and dysfunction or rather stimulates local immune reactions. Previous studies on rejection of NKG2DL-expressing tumor cell lines and on the role of NKG2D in the pathogenesis of diabetes in NOD mice, respectively, suggest the latter [**25,26,45**].

A down-modulation of NKG2D has also been reported in human cancer patients, where tumors express and release substantial amounts of soluble MICA [**28**]. Interestingly, H2-K^b- MICA mice also contain high serum levels of sMICA that exceed levels observed in cancer patients at least tenfold [**29**] and thus is not a peculiarity of

malignant cells. This is in line with the detection of soluble MICA in patients with autoimmune diseases and raises the question whether MICA shedding is of physiological relevance, e. g. in regulating MIC cell surface levels. Characterization of the MIC- shedding activity may resolve this issue. Conflicting results exist regarding the down-regulation of NKG2D by soluble MICA. Whereas MICAcontaining sera of patients with malignancies reportedly cause systemic NKG2D downregulation correlating with reduced NKG2D expression on $CD8^+$ T cells and NK cells in cancer patients [**8,30,46**], NKG2D surface expression is not altered in patients with rheumatoid arthritis and celiac disease in spite of similar sera levels of sMICA [**17,18**]. Our *in vitro* experiments indicate that NKG2D down-regulation in H2-K^b-MICA mice is mainly due to engagement of cell-bound MICA as sMICA had little effect on NKG2D surface expression of non-transgenic NK cells. Possibly, MICA released from tumor cells and benign cells, respectively, may be subjected to different post-translational modifications differentially affecting NKG2D down-regulation.

Irrespective of the exact molecular mechanism, our results now provide direct *in vivo* evidence that persistent MICA expression results in down-modulation of NKG2D and impacts tumor immunity as H2-K^b-MICA mice failed to reject MICA-expressing RMA cells in contrast to nontgLM or RAG2-deficient mice. Though our mouse model does not mirror the localized MICA expression by tumors, it does strongly support the notion that ligand-induced NKG2D down-modulation is detrimental for tumor immunosurveillance.

In H2-K^b-MICA mice, down-modulation of surface NKG2D on NK cells was not complete raising the possibility that the observed dysfunction may in part also be due to an impaired signal transduction. However, lysis of CHO cells by H2-K^b-MICA NK cells was similar to lysis by non-transgenic NK cells suggesting that the DAP12 signaling pathway is not affected. Upon *in vitro* cultivation, H2-K^b-MICA NK cells acquired higher NKG2D expression levels and regained functional activity demonstrating that NKG2D-ligand induced silencing of NKG2D is reversible. Failure to completely restore NKG2D surface expression levels may also be due to a MICA-NKG2D cis-interaction within same cells as postulated for activated NK cells from NOD mice [**31**]. In humans, MICA expression has also been reported for thymic epithelial cells raising the possibility that NKG2D is involved in thymic selection of T cells [**47**]. Since MICA costimulates T cells via NKG2D and represents a ligand of some human γδ TCR, constitutive MICA expression might also affect the generation

and/or expansion of lymphocyte subpopulations bearing NKG2D or γδ TCR [**1,8,15,48,49**]. However, we did not detect any major alterations in the total number or composition of lymphocyte subpopulations in naïve H2-K^b-MICA mice. In particular, numbers of splenic NK cells, CD8$^+$ T cells and γδ T cells were not significantly altered as compared to nontgLM. Recently, a transgenic mouse with a gut-specific MICA expression directed by the T3b-promoter was described with expansions of CD4$^+$CD8αα$^+$ intraepithelial T cells [**37**]. But a functional involvement of NKG2D was not examined and also no other mechanisms presented that may account for this expansion. In H2-K^b-MICA mice, frequencies of CD4$^+$CD8αα$^+$ intraepithelial T cells did not significantly differ from nontgLM.

Since H2-K^b-MICA mice exhibit a profound NKG2D dysfunction, we implemented these mice to address the relevance of NKG2D in staging immune responses towards infectious pathogens. Infection with *Listeria monocytogenes* was chosen, because Listeriae activate both innate and adaptive immune responses. Further, induction of RAE1-expression by macrophages incubated with *L. monocytogenes* has recently been reported [**23**]. When we compared the pathogen load of H2-K^b-MICA mice and nontgLM at days 2 and 3 postinfection, we found no significant differences, indicating that NKG2D dysfunction on NK cells had no major impact at an early stage of infection. However, NKG2DL expression induced by *L. monocytogenes* may trigger cytokine release by NK cells that in turn may contribute to the generation of an anti-Listeria specific T cell response. NK cells of H2-K^b-MICA mice showed an impaired IFNγ production upon NKG2D triggering *ex vivo* that may also result in a impaired anti-Listeria T$_H$1 response *in vivo*. T cells are of major importance for the immune control and clearance of Listeria [**39**]. We analyzed the anti-Listeria T cell response at day 9 post-infection and found the number and frequency of Listeria-specific CD8$^+$ T cells strongly reduced in H2-K^b-MICA, while Listeria-specific CD4$^+$ T cells were not affected. At present, it is unclear why the CD8$^+$ T cell response is impaired in Listeria-infected H2-K^b-MICA mice. Down-regulation of NKG2D on activated CD8$^+$ T cells may reduce costimulatory signals for proliferation and cell survival. In fact, it has been reported that NKG2D-mediated signal transduction via DAP10 also involves activation of the serine/threonine kinase Akt that promotes cellular proliferation [**50**]. Alternatively, an impaired activation of NK cells by NKG2D may result in reduced cytokine secretion and/or cell lysis generating a suboptimal T$_H$1 response.

In summary, we demonstrate that the persistent expression of MICA results in a pronounced down-modulation of NKG2D on NK cells and activated $CD8^+$ T cells *in vivo*. The resulting NKG2D dysfunction strongly impacts immunity against NKG2DL-expressing tumor cells and impairs the generation and/or expansion of Listeria-specific $CD8^+$ T cells emphasizing an important function of NKG2D for immunity against tumors and intracellular pathogens.

2.1.2.6 Acknowledgements

The authors gratefully acknowledge the excellent technical assistance by Beate Pömmerl, Jessica Bigott, and the experimental assistance by Anouk Feitsma and thank Keesook Li of the transgenic mouse facility of the Fred Hutchinson Cancer Research Center. The authors are grateful to Adrian Hayday and colleagues for sharing unpublished data and thank Stefan Bauer for critical reading of the manuscript. The pHSE vector is a kind gift of Hanspeter Pircher.

2.1.2.7 References

1. Bauer, S., V. Groh, J. Wu, A. Steinle, J. H. Phillips, L. L. Lanier, and T. Spies. 1999. Activation of NK cells and T cells by NKG2D, a receptor for stress-inducible MICA. *Science* 285:727.

2. Wu, J., Y. Song, A. B. Bakker, S. Bauer, T. Spies, L. L. Lanier, and J. H. Phillips. 1999. An activating immunoreceptor complex formed by NKG2D and DAP10. *Science* 285:730.

3. Ho, E. L., L. N. Carayannopoulos, J. Poursine-Laurent, J. Kinder, B. Plougastel, H. R. Smith, and W. M. Yokoyama. 2002. Costimulation of multiple NK cell activation receptors by NKG2D. *J. Immunol.* 169:3667.

4. Jamieson, A. M., A. Diefenbach, C. W. McMahon, N. Xiong, J. R. Carlyle, and D. H. Raulet. 2002. The role of the NKG2D immunoreceptor in immune cell activation and natural killing. *Immunity.* 17:19.

5. Diefenbach, A., E. Tomasello, M. Lucas, A. M. Jamieson, J. K. Hsia, E. Vivier, and D. H. Raulet. 2002. Selective associations with signaling proteins

determine stimulatory versus costimulatory activity of NKG2D. *Nat. Immunol.* 3:1142.

6. Gilfillan, S., E. L. Ho, M. Cella, W. M. Yokoyama, and M. Colonna. 2002. NKG2D recruits two distinct adapters to trigger NK cell activation and costimulation. *Nat. Immunol.* 3:1150.

7. Billadeau, D. D., J. L. Upshaw, R. A. Schoon, C. J. Dick, and P. J. Leibson. 2003. NKG2D-DAP10 triggers human NK cell-mediated killing via a Syk-independent regulatory pathway. *Nat. Immunol.* 4:557.

8. Groh, V., R. Rhinehart, J. Randolph-Habecker, M. S. Topp, S. R. Riddell, and T. Spies. 2001. Costimulation of CD8alphabeta T cells by NKG2D via engagement by MIC induced on virus-infected cells. *Nat. Immunol.* 2:255.

9. Zompi, S., J. A. Hamerman, K. Ogasawara, E. Schweighoffer, V. L. Tybulewicz, J. P. Di Santo, L. L. Lanier, and F. Colucci. 2003. NKG2D triggers cytotoxicity in mouse NK cells lacking DAP12 or Syk family kinases. *Nat. Immunol.* 4:565.

10. Raulet, D. H. 2003. Roles of the NKG2D immunoreceptor and its ligands. *Nat. Rev. Immunol.* 3:781.

11. Vivier, E., E. Tomasello, and P. Paul. 2002. Lymphocyte activation via NKG2D: towards a new paradigm in immune recognition? *Curr. Opin. Immunol.* 14:306.

12. Spies, T. 2002. Induction of T cell alertness by bacterial colonization of intestinal epithelium. *Proc. Natl. Acad. Sci. USA* 99:2584.

13. Bacon, L., R. A. Eagle, M. Meyer, N. Easom, N. T. Young, and J. Trowsdale. 2004. Two Human ULBP/RAET1 Molecules with Transmembrane Regions Are Ligands for NKG2D. *J. Immunol.* 173:1078.

14. Cosman, D., J. Mullberg, C. L. Sutherland, W. Chin, R. Armitage, W. Fanslow, M. Kubin, and N. J. Chalupny. 2001. ULBPs, novel MHC class I-related molecules, bind to CMV glycoprotein UL16 and stimulate NK cytotoxicity through the NKG2D receptor. *Immunity.* 14:123.

15. Steinle, A., P. Li, D. L. Morris, V. Groh, L. L. Lanier, R. K. Strong, and T. Spies. 2001. Interactions of human NKG2D with its ligands MICA, MICB, and homologs of the mouse RAE-1 protein family. *Immunogenetics* 53:279.

16. Groh, V., R. Rhinehart, H. Secrist, S. Bauer, K. H. Grabstein, and T. Spies. 1999. Broad tumor-associated expression and recognition by tumor-derived gamma delta T cells of MICA and MICB. *Proc. Natl. Acad. Sci. USA* 96:6879.

17. Groh, V., A. Bruhl, H. El Gabalawy, J. L. Nelson, and T. Spies. 2003. Stimulation of T cell autoreactivity by anomalous expression of NKG2D and its MIC ligands in rheumatoid arthritis. *Proc. Natl. Acad. Sci. USA* 100:9452.

18. Hue, S., J. J. Mention, R. C. Monteiro, S. Zhang, C. Cellier, J. Schmitz, V. Verkarre, N. Fodil, S. Bahram, N. Cerf-Bensussan, and S. Caillat-Zucman. 2004. A direct role for NKG2D/MICA interaction in villous atrophy during celiac disease. *Immunity.* 21:367.

19. Meresse, B., Z. Chen, C. Ciszewski, M. Tretiakova, G. Bhagat, T. N. Krausz, D. H. Raulet, L. L. Lanier, V. Groh, T. Spies, E. C. Ebert, P. H. Green, and B. Jabri. 2004. Coordinated induction by IL15 of a TCR-independent NKG2D signaling pathway converts CTL into lymphokine-activated killer cells in celiac disease. *Immunity.* 21:357.

20. Carayannopoulos, L. N., O. V. Naidenko, D. H. Fremont, and W. M. Yokoyama. 2002. Cutting edge: murine UL16-binding protein-like transcript 1: a newly described transcript encoding a high-affinity ligand for murine NKG2D. *J. Immunol.* 169:4079.

21. Cerwenka, A., A. B. Bakker, T. McClanahan, J. Wagner, J. Wu, J. H. Phillips, and L. L. Lanier. 2000. Retinoic acid early inducible genes define a ligand family for the activating NKG2D receptor in mice. *Immunity.* 12:721.

22. Diefenbach, A., A. M. Jamieson, S. D. Liu, N. Shastri, and D. H. Raulet. 2000. Ligands for the murine NKG2D receptor: expression by tumor cells and activation of NK cells and macrophages. *Nat. Immunol.* 1:119.

23. Hamerman, J. A., K. Ogasawara, and L. L. Lanier. 2004. Cutting edge: Toll-like receptor signaling in macrophages induces ligands for the NKG2D receptor. *J. Immunol.* 172:2001.

24. Girardi, M., D. E. Oppenheim, C. R. Steele, J. M. Lewis, E. Glusac, R. Filler, P. Hobby, B. Sutton, R. E. Tigelaar, and A. C. Hayday. 2001. Regulation of cutaneous malignancy by gammadelta T cells. *Science* 294:605.

25. Cerwenka, A., J. L. Baron, and L. L. Lanier. 2001. Ectopic expression of retinoic acid early inducible-1 gene (RAE-1) permits natural killer cell-mediated rejection of a MHC class I-bearing tumor *in vivo*. *Proc. Natl. Acad. Sci. USA* 98:11521.

26. Diefenbach, A., E. R. Jensen, A. M. Jamieson, and D. H. Raulet. 2001. Rae1 and H60 ligands of the NKG2D receptor stimulate tumour immunity. *Nature* 413:165.

27. Salih, H. R., H. G. Rammensee, and A. Steinle. 2002. Cutting edge: down-regulation of MICA on human tumors by proteolytic shedding. *J. Immunol.* 169:4098.

28. Groh, V., J. Wu, C. Yee, and T. Spies. 2002. Tumour-derived soluble MIC ligands impair expression of NKG2D and T-cell activation. *Nature* 419:734.

29. Salih, H. R., H. Antropius, F. Gieseke, S. Z. Lutz, L. Kanz, H. G. Rammensee, and A. Steinle. 2003. Functional expression and release of ligands for the activating immunoreceptor NKG2D in leukemia. *Blood* 102:1389.

30. Wu, J. D., L. M. Higgins, A. Steinle, D. Cosman, K. Haugk, and S. R. Plymate. 2004. Prevalent expression of the immunostimulatory MHC class I chain-related molecule is counteracted by shedding in prostate cancer. *J. Clin. Invest* 114:560.

31. Ogasawara, K., J. A. Hamerman, H. Hsin, S. Chikuma, H. Bour-Jordan, T. Chen, T. Pertel, C. Carnaud, J. A. Bluestone, and L. L. Lanier. 2003. Impairment of NK cell function by NKG2D modulation in NOD mice. *Immunity.* 18:41.

32. Pircher, H., T. W. Mak, R. Lang, W. Ballhausen, E. Ruedi, H. Hengartner, R. M. Zinkernagel, and K. Burki. 1989. T cell tolerance to Mlsa encoded antigens in T cell receptor V beta 8.1 chain transgenic mice. *EMBO J.* 8:719.

33. Klaunig, J. E., P. J. Goldblatt, D. E. Hinton, M. M. Lipsky, J. Chacko, and B. F. Trump. 1981. Mouse liver cell culture. I. Hepatocyte isolation. *In Vitro* 17:913.

34. Foulds, K. E., L. A. Zenewicz, D. J. Shedlock, J. Jiang, A. E. Troy, and H. Shen. 2002. Cutting edge: CD4 and CD8 T cells are intrinsically different in their proliferative responses. *J. Immunol.* 168:1528.

35. Mittrucker, H. W., M. Kursar, A. Kohler, R. Hurwitz, and S. H. Kaufmann. 2001. Role of CD28 for the generation and expansion of antigen-specific CD8(+) T lymphocytes during infection with *Listeria monocytogenes*. *J. Immunol.* 167:5620.

36. Dunn, C., N. J. Chalupny, C. L. Sutherland, S. Dosch, P. V. Sivakumar, D. C. Johnson, and D. Cosman. 2003. Human cytomegalovirus glycoprotein UL16 causes intracellular sequestration of NKG2D ligands, protecting against natural killer cell cytotoxicity. *J. Exp. Med.* 197:1427.

37. Park, E. J., I. Takahashi, J. Ikeda, K. Kawahara, T. Okamoto, M. N. Kweon, S. Fukuyama, V. Groh, T. Spies, Y. Obata, J. Miyazaki, and H. Kiyono. 2003. Clonal expansion of double-positive intraepithelial lymphocytes by MHC class I-related chain A expressed in mouse small intestinal epithelium. *J. Immunol.* 171:4131.

38. Furukawa, H., K. Iizuka, J. Poursine-Laurent, N. Shastri, and W. M. Yokoyama. 2002. A ligand for the murine NK activation receptor Ly-49D: activation of tolerized NK cells from beta β2-microglobulin-deficient mice. *J. Immunol.* 169:126.

39. Lara-Tejero, M. and E. G. Pamer. 2004. T cell responses to *Listeria monocytogenes*. *Curr. Opin. Microbiol.* 7:45.

40. Lanier, L. L. 2001. A renaissance for the tumor immunosurveillance hypothesis. *Nat. Med.* 7:1178.

41. Wolan, D. W., L. Teyton, M. G. Rudolph, B. Villmow, S. Bauer, D. H. Busch, and I. A. Wilson. 2001. Crystal structure of the murine NK cell-activating receptor NKG2D at 1.95 A. *Nat. Immunol.* 2:248.

42. Li, P., D. L. Morris, B. E. Willcox, A. Steinle, T. Spies, and R. K. Strong. 2001. Complex structure of the activating immunoreceptor NKG2D and its MHC class I-like ligand MICA. *Nat. Immunol.* 2:443.

43. Li, P., G. McDermott, and R. K. Strong. 2002. Crystal structures of RAE-1beta and its complex with the activating immunoreceptor NKG2D. *Immunity.* 16:77.

44. Nomura, E., M. Sato, H. Suemizu, T. Watanabe, T. Kimura, K. Yabuki, K. Goto,

N. Ito, S. Bahram, H. Inoko, N. Mizuki, S. Ohno, and M. Kimura. 2003. Hyperkeratosis and leukocytosis in transgenic mice carrying MHC class I chain-related gene B (MICB). *Tissue Antigens* 61:300.

45. Doubrovina, E. S., M. M. Doubrovin, E. Vider, R. B. Sisson, R. J. O'Reilly, B. Dupont, and Y. M. Vyas. 2003. Evasion from NK cell immunity by MHC class I chain-related molecules expressing colon adenocarcinoma. *J. Immunol.* 171:6891.

46. Hue, S., R. C. Monteiro, S. Berrih-Aknin, and S. Caillat-Zucman. 2003. Potential role of NKG2D/MHC class I-related chain A interaction in intrathymic maturation of single-positive CD8 T cells. *J. Immunol.* 171:1909.

47. Groh, V., A. Steinle, S. Bauer, and T. Spies. 1998. Recognition of stress-induced MHC molecules by intestinal epithelial gammadelta T cells. *Science* 279:1737.

48. Wu, J., V. Groh, and T. Spies. 2002. T cell antigen receptor engagement and specificity in the recognition of stress-inducible MHC class I-related chains by human epithelial gamma delta T cells. *J. Immunol.* 169:1236.

49. Sutherland, C. L., N. J. Chalupny, K. Schooley, T. VandenBos, M. Kubin, and D. Cosman. 2002. UL16-binding proteins, novel MHC class I-related proteins, bind to NKG2D and activate multiple signaling pathways in primary NK cells. *J. Immunol.* 168:671.

2.2 Modulation of the innate immune system

2.2.1 A CD14 domain with lipopolysaccharide-binding and -neutralizing activity

This chapter has been published in *ChemBioChem* **7**(2): 275-286 (2006) by the following authors:

Söhnke Voss, Stefan Welte, Mariola Fotin-Mleczek, Rainer Fischer, Artur J. Ulmer, Günther Jung, Karl-Heinz Wiesmüller and Roland Brock

The author of this thesis performed the site-directed mutagenesis and contributed to the analysis of the CD14 mutants by flow cytometry.

2.2.1.1 Abstract

The interaction of lipopolysaccharide with CD14 plays a key role in signaling that activates an early defense against pathogens but also contributes to the development of sepsis and septic shock. Here we have mapped the entire 356-amino-acid protein with synthetic 20-amino-acid peptides and have identified a new lipopolysaccharide-binding domain with a strong LPS-neutralizing activity. Moreover, analysis of the structure-activity relationship of this peptide, which corresponds to amino acids 81-100 of human CD14, revealed that leucines 87, 91, and 94 are essential for these activities. The functional relevance of these residues was confirmed by cellular expression of mutant CD14 proteins that are no longer able to bind LPS. Furthermore, the peptide provided a basis for the generation of highly soluble analogs with stronger lipopolysaccharide-neutralizing activity.

2.2.1.2 Introduction

Release of lipopolysaccharide (LPS) from the cell walls of Gram-negative bacteria into the blood is a strong immunomodulatory stimulus. Low concentrations in blood produce moderate immune responses in healthy humans, but higher concentrations may induce massive release of cytokines, resulting in life-threatening disorders such as septic shock [**1**]. Once released from the bacterial cell wall, LPS is sequestered by

the serum protein lipopolysaccharide-binding protein (LBP), which transfers LPS to CD14 [**2**]. The endotoxin-CD14 complex binds a heterodimer consisting of Toll-like receptor 4 (TLR4) and the coreceptor MD-2 [**3,4**]. TLR4 belongs to a family of at least eleven receptors that mediate immune responses to a large number of diverse molecules of bacterial and viral origin. CD14 is a 55 kDa glycoprotein of 356 amino acids expressed both in a GPI-anchored and in a soluble form. The GPI-anchored form is preferentially expressed on cells of the myeloid lineage (i.e., monocytes, macrophages, and polymorphonuclear granulocytes) [**5,6**], whilst the soluble form (sCD14) plays a role in the LPS responses of endothelial and epithelial cells [**7-9**]. In addition to LPS, CD14 also binds a panel of components of Gram-negative and -positive bacteria that are implicated in the initiation of signal transduction via TLR2. These components include lipoarabinomannan from Mycobacterium tuberculosis, peptidoglycan, lipoteichoic acid, and spirochetal outer membrane lipoproteins and lipopeptides [**10-13**]. For this reason, CD14 has been defined as a pattern recognition receptor in innate immunity [**14**].

Because of CD14s central role, several studies have focused on the identification of structural elements of this protein involved in ligand recognition and binding. It has been shown that the N-terminal part comprising amino acids 1-152 is sufficient for binding and for enabling cellular responses to LPS, both in the soluble and the membrane-bound forms [**15,16**]. Hydrophilic regions and amino acids within the N-terminal portion were identified for serum-dependent binding of LPS to CD14 through the construction of a series of single and combined deletion mutants of membrane-anchored CD14 [**17**], although only one of these mutations affected the LPS-binding of sCD14 in a further study [**18**]. Because of these discrepancies, the authors proposed that different structural determinants may contribute to LPS receptor function in the soluble and the membrane-anchored forms of CD14. The involvement of individual hydrophilic amino acids within the N-terminal 66 amino acids in the binding of soluble CD14 to LPS was further investigated by serine replacement and charge reversal [**19,20**], but only charge reversal of these amino acid side chains abolished the function of the protein. Amino acids 57 to 64 were found to be protected by LPS from the action of Asp-N protease and chymotrypsin, and deletion of this particular region resulted in a nonfunctional mutant that neither bound LPS nor triggered cellular responses to LPS [**21,22**]. Evidence for a contribution to LPS-binding by amino acids 39 to 44 was obtained from a mutant in

which all these amino acids were exchanged for a stretch of alanine residues [**23**]. Alternatively, a further study suggested that the LPS-binding site might be a conformational epitope comprising several other regions of the protein [**24**]. Furthermore, one report showed that amino acids 9 to 13 and 91 to 101 participate in sCD14-mediated signaling, though not for all of the tested immunologically relevant cell types [**25**]. In summary, in spite of these investigations, many questions on the function of CD14 still remain.

Synthetic peptides corresponding to parts of a protein offer an alternative strategy for the identification of ligand-binding domains. Peptides derived from Tachypleus anti-LPS factor [**26**], Limulus anti-LPS factor (LALF) [**27**,**28**], bactericidal/permeability increasing protein (BPI) [**29**], human cationic antibacterial protein of 18 kDa (hCAP18) [**30,31**], lactoferrin [**32**], LPS-binding protein [**33**], as well as the peptide antibiotic polymyxin B [**34**] have been identified as endotoxin-binding and -neutralizing agents. A structural comparison of these LPS-binding peptides and further analyses of structure-activity relationships showed that an amphiphilic structure with a net positive charge together with a considerable hydrophobicity are a general characteristic of these molecules. The spatial organization of the positive and hydrophobic moieties determines the LPS-binding and -neutralizing activity [**35-37**]. It can be assumed that the positively charged amino acid residues interact with the negatively charged moieties of the LPS, such as the phosphate groups, whereas hydrophobic amino acids may bind to the fatty acid chains of LPS [**38**].

LPS-binding molecules might possess potential as drugs for the treatment of sepsis and septic shock and for the generation of affinity reagents for the removal of LPS from the bloodstream [**31,39-41**]. Analyses of structure-activity relationships of LPS-binding peptides that contribute to an understanding of the mode of binding are therefore highly relevant for the generation of optimized LPS-neutralizing agents.

Here we present the identification of an LPS-binding domain of CD14, obtained from a mapping of the full-length 356-amino-acid protein with 20-amino-acid peptides. This domain includes leucine residues 87, 91, and 94 of human CD14, which are shown to be essential for the LPS-binding activity of the protein. The corresponding peptide, comprising amino acids 81 to 100, is sufficient to bind and neutralize LPS. Analysis of the structure-activity relationship of this peptide resulted in the rational

design of some LPS-neutralizing analog with improved activity.

2.2.1.3 Materials and Methods

Reagents. Lipopolysaccharide (phenol-extracted and purified by ion-exchange chromatography) and fluorescein isothiocyanate- labeled lipopolysaccharide (FITC-LPS), both from *E. coli* serotype O111:B4, lipopolysaccharides from *Pseudomonas aeroginosa*, *Klebsiella pneumoniae*, *Salmonella friedenau*, *Salmonella typhimurium* and Rd-LPS from *E. coli*, 3-(4,5-dimethylthiazol-2-yl)-2,5-diphenyltetrazolium bromide (MTT) and phorbol 12-myristate 13-acetate (PMA) were obtained from Sigma (Taufkirchen, Germany), Limulus amebocyte lysate assay from BioWhittaker (Walkersville, MD, USA). Fmoc amino acids were purchased from Novabiochem (Laufelfingen, Switzerland), Senn Chemicals (Dielsdorf, Switzerland) and Orpegen Pharma (Heidelberg, Germany). The isomeric mixture of 5(6)-carboxyfluorescein was obtained from Fluka (Deisenhofen, Germany). G418 was obtained from Gibco (Karlsruhe, Germany), and hygromycin from PAN Biotech (Aidenbach, Germany). Standard chemicals were purchased from Fluka and Merck (Darmstadt, Germany).

Peptide synthesis and labeling. Parallel peptide amide synthesis was performed by solid-phase Fmoc/tert-butyl chemistry with use of an automated peptide synthesizer for multiple peptide synthesis (Syro, MultiSynTech, Bochum, Germany) by a procedure described elsewhere [**59,60**] Peptide amides were synthesized on Rink amide resin (Rapp Polymere, Tübingen, Germany). N-Terminal labeling of the peptide amides with 5(6)-carboxyfluorescein was performed on the resin as previously described [**42**] Conjugation of biotin to N termini of resin-bound peptides was performed with biotin (5 equiv), 2-(1H-benzotriazol-1-yl)-1,1,3,3-tetramethyluronium tetrafluoroborate (5 equiv), 1-hydroxybenzotriazole (5 equiv) and N,N-diisopropylethylamine in N-methylpyrrolidone (10 equiv) for 16 h. Completeness of all labeling was confirmed by Kaiser test [**61**].

Cell culture. The human myelomonocytic cell line THP-1 was obtained from the Deutsche Sammlung von Mikroorganismen und Zellkulturen (DSMZ, Braunschweig, Germany) [**62**]. The cells were cultured in RPMI 1640 medium (PAN Biotech) supplemented with FCS (10 %, PAN Biotech) in a humidified CO_2 atmosphere (5 %) at 37 °C. HEK 293T cells were cultured in IMDM (PAN Biotech)

supplemented with FCS (10 %). The engineering of the CD14-expressing Chinese hamster ovary (CHO)-K1 reporter cell line CHO/CD14/TLR2.elam.tac has been described previously [**63**]. The cells were grown in RPMI 1640 medium containing FCS (10 %), G418 (400 g ml^{-1}) and hygromycin B (400 units ml^{-1}). Adherent cells were harvested with trypsin/EDTA (Biochrom, Berlin, Germany). Cells were passaged every third to fourth day.

ELISA. THP-1 cells were incubated with peptides at the indicated concentrations for 10 min at 37 ºC. LPS (20 ng ml^{-1}) was added to the samples, and after 5 h cell-free supernatants were collected and frozen at -80 ºC. The supernatants were analyzed by a human IL-8-specific ELISA (clone G265-5 and clone G265-8, BDPharMingen, San Diego, CA, USA) or a human TNFα-specific ELISA (clone MAb1 and clone MAb11, BDPharMingen) according to protocols provided by the manufacturer. To render THP-1 cells competent for LPS-induced TNFα secretion, they were treated with phorbol 12-myristate 13-acetate (PMA; 30 ng ml^{-1}) for 72 h at 37 ºC prior to addition of peptides [**64**].

Cell viability assay. After removal of the supernatant (120 µl) for ELISA, cells were incubated with MTT (1 mg ml-1) for 4 h. The formazan product was solubilized with SDS [10 % (m/v) in HCl (10 mM)]. Cell viability was determined by measuring the absorbance of each sample at 570 nm with the microplate reader.

Detection of FITC-LPS-binding to biotinylated bead-immobilized peptides by laser scanning microscopy. A suspension of high-performance streptavidin-Sepharose in ethanol (20 %, v/v, 100 µl; Amersham Bioscience, Uppsala, Sweden) was washed three times with phosphate-buffered saline (PBS) and resuspended in PBS (1 ml). Biotinylated peptides (20 µM) were incubated with the streptavidin-bead suspension for 60 min at 4 ºC on a shaker. Unbound peptides were removed by washing the beads three times with PBS, and the beads were subsequently resuspended in PBS (350 µl). This suspension (50 µl) was further diluted with PBS (950 L). FITC-LPS was solubilized (2 mg ml^{-1}) by sonication for 5 min at 50 ºC and FITC-LPS (2 µg/ml) was incubated with the bead suspension for a further 60 min on a shaker at 4 ºC. For competition experiments FITC-LPS was incubated with the beads in the presence of an unlabeled LPS-binding peptide (2 and 20 µM) or a 50-fold excess of unlabeled LPS. Subsequently the beads were washed three times with

PBS/Tween 20 (0.2 %, v/v) and imaged by laser scanning microscopy with an inverted LSM510 microscope (Carl Zeiss, Göttingen, Germany) fitted with a Plan-Apochromat 63×1.4 N. A. objective. Fluorescein was excited with a 488 nm argon-ion laser. Fluorescence was detected with a BP 505-550 nm band pass filter.

Inhibition of the Limulus amebocyte lysate response to LPS. LPS (2 endotoxin units per ml) was prepared according to the manufacturer's protocol in endotoxin-free water. Peptide amides were prepared at varying concentrations in endotoxin-free water and the respective peptide amide solution was mixed with the LPS solution at a ratio of 1:1 in a 96-well microtiter plate (Becton Dickinson, Franklin Lakes, NJ, USA) and incubated at 37 °C on a shaker. After 45 min Limulus amebocyte lysate (25 µl, Quantitative Chromogenic LAL Kit, Whittaker Bioproducts, Walkersville, USA) was added to each well and incubation was continued for a further 15 min. Chromogenic substrate (50 µl), prepared according to the manufacturer's specifications, was then added and the reaction was stopped after 10 min by addition of acetic acid (100 µl, 25 % v/v) to each well. Absorbance at 405 nm was determined with a microplate reader.

Inhibition of cellular binding of FITC-LPS by CD14-derived peptide amides. RPMI 1640 (200 µl), containing FITC-conjugated LPS (1.2 µg ml^{-1}), was incubated either in the absence or in the presence of CD14-derived peptide amides for 5 min at 37 °C. Subsequently, this mixture (50 µl) was added to CHO-CD14 cells (1×10^6 cells per mL in 100 µl serum-containing RPMI 1640) in a 96-well plate. After incubation, cells were washed twice with ice-cold medium, detached by trypsinization, suspended in ice-cold PBS and washed once in ice-cold PBS. Binding of FITC-conjugated LPS to the cells was analyzed by flow cytometry (BD FACSCalibur System, Becton Dickinson, Heidelberg, Germany). In each case, the median fluorescence intensity of 8000 vital cells was determined. Vital cells were gated on the basis of sideward and forward scatter.

CD spectroscopy. CD spectra were measured on a JASCO J-720 dichrograph spectrometer (Jasco, Easton, MD, US). Stock solutions of the peptide amides (1 mM) were prepared in 1,1,1,3,3,3-hexafluoropropan-2-ol. CD spectra of peptides (10 µM) were recorded either in sodium phosphate buffer (10 mM, pH 7.4) or in sodium phosphate buffer (10 mM, pH 7.4) diluted with trifluoroethanol (TFE, 20 % v/v) at room temperature from 195 to 250 nm at 0.2 nm intervals, with a spectral band width of 1 nm and a scan speed of 20 nm min^{-1}. The spectra were corrected for buffer alone

and the mean residue molar ellipticity ([Θ]) was plotted versus wavelength. The fractional helical content was estimated by using the spectral deconvolution method JFIT provided by Dr. B. Rupp (Lawrence Livermore National Laboratory, Livermore, CA, USA).

Site-directed mutagenesis. The full-length CD14 ORF was cloned into the pcDNA3 vector. Site-directed mutagenesis was performed with the QuikChange II site-directed mutagenesis kit (Stratagene Europe, Amsterdam, NL) according to the manufacturer's instructions with use of the following primers: 5-ctcagctaccggtaggcgccccgcgtgtgccagcgtactc-3 and 5-gagtacgctggcacacgcgggg cgcctaccggtagctgag-3 for the triple L to P exchange, and 5-ctcagctacaggtaggcgcccagcgtgtgcaagcgtactc-3 and 5-gagtacgcttgcacacgctgggcg cctacctgtagctgag-3 for the triple L to Q exchange (obtained from biomers.net, Ulm, Germany). The correct sequences were verified by sequencing. The plasmid DNA was purified by use of the Endofree Plasmid Maxi Kit from Qiagen (Hilden, Germany).

Analysis of the binding of FITC-LPS to HEK 293T cells expressing wild-type and mutant CD14. For transfection, HEK 293T cells were harvested with trypsin/EDTA, washed with medium and suspended in medium containing the indicated plasmid. Cells (2×10^6 cells per ml) were electroporated in 4 mm cuvettes (Peqlab, Erlangen, Germany), with use of a 15 millisecond pulse (330 V and 1700 µF maximal resistance; Fischer Electroporator, Heidelberg, Germany). After electroporation, cells were incubated in cuvettes for a further 30 min and seeded in 6-well plates (Sarstedt, Nümbrecht, Germany, 500 000 cells per well) or in 8-well chambered cover glasses (Nunc, Wiesbaden, Germany; 40 000 cells per well), for further analysis. For flow cytometry, cells were trypsinized after 16 h at 37 °C and seeded in 96-well plates in serum-containing RPMI 1640 (100 000 per well). Cells were washed with medium, resuspended in medium (200 µl) containing FITC-LPS (1 g ml^{-1}), and incubated for 1 h at 4 °C. Subsequently, cells were washed three times with medium, followed by incubation in ice-cold PBS/BSA (0.1 % v/w, 50 µl) containing a polyclonal sheep anti-human CD14 antibody (R&D Systems, Minneapolis, MN, USA; 5 g ml^{-1}) for 1 h at 4 °C. After washing three times in ice-cold PBS/BSA, cells were incubated with PBS/BSA (50 µl) containing a phycoerythrin-conjugated donkey anti-sheep secondary antibody (Dianova, Hamburg, Germany; 1:100 dilution), for 1 h at 4 °C. After washing, cells were suspended in ice-cold PBS/BSA and measured immediately

by flow cytometry. In each case, the fluorescence of 10 000 vital cells was acquired. For confocal microscopy, electroporated HEK 293T cells were seeded in 8-well chambered cover glasses (40 000 per well). One day later, cells were washed once with serum-containing RPMI 1640, followed by incubation with medium containing FITC-LPS on ice and stained for CD14 by indirect immunofluorescence with use of the same reagents as described above. After staining, living cells were imaged immediately. For double detection of FITC-LPS and phycoerythrin-labeled antibody the 488 nm line of an argon ion laser and the light of a 543 nm helium/neon laser were directed over an HFT UV/488/543/633 beam splitter and fluorescence was detected with an NFT 545 beam splitter in combination with a BP 505-530 band pass filter for fluorescein detection and a BP 560-615 band pass filter for phycoerythrin detection.

2.2.1.4 Results

Screening of overlapping 20-amino-acid peptides for inhibition of LPS-induced IL-8 production in THP-1 cells.

To identify functional domains of human CD14 that would interfere with LPS-dependent signaling, the entire mature 356-amino-acid protein was covered by 35 synthetic 20-amino-acid peptides with 10-amino-acid overlaps. All peptides were synthesized as 5(6)-carboxyfluorescein-labeled (Fluo-labeled) peptide amides by parallel solid-phase peptide synthesis based on 9-fluorenylmethoxycarbonyl (Fmoc) chemistry. N-Terminal coupling of carboxyfluorescein was performed by use of optimized procedures for the parallel labeling of peptide collections with reproducible and uniform yields [**42**]. Labeling with carboxyfluorescein: i) allowed the reliable determination of peptide concentrations from the absorption of the fluorophore, and ii) enabled the detection of potential interactions with living cells by fluorescence microscopy and flow cytometry. Except for the peptide corresponding to amino acids 21 to 40, all peptides were obtained in purities exceeding 75 % as determined by reversed-phase HPLC. For some of the more hydrophobic peptides, precipitate formation was observed upon dilution of dimethyl sulfoxide (Me_2SO) stock solutions into aqueous buffers. This problem was circumvented by first diluting the Me_2SO stock solutions 1:10 in tert-butyl alcohol/H_2O (4:1) followed by dilution in aqueous buffers to the working concentrations.

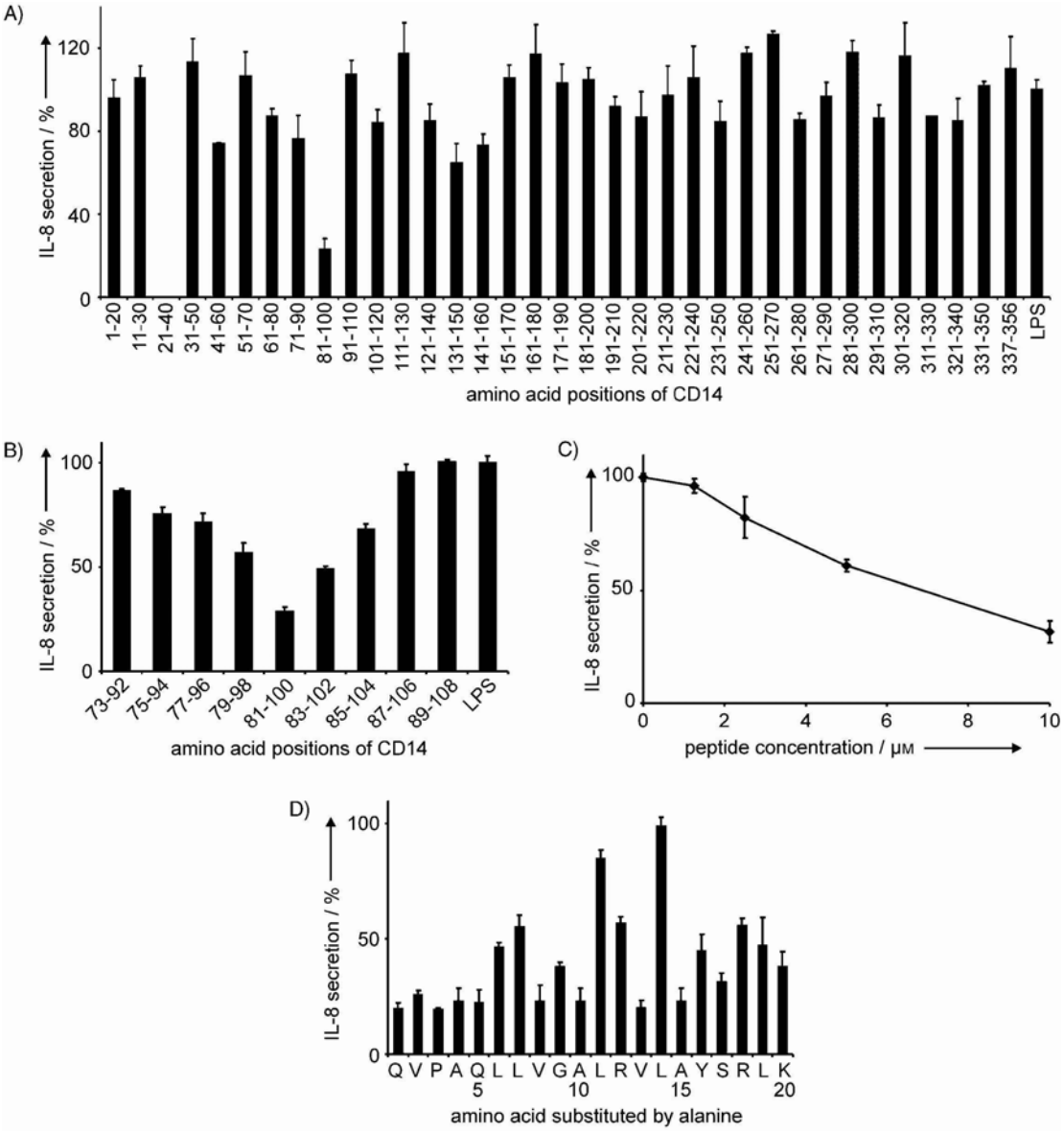

Figure 2.15. Inhibition of LPS-induced IL-8 secretion in THP-1 cells by 20-amino-acid peptide amides derived from human CD14. (**A**) Mapping of the entire human CD14 protein. Despite the use of several synthetic approaches, peptide CD14 (21-40) was not obtained in sufficient purity (>75 %). The individual 20 amino acid peptide amides are specified by their amino acid positions. After 10 min incubation with fluorescein-labeled peptide amides (10 µM), cells were treated with LPS (20 ng ml^{-1}) for 5 h in the presence of peptide amides. (**B**) Fine mapping of the region covering amino acids 73 to 108 of human CD14. (**C**) Concentration dependence of the inhibitory activity of CD14 (81-100). (**D**) To identify residues critical for CD14 (81-100) activity, fluorescent peptide amides with single alanine substitutions were screened for their ability to inhibit the IL-8 production of LPS-stimulated THP-1 cells. The secretion of IL-8 was detected by ELISA in cell-free supernatants. The LPS-induced IL-8 secretion is shown in relation to a sample incubated with buffer only containing solvent at a concentration corresponding to the one of the peptide-containing samples and stimulated with LPS. Error bars represent the standard deviation of triplicates in one representative experiment.

Peptides were tested for their ability to interfere with IL-8 secretion induced by LPS serotype O111:B4 from *E. coli* in human monocyte-derived THP-1 myelomonocytic leukaemia cells. At a concentration of 10 µM, one peptide - corresponding to amino

acids 81 to 100 of human CD14 - reduced the secretion of IL-8 by 80 %. All other peptides exhibited no significant inhibitory activity (**Figure 2.15A**).

For fine mapping of this functional domain of the protein, a further set of eight 20-amino-acid peptides - covering amino acids 73 to 108 with 18-amino-acid overlaps - was synthesized. This second scan again confirmed CD14 (81-100) as the most active peptide (**Figure 2.15B**) and the inhibitory effect was concentration-dependent (**Figure 2.15C**). Viability of cells was fully preserved for all peptides, as determined by an MTT-assay (data not shown).

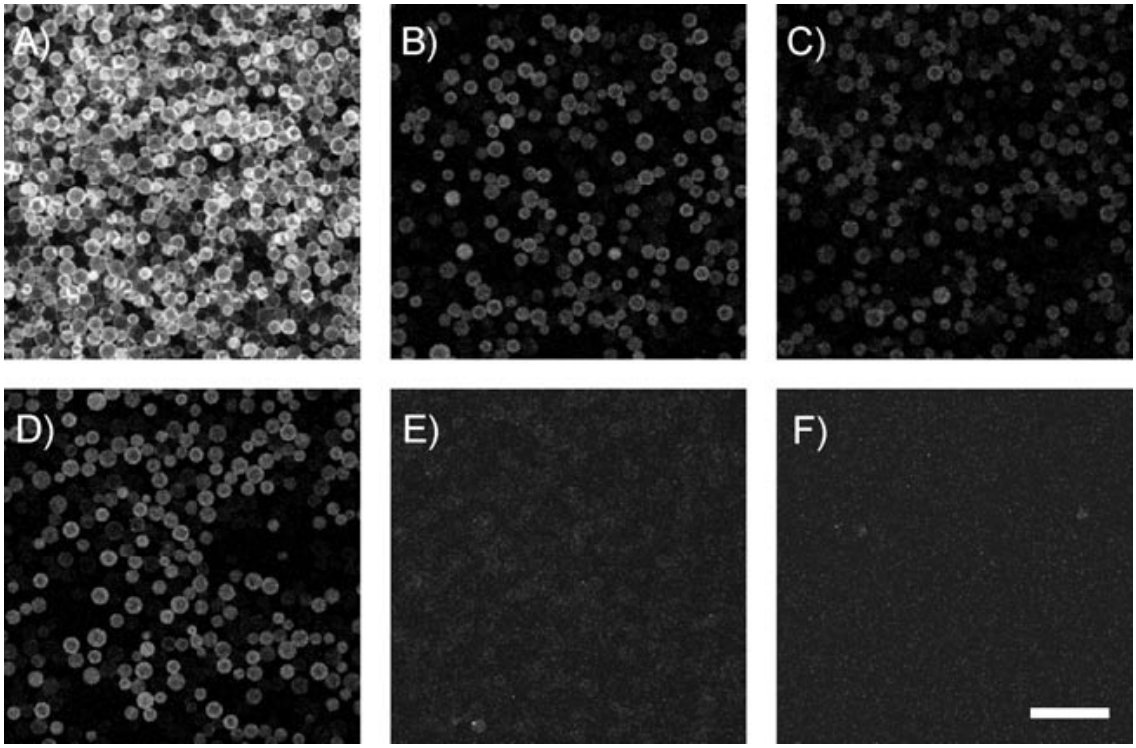

Figure 2.16. LPS-binding by CD14 (81-100). Incubation of streptavidin beads loaded with biotinylated CD14 (81-100) with: (**A**) FITC-LPS (2 µg ml^{-1}), (**B**) coincubation with FITC-LPS and 150 µg ml^{-1} unlabeled LPS, and coincubation with (**C**) 20 µM or (**D**) 2 µM unlabeled peptide 31 (**Table 2.1**). The specificity of LPS binding was confirmed by (**E**) incubation of peptide-free streptavidin beads with FITC-LPS and (**F**) incubation of streptavidin beads loaded with biotinylated peptide CD14 (171-190) with FITC-LPS. Beads were analyzed by fluorescence microscopy. The scale bar corresponds to 200 µm.

Residues important for the inhibitory capacity of CD14 (81-100) were identified by performing an alanine scan through the entire 20-amino-acid sequence (**Figure 2.15D**). When the leucine residues at positions 11 and 14, corresponding to positions 91 and 94 in mature CD14, were replaced by alanine residues the ability of the peptide to inhibit the LPS-induced IL-8 secretion was almost or fully lost. In peptides mutated at the amino acids at positions 6, 7, 9, 12, and 16-20, the capacity to inhibit LPS-induced IL-8 secretion was 50 to 70 % of that of the most active peptide. In contrast,

exchange of amino acids 1-3, 5, 8, and 13 by alanine residues did not affect the activity.

Mode of action of CD14 (81-100).

To clarify whether the inhibitory activity of CD14 (81-100) was associated with an interaction between the peptide and components of the plasma membrane, THP-1 cells were tested for binding of the fluorescein-labeled analog by confocal laser scanning microscopy and flow cytometry. However, no binding of the analog to the cell surface could be detected (data not shown).

We next investigated whether CD14 (81-100) exerted its inhibitory activity on IL-8 secretion through direct interaction with LPS. An analog of CD14 (81-100), N-terminally elongated with two 8-amino-3,6-dioxaoctanoic acid spacer moieties and biotin, was synthesized and bound to streptavidin-conjugated Sepharose beads. The interaction of LPS with the peptide was then investigated by incubation of fluorescein-labeled LPS with beads loaded with CD14 (81-100; **Figure 2.16A**).

Table 2.1. Fluorescein-labeled and acetylated peptide amide analogs of CD14 (81-100). Peptides 11-24 represent analogs with enhanced solubility and amphipathicity relative to the native sequence. In the peptide amides 23 and 24, the leucine residues at positions 11 and 14 were replaced by alanine residues in order to confirm the significance of these residues for the LPS-neutralizing activity.

Peptide	Sequence
Peptide 1	Fluo-QVPAQLLVGALRVLAYSRLK-NH_2
Peptide 11	Fluo-QVPAKLLVKALRKLAYKRLK-NH_2
Peptide 12	Fluo-QVPAKLLVEALRKLAYERLK-NH_2
Peptide 13	Fluo-QVPAELLVKALRELAYKRLE-NH_2
Peptide 14	Fluo-QVPAELLVEALRELAYERLE-NH_2
Peptide 21	Fluo-QVPAQLLVGALRVLAYSRLKKKKK-NH_2
Peptide 22	Fluo-QVPAQLLVGALRVLAYSRLKEEEEE-NH_2
Peptide 23	Fluo-QVPAQLLVGAARVLAYSRLKKKKK-NH_2
Peptide 24	Fluo-QVPAQLLVGALRVAAYSRLKKKKK-NH_2
Peptide 30	Ac-QVPAQLLVGALRVLAYSRLK-NH_2
Peptide 31	Ac-QVPAKLLVKALRKLAYKRLK-NH_2
Peptide 32	Ac-QVPAKLLVKAARKLAYKRLK-NH_2
Peptide 33	Ac-QVPAKLLVKAARKAAYKRLK-NH_2
Peptide 34	Ac-QVPAKLLVKAQRKLAYKRLK-NH_2
Peptide 35	Ac-QVPAKLLVPALRKLAYKRLK-NH_2
Peptide 36	Ac-QVAAKLLVKALRKLAYKRLK-NH_2
Peptide 37	Ac-QVPAQLLVGAARVLAYSRLK-NH_2

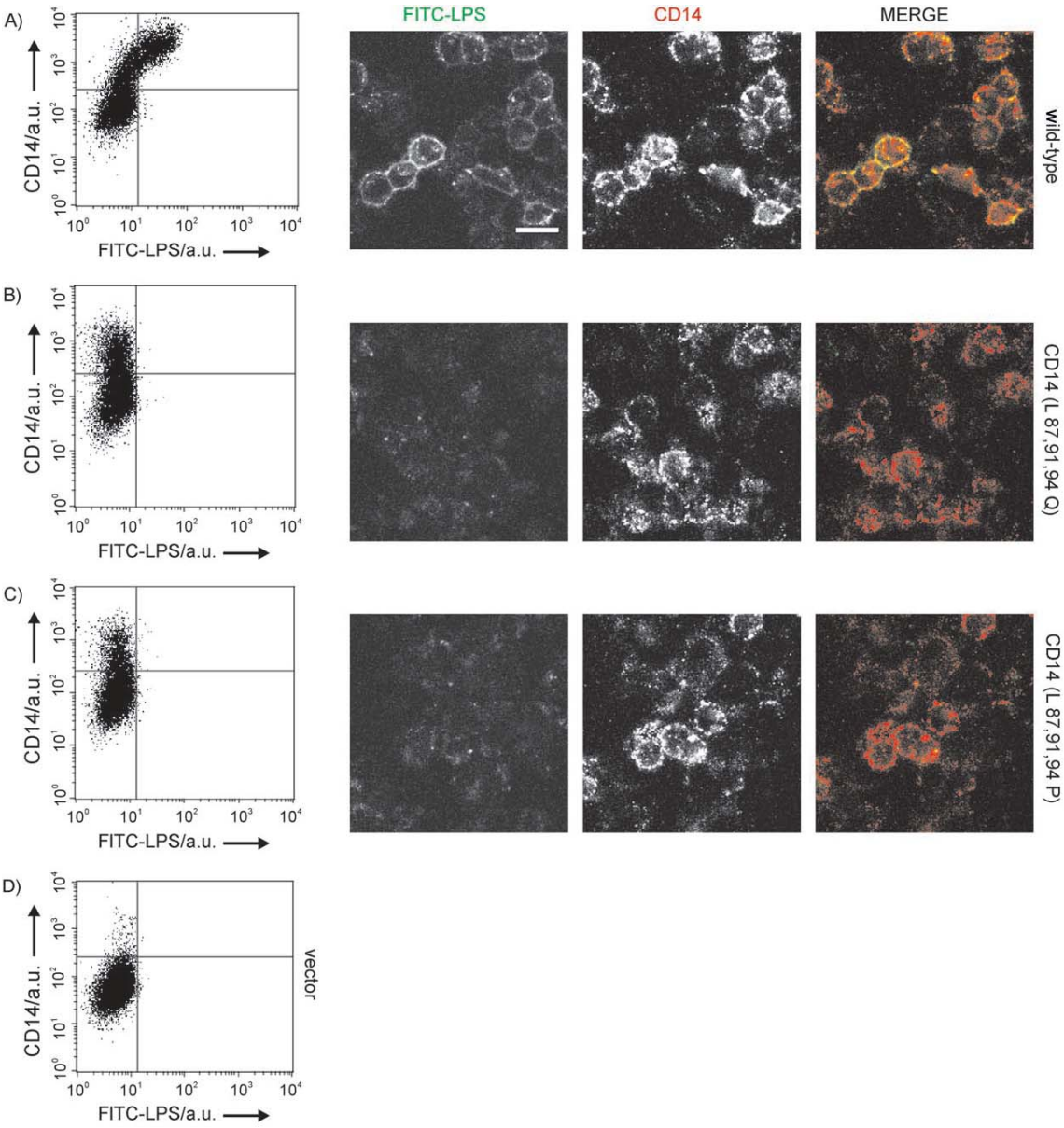

Figure 2.17. Binding of LPS to HEK 293 T cells expressing wild-type and mutated CD14. (**A**) Wild-type CD14, (**B**) CD14 [Leu87, 91, 94 Gln], and (**C**) [Leu87, 91, 94 Pro] were expressed in HEK 293T cells, and binding of FITC-LPS was determined by flow cytometry and fluorescence microscopy. (**D**) Cells electroporated with the vector alone served as a negative control. Electroporated cells were seeded at a density of 100 000 per well in 96-well plates or 40 000 cells per well in 8-well chambered cover glasses for analysis by flow cytometry or confocal laser scanning microscopy, respectively. Cells were incubated with FITC-LPS (1 g ml^{-1}) for 1 h at 4 °C and were then incubated with a polyclonal sheep anti-human CD14 antibody (5 µg ml^{-1}), followed by incubation with a phycoerythrin-conjugated donkey anti-sheep antibody (1:100 dilution) for 1 h in each case. Dot plots of phycoerythrin-fluorescence versus fluorescein fluorescence of cells analyzed by flow cytometry and confocal microscopy images of HEK 293T cells expressing the wild-type or mutant proteins are shown. The scale bar represents 20 µm. The cell-associated fluorescence is given in arbitrary units.

Validation of the LPS-binding site in the full-length protein.

The alanine scan suggested that leucine residues are required for the LPS-binding activity in the CD14-derived peptide. We next investigated whether this domain, and especially the leucine residues, contribute to the LPS-binding domain of the entire protein. Mutant CD14 proteins in which the relevant leucine residues had been replaced by either glutamine or proline residues were therefore expressed in HEK 293T cells, and binding of FITC-LPS was analyzed by flow cytometry and confocal laser scanning microscopy (**Figure 2.17**).

Cells expressing the wild-type CD14 protein bound FITC-LPS efficiently, whereas cells expressing the mutant CD14 proteins at comparable levels did not show any LPS-binding capacity. Cells expressing high levels of the mutant proteins at the plasma membrane were specifically investigated by confocal laser scanning microscopy. Again, no binding of FITC-LPS was detected, demonstrating that the exchange of these residues had abolished LPS binding.

LPS-neutralizing activity of higher-solubility derivatives of CD14 (81-100).

LPS-binding peptides derived from LPS-binding proteins represent a valuable source of LPS-neutralizing agents with therapeutic potential. However, CD14 (81-100) exhibited only poor solubility, so we sought to generate analogs of CD14 (81-100) with improved solubility in aqueous buffers. Two different strategies to enhance peptide solubility were pursued: i) C-terminal elongation of the peptide with a tetralysine or a pentaglutamic acid stretch, and ii) replacement of uncharged amino acids within the peptide by lysine and glutamic acid residues. The results of the alanine scan (**Figure 2.15D**) suggested that the amino acids at positions 5, 9, 13, and 17 should be exchangeable with minimum loss of biological activity. A total of four internally substituted analogs with either lysine or glutamic acid residues in all four positions or with alternating substitutions of lysine/glutamic acid or glutamic acid/lysine residues were synthesized (**Table 2.1**). The substitutions markedly increased the solubilities of all peptides, so that concentrations up to 50 µM could be tested in aqueous buffers. However, only for the peptide in which all residues had been substituted by lysine residues (peptide 11) and the peptide with the C-terminal tetra-lysine stretch (peptide 21) were the capacities to inhibit IL-8 secretion preserved or even improved (**Figure 2.18A,B**). For the latter an IC_{50} value of about 500 nM and a maximum inhibition of 80 % at a concentration of 1 µM were determined, whilst for peptide 11, with the internal lysine substitutions, IL-8 secretion was

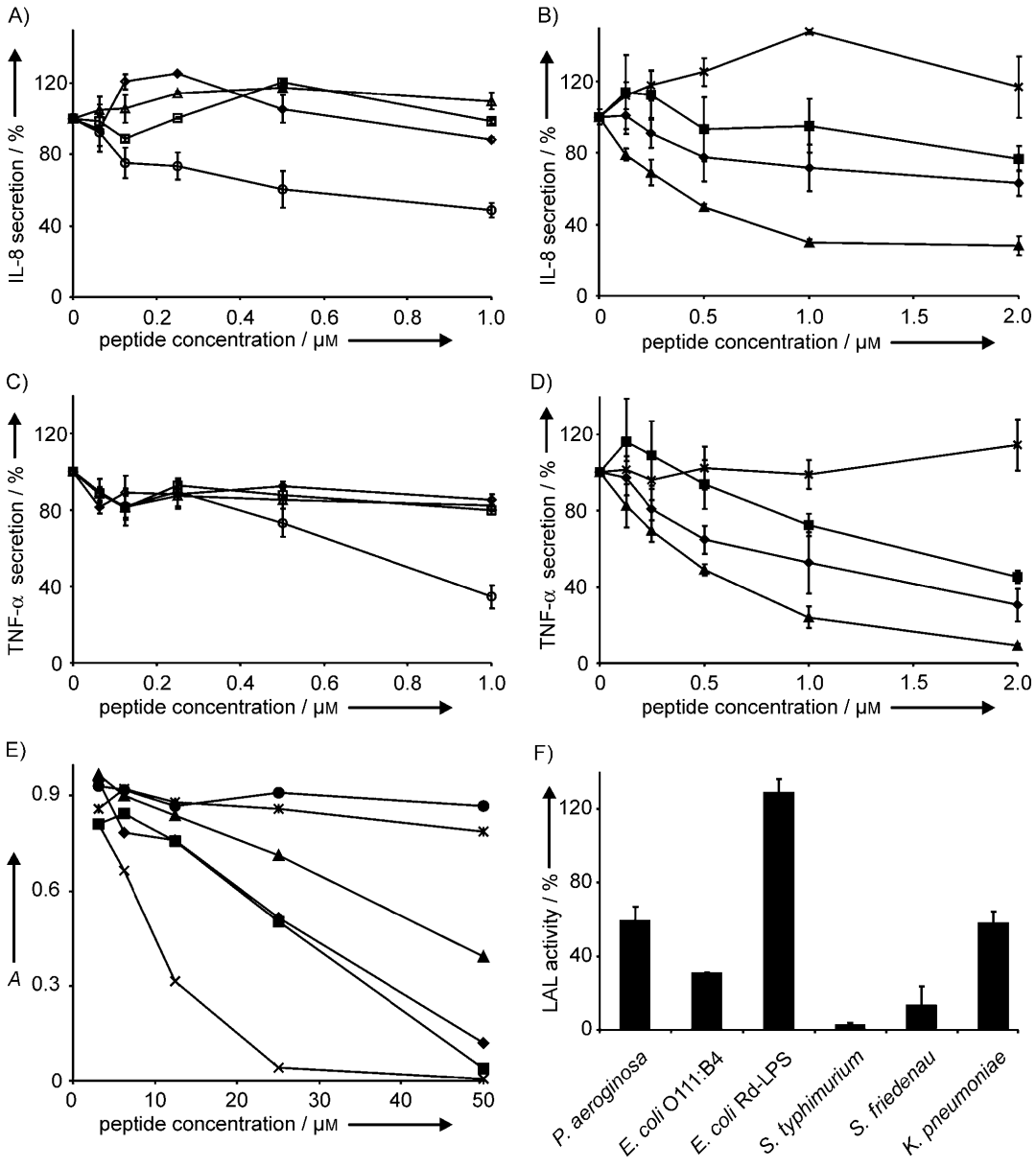

Figure 2.18. LPS-neutralizing activities of CD14 (81-100) analogs with increased solubility. The peptides were tested for their abilities to suppress LPS-induced IL-8 secretion in THP-1 cells (**A,B**) and LPS-induced TNFα-secretion in THP-1 cells differentiated with PMA (**C,D**). After incubation with varying concentrations of fluorescent peptide amides (10 min), cells were stimulated with LPS (20 ng ml^{-1}) for 5 h. The higher toxicities of the analogs with substitutions within the peptide (peptides 11-14) precluded testing of concentrations above 1 µM. The symbols correspond to the following fluorescent peptide amides (see **Table 2.1**): peptide 11: ○; peptide 12: ◊; peptide 13: □; peptide 14: △; peptide 21: ▲; peptide 22: x; peptide 23: ♦; peptide 24: ■. Error bars represent the standard deviations of triplicates. (**E**) Inhibition of the endotoxin-induced LAL reaction by acetylated peptide amide analogs of CD14 (81-100). Increasing concentrations of peptide amides were incubated with LPS (1 endotoxin unit) for 45 min and subsequently the LAL reaction was performed. Absorbance was quantitated at a wavelength of 405 nm. Symbols correspond to the following acetylated peptide amides (**Table 2.1**): peptide 31: ♦; peptide 32: ■; peptide 33: ▲; peptide 34: ●; peptide 35: ✱; peptide 36: **x**. (**F**) Inhibition of the LAL reaction induced by *P. aeroginosa*, *K. pneumoniae*, *S. friedenau*, *S. typhimurium* and *E. coli* Rd-LPS and O111:B4 LPS by the acetylated peptide amide analog of CD (81-100) with enhanced solubility. Peptide 31 (50 µM) was incubated with LPS (2 endotoxin units) for 45 min prior to the LAL reaction. The activity in the LAL assay for various LPSs in the presence of peptide in relation to the activity in the absence of peptide is shown. Error bars represent mean deviations of triplicates.

inhibited by 50 % at a concentration of 1 µM. In agreement with the results of the alanine scan, lysine-elongated analogs containing alanine substitutions of leucine residues at positions 11 (peptide 23) or 14 (peptide 24) exhibited significant decreases in antagonistic activity in the applied concentration range.

In view of the significance of TNFα in the clinical progression of septic shock [**43, 44**], the analogs with higher solubilities were also tested for their capacity to inhibit the secretion of this cytokine. Peptides 11 and 21 inhibited LPS-induced TNFα-secretion in a dose-dependent manner (**Figure 2.18C,D**). Consistently with the results obtained for the inhibition of IL-8 induction, the introduction of negative charges within the peptide (peptides 12, 13, and 14) or at the C terminus (peptide 22) abolished the antagonistic activity. Substitution of the leucine residues at positions 11 (peptide 23) and 14 (peptide 24) reduced but did not fully abolish the inhibitory activity of the peptides.

To validate the LPS-neutralizing capacity of the CD14-derived peptides by a further well established assay, the chromogenic Limulus amebocyte lysate (LAL) assay was performed. Initial experiments had shown that peptide concentrations in the lower to mean micromolar range were required to determine the activity in the LAL test, so this analysis was restricted to the analogs with higher solubility containing lysine substitutions at positions 5, 9, 13, and 17. To exclude disturbance of the readout of the LAL test by the fluorescein moiety, all peptides for this study were N-terminally acetylated instead of fluorescein-labeled (**Table 2.1**).

Unlike in the native sequence, the substitution of a relevant leucine residue at position 11 by an alanine residue (peptide 32) in this assay did not decrease the antagonistic activity. However, when both relevant leucine residues at positions 11 and 14 were replaced by alanine residues (peptide 33), a decrease in activity of about 50 % was observed. Both the exchange of the leucine residue at position 11 for a glutamine residue (peptide 34) and the exchange of a lysine residue for a proline residue at position 9 (peptide 35) resulted in complete loss of activity in the tested concentration range of up to 50 µM. In contrast, substitution of the naturally occurring proline residue at position 3 by an alanine residue (peptide 36) increased the activity more than twofold, yielding an IC_{50} of about 10 µM (**Figure 2.18E**).

Inhibition of the cellular binding of FITC-LPS by CD14-derived peptides

To define the inhibitory mode of action of the CD14-derived peptides further, we lastly determined whether these peptides prevented LPS from binding to cells or whether the LPS-peptide complexes could still bind but failed to activate the receptor. For this purpose CD14-expressing CHO cells were incubated with FITC-conjugated LPS in the presence or absence of CD14-derived peptides, and the cell-associated fluorescence was determined by flow cytometry. Peptide amides 30, 31, and 36 reduced the binding of FITC-LPS by 70 to 80 % at concentrations of 16, 6.5, and 2.5 µM respectively (**Figure 2.19A**). Peptides with enhanced amphipathicity (peptides 31 and 36) were more efficient than the peptide corresponding to the native sequence (peptide 30) in inhibiting the binding of FITC-LPS. The highest activity was again observed for the peptide in which the proline residue at position 3 had been exchanged for an alanine residue (peptide 36). In contrast, peptides 34 (Leu11 to Gln) and 35 (Lys9 to Pro) at concentrations of 2.5 µM had no inhibitory effect (**Figure 2.19B**).

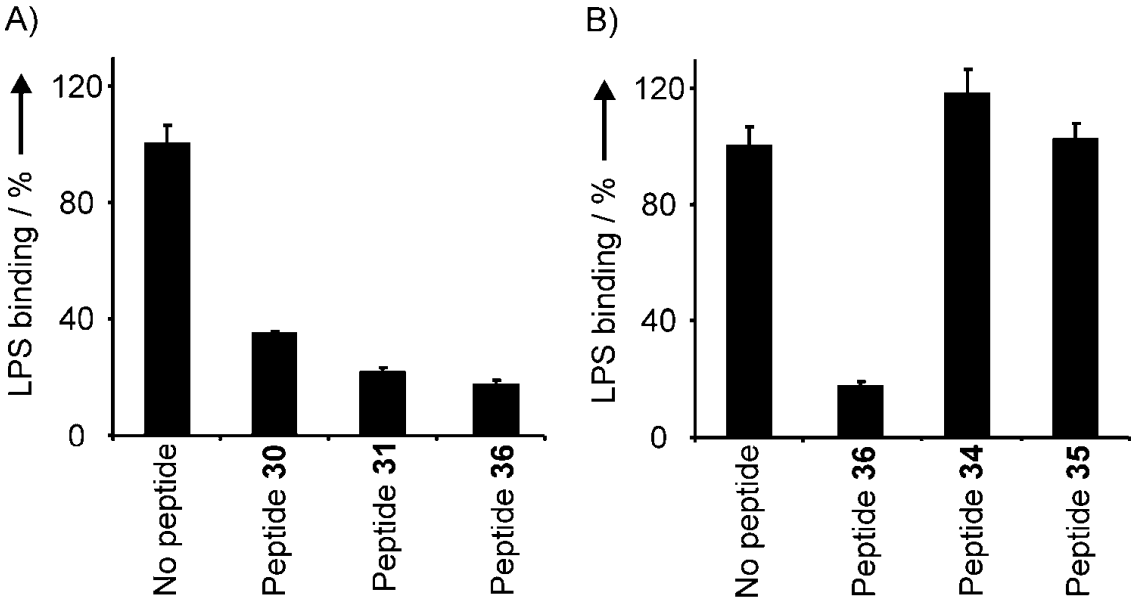

Figure 2.19. Effects of CD14-derived acetylated peptide amides on the binding of FITC-LPS to CHO-CD14 cells. Cells were incubated with FITC-LPS (400 ng ml^{-1}) in the presence of: (**A**) peptide 30 (15 µM), peptide 31 (6.5 µM), peptide 36 (2.5 µM), or (**B**) peptides 34-36 (2.5 µM) for 2 h at 37 °C. For peptides 30, 31, and 36 the concentrations of the individual peptides were selected according to their ability to inhibit the binding of FITC-LPS by 70 to 80 %. After the cells had been washed twice with medium, trypsinized and washed once with PBS, fluorescence was determined by flow cytometry. Columns represent median fluorescence of vital cells in the presence of peptide and FITC-LPS relative to cells treated only with FITC-LPS. Error bars represent the mean deviations of duplicates.

Determination of peptide conformation by CD spectroscopy

An α-helical conformation is a prerequisite for the alignment of the leucine side chains required for the LPS-neutralizing activity of the peptide on one face of the molecule. Circular dichroism measurements allowed estimations of the α-helical contents of these peptides. In phosphate buffer, peptides 30 (native sequence), 31 (more soluble analog), and 37 (leucine residue in position 11 substituted by an alanine) possessed little secondary structure, as evidenced by negative ellipticity at 200 nm (**Figure 2.20A**). Addition of 20 % (v/v) TFE, an organic solvent often used as a membrane mimetic, strongly increased the estimated α-helix contents to 52, 64, and 62 % for peptides 30, 31, and 37, respectively. The CD spectra of the individual peptides were almost indistinguishable from each other (**Figure 2.20B**). The reduced hydrophobicity and enhanced amphipathicity of peptide 31 only slightly enhanced the α-helical content relative to the native sequence. These results indicate that the lower activities of the peptides with leucine to alanine residue exchanges were not due to structural effects but rather to loss of molecular contacts required for tight binding of LPS.

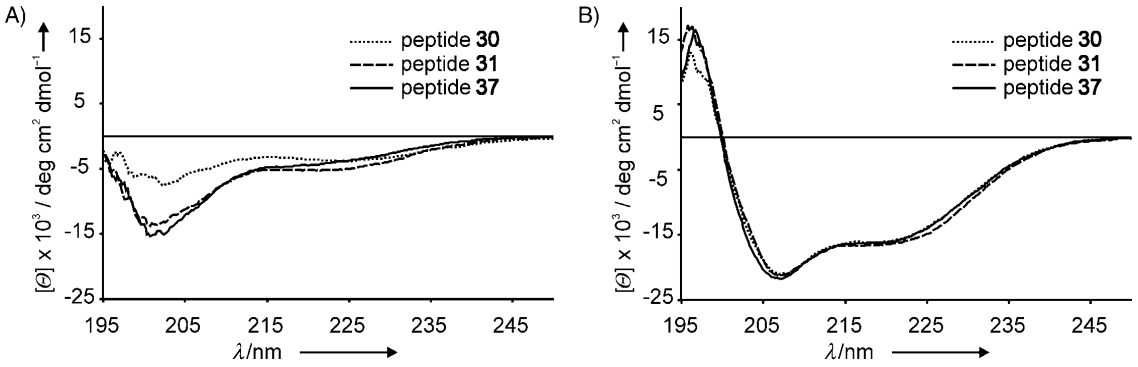

Figure 2.20. Secondary structures of CD14 (81-100) and analogs in solution. The secondary structures of CD14-derived peptides were determined by CD spectroscopy. Far UV-CD spectra of three CD14-derived acetylated peptide amides are shown as mean residue molar ellipticity ([Θ]) versus wavelength (nm). The spectra were recorded at peptide concentrations of 10 µM at room temperature: (**A**) in 10 mM sodium phosphate buffer, pH 7.4, or (**B**) in 10 mM phosphate buffer to which TFE had been added to 20 % (v/v).

2.2.1.5 Discussion

LPS-binding domain of CD14

Mapping of the full-length human CD14 protein with synthetic 20-amino-acid peptide amides overlapping by 10 amino acids identified a single peptide amide with

LPS-neutralizing activity, corresponding to amino acids 81-100 of the mature protein. By using peptide-functionalized Sepharose beads it was shown that this peptide binds FITC-LPS from *E. coli* serotype O111:B4. A crystal structure of murine CD14, obtained in the absence of ligand, was recently published [**45**]. Amino acids 82-94 comprise an α-helix with one side oriented towards an intramolecular pocket and the other side directed outwards. Analysis of the structure-activity relationship of the peptide revealed that the leucine residues corresponding to residues 87, 91, and 94 are required for biological activity. These residues are all located on the side of the helix facing into the interior of the protein. The physiological significance of these residues for binding of LPS was confirmed by the failure of mutant proteins in which these residues had been exchanged for either glutamine or proline residues to bind LPS. Our peptide mapping approach therefore provides strong evidence that the LPS-binding domain of CD14 is located in the interior of the protein and identifies residues directly involved in binding of LPS (**Figure 2.21**).

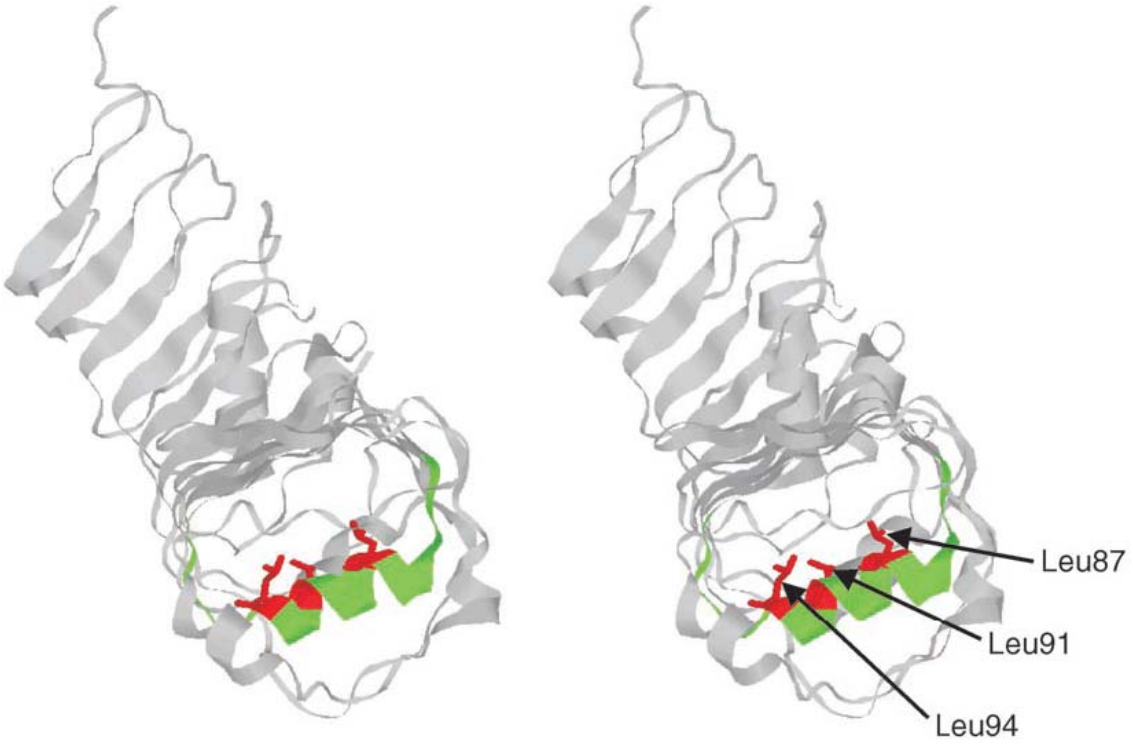

Figure 2.21. Structure of murine CD14. Residues 81-100, comprising helix 4, are in green, whilst side chains of leucine residues 87, 91 and 94 are highlighted in red. The leucine side chains point into the N-terminal pocket, which represents a putative LPS-binding site of the protein.

Several studies have focused on the identification of LPS-binding and -signal-transducing domains of human CD14. The failure to detect the LPS-binding activity of amino acids 81 to 100 previously may be due to the different strategies applied for the identification of the binding sites. For an LPS-binding domain formed by several

separate binding sites, limited mutation of only one site may only slightly affect the affinity of the entire protein. Through our analysis of the structure–activity relationship for the peptide we have been able to identify amino acids involved in LPS binding and to confirm their relevance for the full-length protein by simultaneous site-specific mutation for amino acids with different physicochemical properties or conformational characteristics. The reason why CD14 (81–100) was the only peptide to exhibit LPS-neutralizing activity in our assays might be that this peptide be the only one, among those peptides corresponding to parts of the LPS-binding domain, to assume a conformation similar to that of the corresponding region in the native protein. CD spectroscopy confirmed that peptides derived from CD14 (81–100) displayed considerable α-helix contents under relatively mild helix-inducing conditions, consistently with the secondary structure of this domain observed in the crystal structure.

Given the previous observation that mutations of residues 91 to 101 affected the signal-transducing capacity, we hypothesized that CD14 (81–100) might also have the ability to mimic the functional domain of CD14 responsible for binding to cellular receptors. However, no binding could be detected when the fluorescein-labeled analog of the peptide was incubated with signaling-competent THP-1 cells.

The CD14-derived peptide with enhanced solubility (peptide 31) neutralized smooth LPS from different bacterial strains in the LAL assay but failed to inhibit the LAL reaction induced by rough LPS. This differential activity might be due to an interaction of the peptide with the O-antigen of LPS rather than the lipid A moiety. Conflicting results have been presented with respect to the discrimination of rough and smooth LPS by CD14. In an investigation of the interaction of different LPS with CD14-transfected cells, interaction of both rough and smooth LPS was shown [**46**], although this interaction depended strongly on the presence of LBP. In contrast, Gangloff *et al.* have very recently demonstrated that CD14 preferentially mediates cellular activation by LPS containing the O-antigen [**47**]. With truncation of the carbohydrate moiety, activation of cells by rough LPS variants was increasingly CD14-independent and needed higher concentrations to achieve comparable activation of cells. Additional experiments will be required to reveal the basis of these discrepancies and to better understand the contributions of individual domains in CD14 to the recognition of different LPS ligands.

Our data indicate that the CD14-derived peptides neutralize the cell-stimulating and -binding properties of LPS through complex formation. We did not directly determine

whether the binding of LPS with other LPS-binding molecules involved in the activation of TLR4 was inhibited by our peptide or whether the peptide interfered with the activity once LPS was bound to one of these molecules. Effective molecular recognition of endotoxin requires the concerted action of several extracellular and cell surface proteins (in addition to TLR4) that bind and transfer LPS. In serum, LPS micelles form complexes with the lipid transfer protein LBP. LBP potently enhances the agonistic activity of LPS [**48,49**] by accelerating the transfer of monomeric LPS molecules to CD14 [49-51]. CD14-bound endotoxin is then transferred to MD-2 and TLR4 [**52,53**]. Given this molecular mechanism it seems unlikely that LPS (once bound to a cofactor) is accessible to the LPS neutralizing peptides. In our experiments, we observed that the inhibitory activity of the CD14-derived peptides was enhanced when the dilution of the LPS stock solution to working concentrations was performed under serum-free conditions. Serum represents a source of LBP, so complex formation between LPS and LBP during dilution in a serum-containing buffer might therefore limit the inhibitory activity of the peptides. It was previously shown that several structurally diverse LPS-neutralizing cationic peptides inhibit the interaction of LPS with LBP [**54**]. From these observations and our own, we propose that our peptides might block the initial binding to LBP. However, this still needs to be determined in future experiments.

Comparison of CD14 (81–100) with LPS-binding peptides from other proteins

Recent approaches to the development of molecules that neutralize endotoxin have concentrated on characterizing LPS-binding regions fromendotoxin-binding peptides and proteins. The crystal structure of LALF revealed a positively charged amphipathic loop with the basic residues facing to one side of the molecule that contributes to LPS binding [**27**]. Similar motifs have been proposed for other endotoxin-binding proteins: namely BPI, LBP [**27,28**], heparin-binding protein [**55**], and lactoferrin [**56**].

In addition, a variety of α-helical cationic peptides exhibit strong LPS-binding and -neutralizing activity. These include antimicrobial peptides derived from silk moth cecropin and bee mellitin [**57,40**], human CAP18 [**30,31**], and guinea-pig CAP11 [**58**].

The results obtained from the analysis of the structure–activity relationship and CD spectroscopy revealed that the CD14-derived LPS-neutralizing peptides share properties characteristic of the class of α-helical peptides with antimicrobial activity.

The leucine residues 11 and 14 critical for biological activity are three residues apart. In addition, the lysine-substituted variant of the native sequence exhibits a pattern of aliphatic and cationic amino acid residues that is characteristic of cationic amphipathic a-helices. Similar properties have been reported for the LPS-binding and -neutralizing 18-amino-acid peptide derived fromthe C-terminal part of CAP18 [**31,37**]. Further evidence for an α-helical conformation of CD14 (81–100) was obtained by removal or introduction of proline residues. Mutation of the proline to an alanine residue at position 3 yielded a more potent peptide as shown by the significantly enhanced LPSneutralizing activity in the LAL test. In contrast, the activity of the peptide was significantly reduced when the lysine residue at position 9 was substituted by a proline residue. Moreover, the more soluble CD14 (81–100) analog (peptide 31) inhibited growth of *E. coli* down to a concentration of 1 mM (data not shown).

Up to this point it has not been possible to determine the degree to which the increases in activity of the lysine-substituted analog and the analog containing a tetra-lysine stretch were due to enhanced peptide solubility or to additional molecular interactions of the positively charged amino acid side chains with the negatively charged groups of LPS. The observation that the C-terminal elongation of the peptide increased the activity even more strongly than the internal lysine substitutions indicates that the higher solubility was the major contribution to the higher activity.

2.2.1.6 Acknowledgements

The authors thank Nicole Sessler for excellent technical assistance in peptide synthesis, Aleksandra Velkova for help in the biological testing of the peptides and Aphrodite Kapurniotu for support with CD measurements. The coordinates of the CD14 crystal structure were obtained from J. O. Kim. This work was supported by the BioChance program of the Federal Ministry of Education and Research (grant no. 0312662). R.B. gratefully acknowledges financial support from the Volkswagen Foundation (Nachwuchsgruppen an Universitäten).

2.2.1.7 References

1. Ulevitch, R. J. 1993. Recognition of bacterial endotoxins by receptor-dependent mechanisms. *Adv Immunol.* 53:267-289.

2. Tobias, P. S., K. Soldau, J. A. Gegner, D. Mintz, and R. J. Ulevitch. 1995. Lipopolysaccharide binding protein-mediated complexation of lipopolysaccharide with soluble CD14. *J.Biol.Chem.* 270:10482-10488.

3. Shimazu, R., S. Akashi, H. Ogata, Y. Nagai, K. Fukudome, K. Miyake, and M. Kimoto. 1999. MD-2, a molecule that confers lipopolysaccharide responsiveness on Toll-like receptor 4. *J.Exp.Med.* 189:1777-1782.

4. Poltorak, A., X. He, I. Smirnova, M. Y. Liu, C. Van Huffel, X. Du, D. Birdwell, E. Alejos, M. Silva, C. Galanos, M. Freudenberg, P. Ricciardi-Castagnoli, B. Layton, and B. Beutler. 1998. Defective LPS signaling in C3H/HeJ and C57BL/10ScCr mice: mutations in Tlr4 gene. *Science* 282:2085-2088.

5. Ulevitch, R. J. and P. S. Tobias. 1995. Receptor-dependent mechanisms of cell stimulation by bacterial endotoxin. *Annu.Rev.Immunol.* 13:437-457.

6. Wright, S. D., R. A. Ramos, P. S. Tobias, R. J. Ulevitch, and J. C. Mathison. 1991. CD14, a receptor for complexes of lipopolysaccharide (LPS) and LPS binding protein. *science* 252:1321-1322.

7. Frey, E. A., D. S. Miller, T. G. Jahr, A. Sundan, V. Bazil, T. Espevik, B. B. Finlay, and S. D. Wright. 1992. Soluble CD14 participates in the response of cells to lipopolysaccharide. *J.Exp.Med.* 176:1665-1671.

8. Pugin, J., C.-C. Schürer-Maly, D. Leturcq, A. Moriarty, R. J. Ulevitch, and P. S. Tobias. 1993. Lipopolysaccharide activation of human endothelial and epithelial cells is mediated by lipopolysaccharide-binding protein and soluble CD14. *Proc.Natl.Acad.Sci.U.S.A.* 90:2744-2748.

9. Pugin, J., R. J. Ulevitch, and P. S. Tobias. 1993. A critical role for monocytes and CD14 in endotoxin-induced endothelial cell activation. *J.Exp.Med.* 178:2193-2200.

10. Zhang, Y., M. Doerfler, T. C. Lee, B. Guillemin, and W. N. Rom. 1993. Mechanisms of stimulation of interleukin-1 beta and tumor necrosis factor-alpha by Mycobacterium tuberculosis components. *J.Clin.Invest.* 91:2076-2083.

11. Weidemann, B., J. Schletter, R. Dziarski, S. Kusumoto, F. Stelter, E. T. Rietschel, H.-D. Flad, and A. J. Ulmer. 1997. Specific binding of soluble

peptidoglycan and muramyldipeptide to CD14 on human monocytes. *Infect.Immun.* 65:858-864.

12. Cleveland, M. G., J. D. Gorham, T. L. Murphy, E. Tuomanen, and K. M. Murphy. 1996. Lipoteichoic acid preparations of gram-positive bacteria induce interleukin-12 through a CD14-dependent pathway. *Infect.Immun.* 64:1906-1912.

13. Sellati, T. J., D. A. Bouis, M. V. Norgard, and J. D. Randolf. 1998. Treponema pallidum and Borrelia burgdorferi lipoproteins and synthetic lipopeptides activate monocytic cells via a CD14-dependent pathway distinct from that used by lipopolysaccharide. *J.Immunol.* 160:5455-5464.

14. Pugin, J. and R. J. Ulevitch. 1994. CD14 is a pattern recognition receptor. *Immunity* 1:509-516.

15. Juan, T. S. C., M. J. Kelley, D. A. Johnson, L. A. Busse, E. Hailman, S. D. Wright, and H. S. Lichenstein. 1995. Soluble CD14 truncated at amino acid 152 binds lipopolysaccharide (LPS) and enables cellular response to LPS. *J.Biol.Chem.* 270:1382-1387.

16. Viriyakosol, S. and T. N. Kirkland. 1996. The N-terminal half of membrane CD14 is a functional cellular lipopolysaccharide receptor. *Infect.Immun.* 64:653-656.

17. Viriyakosol, S. and T. N. Kirkland. 1995. A region of human CD14 required for lipopolysaccharide binding. *J.Biol.Chem.* 270:361-368.

18. Viriyakosol, S., J. C. Mathison, P. S. Tobias, and T. N. Kirkland. 2000. Structure-function analysis of CD14 as a soluble receptor for lipopolysaccharide. *J.Biol.Chem.* 275:3144-3149.

19. Cunningham, M. D., R. A. Shapiro, C. Seachord, K. Ratcliffe, L. Cassiano, and R. P. Darveau. 2000. CD14 employs hydrophilic regions to "capture" lipopolysaccharides. *J.Immunol.* 164:3255-3263.

20. Shapiro, R. A., M. D. Cunningham, K. Ratcliffe, C. Seachord, J. Blake, J. Bajorath, A. Aruffo, and R. P. Darveau. 1997. Identification of CD14 residues involved in specific lipopolysaccharide recognition. *Infect.Immun.* 65:293-297.

21. McGinley, M. D., L. O. Narhi, M. J. Kelley, E. Davy, J. Robinson, M. F. Rohde, S. D. Wright, and H. S. Lichenstein. 1995. CD14: physical properties and identification of an exposed site that is protected by lipopolysaccharide. *J.Biol.Chem.* 270:5213-5218.

22. Juan, T. S. C., E. Hailman, M. J. Kelley, L. A. Busse, E. Davy, C. J. Emping, L. O. Narhi, S. D. Wright, and H. S. Lichenstein. 1995. Identification of a lipopolysaccharide binding domain in CD14 between amino acids 57 and 64. *J.Biol.Chem.* 270:5219-5224.

23. Stelter, F., M. Bernheiden, R. Menzel, R. S. Jack, S. Witt, X. Fan, M. Pfister, and C. Schütt. 1997. Mutation of amino acids 39-44 of human CD14 abrogates binding of lipopolysaccharide and Escherichia coli. *Eur.J.Biochem.* 243:100-109.

24. Stelter, F., M. Bernheiden, R. Menzel, S. Witt, R. S. Jack, U. Grunwald, X. Fan, and C. Schutt. 1998. The molecular basis for therapeutic concepts utilizing CD14. *Prog.Clin.Biol.Res.* 397:301-313.

25. Stelter, F., H. Loppnow, R. Menzel, U. Grunwald, M. Bernheiden, R. S. Jack, A. J. Ulmer, and C. Schütt. 1999. Differential impact of substitution of amino acids 9-13 and 91-101 of human CD14 on soluble CD14-dependent activation of cells by lipopolysaccharide. *J.Immunol.* 163:6035-6044.

26. Kloczewiak, M., K. M. Black, P. Loiselle, J. M. Cavaillon, N. Wainwright, and H. S. Warren. 1994. Synthetic peptides that mimic the binding site of horseshoe crab antilipopolysaccharide factor. *J.Infect.Dis.* 170:1490-1497.

27. Hoess, A., S. Watson, G. R. Siber, and R. Liddington. 1993. Crystal structure of an endotoxin-neutralizing protein from the horseshoe crab, Limulus anti-LPS factor, at 1.5 A resolution. *EMBO J.* 12:3351-3356.

28. Ried, C., C. Wahl, T. Miethke, G. Wellnhofer, C. Landgraf, J. Schneider-Mergener, and A. Hoess. 1996. High affinity endotoxin-binding and neutralizing peptides based on the crystal structure of recombinant Limulus anti-lipopolysaccharide factor. *J.Biol.Chem.* 271:28120-28127.

29. Little, R. G., D. N. Kelner, E. Lim, D. J. Burke, and P. J. Conlon. 1994. Functional domains of recombinant bactericidal/permeability increasing

protein (rBPI23). *J.Biol.Chem.* 269:1865-1872.

30. Larrick, J. W., M. Hirata, R. F. Balint, J. Lee, J. Zhong, and S. C. Wright. 1995. Human CAP18: a novel antimicrobial lipopolysaccharide-binding protein. *Infect.Immun.* 63:1291-1297.

31. Kirikae, T., M. Hirata, H. Yamasu, F. Kirikae, H. Tamura, F. Kayama, K. Nakatsuka, T. Yokochi, and M. Nakano. 1998. Protective effects of a human 18-kilodalton cationic antimicrobial protein (CAP18)-derived peptide against murine endotoxemia. *Infect.Immun.* 66:1861-1868.

32. Zhang, G.-H., D. M. Mann, and C.-H. Tsai. 1999. Neutralization of endotoxin *in vitro* and *in vivo* by a human lactoferrin-derived peptide. *Infect.Immun.* 67:1353-1358.

33. Taylor, A. H., G. Heavner, M. Nedelman, D. Sherris, E. Brunt, D. Knight, and J. Ghrayeb. 1995. Lipopolysaccharide (LPS) neutralizing peptides reveal a lipid A binding site of LPS binding protein. *J.Biol.Chem.* 270:17934-17938.

34. Rustici, A., M. Velucchi, R. Faggioni, M. Sironi, P. Ghezzi, S. Quataert, B. Green, and M. Porro. 1993. Molecular mapping and detoxification of the lipid A binding site by synthetic peptides. *Science* 259:361-365.

35. Iwagaki, A., M. Porro, and M. Pollack. 2000. Influence of synthetic antiendotoxin peptides on lipopolysaccharide (LPS) recognition and LPS-induced proinflammatory cytokine responses by cells expressing membrane-bound CD14. *Infect.Immun.* 68:1655-1663.

36. Mayo, K. H., J. Haseman, E. Ilyina, and B. Gray. 1998. Designed beta-sheet-forming peptide 33mers with potent human bactericidal/permeability increasing protein-like bactericidal and endotoxin neutralizing activities. *Biochim.Biophys.Acta* 1425:81-92.

37. Nagaoka, I., S. Hirota, F. Niyonsaba, M. Hirata, Y. Adachi, H. Tamura, S. Tanaka, and D. Heumann. 2002. Augmentation of the lipopolysaccharide-neutralizing activities of human cathelicidin CAP18/LL-37-derived antimicrobial peptides by replacement with hydrophobic and cationic amino acid residues. *Clin.Diagn.Lab.Immunol.* 9:927-982.

38. Porro, M. 1994. Structural basis of endotoxin recognition by natural polypeptides. *Trends Microbiol.* 2:65-67.

39. Giacometti, A., O. Cirioni, R. Ghiselli, F. Mocchegiani, M. S. Del Prete, C. Viticchi, W. Kamysz, E. Lempicka, V. Saba, and G. Scalise. 2002. Potential therapeutic role of cationic peptides in three experimental models of septic shock. *Antimicrob.Agents Chemother.* 46:2132-2136.

40. Gough, M., R. E. W. Hancock, and N. M. Kelley. 1996. Antiendotoxin activity of cationic peptide antimicrobial agents. *Infect.Immun.* 64:4922-4927.

41. Hanasawa, K. 2002. Extracorporeal treatment for septic patients: new adsorption technologies and their clinical application. *Ther.apher.* 6:290-295.

42. Fischer, R., O. Mader, G. Jung, and R. Brock. 2003. Extending the applicability of carboxyfluorescein in solid-phase synthesis. *Bioconjugate Chem.* 14:653-660.

43. Beutler, B., I. W. Milsark, and A. C. Cerami. 1985. Passive immunization against cachectin/tumor necrosis factor protects mice from lethal effect of endotoxin. *Science* 229:869-871.

44. Tracey, K. J., Y. Fong, D. G. Hesse, K. R. Manogue, A. T. Lee, G. C. Kuo, S. F. Lowry, and A. Cerami. 1987. Anti-cachectin/TNF monoclonal antibodies prevent septic shock during lethal bacteraemia. *Nature* 330:662-664.

45. Kim, J. I., C. J. Lee, M. S. Jin, C. H. Lee, S. G. Paik, H. Lee, and J. O. Lee. 2005. Crystal structure of CD14 and its implications for lipopolysaccharide signaling. *J.Biol.Chem.* 280:11347-11351.

46. Triantafilou, M., K. Triantafilou, and N. Fernandez. 2000. Rough and smooth forms of fluorescein-labeled bacterial endotoxin exhibit CD14/LBP dependent and independent binding that is influencedby endotoxin concentration. *Eur.J.Biochem.* 267:2218-2226.

47. Gangloff, S. C., U. Zahringer, C. Blondin, M. Guenounou, J. Silver, and S. M. Goyert. 2005. Influence of CD14 on ligand interactions between lipopolysaccharide and its receptor complex. *J.Immunol.* 175:3940-3945.

48. Schumann, R. R., S. R. Leong, G. W. Flaggs, P. W. Gray, S. D. Wright, J. C. Mathison, P. S. Tobias, and R. J. Ulevitch. 1990. Structure and function of

lipopolysaccharide binding protein. *Science* 249:1429-1431.

49. Mathison, J. C., P. S. Tobias, E. Wolfson, and R. J. Ulevitch. 1992. Plasma lipopolysaccharide (LPS)-binding protein. A key component in macrophage recognition of gram-negative LPS. *J.Immunol.* 149:200-206.

50. Wright, S. D., R. A. Ramos, P. S. Tobias, R. J. Ulevitch, and J. C. Mathison. 1990. CD14, a receptor for complexes of lipopolysaccharide (LPS) and LPS binding protein. *Science* 249:1431-1433.

51. Hailman, E., H. S. Lichenstein, M. M. Wurfel, D. S. Miller, D. A. Johnson, M. Kelley, L. A. Busse, M. M. Zukowski, and S. D. Wright. 1994. Lipopolysaccharide (LPS)-binding protein accelerates the binding of LPS to CD14. *J.Exp.Med.* 179:269-277.

52. Gioannini, T. L., A. Teghanemt, D. Zhang, N. P. Coussens, W. Dockstader, S. Ramaswamy, and J. P. Weiss. 2004. Isolation of an endotoxin-MD-2 complex that produces Toll-like receptor 4-dependent cell activation at picomolar concentrations. *Proc.Natl.Acad.Sci.U.S.A* 101:4186-4191.

53. da Silva, C. J., K. Soldau, U. Christen, P. S. Tobias, and R. J. Ulevitch. 2001. Lipopolysaccharide is in close proximity to each of the proteins in its membrane receptor complex. transfer from CD14 to TLR4 and MD-2. *J.Biol.Chem.* 276:21129-21135.

54. Scott, M. G., A. C. Vreugdenhil, W. A. Buurman, R. E. Hancock, and M. R. Gold. 2000. Cutting edge: cationic antimicrobial peptides block the binding of lipopolysaccharide (LPS) to LPS binding protein. *J.Immunol.* 164:549-553.

55. Iversen, L. F., J. S. Kastrup, S. E. Bjorn, P. B. Rasmussen, F. C. Wiberg, H. J. Flodgaard, and I. K. Larsen. 1997. Structure of HBP, a multifunctional protein with a serine proteinase fold. *Nat.Struct.Biol.* 4:265-268.

56. Elass-Rochard, E., A. Roseanu, D. Legrand, M. Trif, V. Salmon, C. Motas, J. Montreuil, and G. Spik. 1995. Lactoferrin-lipopolysaccharide interaction: involvement of the 28-34 loop region of human lactoferrin in the high-affinity binding to Escherichia coli 055B5 lipopolysaccharide. *Biochem.J.* 312:839-845.

57. Scott, M. G., H. Yan, and R. E. W. Hancock. 1999. Biological properties of

structurally related alpha-helical cationic antimicrobial peptides. *Infect.Immun.* 67:2005-2009.

58. Nagaoka, I., S. Hirota, F. Niyonsaba, M. Hirata, O. Adachi, H. Tamura, and D. Heumann. 2001. Cathelicidin family of antibacterial peptides CAP18 and CAP11 inhibit the expression of TNF-alpha by blocking the binding of LPS to CD14(+) cells. *J.Immunol.* 167:3329-3338.

59. Jung, G. 1996. Combinatorial Peptide and Nonpeptide libraries. *Wiley-VCH, Weinheim*.

60. Fischer, R., K. Kohler, M. Fotin-Mleczek, and R. Brock. 2004. A stepwise dissection of the intracellular fate of cationic cell-penetrating peptides. *J.Biol.Chem.* 279:12625-12635.

61. Sarin, V. K., S. B. H. Kent, J. P. Tam, and R. B. Merrifield. 1981. Quantitative monitoring of solid phase peptide synthesis by the ninhydrin reaction. *Anal.Biochem.* 117:147-157.

62. Tsuchiya, S., M. Yamabe, Y. Yamaguchi, Y. Kobayashi, T. Konno, and K. Tada. 1980. Establishment and characterization of a human acute monocytic leukemia cell line (THP-1). *Int.J.Cancer* 26:171-176.

63. Yoshimura, A., E. Lien, R. R. Ingalls, E. Toumanen, R. Dziarski, and D. T. Golenbock. 1999. Cutting edge: recognition of Gram-positive bacterial cell wall components by the innate immune system occurs via Toll-like receptor 2. *J.Immunol.* 163:1-5.

64. Tsuchiya, S., Y. Kobayashi, Y. Goto, H. Okumura, S. Nakae, T. Konno, and K. Tada. 1982. Induction of maturation in cultured human monocytic leukemia cells by a phorbol diester. *Cancer Res.* 42:1530-1536.

2.2.2 Mutual activation of natural killer cells and monocytes mediated by interaction between the human NK receptor NKp80 and the myeloid-specific receptor AICL

This chapter has been published in *Nat.Immunol.* **7** (12):1334-42 (2006) by the following authors:

Stefan Welte, Sabrina Kuttruff, Inja Waldhauer and Alexander Steinle

The author of this thesis designed and performed all experiments described herein, except the CD107a degranulation and intracellular cytokine assays (**Figure 2.24d-f**, Sabrina Kuttruff), Western Blotting (**Figure 2.28f**, Inja Waldhauer), BIAcore measurements (Alexander Steinle, **Figure 2.26d,e**) and the contributions by others mentioned in the acknowledgements section.

2.2.2.1 Abstract

Receptors encoded by the natural killer gene complex (NKC) (e.g. NKG2D) govern reactivity of natural killer (NK) cells. However, the function and ligand(s) of the NKC-encoded human NK receptor NKp80 remain elusive. Here we demonstrated that NKp80 binds to the genetically linked orphan receptor AICL, which like NKp80 is absent in rodents. We defined AICL as a myeloid-specific activating receptor that is up-regulated by Toll-like receptor stimulation. AICL-NKp80 interactions promoted NK cell-mediated cytolysis of malignant myeloid cells. In addition, during cross-talk between NK cells and monocytes, NKp80 stimulated the release of pro-inflammatory cytokines from both cell types. Thus, by specifically bridging NK cells and myeloid cells, NKp80-AICL interactions may contribute to the initiation and maintenance of immune responses at sites of inflammation.

2.2.2.2 Introduction

Originally, natural killer (NK) cells were primarily considered to be innate immune effector cells capable of spontaneously destroying infected or transformed cells [**1**]. NK cells detect malignant or virus-infected cells through the recognition modes of

'missing-self' and 'induced-self', which regulate cytokine secretion and cytotoxicity and ultimately lead to the elimination of harmful cells [**2,3**].

Emerging evidence now also attributes to NK cells an important role in the initiation and modulation of adaptive immune responses [**4,5**]. Specifically, by providing an early source of interferon-γ (IFNγ), NK cells are instrumental in initiating T helper type 1 (T_H1) T cell responses [**6**]. However, the molecular and cellular events involving NK cells at the initiation of adaptive immune responses remain unclear. In this regard, the cellular cross-talk between NK cells and myeloid cells is currently of major interest, since it is thought to crucially program subsequent immune responses. Several studies demonstrated a mutual activation of NK cells and dendritic cells (DCs), in which both soluble factors and cell contact-dependent events have been implicated [**5,7-10**]. Other recent reports also define a reciprocal activation between human NK cells and monocytes and macrophages [**11,12**]. Like NK-DC interactions, the stimulatory cross-talk between NK cells and monocytes is partially cell contact-dependent; hence an involvement of hitherto undefined receptors was postulated [**12**].

NK cell activation is balanced by inhibitory signals provided by MHC class I-specific NK receptors (which allow detection of 'missing-self') and activating signals received by several immunoglobulin-like and C-type lectin-like receptors like NKG2D (which allows detection of 'induced self'). In humans, a number of activating NK receptors including NKp30, NKp44, NKp46, NKp80 and NKG2D has been characterized, but apart from NKG2D, the unidentified nature of the corresponding cellular ligands strongly hampers further advances in understanding their role in NK cell-mediated immunoregulation and immunosurveillance [**3,13**].

NKG2D and NKp80 (also called KLRF1) are both C-type lectin-like homodimeric receptors encoded within the human NKC [**14-17**]. NKG2D is expressed by virtually all human NK cells, γδ T cells and $CD8^+$ T cells and, together with the adaptor protein DAP10, assembles into an activating immunoreceptor complex [**3,14**]. Upon recognition of its MHC class I-related, stress-inducible ligands encoded by the MIC and ULBP genes, NKG2D stimulates NK cytotoxicity and cytokine secretion [**14,18**]. Since NKG2D ligands are inducibly expressed in cells subjected to genotoxic stress and are associated with malignant transformation, the hypothesis was put forward that NKG2D may detect and orchestrate the elimination of harmful infected or transformed cells [**3,14,19,20**]. In fact, recent studies illustrate that NKG2D provides protection from spontaneous tumors *in vivo* [**21,22**].

In comparison, much less is known about NKp80 which, unlike NKG2D, has been reported to be expressed exclusively on NK cells [**16**]. In fact, NKp80 was described during the course of a search for novel NK cell-specific surface markers [**26**]. Like NKG2D, NKp80 stimulates NK cell cytotoxicity and induces Ca^{2+} influx in human NK cells upon triggering by appropriate antibodies [**16**]. In contrast to NKG2D, NKp80 lacks charged amino acids in its transmembrane domain (thereby disfavouring association with activating adaptor proteins like CD3ζ, DAP12, DAP10 or FcεRIγ) and consensus activation motifs in its cytoplasmic domain. Also in contrast to NKG2D, NKp80 lacks a homologue in rodents [**17**]; this distinction may have impeded investigation of NKp80 function *in vivo*. Recently, two studies of non-human primates confirmed that NKp80 is an NK cell-specific stimulatory receptor [**23,24**]. However, these reports also were limited by the unknown identity of NKp80 ligand(s).

Driven by the knowledge that characterization of NKG2D ligands profoundly improved our understanding of NK cell activation, we set out to identify ligand(s) of NKp80, the only known NKC-encoded activating receptor exclusively expressed on human NK cells. Here, we identified the NKC-encoded orphan receptor AICL (also called CLEC2B) as a ligand of NKp80. Using newly generated AICL-specific monoclonal antibodies we showed that AICL is a novel myeloid-specific receptor expressed by monocytes, macrophages and granulocytes. Cross-linking of both NKp80 and AICL stimulated secretion of pro-inflammatory cytokines, and in co-cultures of NK cells and monocytes, cytokine release was partially dependent on NKp80 engagement. Hence, our findings suggest that the NKp80-AICL interaction is involved in the activating cross-talk between NK cells and myeloid cells, and thus may influence the initiation and maintenance of immune responses in humans.

2.2.2.3 Materials and Methods

Cells. Peripheral blood leukocytes of healthy donors were isolated according to the guidelines of and as approved by the local ethic committee and cultured in X-Vivo 15 (Cambrex) with 10% FCS. NK cells were purified by the NK cell isolation kit II and monocytes by the $CD16^+$ Monocyte Isolation Kit (for NK co-culture), by the Monocyte Negative Isolation Kit (for cytokine secretion assays), or by CD14 microbeads (all from Miltenyi). Cell purity was between 90-98%. Granulocytes were isolated as described [**40**]. Monocytes were differentiated to macrophages with 50

ng/ml hM-CSF. Cytokines were from R&D Systems except hIL-15 and hIL-2 (PromoCell). Monocytes were cultured 24 h with 1 µg/ml LPS from *S. typhimurium,* 50 µg/ml poly(I:C) (Sigma), 1 µM S-[2,3-bis(palmitoyloxy)propyl]-cysteine-$(Lys)_4$ (Pam_2Cys SK4; EMC Microcollections), and 10 ng/ml R-848 (S. Bauer, Munich). NK cells and $CD16^+$ monocytes were co-cultured at 4×10^5 cells/well for 12 h at a 1:1 ratio (total 8×10^5 cells/well) with 100 U IL-2/ml. IL-15 and IL-18 (both at 10 ng/ml), and $F(ab')_2$ of 5D12, 7F12, or NP (4-hydroxy-3-nitrophenylacetyl)-specific IgG_1 (all at 10 µg/ml), respectively, were added where indicated. $CD56^+$ cells were stained for intracellular IFNγ, and $CD14^{dim}16^+$HLA-DR^{bright} cells for intracellular TNF. To calculate monocyte-dependent increases in frequencies of IFNγ-producing NK cells, monocyte-dependent increase in presence of NP-specific IgG_1 (Fab')2 was set as 100% ((%IFNγ-producing NK cells with monocytes) - (%IFNγ-producing NK cells without monocytes) = 100%). Increase in frequencies of TNF^+ monocytes by co-cultivation with NK cells was calculated accordingly.

NKp80- and AICL-specific monoclonal antibodies. Splenocytes of mice repeatedly immunized with NKp80-ED or AICL-ED, respectively, were fused with P3X63Ag8.653 myeloma cells as described [**41**]. Hybridoma supernatants were screened with mixtures of Jurkat-neo or Jurkat-NKp80 transfectants and mixtures of AICL-ED or LLT1-ED-coated microspheres by immunofluorescence. Immunoglobulins were purified from supernatants with Protein A (Biorad). 5D12, 10E4 and 12D11 antibodies are NKp80-specific, 7F12 and 7G4 antibodies are AICL-specific, and all antibodies are of IgG_1 isotype. Antibodies were labeled using Alexa Fluor 647 carboxylic acid-succinimidyl ester according to the manufacturer's protocol (Molecular Probes). $(Fab')_2$ fragments were generated by pepsin digestion und purified from endotoxin by Triton 114 extraction [**42**]. Endotoxins in mAb and $(Fab')_2$ preparations were tested using a *Limulus* amebocyte lysate assay (QCL-1000, Cambrex) and were below 0.1 EU/µg antibody.

Antibodies. PE-conjugated anti-NKp46 and anti-CD56 were from Immunotech, CD14-FITC and isotype control from Immunotools, CD14-PE-Cy7 and isotype control from BioLegend, anti-NKp46 and anti-TREM-1 from R&D Systems, anti-FLAG M2 from Sigma, anti-penta-His from Qiagen, and goat anti-mouse-Ig-PE conjugate from Jackson Laboratories. The anti-NP IgG_1 mAb was a kind gift from Jörg Kirberg, Max-Planck-Institute for Immunobiology, Freiburg, Germany. All other

antibodies were from BD Biosciences.

Cytotoxicity, degranulation and cytokine analysis. Cytotoxicity was analyzed in a 4 h ^{51}chromium-release assay as described [**41**]. Degranulating NK cells were quantified by analysis of surface CD107a after 6 h incubation with plate-bound antibody in the presence of 10 µg/ml Brefeldin A (Sigma) as described [**43**]. Likewise, frequencies of cytokine-producing NK cells were determined by intracellular staining with PE-anti-IFNγ after 6 h incubation with plate-bound antibody in the presence of 10 µg/ml Brefeldin A and 100 U IL-2/ml. Ionomycin (Sigma) and PMA (Cell Signaling Technology) were used at concentrations of 1 nM and 10 ng/ml, respectively. TNF levels in supernatants of purified NK cells stimulated for 24 h with plate-bound antibody and 100 U IL-2/ml were determined using ELISA CytoSets from BioSource. TNF in supernatants of purified monocytes was measured after 24 h stimulation with plate-bound, endotoxin-low antibody.

Soluble ectodomains (ED) of C-type lectin-like receptors. Ectodomains of NKp80 (Gln64 through Tyr231), AICL (Lys26 through His149), LLT1 (Ala61 through Val191), and CD161 (Ile66 through Ser225) were expressed in 293T cells transfected with the corresponding cDNA containing an N-terminal BirA-tag and C-terminal c-myc- and six-histidine-tags. EDs were isolated from supernatants of 293T-transfectants by affinity chromatography with anti-c-myc columns and biotinylated using BirA Ligase [**41**] and purified by size exclusion chromatography. Before use, biotinylated EDs were either immobilized on streptavidin-coated microspheres (Bangs Laboratories) or tetramerized using PE- or APC-labeled streptavidin (Molecular Probes).

SPR measurements. Using a BIAcore X apparatus (BIAcore AB) AICL ectodomains were immobilized to CM5 chips by amine coupling. In kinetic analyses (flow rate: 50 µl/min), RU from the control flow cell ($_{im}$LLT1-ED) were subtracted from RU of the AICL-derivatized surface (black traces) with overlayed gray traces representing fitting of a 1:1 Langmuir model to the association and dissociation phases. In steady-state analyses (15 µl/min) RU from the AICL-derivatized surface were corrected by RU from the non-derivatized control cell. Raw data were analyzed and illustrated using the BIAevaluation software (BIAcore AB).

Immunoblot analysis. Immunoblotting was performed as previously described [**44**]. Treatment with Peptide:*N*-Glycanase F (PNGaseF) (New England Biolabs) was for 1 h at 37°C. Samples were blotted and analyzed with 30 µg 7F12/ml.

Statistical analysis. Statistical analysis was done either using the two-tailed unpaired Student's t test or the nonparametric two-tailed Mann-Whitney Rank Sum test both with $\alpha = 0.050$ and SigmaStat 3.1 software (Systat Software). *P*-values less than 0.04 were considered significant.

Real-time RT-PCR. Total RNA was prepared using TRIZOL (Invitrogen) and reverse transcribed by SuperScript II (Invitrogen). cDNA was amplified with NKp80, AICL and 18S rRNA-specific primer pairs in duplicates (40 cycles, 95°C for 15 s, 60°C for 1 min) using SYBRGreen chemistry on the ABI PRISM 7000 Sequence Detection System (Applied Biosystems). Primers were designed to flank an intron, where possible, and specificity was validated using cloned cDNA. Data analysis was by the ΔCT method for relative quantification. Similar amplification efficiencies for NKp80, AICL and 18S were demonstrated by analyzing serial cDNA dilutions with values of the slope of log cDNA amount vs. ΔCT of < 0.1. Oligonucleotide sequences (forward; reverse) were 18S rRNA: 5´-CGGCTACCACATCCAAGGAA-3´; 5´-GCTGGAATTACCGCGGCT-3´; NKp80: 5´- TTCAGTGACGTTGCACTGGT-3´; 5´-CTCCCTGAGAAACCAACAGGA-3´; AICL: 5´-TACCAAATCGTTTGGCATGA-3´; 5´-CTGCAAATCCATTTTCTTTCG-3´. Purity of PCR products was analyzed on 3% agarose gels.

Transfectants. Jurkat cells were transfected by electroporation with an NKp80-hybrid cDNA encoding the cytoplasmic and transmembrane domains of human CD69 (Met1 through Gly70), the NKp80 ectodomain (Gly85 through Tyr231), and a C-terminal FLAG-tag followed by a six-histidine-tag in RSV.5 neo. COS-7 cells were transiently transfected using FuGene6 (Roche) with an AICL hybrid cDNA encompassing the cytoplasmic domain of mouse CD3ζ (Arg52 through Arg164), the transmembrane domain of mouse Ly-49A (Ser40 through Met90), the AICL ectodomain (Lys26 through His149), and a C-terminal FLAG-tag followed by a six-histidine-tag in RSV.5 neo or with a bicistronic expression vector with full-length cDNA of AICL or LLT1 (first cistron) followed by the EGFP cDNA (second cistron).

2.2.2.4 Results

NKp80 stimulates NK cell degranulation and cytokine release

To analyze NKp80 expression and function, we generated a panel of NKp80-specific monoclonal antibodies by immunizing mice with the NKp80 ectodomain (NKp80-ED). The tagged NKp80-ED construct was expressed in 293T cells and purified from supernatants by affinity chromatography (**Figure 2.22**).

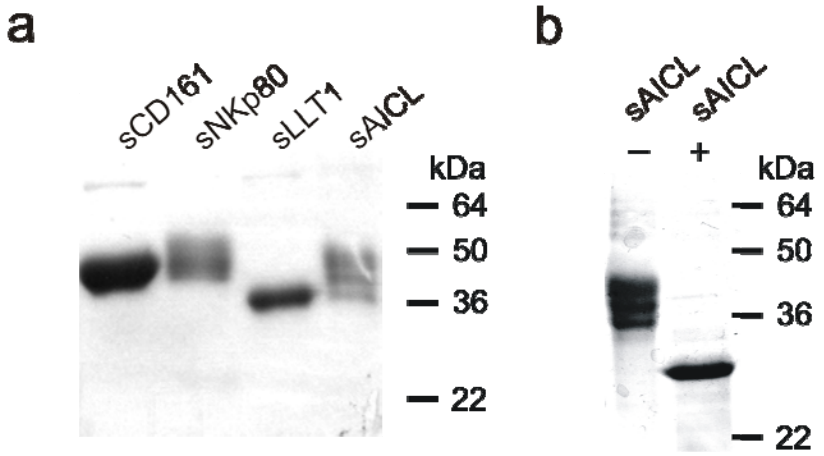

Figure 2.22 Recombinant soluble ectodomains (ED) of various C-type lectin-like receptors. (**a**) SDS-PAGE of soluble CD161-ED, NKp80-ED, LLT1-ED, and AICL-ED affinity-purified from supernatants of transfected 293T cells. (**b**) SDS-PAGE of soluble AICL-ED untreated (–) or treated (+) with PNGase F.

Specificity of the resulting NKp80-specific antibodies 5D12, 10E4, and 12D11 was verified in binding analyses using microsphere-immobilized NKp80-ED and NKp80-transfected Jurkat cells (**Figure 2.23**). In accord with previous reports, the NKp80-specific antibody bound to nearly all freshly isolated human NK cells [**16**] (**Figure 2.24a**). We also noted that the $CD56^{bright}$ NK subset, which is a primary source of monokine-stimulated NK cell cytokine production [**25**], also expressed high amounts of NKp80. NKp80 expression has also been reported to be expressed on $CD3^{+}CD56^{+}$ cells from some donors [**16**]. Accordingly, we found NKp80 on varying fractions of $CD56^{+}CD3^{+}$ cells (range 29-61%, median 43%) (**Figure 2.24b**).

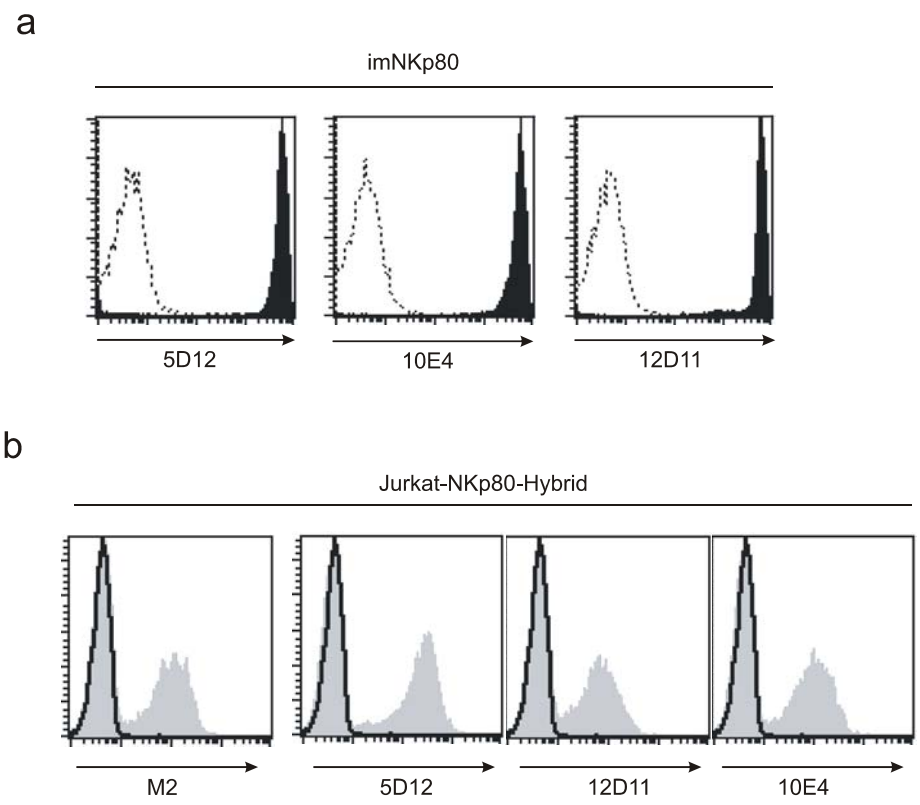

Figure 2.23 Specificity of NKp80-specific antibodies 5D12, 10E4, and 12D11. (**a**) 5D12, 10E4, and 12D11 binding to microsphere-immobilized NKp80 ($_{im}$NKp80) (filled histograms) and $_{im}$LLT1 (open histograms). (**b**) 5D12, 10E4, 12D11, and anti-FLAG binding to a mixture of Jurkat cells transfected with the FLAG-tagged NKp80-CD69 hybrid cDNA and NKp80-hybrid-negative Jurkat transfectants (gray histograms). Black line represents the isotype control staining.

However, we also detected NKp80 on a substantial proportion of γδ T cells. This expression varied widely among individual donors (range 16%-70%, median 26%), and likely accounted for the few NKp80$^+$ CD56$^-$CD3$^+$ T cells (**Figure 2.24b**). In contrast, B cells, monocytes, and other T cells subsets including CD4$^+$ and CD8$^+$ αβ T cells (CD3$^+$CD56$^-$) were devoid of surface NKp80, as were all tested cell lines (data not shown). These findings were supported by real-time RT-PCR analyses, which revealed a high abundance of transcripts encoding NKp80 in NK cells (**Figure 2.25**). The impact of NKp80 triggering on cytokine release by NK cells has not yet been addressed. To investigate the consequences of NKp80 triggering on NK cell effector functions independently of other NK receptors, we incubated freshly purified NK cells with plate-bound anti-NKp80 NKp80 cross-linking triggered secretion of TNF (**Figure 2.24c**). Simultaneous stimulation with anti-NKp80 and anti-NKp46 further amplified TNF secretion. Similar results were obtained when assessing NK cell IFNγ production (**Figure 2.24d**). In accordance with published data on NKp80-mediated stimulation of NK cell cytotoxicity [**16**], we observed that immobilized anti-NKp80

also induced enhanced cell surface exposure of CD107a (also called lysosomal-associated membrane protein (LAMP-1)) which is indicative of NK cell degranulation, in a manner similar to anti-NKp46, again with a pronounced cooperative effect of simultaneous ligation of both receptors (**Figure 2.24e, f**).

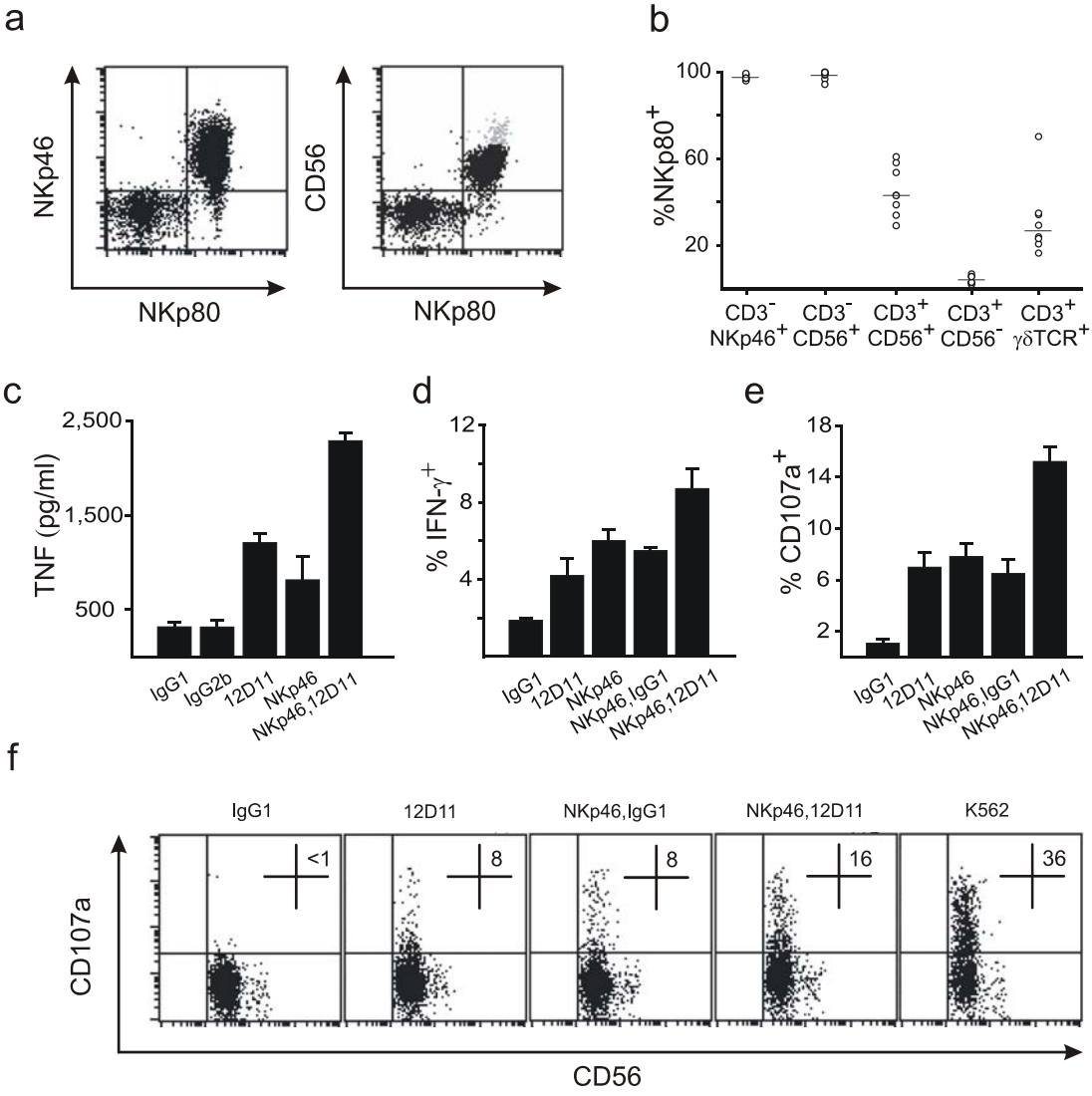

Figure 2.24. NKp80 stimulates granule exocytosis and cytokine secretion. (**a**) Expression of the indicated molecules on the surface of human resting NK cells was determined by flow cytometry. Plots depict freshly isolated PBMC where $CD3^+$ cells were excluded by electronic gating. (**b**) Frequencies of $NKp80^+$ cells among indicated subpopulations from eight healthy donors. Medians are indicated by horizontal bars, and each dot depicts one individual donor. (**c-f**) Freshly purified NK cells were incubated with the indicated plate-bound antibodies. (**c**) Concentrations of TNF in culture supernatants were determined by ELISA. Results depict means of triplicate samples, and error bars represent s.d. Results are representative of 3 independent experiments. (**d**,**e**) Frequencies of $IFN\gamma^+$ cells (**d**) and $CD107a^+$ cells (**e**) among $CD56^+$ NK cells were determined by flow cytometry. Results are shown as means of triplicates with s.d. (**f**) Representative analysis of $CD107a^+$ NK cells after stimulation with indicated immobilized antibodies or K562 cells. Percentages of $CD107a^+$ cells of all $CD56^+$ NK cells (upper right quadrant) are depicted. Results in (**d-f**) are representative of 6 independent experiments.

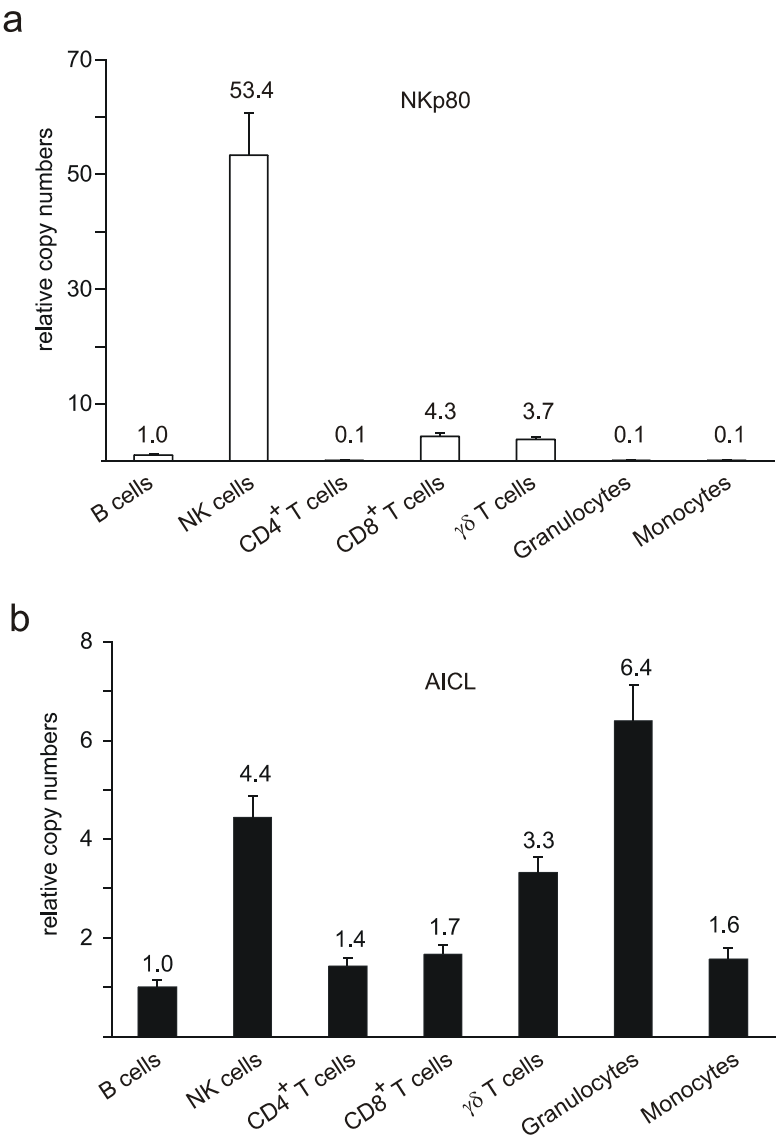

Figure 2.25. Abundance of AICL and NKp80 transcripts in leukocyte subpopulations. (**a, b**) $CD3^+CD8^+$ ($CD8^+$ T cells), $CD3^+CD4^+$ ($CD4^+$ T cells), $CD3^+\gamma\delta\ TCR^+$ ($\gamma\delta$ T cells), $CD19^+$ (B cells), $CD66b^+$ (granulocytes), $CD14^+$ (monocytes) and $CD3{-}CD56^+$ (NK cells) cells were sorted from the peripheral blood of a healthy donor. C_T values for NKp80 (**a**) and AICL (**b**) transcripts were calculated by normalization with 18S RNA and relative copy numbers were determined by setting the ΔC_T value of B cells as 1.

NKp80 engages AICL

Further elucidation of the immunological relevance of NKp80-mediated NK cell activation necessitated the identification of NKp80 ligands (NKp80-L). We attempted to identify NKp80-L bearing cells by using BWZ.36 cells expressing NKp80-CD3ζ reporter constructs, because ligands of the NKC-encoded mouse Nkrp1 receptors were previously identified using BWZ.36 cells expressing Nkrp1-CD3ζ reporter constructs [**26,27**]. These reports revealed that mouse Nkrp1 receptors and their ligands, called C-type lectin-related (Clr) molecules, are all encoded in close genetic linkage within the NKC [**17,26,27**].

Because this strategy failed to identify NKp80-L expressing cells, we considered the possibility that, like Nkrp1-Clr receptor-ligand pairs, the orphan genes encoding Lectin-Like Transcript 1 (LLT1) and Activation-Induced C-type Lectin (AICL), which are located in close proximity to the gene encoding NKp80 in the human NKC, might be ligands of NKp80 (**Figure 2.26a**). In fact, while this work was in progress, LLT1 was reported as a ligand of the single human representative of the Nkrp1 receptor family, NKR-P1A (also called CD161) [**28,29**]; this receptor-ligand pair is also genetically linked within the NKC. In contrast to CD161, no known mouse homologues of NKp80 or for AICL have been identified [**17**]. Hence, to directly assay a possible interaction between NKp80 and AICL or LLT1, we produced soluble ectodomains of AICL (AICL-ED) and LLT1 (LLT1-ED) using stably transfected 293T cells (**Figure 2.22**). AICL-ED or LLT1-ED, respectively, were immobilized on streptavidin-coated microspheres and directly tested for binding to fluorochrome-labeled NKp80-ED or CD161-ED tetramers, respectively, via flow cytometry. As expected, CD161-ED-tetramers bound immobilized LLT1, although staining was fairly weak, indicating a low affinity interaction in agreement with recent reports [**28,29**] (**Figure 2.26b**). In contrast, NKp80-ED-tetramers did not bind to LLT1, but exhibited strong binding to immobilized AICL (**Figure 2.26b**). Similar results were obtained in a 'reverse' setting in which immobilized NKp80-ED specifically interacted with AICL-ED-tetramers (**Figure 2.26c**). These data suggest that AICL, but not LLT1, is a ligand for NKp80.

Using surface plasmon resonance (SPR) technology, we determined the affinity of the NKp80-AICL interaction. Soluble NKp80 ectodomains bound to immobilized AICL-ED with an intermediate association rate (k_{on} = 1.6 × 10^4 $M^{-1}s^{-1}$) and dissociated relatively rapidly (k_{off} = 6.7 × 10^{-2} s^{-1}) (**Figure 2.26d**). The affinity for the NKp80-AICL interaction calculated from on- and off-rates ($K_{D,calc}$ = 4.1 µM at 25°C) is comparable to the affinity determined during steady-state analyses (K_D ~ 2.3 µM at 25°C) (**Figure 2.26e**). Pre-incubation of NKp80-ED-coated microspheres with various NKp80-specific antibodies blocked binding of AICL-ED-tetramers (**Figure 2.26f**). Importantly, AICL-ED-tetramers also stained freshly isolated NK cells and binding was blocked by pre-treatment of NK cells with NKp80-specific antibodies, demonstrating that AICL is a natural ligand of NKp80 (**Figure 2.26g**).

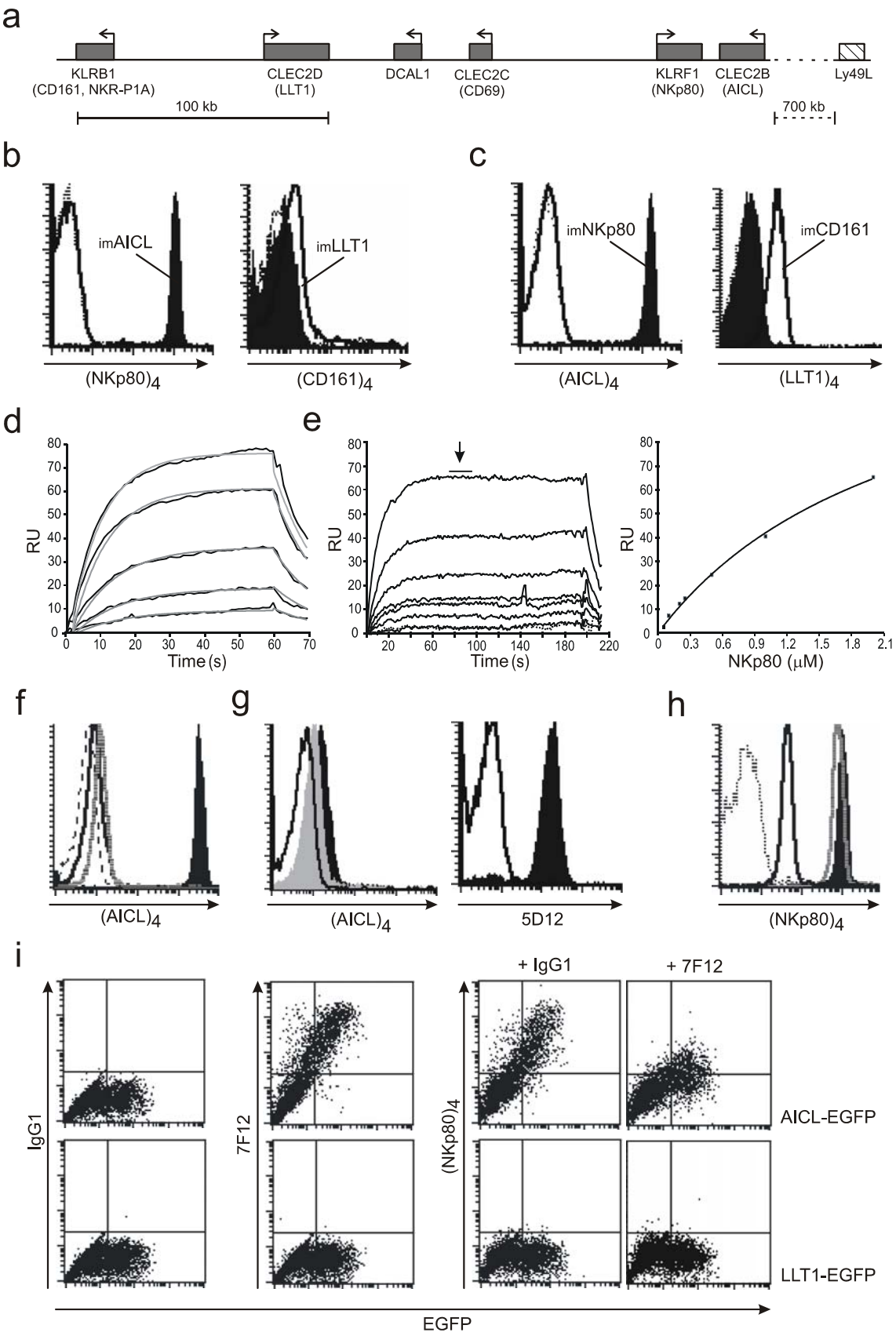

Figure 2.26. NKp80 engages AICL. (**a**) Scheme of a subregion of the human NKC with *KLRF1* and *CLEC2B* encoding NKp80 and AICL, respectively. Ly49L marks the centromeric end of the NKC. Boxes and arrows represent genes and transcriptional orientation, respectively. (**b**) Staining of immobilized sAICL-ED ($_{im}$AICL) (black fill), $_{im}$LLT1 (black line) or $_{im}$NKp80 (dashed line) with indicated tetramers. (**c**) Staining of $_{im}$NKp80 (black fill), $_{im}$CD161 (black line), $_{im}$AICL (dashed line, left panel) or $_{im}$LLT1 (dashed line, right panel) with indicated tetramers. (**d**)

Kinetics of binding of sNKp80-ED (0.12, 0.25, 0.5, 1.0, 2.0 µM) to immobilized AICL-ED as described in Methods. RU, resonance units. (**e**) Affinity of NKp80 to AICL was determined by injecting sNKp80-ED (0.05, 0.1, 0.2, 0.25, 0.5, 1.0, 2.0 µM) over immobilized AICL (left panel). Dotted trace indicates control injection (2 µM sCD161-ED) and arrow averaged interval for a best-fit curve (right panel) (**f**) Binding of sAICL-ED tetramer to NKp80 after pre-incubation with 5D12 (gray line) and 10E4 (dashed line), IgG_1 isotype control (black fill), or to $_{im}$AICL (black line). (**g**) Left, binding of sAICL-ED tetramers to NK cells after pre-incubation with 10E4 (gray fill) and IgG_1 control (black fill) or of sCD161-ED tetramers (black line) to NK cells. Right, surface NKp80 detected by 5D12 (black fill) and isotype control (black line). (**h**) Binding of sNKp80-ED tetramers to $_{im}$AICL after incubation with 7F12 (black line) and 7G4 (gray line) or IgG_1 isotype control (black fill). Staining of $_{im}$NKp80 served as negative control (dotted line). (**i**) Binding of indicated reagents to COS-7 cells transfected with indicated bicistronic EGFP constructs after pre-incubation with indicated antibodies. Data (**b-i**) are representative of at least two independent experiments.

AICL is a myeloid-specific surface receptor

A single study reported differential expression of AICL mRNA expression in T and B lymphocytes, monocytes and granulocytes [**30**]. By real-time PCR, we confirmed that AICL transcripts were most abundantly expressed in granulocytes, and found these more prominently in NK cells and γδ T cells than in αβ T cells or B cells (**Figure 2.25**). However, due to a prior lack of AICL-specific antibodies, AICL protein expression was not examined in previous studies. Thus, to explore AICL expression, we generated AICL-specific antibodies by immunizing mice with AICL-ED. Two antibodies, 7F12 and 7G4, bound immobilized AICL-ED, but not LLT1-ED, NKp80-ED or CD161-ED; these antibodies also stained COS-7 cells transiently transfected with AICL-Ly49A-CD3ζ hybrid constructs, in which transmembrane and cytoplasmic sequences of AICL were replaced by those of mouse Ly49A (transmembrane) and mouse CD3ζ (cytoplasmic) sequences (**Figure 2.27**, and data not shown).

Pre-incubation of microsphere-immobilized AICL with 7F12, but not with 7G4, reduced binding of NKp80-ED tetramers indicating that 7F12 partially hinders the NKp80-AICL interaction (**Figure 2.26h**). Importantly, NKp80-ED tetramers also bound AICL expressed on the surface of transfected COS-7 cells, and addition of 7F12 interfered with binding (**Figure 2.26i** and **Figure 2.27**).

Next, we analyzed AICL surface expression on various cell lines, and detected AICL on the surface of myeloid cell lines U937, THP-1 and MEG-01 (**Figure 2.28a** and **Table 2.2**). U937 cells, which expressed the highest amounts of AICL, also bound high amounts of NKp80-ED tetramers, and pre-incubation with 7F12 markedly reduced NKp80-ED binding (**Figure 2.28b**).

In contrast to myeloid cell lines, AICL was not detectable on non-myeloid hematopoietic or on non-hematopoietic cell lines (**Figure 2.28a** and **Table 2.2**) suggesting that AICL is preferentially expressed on the surface of myeloid cells.

Thus, we analyzed AICL expression on peripheral blood leukocytes and observed specific binding of 7F12 and 7G4 to monocytes, macrophages and granulocytes, but not to T cells, B cells, or NK cells (**Figure 2.28c,d** and **Figure 2.27**). Among monocytes, the $CD14^{dim}CD16^{+}$ subset, which is a major source of TNF [**31**] exhibited substantially higher AICL surface expression than the $CD14^{bright}CD16^{-}$ subset (**Figure 2.28d**).

We also assessed AICL expression on DCs, because the cellular cross-talk between NK cells and DCs has attained much interest [**5**]. Interestingly, AICL expression decreased when monocytes were differentiated *in vitro* to immature DCs (**Figure 2.28e**) indicating that NKp80-AICL interactions may not be involved in the interaction of NK cells with monocyte-derived DCs. A previous report suggested that NKp80-L may be expressed on activated T cells, because NK cell-mediated cytotoxicity against PHA-activated T cells was partially reduced by addition of NKp80-specific antibodies [**42**]. However, we were unable to detect AICL on the surface of activated T cells (**Table 2.2**). Myeloid-specific AICL expression was surprising given that a previous report [**30**] and our analyses detected AICL transcripts also in lymphocytes.

Therefore we analyzed AICL protein in whole cell lysates using 7F12 and detected AICL in lysates of U937 cells and monocytes, but not in lysates of non-myeloid cell lines or lymphocytes (**Figure 2.28f**). Together these data define AICL as a myeloid-specific surface receptor capable of binding NKp80 on NK cells.

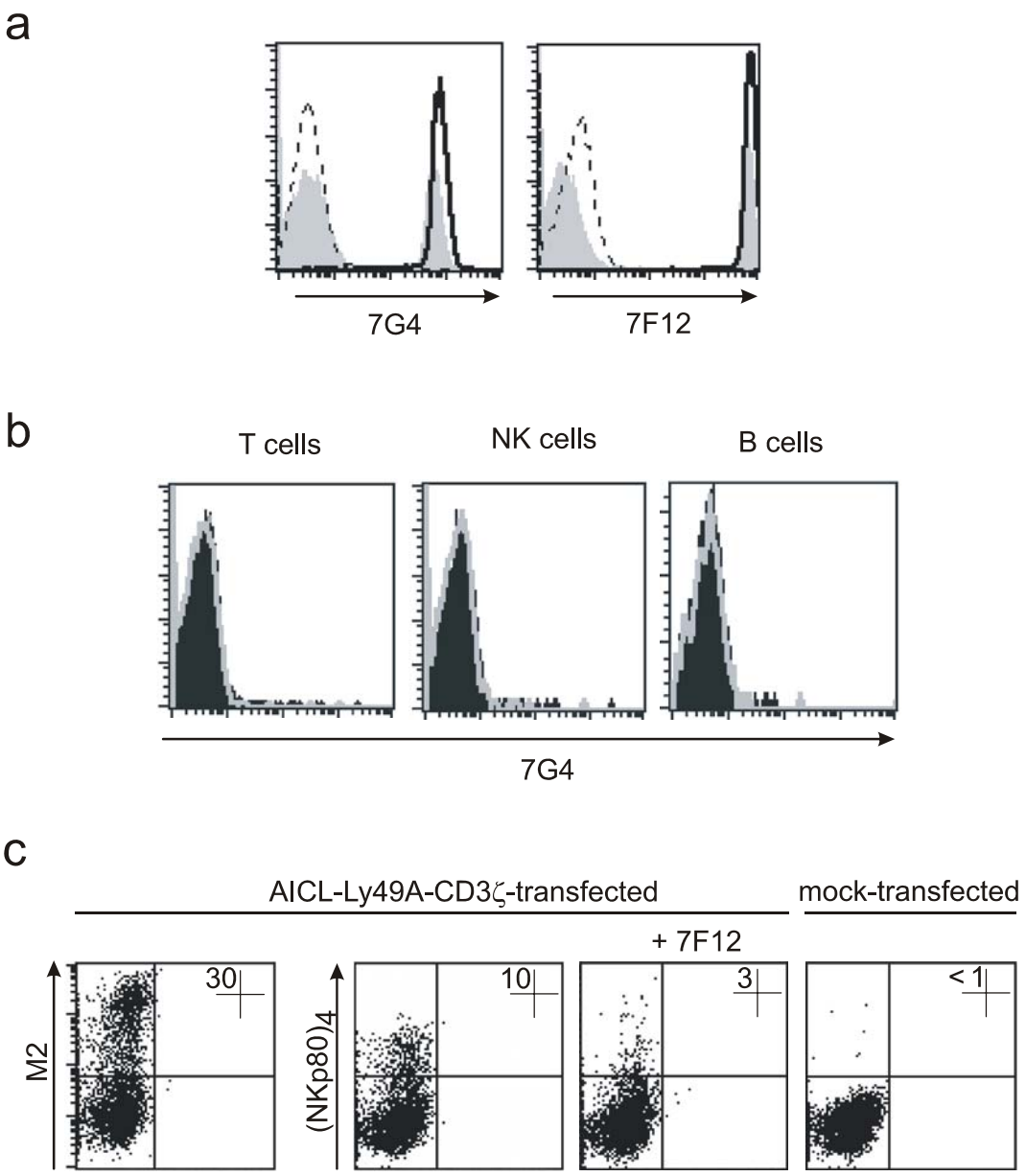

Figure 2.27. (**a**) 7F12 and 7G4 binding to microsphere-immobilized AICL ($_{im}$AICL) (solid line), to $_{im}$NKp80 (dashed line), and to a 2:1 mixture of $_{im}$NKp80-microspheres and $_{im}$AICL-microspheres (gray histograms). (**b**) Staining of 7G4 of freshly isolated T cells ($CD3^+$), NK cells ($CD56^+$) and B cells ($CD19^+$) (filled histogram). Open histograms represent isotype control stainings. (**c**) NKp80-ED tetramer binding to COS-7 cells transiently transfected with an AICL-Ly49A-CD3ζ hybrid after pre-incubation with or without 7F12. NKp80-ED tetramer binding to mock-transfected COS-7 cells is indicated. AICL-hybrid expression was monitored by staining with the FLAG-specific antibody M2. Percentages of stained cells (upper left quadrant) are given.

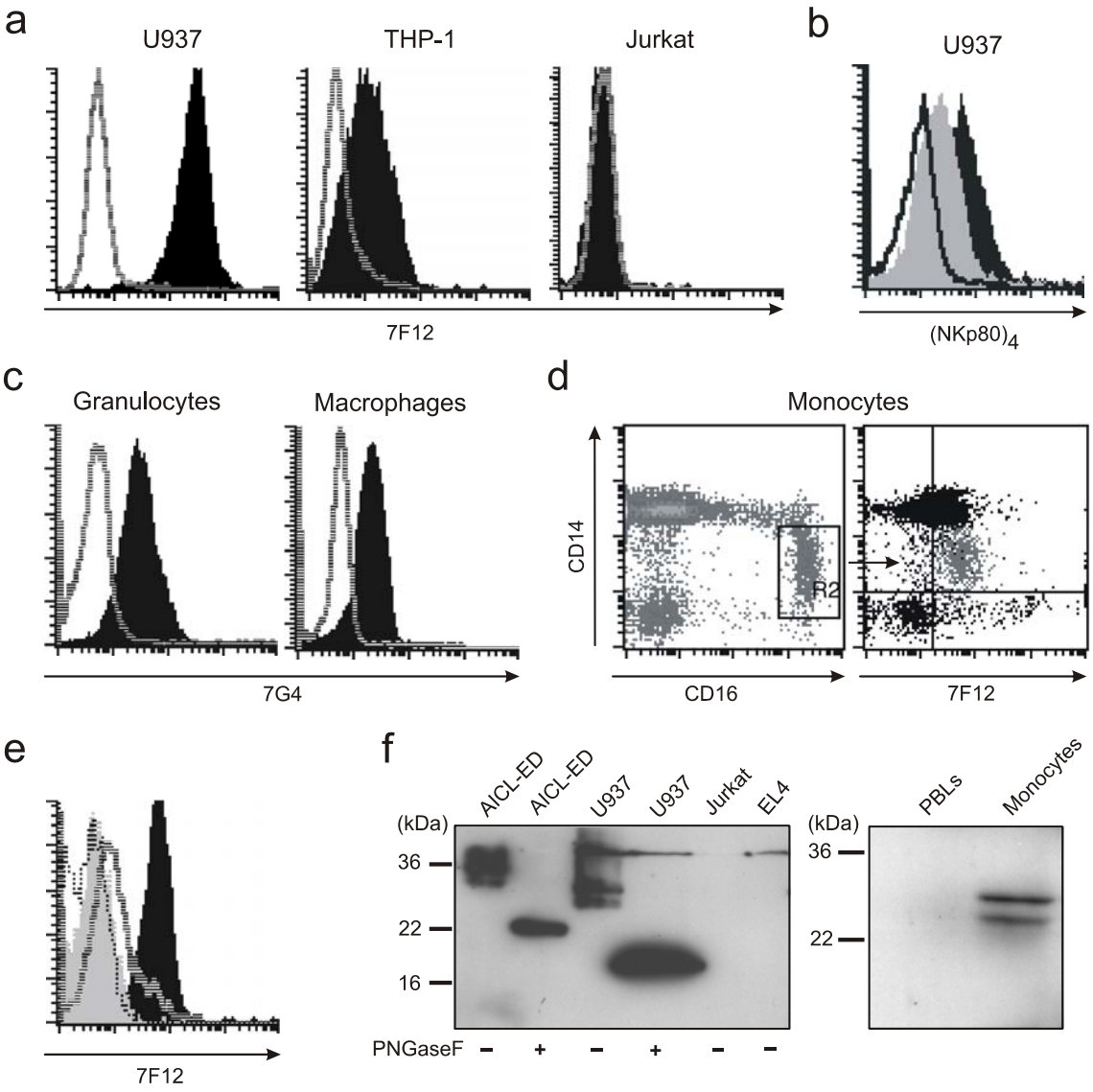

Figure 2.28. AICL is a myeloid-specifc receptor. (**a**) Staining with AICL-specific antibody 7F12 (black fill) or IgG_1 isotype control (gray line) on myeloid cell lines U937 and THP-1 and the T cell line Jurkat, as determined by flow cytometry. (**b**) Binding of NKp80-ED tetramers to U937 cells with and without pre-incubation with 7F12 (gray fill) or IgG_1 isotype control (black fill). Negative control, staining with PE-conjugated streptavidin (black line). (**c**) Staining of freshly isolated granulocytes and *in vitro* matured macrophages with AICL-specific antibody 7G4 (black fill) and IgG_1 isotype control (gray line). (**d**) Expression of indicated molecules on the surface of freshly isolated monocytes. Gray cells in right panel depict cells within R2 in left panel. (**e**) AICL expression on purified monocytes at day 0 (black fill) or after 6 days culture with GM-CSF and IL-4 (gray line). IgG_1 isotype control stainings at day 0 (dashed line) and day 6 (gray fill) are indicated. (**f**) AICL in lysates of indicated cell lines (left), freshly isolated monocytes and lymphocytes (PBLs) (right) was detected by immunoblotting with 7F12. Lysates were deglycosylated with PNGase F where indicated. Recombinant AICL-ED is included as positive control. Data (**a-f**) are representative of at least two independent experiments.

Table 2.2. AICL surface expression on human primary cells and tumor cell lines. Primary cells and tumor cell lines were analyzed by flow cytometry for reactivity with AICL-specific antibodies 7F12 and 7G4. Mean fluorescence intensity (MFI): 10 (-); 10 to 15 (+/-); 15 to 50 (+); 50 to 200 (++), above 200 (+++). nd (not done).

Cells	Histotype	7F12	7G4
Resting NK cells		-	-
Activated NK cells		-	-
Resting T cells		-	-
PHA blasts		-	-
Resting B cells		-	-
Monocytes		+	+
LPS-activated monocytes		++	++
Granulocytes		+	+
Macrophages		+	+
immature monocyte-derived DC		-/+	nd
mature monocyte-derived DC		-	nd
YT	NK cell line	-	-/+
NKL	NK cell line	-	-
CEM	T leukemia	-	-
MOLT4	T leukemia	-	-
Jurkat	T leukemia	-	-
HBP	EBV-transformed B cell line	-	-
LCL 721.221	EBV-transformed B cell line	-	-
WT51	LCL	-	-
T1	B-LCL 721.174xCEMR.3	-	-
C1R	EBV-transformed B cell line	-	-
RPMI 8866	EBV-transformed B cell line	-	-
K562	erythroleukemia	-	-
THP-1	acute monocytic leukemia	+	+
MEG-01	chronic myelogenous leukemia	++	++
U937	human histiocytic lymphoma	+++	+++
HL60	acute promyelocytic leukemia	-	-
NB4	acute promyelocytic leukemia	-	-
293T	embryonic fibroblasts	-	-
AML-01	acute myeloid leukemia	-	-
BV173	chronic myeloid leukemia	-	-
KYO-1	chronic myeloid leukemia	-/+	-/+
CaCo-2	colon carcinoma	-	-
MelJuso	melanoma	-	-
Ma-Mel-8a	melanoma	-	-
HCT116	colon carcinoma	-	-
SW756	cervix carcinoma	-	-
MG63	osteosarcoma	-	-
WEHI-3B	mouse myelomonocytic leukemia	-	-

AICL triggers monocyte cytokine release

Ligands of Toll-like receptors (TLRs) modulate the cell surface expression of various immunoreceptors, including TREM-1, CD80 and CD83 [**32**]. Hence, we determined whether TLR stimulation modulated AICL surface expression. AICL was markedly up-regulated within 24 h of exposure of monocytes to the TLR ligands LPS, poly (I:C), R848, or Pam_2Cys SK4 (**Figure 2.29a** and data not shown). In accord with the lack of TLR9 expression by human monocytes stimulation with the TLR9 ligand CpG DNA did not affect AICL surface expression.

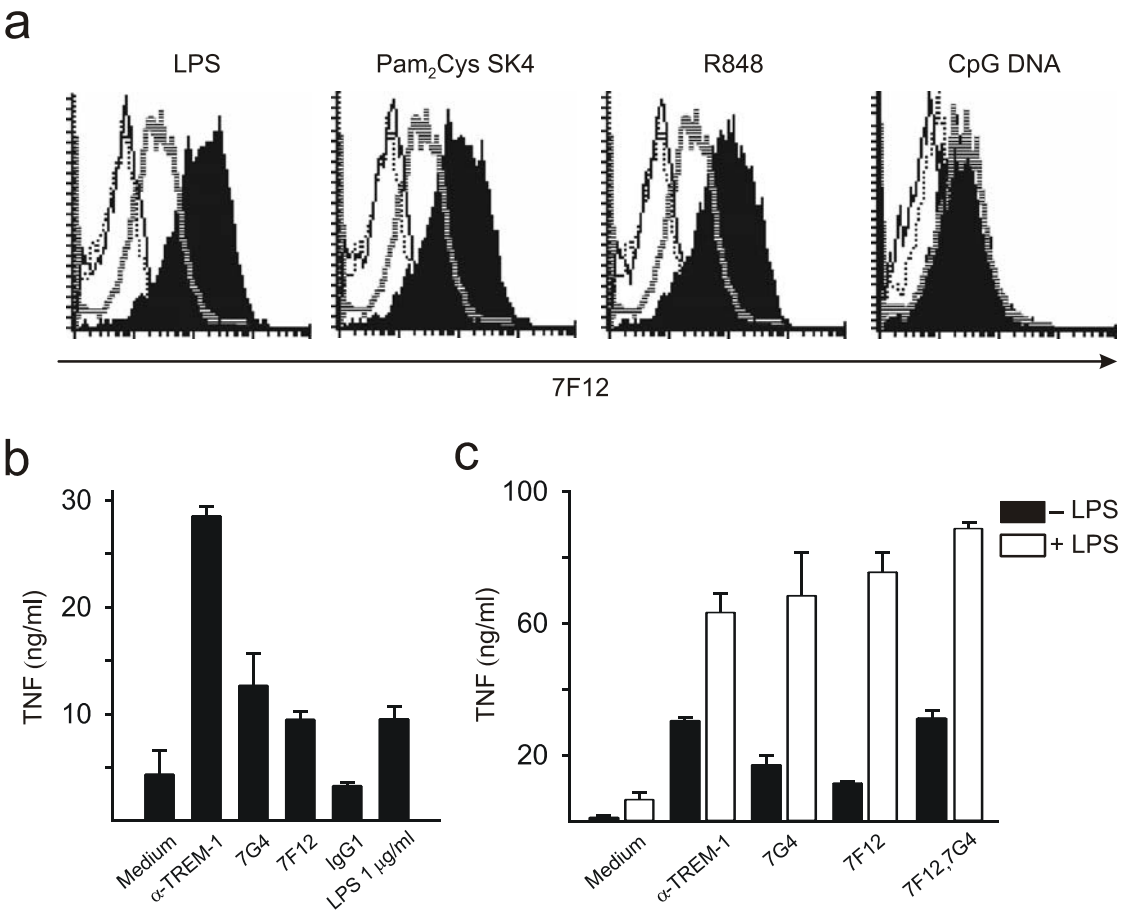

Figure 2.29. AICL is up-regulated by TLR stimulation and stimulates TNF release. (**a**) Freshly purified monocytes stimulated for 24 h with indicated TLR ligands were stained with AICL-specific antibody 7F12 (black fill) or IgG_1 isotype control (dotted line). Stainings of mock-treated monocytes with 7F12 (gray line) or IgG_1 isotype control (black line) are shown. (**b**) TNF in supernatants of freshly isolated monocytes cultivated for 24 h with indicated plate-bound antibodies was measured by ELISA. (**c**) TNF in supernatants of freshly isolated monocytes stimulated for 24 h with indicated plate-bound antibodies in the presence (open bars) or absence of LPS (black bars) was measured by ELISA. In (**b**) and (**c**) means of triplicates are shown, error bars represent s.d. All results are representative of at least 3 independent experiments.

Next, we determined whether AICL ligation could stimulate monocytes. Like stimulation with LPS or with TREM-1-specific antibodies, AICL cross-linking

enhanced monocyte TNF production (**Figure 2.29b**). In addition, LPS exerted a strong additive effect on AICL-stimulated TNF release (**Figure 2.29c**).

NKp80 promotes lysis of AICL$^+$ target cells

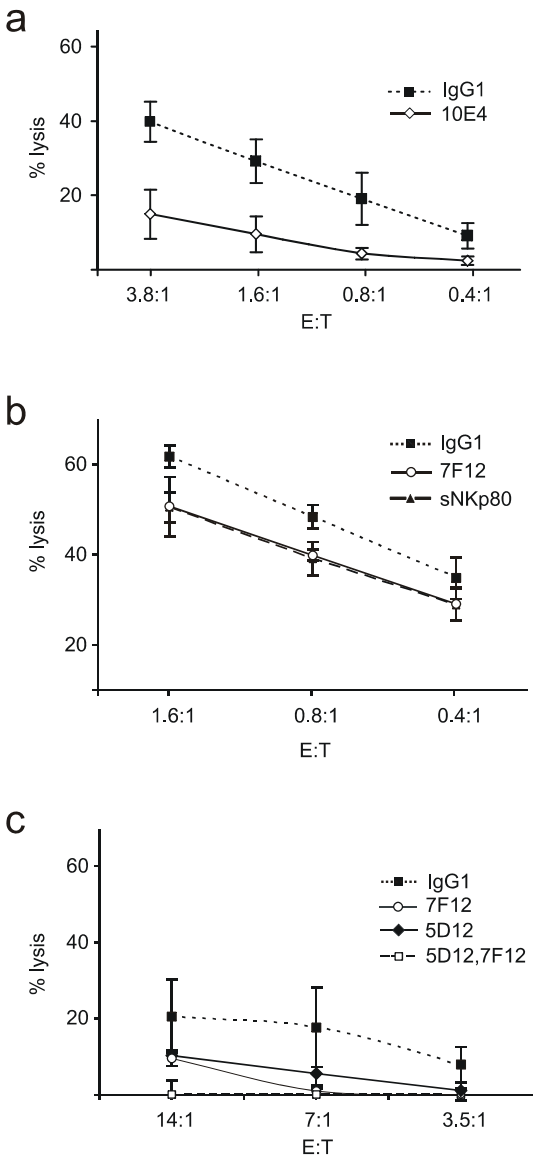

Figure 2.30. NKp80-AICL interaction promotes NK cell-mediated cytolysis of myeloid cells. (**a**-**c**) Cytotoxic activity of freshly purified NK cells was measured during a 4 h ^{51}chromium-release assay (**a**,**b**) Lysis of U937 cells in presence of indicated antibodies. Results are representative of four (**a**) and two (**b**) independent experiments. (**c**) Lysis of LPS-activated, CD14$^+$ monocytes in the presence of indicated antibodies. Results are representative of two independent experiments with cells from different donors. F(ab')$_2$ fragments were used in all experiments. NK cells in (**a**-**c**) were from different donors with data depicted as means of quadruplicate (**a**,**b**) or triplicate (**c**) samples. Errors bars represent s.d.

Previous studies demonstrated that NKp80 stimulates NK cytotoxicity in redirected lysis assays when cross-linked by NKp80-specific antibodies [**16,23,24**]. However, due to the unknown nature of NKp80-L, the importance of NKp80-dependent

cytotoxicity in a biologically relevant setting could not be assessed. Here, we addressed the impact of NKp80 on NK cell cytotoxicity towards myeloid cells expressing AICL. U937 cells express high amounts of AICL, but also of ligands for the activating NK receptor DNAM-1 [**33**].

Accordingly, freshly isolated NK cells strongly lyzed U937. U937 lysis was partially blocked by anti-NKp80 10E4, suggesting that NKp80 markedly contributes to NK cell-mediated cytolysis of U937 cells (**Figure 2.30a**). Furthermore, addition of either 7F12 or soluble NKp80 also reduced NK cytotoxicity against U937 cells (**Figure 2.30b**). In contrast to U937 cells, non-malignant myeloid cells like monocytes express low amounts of AICL and DNAM-1 ligands and are largely resistant to NK cell-mediated cytolysis (data not shown). However, after 24 h of LPS treatment, in two out of four donors, we observed moderate NK cell-mediated cytolysis of autologous monocytes, which was inhibited by treatment with NKp80- and AICL-specific antibodies (**Figure 2.30c** and data not shown). These data indicate that TLR-mediated activation may render monocytes susceptible to NKp80-dependent NK cell-mediated cytolysis.

NKp80-dependent NK-monocyte cross-talk

A recent report [**12**] described a bi-directional activation pathway between NK cells and monocytes that results in secretion of IFNγ and TNF by NK cells and monocytes, respectively. It was suggested that this mutual activation may occur at sites of inflammation, particularly during chronic inflammatory autoimmune diseases when activated $CD56^{bright}$ NK cells and monocytes are prominent [**12**]. Co-culture of NK cells and monocytes in the presence of monokines results in increased secretion of pro-inflammatory cytokines by NK cells and monocytes, and this increase is partially dependent on cell contact [**12**]. However, the receptors involved in this cell contact-dependent NK cell-monocyte cross-talk remain unidentified.

Here we here adopted this same experimental system to confirm that co-culture of freshly isolated autologous NK cells and monocytes results in increased frequencies of IFNγ-secreting NK cells and TNF-secreting monocytes, respectively, as compared to cultures of either NK cells or monocytes alone (**Figure 2.31**). In accordance with previous studies, $CD56^{bright}$ NK cells were more prone to produce IFNγ than $CD56^{dim}$ NK cells [**25**] (**Figure 2.31b**, and **Table 2.3**). Importantly, addition of IL-15 and IL-18 monokines was essential to induce cytokine secretion.

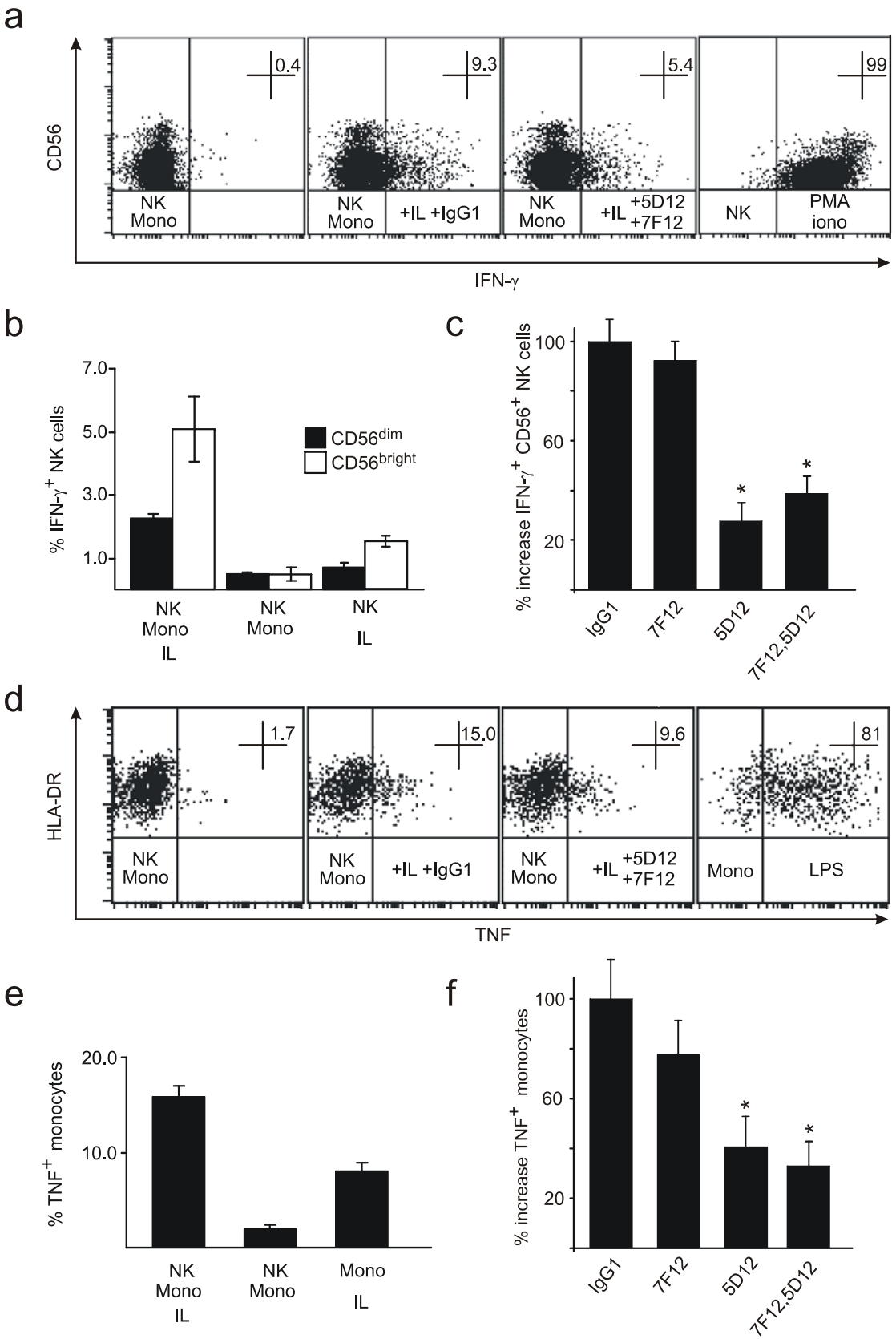

Figure 2.31. NKp80-dependent stimulation of cytokine release. (**a-c**) Frequency of IFN-γ-producing NK cells after 12 h culture with autologous $CD14^{dim}CD16^{+}$ monocytes. (**a**) Representative analysis of NK cells cultured with monocytes (Mono) or monokines (IL) in the

presence of indicated antibodies. Stimulation with PMA and ionomycin served as a positive control (right panel). Percentages of IFN-γ^+ cells of all $CD56^+$NK cells (upper right quadrant) are indicated. (**b**) Frequency of IFN-γ^+CD56^{dim} NK cells (black bars) or IFNγ^+CD56^{bright} NK cells (open bars) after culture with monocytes, monokines or both. (**c**) Change in frequency of IFN-γ^+ NK cells after co-culture with monocytes in the presence of monokines and indicated antibodies. (**d-f**) Frequency of $TNF^+CD14^{dim}CD16^+$ monocytes after 12 h culture with autologous NK cells. (**d**) Representative analysis of monocytes cultured with NK cells in the presence of monokines and indicated antibodies. Stimulation with LPS served as a positive control (right panel). Percentages of TNF^+ cells of all HLA-DR^+ monocytes (upper right quadrant) are indicated. (**e**) Frequency of TNF^+ monocytes after culture with NK cells, monokines or both. (**f**) Change in frequency of TNF^+ monocytes after culture with NK cells in the presence of monokines and indicated antibodies. In (**c**) and (**f**) the frequency of cytokine-producing cells after culture with isotype control IgG_1 is set as 100% (for details see Methods). All data are means of triplicate (**a**, donor 6) or quadruplicate (**b-f**, donor 3) samples, and errors bars represent s.d. *P*-values were calculated using the two-tailed Student's t test and * indicates a significant difference ($P < 0.001$) to the IgG_1 isotype control.

To investigate whether NKp80-AICL interactions may contribute to this cell contact-dependent NK cell-monocyte cross-talk, we added $F(ab')_2$ fragments of the NKp80-specific antibody 5D12 and/or the AICL-specific antibody 7F12 to NK cell-monocyte co-cultures. Blockade of NKp80-AICL interactions strongly reduced the monocyte-dependent increase in NK cell IFNγ secretion, demonstrating that NKp80-AICL interactions are crucially involved in the activating NK-monocyte crosstalk (**Figure 2.31a,c**). Although the frequencies of IFNγ-secreting $CD56^{bright}$ NK cells varied widely between various donors (range 3.8% to 40.2%), NKp80 blockade always resulted in a strong reduction of responsive cells (**Table 2.3**). Similarly, frequencies of IFNγ-secreting $CD56^{dim}$ NK cells (range 1.7% to 25.2 %) were markedly reduced in four out of five donors analyzed. In contrast, 7F12 did not significantly affect IFNγ-secretion by NK cells, presumably due to its inefficient blocking capability. Conversely, enhanced TNF secretion by monocytes co-cultured with NK cells ranged between 5% and 62%. In four out of five donors TNF secretion was notably reduced when NKp80 was blocked (**Figure 2.31d,f** and **Table 2.3**). These results indicate that NKp80 engagement also influences cell contact-dependent TNF secretion by monocytes. Finally, a contribution of NKp80 to monocyte-induced IFNγ secretion by NK cells was also observed in a setting where experimental addition of monokines was substituted with LPS treatment of monocytes (**Figure 2.32**).

Table 2.3. Frequencies of IFNγ$^+$ NK cells and TNFα$^+$ CD14^{dim}CD16$^+$ monocytes in NK-monocyte co-cultures. Data represent percentages of IFNγ$^+$ NK cells (columns 2-11) and TNFα$^+$ CD14^{dim}CD16$^+$ monocytes (columns 12-16) in 12h NK-monocyte co-cultures from six unrelated donors with monokines IL-15 and IL-18 (IL) or without monokines (columns 6, 11, 16). Significant reductions of frequencies in presence of 7F12, 5D12 or 7F12/5D12 as compared to control IgG_1 (endotoxin-low $(Fab')_2$ –fragments were used throughout) are marked by: *, $p < 0.04$ or **, $p < 0.001$ (p-values were calculated using the two-tailed Student's t test). Data are means of n = 3 (Donor 1, 2, 4, 6) or n = 4 (Donor 3) or n = 6 (Donor 5) ± s.d. nd = not done.

	CD56^{bright} NK cells					CD56^{dim} NK cells					CD14^{dim}CD16$^+$ Monocytes				
	NK Mono IL				NK Mono	NK Mono IL				NK Mono	NK Mono IL				NK Mono
Donor	IgG1	5D12	7F12	5D12 7F12	-	IgG1	5D12	7F12	5D12 7F12	-	IgG1	5D12	7F12	5D12 7F12	-
1	14.1 ± 0.9	9.1** ± 2.2	13.1 ± 1.5	9.4* ± 0.4	1.6 ± 1.7	6.4 ± 0.6	4.8* ± 0.4	6.2 ± 0.7	4.1* ± 0.2	1.4 ± 0.1	51.7 ± 1.2	47.2* ± 2.2	49.1 ± 1.8	46.8* ± 1.3	14.7 ± 0.7
2	40.2 ± 2.8	25.5* ± 4.3	nd	27.5** ± 4.8	1.0 ± 0.4	25.2 ± 0.9	17.3* ± 2.6	nd	18.6* ± 3.4	1.2 ± 0.1	35.6 ± 1.4	28.9* ± 1.1	nd	30.7* ± 0.6	8.2 ± 0.7
3	4.4 ± 0.1	1.7** ± 0.3	3.6* ± 0.5	1.6** ± 0.3	0.5 ± 0.2	2.0 ± 0.1	1.1** ± 0.1	1.8 ± 0.03	1.4** ± 0.1	0.5 ± 0.1	13.8 ± 0.9	10.4** ± 0.6	12.6 ± 0.7	10.0** ± 0.4	1.9 ± 0.2
4	9.7 ± 1.1	6.7* ± 0.9	13.4 ± 2.3	7.0 ± 1.4	2.1 ± 0.7	3.0 ± 0.3	2.5 ± 0.2	3.0 ± 0.1	2.6 ± 0.2	0.6 ± 0.1	25.7 ± 0.5	22.3 ± 1.6	24.1 ± 1.5	21.4** ± 0.7	10.7 ± 0.9
5	3.8 ± 0.3	1.5** ± 0.3	3.5 ± 0.7	1.7** ± 0.4	0.9 ± 0.4	1.7 ± 0.2	1.2* ± 0.2	1.6 ± 0.2	1.1* ± 0.2	1.0 ± 0.2	5.2 ± 0.5	4.0* ± 0.3	4.6 ± 0.4	3.7* ± 0.4	1.3 ± 0.2
6	8.1 ± 0.9	nd	nd	5.5* ± 0.5	0.3 ± 0.04	11.1 ± 2.6	nd	nd	8.2 ± 1.1	2.1 ± 0.7	61.9 ± 4.4	nd	nd	54.1* ± 1.5	24.1 ± 4.8

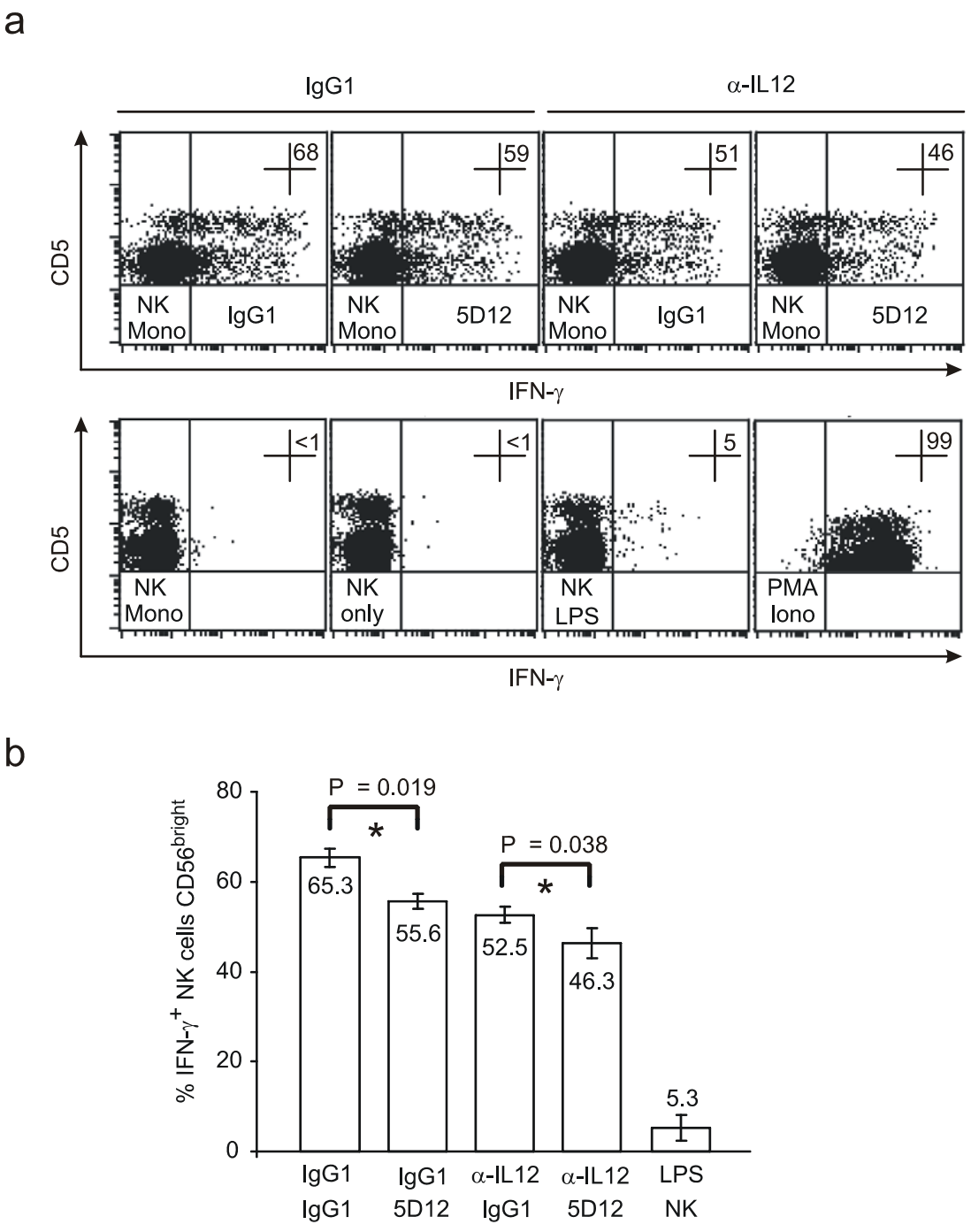

Figure 2.32. Frequencies of IFNγ-producing NK cells after 12 h co-culture with autologous $CD14^{dim}CD16^{+}$ monocytes in the presence of LPS. (**a**) Top, representative analysis of NK cells cultured with monocytes and 0.1 μg/ml LPS in the presence (right panels) or absence (left panels) of neutralizing anti-IL-12 (α-IL12) and in the presence of anti-NKp80 5D12 or an isotype control IgG_1. Bottom, various controls. Percentages of IFN-γ^{+} $CD56^{bright}$ NK cells (upper right quadrant) are given. 5D12 and corresponding IgG_1 control were $F(ab')_2$ –fragments and all antibodies were used at 20 μg/ml. (**b**) Frequencies of IFN-γ^{+} $CD56^{bright}$ NK cells after co-culture with monocytes in presence of LPS as described in (**a**). All data are means of pentaplicates, errors bars represent s. d. *P*-values were calculated using the Mann-Whitney Rank Sum test and * indicates a significant difference. The experiment in (**b**) is representative of 2 independent experiments.

2.2.2.5 Discussion

NK cell activity is governed by the complex interplay of multiple activating, inhibitory and co-stimulatory receptors [**3**]. Hence, a thorough understanding of NK cell biology requires the functional definition of these various receptors and their ligands. Identification of MHC class I-related ligands and characterization of their stress-inducible regulation was key to understanding NKG2D function [**14**] and its role in immunosurveillance of viral infections and malignancies as well as in the pathogenesis of autoimmune diseases [**3,19**]. Like NKG2D, NKp80 is a homodimeric NKC-encoded activating NK receptor without a known inhibitory counterreceptor [**16,17**]. In contrast to NKG2D, NKp80 is predominantly expressed on NK cells and is absent in rodents. Hence, characterization of NKp80 ligands would likely aid the attempt to further decipher human NK cell biology.

We here identify AICL as a ligand of NKp80 and provide the first characterization of AICL as a myeloid-specific, activating receptor. AICL shares several features with TREM-1 including myeloid-specific expression, up-regulation in response to TLR stimulation and down-regulation during differentiation from monocytes to immature DCs [**32**]. In fact, AICL transcripts are among the most prominently down-regulated transcripts during *in vitro* generation of DCs from monocytes [**34**]. Like TREM-1, cross-linking of AICL triggered TNF release by monocytes, which was further enhanced by LPS stimulation [**32**]. However, unlike AICL, TREM-1 is a member of the immunoglobulin superfamily with yet unidentified ligands, is not expressed on $CD14^{dim}CD16^{+}$ monocytes and contains a positively charged amino acid in the transmembrane domain that allows pairing with the ITAM-bearing adaptor protein DAP12 [**32**]. The cytoplasmic domain of AICL is rather short (7 amino acids) and the transmembrane domain lacks charged residues, suggesting that AICL does not associate with DAP10, DAP12 or FcεRIγ adaptor proteins.

Recently, association of the distant AICL relative CD69 with sphingosine-1-phosphate receptor 1 has been reported [**35**]. In ongoing studies we will attempt to identify AICL-associated proteins and to assess a potential association between AICL and human sphingosine-1-phosphate receptors. Similarly, the signal transducing elements associated with NKp80 have not yet been defined. Moretta and colleagues originally reported that tyrosine phosphorylation of NKp80 was detected upon treatment of NK cells with pervanadate, but immunoprecipitation experiments failed to identify NKp80-associated signaling molecules [**16**].

Certainly, it will be important to determine whether NKp80-AICL interactions influence NK cell reactivity and immune responses *in vivo*. Since both receptors have no corresponding sequence homologues in rodents, addressing this issue *in vivo* remains difficult. Here we provide *in vitro* data that can be conceptualized in two non-exclusive ways. First, we show that expression of AICL, which engages NKp80, increased susceptibility of myeloid cells to NK cell-mediated cytolysis. However, whereas malignant U937 cells were strongly lyzed by NK cells, NK cell-mediated cytolysis of autologous LPS-activated monocytes was considerably lower or even absent depending on the donor. NK cell-mediated killing of infected monocytes and macrophages has been reported [**36**], and in these situations TLR-induced AICL expression may aid in the elimination of macrophages and other myeloid cells exposed to or infected by pathogens. Second, we demonstrated that secretion of pro-inflammatory cytokines in co-cultures of NK cells and monocytes in the presence of monokines was strongly augmented by NKp80 engagement, and that NKp80-AICL interactions account, at least in part, for the previously described cell contact-dependency of the activating cellular cross-talk [**12**]. Since this reciprocal activation involves multiple cytokines and possibly several receptor-ligand interactions, it is not unexpected that it was not completely blocked by anti-NKp80 treatment. Of the two AICL-specific antibodies generated, 7G4 does not block NKp80 binding, and 7F12 only partially inhibits NKp80 binding as judged from binding assays with recombinant proteins. This may account for the inefficient inhibition of cytokine production in NK-monocyte co-cultures by 7F12. However, our data do not exclude the possibility that a second unidentified NKp80-L on monocytes may also contribute to this cross-talk.

Our data establish the affinity of the NKp80-AICL interaction in the range of 2-5 µM. Affinities of other NKC-encoded homodimeric C-type lectin-like receptor-ligand pairs are not available for comparison. Reported affinities for NKC-encoded NK receptors interacting with MHC class I molecules or MHC class I-related molecules vary between 10 nM and 100 µM [**17**] (e.g. kinetic data of NKG2D-MICA interactions are similar to those of NKp80-AICL interactions [**37**]).

Yokoyama and colleagues were the first to describe the genetic linkage of certain receptor-ligand pairs within the NKC [**27**]. This observation aided the recent characterization of LLT1 as ligand of human CD161 [**28,29**], as well as the identification of AICL as ligand of NKp80 presented here. In light of these findings, it is tempting to speculate that other adjacent genes (e.g. those encoding DCAL1 and CD69) located within this NKC subregion may encode receptor-ligand pairs.

Whereas the NKC of mice contains genes encoding several inhibitory and activating Nkrp1 receptors, the single human Nkrp1 homologue NKRP1A is an inhibitory receptor [**17**]. Since Nkrp1 receptors and their Clr ligands in mice are clustered in a subregion of the NKC orthologous to the human NKC subregion encoding NKRP1A, LLT1, NKp80, and AICL, NKp80 may be a human equivalent of an activating mouse Nkrp1 receptor. Interestingly, transcripts for Clr-b and Clr-g, ligands of the inhibitory Nkrp1d and the activating Nkrp1f receptors, respectively, were reported to be expressed by myeloid cells [**27**]. However, lack of specific antibodies impeded detailed characterization of Clr protein expression. It has been proposed that the tight genetic linkage of Nkpr1-Clr receptor-ligand pairs reflects genetic strategies of ancient histocompatibility systems [**27**]. At least for humans, our analyses of AICL expression as well as our studies of LLT1 expression (J. Pfeiffer and A.S., unpublished observations) show that these ligands are specifically expressed by distinct subsets of hematopoietic cells, suggesting that these NKC-encoded receptor-ligand pairs may have evolved to orchestrate immune interactions between various leukocyte subpopulations.

In contrast to the activating receptor NKG2D, which is thought to alert NK cells towards 'dangerous' (e.g. infected or malignant) cells by detecting stress-induced self-ligands [**3,19**], NKp80 may mediate cell contact-dependent communication between NK cells and myeloid cells during early phases of infection or during chronic inflammatory reactions. Recent studies indicate that NK cells are activated by mycobacteria-infected monocytes and respond to Plasmodium-infected erythrocytes in concert with monocytes and macrophages [**11,38,39**]. Hence, addressing an involvement of the NKp80-AICL interaction in the immune control of these pathogens is of immediate interest.

In summary, here we identify the orphan AICL as a ligand of the human activating NK receptor NKp80 and characterize AICL as a myeloid-specific activating receptor (**Figure 2.33**). We provide evidence that NKp80 engagement by AICL not only promotes cytolysis of myeloid cells, but is also critically involved in the mutual activation of NK cells and monocytes.

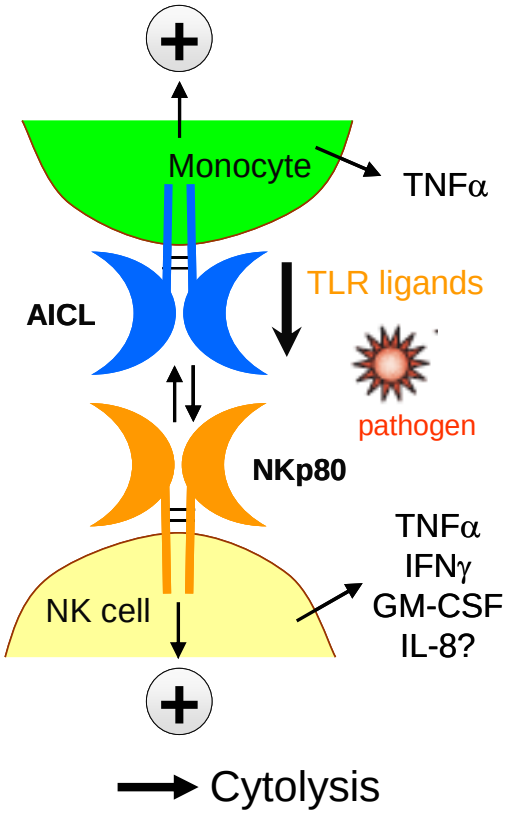

Figure 2.33. Activating cellular cross-talk between NK cells and monocytes is partially dependent on the NKp80-AICL interaction. AICL is a physiological ligand of the NK receptor NKp80. AICL is specifically expressed only on cells of the myeloid linage and is markedly induced by TLR ligands (e.g. LPS-containing pathogens). Cross-linking of AICL stimulated TNFα-release by monocytes and the NKp80-AICL interaction promoted lysis of AICL-expressing cells by NK cells. Finally resulted NKp80 blocking in a reduced sectretion of pro-inflammatory cytokines, i.e IFNγ from NK cells and TNFα from monocytes. Therefore the activating cellular cross-talk between NK cells and monocytes is partially dependent on the NKp80-AICL interaction.

To our knowledge, this is the first report describing a cellular cross-talk between human NK cells and monocytes mediated by cell-type specific receptors. Therefore these findings may provide insight into communication within the innate immune system in acute and chronic inflammatory situations, and may aid in the elucidation of processes of innate immune defense against human pathogens.

2.2.2.6 Acknowledgements

We thank W. Ruschmeier for technical assistance, J. Bukur for CD161-ED, J. Pfeiffer for real-time PCR (**Figure 2.25.**), A. Kelp for EGFP constructs, S. Stevanović for mass spectrometry and H.-G. Rammensee for long-term support and critical remarks. This work was supported by grants of the Deutsche Forschungsgemeinschaft (STE 828/3-1 and SFB 685 TP A1).

2.2.2.7 References

1. Trinchieri, G. 1989. Biology of natural killer cells. *Adv.Immunol.* 47:187-376.

2. Karre, K. 2002. NK cells, MHC class I molecules and the missing self. *Scand.J.Immunol.* 55:221-228.

3. Lanier, L. L. 2005. NK cell recognition. *Annu.Rev.Immunol.* 23:225-274.

4. Raulet, D. H. 2004. Interplay of natural killer cells and their receptors with the adaptive immune response. *Nat.Immunol.* 5:996-1002.

5. Degli-Esposti, M. A. and M. J. Smyth. 2005. Close encounters of different kinds: dendritic cells and NK cells take centre stage. *Nat.Rev.Immunol.* 5:112-124.

6. Martin-Fontecha, A., L. L. Thomsen, S. Brett, C. Gerard, M. Lipp, A. Lanzavecchia, and F. Sallusto. 2004. Induced recruitment of NK cells to lymph nodes provides IFN-gamma for T(H)1 priming. *Nat.Immunol.* 5:1260-1265.

7. Ferlazzo, G., M. L. Tsang, L. Moretta, G. Melioli, R. M. Steinman, and C. Munz. 2002. Human dendritic cells activate resting natural killer (NK) cells and are recognized via the NKp30 receptor by activated NK cells. *J.Exp.Med.* 195:343-351.

8. Fernandez, N. C., A. Lozier, C. Flament, P. Ricciardi-Castagnoli, D. Bellet, M. Suter, M. Perricaudet, T. Tursz, E. Maraskovsky, and L. Zitvogel. 1999. Dendritic cells directly trigger NK cell functions: cross-talk relevant in innate anti-tumor immune responses *in vivo*. *Nat.Med.* 5:405-411.

9. Gerosa, F., B. Baldani-Guerra, C. Nisii, V. Marchesini, G. Carra, and G. Trinchieri. 2002. Reciprocal activating interaction between natural killer cells and dendritic cells. *J.Exp.Med.* 195:327-333.

10. Piccioli, D., S. Sbrana, E. Melandri, and N. M. Valiante. 2002. Contact-dependent stimulation and inhibition of dendritic cells by natural killer cells. *J.Exp.Med.* 195:335-341.

11. Baratin, M., S. Roetynck, C. Lepolard, C. Falk, S. Sawadogo, S. Uematsu, S. Akira, B. Ryffel, J. G. Tiraby, L. Alexopoulou, C. J. Kirschning, J. Gysin, E. Vivier, and S. Ugolini. 2005. Natural killer cell and macrophage cooperation in

MyD88-dependent innate responses to Plasmodium falciparum. *Proc.Natl.Acad.Sci.U.S.A* 102:14747-14752.

12. Dalbeth, N., R. Gundle, R. J. Davies, Y. C. Lee, A. J. McMichael, and M. F. Callan. 2004. CD56bright NK cells are enriched at inflammatory sites and can engage with monocytes in a reciprocal program of activation. *J.Immunol.* 173:6418-6426.

13. Moretta, A., C. Bottino, M. Vitale, D. Pende, C. Cantoni, M. C. Mingari, R. Biassoni, and L. Moretta. 2001. Activating receptors and coreceptors involved in human natural killer cell-mediated cytolysis. *Annu.Rev.Immunol.* 19:197-223.

14. Bauer, S., V. Groh, J. Wu, A. Steinle, J. H. Phillips, L. L. Lanier, and T. Spies. 1999. Activation of NK cells and T cells by NKG2D, a receptor for stress-inducible MICA. *Science* 285:727-729.

15. Roda-Navarro, P., I. Arce, M. Renedo, K. Montgomery, R. Kucherlapati, and E. Fernandez-Ruiz. 2000. Human KLRF1, a novel member of the killer cell lectin-like receptor gene family: molecular characterization, genomic structure, physical mapping to the NK gene complex and expression analysis. *Eur.J.Immunol.* 30:568-576.

16. Vitale, M., M. Falco, R. Castriconi, S. Parolini, R. Zambello, G. Semenzato, R. Biassoni, C. Bottino, L. Moretta, and A. Moretta. 2001. Identification of NKp80, a novel triggering molecule expressed by human NK cells. *Eur.J.Immunol.* 31:233-242.

17. Yokoyama, W. M. and B. F. Plougastel. 2003. Immune functions encoded by the natural killer gene complex. *Nat.Rev.Immunol.* 3:304-316.

18. Cosman, D., J. Mullberg, C. L. Sutherland, W. Chin, R. Armitage, W. Fanslow, M. Kubin, and N. J. Chalupny. 2001. ULBPs, novel MHC class I-related molecules, bind to CMV glycoprotein UL16 and stimulate NK cytotoxicity through the NKG2D receptor. *Immunity.* 14:123-133.

19. Raulet, D. H. 2003. Roles of the NKG2D immunoreceptor and its ligands. *Nat.Rev.Immunol.* 3:781-790.

20. Vivier, E., E. Tomasello, and P. Paul. 2002. Lymphocyte activation via NKG2D:

towards a new paradigm in immune recognition?. *Curr.Opin.Immunol.* 14:306-311.

21. Oppenheim, D. E., S. J. Roberts, S. L. Clarke, R. Filler, J. M. Lewis, R. E. Tigelaar, M. Girardi, and A. C. Hayday. 2005. Sustained localized expression of ligand for the activating NKG2D receptor impairs natural cytotoxicity *in vivo* and reduces tumor immunosurveillance. *Nat.Immunol.* 6:928-937.

22. Smyth, M. J., J. Swann, E. Cretney, N. Zerafa, W. M. Yokoyama, and Y. Hayakawa. 2005. NKG2D function protects the host from tumor initiation. *J.Exp.Med.* 202:583-588.

23. Biassoni, R., M. Fogli, C. Cantoni, P. Costa, R. Conte, G. Koopman, A. Cafaro, B. Ensoli, A. Moretta, L. Moretta, and A. De Maria. 2005. Molecular and functional characterization of NKG2D, NKp80, and NKG2C triggering NK cell receptors in rhesus and cynomolgus macaques: monitoring of NK cell function during simian HIV infection. *J.Immunol.* 174:5695-5705.

24. Mavilio, D., J. Benjamin, D. Kim, G. Lombardo, M. Daucher, A. Kinter, E. Nies-Kraske, E. Marcenaro, A. Moretta, and A. S. Fauci. 2005. Identification of NKG2A and NKp80 as specific natural killer cell markers in rhesus and pigtailed monkeys. *Blood* 106:1718-1725.

25. Cooper, M. A., T. A. Fehniger, S. C. Turner, K. S. Chen, B. A. Ghaheri, T. Ghayur, W. E. Carson, and M. A. Caligiuri. 2001. Human natural killer cells: a unique innate immunoregulatory role for the CD56(bright) subset. *Blood* 97:3146-3151.

26. Carlyle, J. R., A. M. Jamieson, S. Gasser, C. S. Clingan, H. Arase, and D. H. Raulet. 2004. Missing self-recognition of Ocil/Clr-b by inhibitory NKR-P1 natural killer cell receptors. *Proc.Natl.Acad.Sci.U.S.A* 101:3527-3532.

27. Iizuka, K., O. V. Naidenko, B. F. Plougastel, D. H. Fremont, and W. M. Yokoyama. 2003. Genetically linked C-type lectin-related ligands for the NKRP1 family of natural killer cell receptors. *Nat.Immunol.* 4:801-807.

28. Aldemir, H., V. Prod'homme, M. J. Dumaurier, C. Retiere, G. Poupon, J. Cazareth, F. Bihl, and V. M. Braud. 2005. Cutting edge: lectin-like transcript 1 is a ligand for the CD161 receptor. *J.Immunol.* 175:7791-7795.

29. Rosen, D. B., J. Bettadapura, M. Alsharifi, P. A. Mathew, H. S. Warren, and L. L. Lanier. 2005. Cutting edge: lectin-like transcript-1 is a ligand for the inhibitory human NKR-P1A receptor. *J.Immunol.* 175:7796-7799.

30. Hamann, J., K. T. Montgomery, S. Lau, R. Kucherlapati, and R. A. van Lier. 1997. AICL: a new activation-induced antigen encoded by the human NK gene complex. *Immunogenetics* 45:295-300.

31. Belge, K. U., F. Dayyani, A. Horelt, M. Siedlar, M. Frankenberger, B. Frankenberger, T. Espevik, and L. Ziegler-Heitbrock. 2002. The proinflammatory CD14+CD16+DR++ monocytes are a major source of TNF. *J.Immunol.* 168:3536-3542.

32. Bouchon, A., J. Dietrich, and M. Colonna. 2000. Cutting edge: inflammatory responses can be triggered by TREM-1, a novel receptor expressed on neutrophils and monocytes. *J.Immunol.* 164:4991-4995.

33. Pende, D., R. Castriconi, P. Romagnani, G. M. Spaggiari, S. Marcenaro, A. Dondero, E. Lazzeri, L. Lasagni, S. Martini, P. Rivera, A. Capobianco, L. Moretta, A. Moretta, and C. Bottino. 2006. Expression of the DNAM-1 ligands, Nectin-2 (CD112) and poliovirus receptor (CD155), on dendritic cells: relevance for natural killer-dendritic cell interaction. *Blood* 107:2030-2036.

34. Le Naour, F., L. Hohenkirk, A. Grolleau, D. E. Misek, P. Lescure, J. D. Geiger, S. Hanash, and L. Beretta. 2001. Profiling changes in gene expression during differentiation and maturation of monocyte-derived dendritic cells using both oligonucleotide microarrays and proteomics. *J.Biol.Chem.* 276:17920-17931.

35. Shiow, L. R., D. B. Rosen, N. Brdickova, Y. Xu, J. An, L. L. Lanier, J. G. Cyster, and M. Matloubian. 2006. CD69 acts downstream of interferon-alpha/beta to inhibit S1P1 and lymphocyte egress from lymphoid organs. *Nature* 440:540-544.

36. Vankayalapati, R., A. Garg, A. Porgador, D. E. Griffith, P. Klucar, H. Safi, W. M. Girard, D. Cosman, T. Spies, and P. F. Barnes. 2005. Role of NK cell-activating receptors and their ligands in the lysis of mononuclear phagocytes infected with an intracellular bacterium. *J.Immunol.* 175:4611-4617.

37. Li, P., D. L. Morris, B. E. Willcox, A. Steinle, T. Spies, and R. K. Strong. 2001.

Complex structure of the activating immunoreceptor NKG2D and its MHC class I-like ligand MICA. *Nat.Immunol.* 2:443-451.

38. Korbel, D. S., K. C. Newman, C. R. Almeida, D. M. Davis, and E. M. Riley. 2005. Heterogeneous human NK cell responses to Plasmodium falciparum-infected erythrocytes. *J.Immunol.* 175:7466-7473.

39. Zhang, R., X. Zheng, B. Li, H. Wei, and Z. Tian. 2006. Human NK cells positively regulate gammadelta T cells in response to Mycobacterium tuberculosis. *J.Immunol.* 176:2610-2616.

40. Radsak, M. P., N. Hilf, H. Singh-Jasuja, S. Braedel, P. Brossart, H. G. Rammensee, and H. Schild. 2003. The heat shock protein Gp96 binds to human neutrophils and monocytes and stimulates effector functions. *Blood* 101:2810-2815.

41. Welte, S. A., C. Sinzger, S. Z. Lutz, H. Singh-Jasuja, K. L. Sampaio, U. Eknigk, H. G. Rammensee, and A. Steinle. 2003. Selective intracellular retention of virally induced NKG2D ligands by the human cytomegalovirus UL16 glycoprotein. *Eur.J.Immunol.* 33:194-203.

42. Aida, Y. and M. J. Pabst. 1990. Removal of endotoxin from protein solutions by phase separation using Triton X-114. *J.Immunol.Methods* 132:191-195.

43. Alter, G., J. M. Malenfant, and M. Altfeld. 2004. CD107a as a functional marker for the identification of natural killer cell activity. *J.Immunol.Methods* 294:15-22.

44. Waldhauer, I. and A. Steinle. 2006. Proteolytic release of soluble UL16-binding protein 2 from tumor cells. *Cancer Res.* 66:2520-2526.

3 Summary

NK cell activity is governed by the complex interplay of multiple activating, inhibitory and co-stimulatory receptors. Therefore, a thorough understanding of NK cell biology requires the functional definition of these various receptors and their ligands. The NKC-encoded, homodimeric C-type lectin-like molecule NKp80 has been described as an activating orphan receptor, which is almost exclusively expressed by NK cells and stimulates NK cytolysis.

This thesis identifies the adjacently encoded C-type lectin-like molecule AICL as a physiological ligand of NKp80. It also defines AICL as a myeloid-specific, activating receptor expressed on monocytes, macrophages and granulocytes. AICL is up-regulated in response to TLR stimulation and down-regulated during differentiation of monocytes to immature DCs. Cross-linking of AICL stimulated TNFα-release by monocytes, which was further enhanced by LPS stimulation. Additionally, it was shown that the NKp80-AICL interaction promotes lysis of AICL-expressing cells by NK cells. Malignant U937 cells were strongly lyzed by NK cells, whereas cytolysis of autologous LPS-activated monocytes was considerably lower or even absent depending on the donor. In other studies NK cell-mediated killing of infected monocytes and macrophages has been reported, and in these situations TLR-induced AICL expression may aid in the elimination of cells exposed to or infected by pathogens.

Further, this work shows that secretion of pro-inflammatory cytokines, i.e. IFNγ from NK cells and TNFα from monocytes, in co-cultures of NK cells and monocytes was strongly augmented by NKp80 engagement, and that the NKp80-AICL interaction accounts, at least in part, for the previously described cell contact-dependency of the activating cellular cross-talk between monocytes and NK cells. This thesis is the first report describing cell-type specific receptors mediating an activating cellular cross-talk between human NK cells and monocytes, which is thought to play a role in acute and chronic inflammatory situations. Therefore these findings provide novel insights into the communication within the innate immune system and may have important implications for the immune defence of certain pathogens and the pathogenesis of autoimmune disorders.

Zusammenfassung

Die NK-vermittelte Zelllyse wird durch ein komplexes Zusammenspiel von inhibierenden, aktivierenden und costimulierenden Rezeptoren gesteuert. Für ein umfassendes Verständnis der NK-Zellbiologie ist eine funktionelle Charakterisierung dieser verschiedenen Rezeptoren und deren Liganden notwendig. Der NKC-kodierte C-Typ lektin-ähnliche aktivierende NK-Rezeptor NKp80 wird als Homodimer fast ausschließlich auf NK-Zellen exprimiert und ist in der Lage NK Cytotoxizität zu vermitteln.

Diese Arbeit identifiziert AICL als physiologischen Liganden von NKp80 und etabliert AICL als myeloidspezifischen, aktivierenden Rezeptor, der auf Monozyten, Makrophagen und Granulozyten exprimiert wird. AICL wird nach TLR-Stimulation hochreguliert, während AICL bei der Differenzierung von Monozyten zu unreifen DCs herunterreguliert wird. Die AICL-Aktivierung führt zur TNFα-Freisetzung durch Monozyten, was durch die Stimulation mit LPS noch verstärkt wird. Im Rahmen dieser Arbeit konnte gezeigt werden, dass AICL-exprimierende Zellen NKp80-vermittelt lysiert werden. Maligne U937-Zellen werden durch NK-Zellen in hohem Maße lysiert, autologe LPS-stimulierte Monozyten dagegen spenderabhängig kaum oder gar nicht. Es ist bekannt, dass infizierte Monozyten und Makrophagen NK-vermittelt lysiert werden. In diesem Fall könnte die TLR-induzierte AICL-Expression zur Eliminierung von infizierten Zellen führen.

Es konnte weiterhin gezeigt werden, dass bei der Kokultur von Monozyten und NK-Zellen NKp80-vermittelt entzündungsfördernde Cytokine freigesetzt werden, d.h TNFα durch Monozyten und IFNγ durch NK-Zellen. Die NKp80/AICL-Interaktion ist zumindest teilweise für die beschriebene Zell-Zell-Kontaktabhängigkeit dieser reziproken Aktivierung verantwortlich. Diese Arbeit liefert die erste Beschreibung von zelltypspezifischen Rezeptoren, die an dieser reziproken Aktivierung zwischen NK Zellen und Monozyten beteiligt sind, für die eine Rolle bei akuten oder chronischen Entzündungen postuliert wird. Diese hier beschriebene NKp80-AICL-Interaktion liefert neue Einblicke in die Kommunikation innerhalb des angeborenen Immunsystems und könnte bei der Immunantwort gegen bestimmte Pathogene oder bei der Pathogenese von Autoimmunerkrankungen bedeutend sein.

4 Abbreviations

α	anti
α-MEM	α-minimum essential medium
aa	amino acids
Ab	antibody
ADCC	antibody-dependent cell-mediated cytotoxicity
APCs	antigen presenting cells
APC	allophycocyanin
bp	base pairs
BSA	bovine serum albumin
CD	cluster of differentiation
cDNA	complementary deoxyribonucleic acid
CML	chronic myeloid leukemia
CTL	cytotoxic T lymphocyte
DC	dendritic cell
DMEM	Dulbecco's Modified Eagle's Medium
DMSO	dimethyl sulfoxide
dNTP	deoxynucleoside triphosphate
DTT	dithiothreitol
EDTA	ethylenediaminetetraacetic acid
EGFP	enhanced green fluorecent protein
ELISA	enzyme-linked immunosorbent assay
Endo H	endoglycosidase H
ER	endoplasmatic reticulum
Fc	constant fragment
FCS	fetal calf serum
G418	neomycin
GlcNac	N-acetyl-D-glycosamine
GM-CSF	granulocyte-macrophage colony stimulating factor
GPI	glycosylphosphatidyl inositol
GvHD	graft-versus-host disease
GvT	graft-versus-tumor
HBSS	Hank’s Balanced Salt Solution
HLA	human leukocyte antigen
HPLC	high performance liquid chromatography
HRP	horse radish peroxidase
IFN	interferon
Ig	immunoglobulin
IL	interleukin
IMDM	Iscove’s modified Dulbeccos’s medium
kb	kilo bases
kDa	kilo dalton
KLH	keyhole limpet hemocyanin
mAb	monoclonal antibody
MAP-kinase	mitogen-activated kinase
MBP	mannose binding protein
M-CSF	macrophage colony stimulating factor
MHC	major histocompatibility complex
MIC	MHC class I chain–related molecule
MW	molecular weight
NCR	natural cytotoxicity receptor
NK cell	natural killer cell
NKG2D	= KLRK1, killer cell lectin-like receptor subfamily K, member 1
NKG2D-L	NKG2D-ligands
NKp80-L	NKp80-ligands

NKT cell	natural killer T cell
NTP	nucleoside triphosphate
ORF	open reading frame
p.i	post infection
PBL	peripheral blood leukocytes
PBMC	peripheral blood mononuclear cells
PBS	Dulbecco's phoshate buffered saline
PCR	polymerase chain reaction
PDI	proteindisulfidisomerase
PE	phycoerythrin
PI3K	phosphatidylinositol-3-kinase
PMA	phorbol 12-myristate 13-acetate
qPCR	quantitative real-time PCR
RNAsin	RNAse-Inhibitor
ROS	reactive oxygen species
RPMI	Roswell Park Memorial lnstitute
rRNA	ribosomal ribonucleic acid
RT	room temperature
RT-PCR	reverse transcriptase PCR
s	soluble
SDS	sodium dodecyl sulfate
SN	supernatant
ss/dsRNA	single stranded/double stranded ribonucleic acid
SV40	simian virus 40
TBS	Tris-buffered saline
TCR	T cell receptor
TERT	telomerase reverse transcriptase
T_H1, T_H2 cell	T helper 1 cell, T helper 2 cell
TIL	tumor infiltrating lymphocyte
TLR	toll-like receptor
TNF	tumor necrosis factor
TNP	trinitrophenol
T_{Reg} cell	regulatory T cell
ULBP	UL16-binding proteins

5 Acknowledgements

Herrn PD Dr. Alexander Steinle und Herrn Prof. Dr. Hans-Georg Rammensee danke ich sehr herzlich für ihre intensive Förderung, das fortwährende Interesse an meiner Arbeit, die Freiheit in der Umsetzung des gestellten Themas, die exzellenten Arbeitsbedingungen und ihr mir entgegengebrachtes Vertrauen. Besonders dankbar bin ich Alexander Steinle auch dafür, dass er mir über die gesamte Dauer meines Projektes immer die finanziellen Freiheiten gab, Neues und Riskantes auszuprobieren und nie den Glauben an das Gelingen dieser Arbeit verloren hat.

Herzlich bedanken möchte ich mich bei den jetzigen und ehemaligen Laborkollegen der AG Steinle Dr. Katrin Wiemann, Sabrina Kuttruff, Inja Waldhauer, Alexandra Kelp, Mareike Wittenbrinck, Jessica Spreu, Dr. Maya Banerjea, Judith Pfeiffer, Steffen Müller, Dr. Ute Feger, Dr. Jürgen Bukur, Dr. Adrian Chudyk, Gernot Hahne und Anouk Feitsma und vielen anderen für das angenehme Arbeitsklima und Hilfsbereitschaft bedanken. Insbesondere danke ich ganz speziell Sabrina Kuttruff, Inja Waldhauer und Alexandra Kelp sowie Jürgen Bukur und Judith Pfeiffer für die erfolgreiche Zusammenarbeit, Hilfe und Diskussionen bei meinen NKp80/AICL Projekten. Hat Spaß gemacht!

Frau Beate Pömmerl ist die zentrale Anlauftstelle für alles, von Klonierungsfragen über Sequenzierungen bis zu Fahrdiensten. Ganz herzlichen Dank dafür.

Frau Wiebke Ruschmeier hat mir sehr viel Arbeit in der Zellkultur und mit dem Stickstofftank abgenommen. Dankeschön!

Bei der Arbeitsgruppe von PD Dr. Roland Brock möchte ich mich neben dem Leiter selbst noch besonders bei seinen Mitarbeitern Dr. Söhnke Voss, Dr. Mariola Fotin-Mlcezek und Dr. Rainer Fischer für die Zusammenarbeit bei verschiedenen Projekten bedanken.

Dank für vielfältige Hilfsbereitschaft möchte ich auch an Falk Duchardt, Karsten Köhler und Oda Stoevesandt aussprechen, wobei mit dieser Arbeit auch der gemeinsame Weg von Karsten, Oda und mir endet, der mit dem ersten Semster hier

in Tübingen begonnen hat.

Franziska Löwenstein, Patricia Hrstic, Claudia Falkenburger, Gerhard Hörr und Lynne Yakes danke ich für ihre extrem zuverlässige Organisationsarbeit und ihren Einsatz, der uns Doktoranden viel Arbeit abnimmt und wirklich ein (fast) sorgenfreies Arbeiten möglich macht. Viele Serviceleistungen sind wirklich etwas besonders und manche wird man wohl erst richtig zu würdigen wissen, wenn man diese nicht mehr zur Verfügung hat. Insbesondere war es eine Freude mit dem immer gutgelaunten und sehr hilfbereiten Team aus 3.008 Lynne Yakes und Gerhard Hörr zusammenarbeiten. Gerhard wurde nie müde mich nach meinem Fortschritt beim „Kuchen backen“ zu fragen, wie er meine Doktorarbeit öfters umschrieb.

Drs. Ludger Grosse-Hovest, Cécile Gouttefangeas und Patrice Decker danke ich für fachliche Hilfe und freundliche Gespräche.

Danke an Tanja Herrmann, Andi Weinzierl, Lothar Dietrich und Tina Otz und viele mehr, ihr wart prima Kollegen!

In der Arbeitsgruppe von Prof. Stefan Stevanović danke ich Despina Rudolf für die sehr zuverlässige und auch oft kurzfristige Beschaffung von Apharese-Produkten aus der Blutbank und an dieser Stelle gebührt auch großer Dank an die unzählbaren Blutspender, die sich für mich all die Jahre „picksen“ ließen, sowie an die Vampire, die das Blutabnehmen für mich gemacht haben, stellvertretend soll hier nur Prof. Gundram Jung, Tanja Herrmann und Vicky Wolf genannt werden.

Unserem Computerhiwi Matthias Wenzel möchte ich für seine sehr zuverlässige Arbeit danken, was mir im letzten Jahr sehr viel Arbeit abgenommen hat.

Besonders bedanken möchte ich mich bei Söhnke Voss und Jochen Probst für die Freundschaft, Anregungen, Hilfe und Zuspruch innerhalb der letzten Jahre. Ich sage nur Weltklasse!

Oliver Schoor war nicht nur ein besonderer, hilfsbereiter und kompetenter Kollege, sondern ist auch ein wunderbarer Freund vom ersten gemeinsamen Semester an!

Allen Kolleginnen und Kollegen, die nicht namentlich erwähnt worden sind, danke

ich für das sehr kollegiale Arbeitsklima.

Dank geht an die Bischöfliche Studienförderung Cusanuswerk, die mir dieses sorgenfreie Studium und viele unvergessliche Begegnungen, Erfahrungen und Reisen ermöglicht hat.

Ein besonderer Dank geht an meine Familie, die mich stets meinen Weg gehen ließ, mich unterstützt und gefördert hat.

Katrin, diese Suche nach dem NKp80 Ligand war auch für uns eine Herausforderung und nur wir wissen wie viel Du mir dabei geholfen hast.

6 Publications

1. Sathiyaseelan, T., B. Naiman, **S. Welte**, N. Machugh, S. J. Black, and C. L. Baldwin. 2002. Immunological characterization of a gammadelta T-cell stimulatory ligand on autologous monocytes. *Immunology* 105:181-189.

2. Rogers, A. N., S. **Welte, S.** J. Black, and C. L. Baldwin. 2002. Partial cDNA sequences of bovine CD72 and CD166/ALCAM, ligands for SRCR-family accessory molecules CD5 and CD6. *Vet.Immunol.Immunopathol.* 85:233-239.

3. **Welte, S. A.,** C. Sinzger, S. Z. Lutz, H. Singh-Jasuja, K. L. Sampaio, U. Eknigk, H. G. Rammensee, and A. Steinle. 2003. Selective intracellular retention of virally induced NKG2D ligands by the human cytomegalovirus UL16 glycoprotein. *Eur.J.Immunol.* 33:194-203.

4. Wiemann, K., H. W. Mittrücker, U. Feger, **S. A. Welte**, W. M. Yokoyama, T. Spies, H. G. Rammensee, and A. Steinle. 2005. Systemic NKG2D down-regulation impairs NK and CD8 T cell responses *in vivo*. *J.Immunol.* 175:720-729.

5. Fotin-Mleczek, M., **S. Welte,** O. Mader, F. Duchardt, R. Fischer, H. Hufnagel, P. Scheurich, and R. Brock. 2005. Cationic cell-penetrating peptides interfere with TNF signalling by induction of TNF receptor internalization. *J.Cell Sci.* 118:3339-3351.

6. Voss, S., **S. Welte**, M. Fotin-Mleczek, R. Fischer, A. J. Ulmer, G. Jung, K. H. Wiesmüller, and R. Brock. 2006. A CD14 domain with lipopolysaccharide-binding and -neutralizing activity. *Chembiochem.* 7:275-286.

7. **S. Welte**, S. Kuttruff, I. Waldhauer and A. Steinle. 2006. Mutual activation of natural killer cells and monocytes mediated by interaction between the human NK receptor NKp80 and the myeloid-specific receptor AICL. *Nat.Immunol.* (12):1334-42.

7 Scholarships

04/1998 -09/02	scholar of the Cusanvswerk Foundation of the German Catholic church
09/02	graduate scholar of the doctoral program “Cellular mechanisms of Immune-Associated Processes” supported by the German Research Council (Deutsche Forschungsgemeinschaft, DFG)
11/2000	e-fellows.net online scholarship
10/2004	poster prize for cell biology at the research colloquium of the Medical Faculty, University of Tübingen
07/1995	Karl-von-Frisch-Award of the German Foundation of Biologists

8 Academic Teachers

Academic teachers at the Eberhard-Karls-Universität, Tübingen

Prof. Bisswanger , Prof. Bock, Prof. Bohley, Prof. Duszenko, Prof. Eisele, Prof. Gönnenwein, Prof. Grabmayr, Dr. Günzl, Prof. Häfelinger, Prof. Hagenmaier, Prof. Hamprecht, Prof. Hanack, Prof. Jung, Dr. Kalbacher, Prof. Lindner, PD Dr. Maier, Prof. Mayer, Prof. Mecke, Prof. Nakel, Prof. Oberhammer, Prof. Pfeiffer, PD Dr. Pommer, Prof. Poralla, Prof. Probst, Prof. Rammensee, Prof. Reutter, Prof. Schild, Prof. Schwarz, PD Dr. Selzer, PD Dr. Steinle, Prof. Stevanović, PD Dr. Stoeva, Prof. Strähle, Prof. Voelter, Prof. Wegmann, Prof. Weber, Prof. Weser, Prof. Wohlleben.

Academic teachers at the University of Massachusetts, Amherst, MA, USA

Prof. Baldwin, Prof Black, Prof. Fitzgerald-Hayes, Prof Good, Prof. Gross, Prof. Martz, Prof. Norkin, Prof. Normanly.

9 Curriculum Vitae

Name:	Stefan Welte
Date of birth:	13/01/1976
Place of birth:	Tettnang (Bodenseekreis), Germany

09/2002 - 09/2006	PhD thesis at the Institute for Cell Biology, Department of Immunology, University of Tübingen supervised by Prof. Dr. Hans-Georg Rammensee and PD Dr. Alexander Steinle Title: AICL is a ligand for the human NK receptor NKp80/KLRF1 and mediates an activating crosstalk between NK cells and monocytes
08/2002	Diploma in Biochemistry
01/2002 - 08/2002	Diploma thesis at the Institute for Cell Biology, Department of Immunology, University of Tübingen supervised by Prof. Dr. Hans-Georg Rammensee and PD Dr. Alexander Steinle. Title: Selective intracellular retention of virally induced NKG2D ligands by the human cytomegalovirus UL16 glycoprotein
09/1999 - 08/2000	Studies in the Molecular and Cellular Biology Program at the University of Massachusetts, Amherst, MA, USA
10/1996 - 08/2002	Studies in Biochemistry, Eberhard Karls Universität Tübingen, Germany
07/1995 - 10/1996	Military service on bases in Bruchsal, Ulm und Primošten
1992 - 1995	final secondary-school examinations (Abitur) at the Edith-Stein-Schule, Ravensburg, Germany (specialized in agricultural science)
1986 - 1992	Realschule Tettnang, Tettnang, Germany

Lebenslauf

Name:	Stefan Welte
Geburtsdatum:	13.01.1976
Geburtsort:	Tettnang (Bodenseekreis), Deutschland

09/2002 - 09/2006	Doktorarbeit am Interfakultären Institut für Zellbiologie, Abteilung Immunologie, Universität Tübingen unter Anleitung von Prof. Dr. Hans-Georg Rammensee und PD Dr. Alexander Steinle. Titel: „AICL ist ein Ligand des humanen NK Rezeptors NKp80 und vermittelt eine aktivierende Interaktion zwischen NK-Zellen und Monozyten“
08/2002	Diplom in Biochemie
01/2002 - 08/2002	Diplomarbeit am Interfakultären Institut für Zellbiologie, Abteilung Immunologie, Universität Tübingen unter Anleitung von Prof. Dr. Hans-Georg Rammensee und PD Dr. Alexander Steinle Titel: „Interaktion des HCMV-induzierten UL16-Proteins mit dem NKG2D-Ligandensystem“
09/1999 - 08/2000	Einjähriger Auslandsstudienaufenthalt im „Molecular and Cellular Biology Program“ an der University of Massachusetts, Amherst, MA, USA
10/1996 - 08/2002	Studium der Biochemie, Eberhard Karls Universität Tübingen
07/1995 - 10/1996	Grundwehrdienst und Soldat auf Monate in Bruchsal, Ulm und Primošten
1992 - 1995	Abitur am “Agrarwissenschaftlichen Gymnasium”, Edith-Stein-Schule, Ravensburg
1986 - 1992	Realschule Tettnang, Tettnang